Universitat Internacional de Catalunya
Facultat de Medicina i Ciències de la Salut.
Ciències Bàsiques

Tesis doctoral

CDK-mediated phosphorylation of Yku80and its role in DNA repair

María de los Reyes Carballar Ruiz

Aquesta tesi doctoral està subjecta a la licencia Reconeixement-NoComercial-SenseObraDerivada 4.0 Internacional (CC BY-NC-ND 4.0)

Esta tesis doctoral está sujeta a la licencia Reconocimiento-NoComercial-SinObraDerivada 4.0 Internacional (CC BY-NC-ND 4.0)

This doctoral thesis is licensed under the Attribution-NonCommercial-NoDerivatives 4.0 International (CC BY-NC-ND 4.0)

CDK-mediated phosphorylation of Yku80 and its role in DNA repair

María de los Reyes Carballar Ruiz
Tesis Doctoral
2021

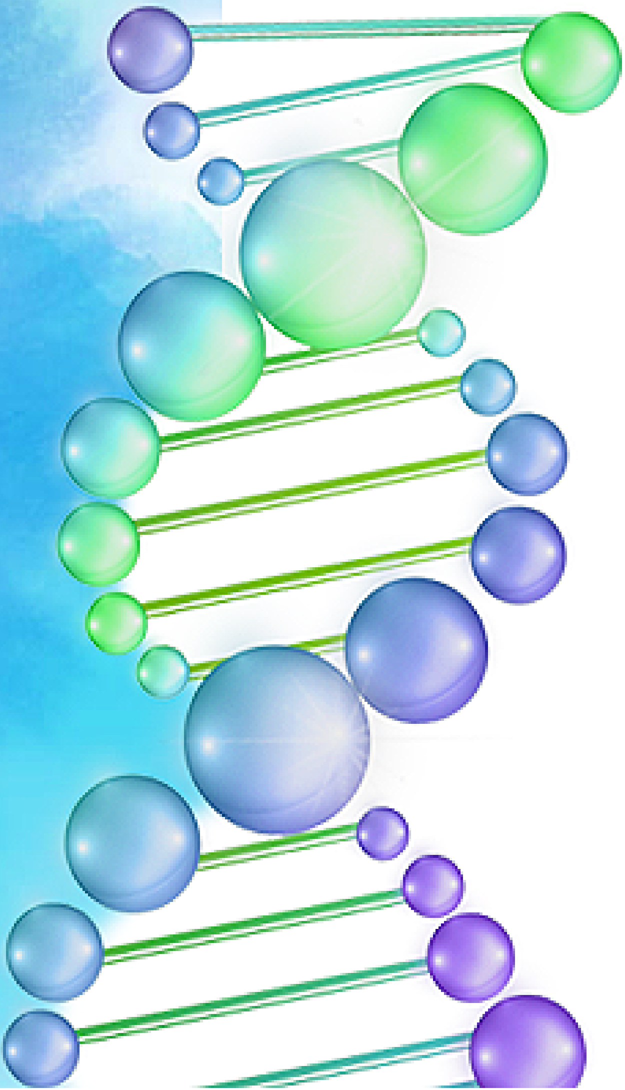

uic
barcelona

CDK-mediated phosphorylation of Yku80 and its role in DNA repair

María de los Reyes Carballar Ruiz

Memoria presentada para optar al título de doctor por la
Universidad Internacional de Cataluña,
Barcelona 2021

Trabajo codirigido por el Dr. Javier Jiménez Jiménez y el Dr.
Samuel Bru Rullo del Departamento de Ciencias Básicas de la
Universidad Internacional de Cataluña

Programa de Doctorado en Ciencias de la Salud de la
Universidad Internacional de Cataluña

Dr. Javier Jiménez Jiménez
Codirector de tesis

Dr. Samuel Bru Rullo
Codirector de tesis

María de los Reyes Carballar Ruiz
Doctorando

A las tres mujeres que siempre han creído y confiado en mí:

mi abuela, mi madre y mi hermana

ACKNOWLEDGEMENTS

Esta tesis ha sido posible gracias al apoyo incondicional de muchas personas a las que me gustaría dedicarles unas palabras de agradecimiento. Sin vosotros, este trabajo no habría sido posible.

En primer lugar, me gustaría agradecer a Josep Clotet la oportunidad que me brindó para formarme como investigadora y docente en la Universidad Internacional de Cataluña. Gracias a Javier Jiménez y Samuel Bru, los codirectores de mi tesis. A Javi me gustaría agradecerle sobre todo cada desafío intelectual y puesta a prueba de mis capacidades y límites. A Samuel Bru, el jefesito, me gustaría agradecerle su apoyo tanto en el ámbito personal como en el laboratorio donde más de una vez me ha sacado de algún que otro apuro.

I would like to express my gratitude to P. Belhumeur for the silencing strains, T.Wilson for the suicide system strains, J. Haber who kindly provided me with the yeast strains to measure HR and J. Masson for human Ku80. Also, I would like to thank Aidan Doherty for his help and showing interest in my work. The time and support have proven invaluable.

Me gustaría darles las gracias a todos y cada uno de los miembros de mi grupo. Gracias Mariana por tu positividad y siempre animarme a ver el lado bueno de las cosas. A Núria por esas charlas en el laboratorio a altas horas de la noche donde nos hacíamos compañía. A Laura, gracias por tu interés y por los ánimos en los momentos de agobio. Gracias a los pollitos, Ana,

Alessandro y en especial a Joan por estar siempre dispuesto a ayudarme y aprender.

Gracias a las que ya considero mis amigas. Marta Pérez, gracias por esa alegría que transmites, por tu risa fácil, por tu capacidad resolutiva y, sobre todo, por animarme cada vez que pensaba que no podía más. Eva Q gracias por tu serenidad y calma, por mostrarme un punto de vista diferente (y más coherente) de las cosas y las infinitas conversaciones y recomendaciones de series y películas. Bàrbara, gracias por ser mi compañera en esta etapa y hacerla mucho más llevadera, por demostrarme que el cansancio no existe y siempre hay tiempo para pasarlo bien y por las risas e innumerables charlas poyata a poyata. A Bob, que llego a última hora, pero pisando fuerte, gracias por tu ayuda y levantarme el ánimo simplemente siendo tú mismo. Gracias a Abril y Marta Palomo por ser mi trocito de Sur en el norte. Compartir parte de esta etapa con vosotras ha sido fundamental y quería agradeceros cada charla, risa y apoyo en momentos de desesperación y por no dejarme olvidar la tierra tan maravillosa de dónde venimos.

Gracias al resto del Verdu tándem, Mari Carmen, Nati y Sara H que a pesar de su veteranía y no haber compartido poyata con ellas, desde el principio me han hecho sentir parte del grupo.

No quiero olvidarme agradecer al grupo de Nuria Casals por su disposición y ayuda en cada momento. Solo tengo palabras de agradecimiento para cada uno de los miembros del grupo. Gracias a Jesús, Xavi, Rut y Rocío por su ayuda. Al Cuqui tándem: María, Cris y Helena por siempre transmitir buena energía. A Miguel, mi eterno y fiel compañero de mesa, gracias por resistir y por cada charla que hemos compartido. A Anna, por su vitalidad, perseverancia y convicción para conseguir lo que se propone. A Cris por su energía, ganas de trabajar y siempre estar dispuesta a todo. A mi Marta Perita, gracias por transmitir tu locura y manera de ver la vida, sé que me llevo una amiga. Y, por último, mi Rosi por esas tardecitas en tu terraza, todos los consejos y risas, gracias, amiga.

Al grupo de Mayka Sánchez gracias por estar dispuestos a ayudar siempre que podéis. Gracias a Ferrán, Gonzalo y Lidia por esos ratitos en las salas de cultivos. A Vero, gracias por muchas cosas, pero sobre todo por transmitirme tu alegría y entusiasmo por la ciencia. Las horas en la sala de virus se hacían más llevaderas contigo.

Gracias a mi super técnico, Andrea. Sin lugar a duda esta tesis no la podría haber hecho sin ti, tus medios y millones de placas. Gracias por tu paciencia y ayuda estos años.

A Erola gracias por todas las risas y charlas que hemos compartido en el lab y por dejarme el incubador de 37°C en momentos de desesperación. Y a Pau gracias por tu manera de ver la vida y por todas las veces que me has hecho reír.

No puedo olvidarme de darle las gracias también a los estadísticos: Juan Carlos, Adri, Cris, Queralt y Àurea. Especialmente quería agradecer a mis dos niñas: Queralt y Àurea cada confidencia y palabra de ánimo que me han ayudado a superar números baches.

Y fuera del laboratorio me gustaría agradecer a mis amigas de Sevilla: Ursu, Cris, Sara, Ana Alexandra, Alba, María y Ana por su apoyo y las incontables horas que me han escuchado quejándome. Gracias también a Alex y Mike, dos amigos con los que he compartido todo durante estos 5 años en Barcelona y siempre me han animado cuando más lo necesitaba.

I'd like to thank my boyfriend, Whitby, the endless h listening to my days and frustration and all the support which he has given me during this journey. Thank you for that and more.

Y, por último, gracias a mi familia que ha hecho posible que hoy yo esté presentando este manuscrito para optar al título de Doctora. En especial, gracias a mi madre y mi hermana. Sois un pilar fundamental en mi vida y sin vuestro esfuerzo, apoyo y palabras de ánimo esto no hubiera sido posible.

ABSTRACT

DNA double-strand breaks (DSBs) are considered the most deleterious lesions of DNA and they are repaired by means of two main mechanisms: homologous recombination (HR) and non-homologous end-joining (NHEJ). These mechanisms are regulated throughout the cell cycle being HR restricted to the S/G2 phases while NHEJ is active during the different phases of the cell cycle. Here I presented evidence of NHEJ regulation by CDK phosphorylation of one of the key proteins of the NHEJ repair pathway, Yku80. Yku80 is phosphorylated both *in vitro* and *in vivo* by the CDK Pho85 in association with the G1 cyclin Pcl1. A non-phosphorylatable version of Yku80 (*yku80*-S623A) shows increased NHEJ activity, reduced HR events and higher sensitivity upon bleomycin treatment, a DSB-inducing agent, specifically when DNA damage was induced during the G2 phase of the cell cycle. Interestingly, the overexpression of the non-phosphorylatable version of human Ku80 (Ku80^{T629A}) increased bleomycin sensitivity in different cancer lines suggesting Ku80 phosphorylation and its role in DSB repair regulation might be conserved. Thus, the results presented in this work provide evidence of a new mechanism to regulate DSB repair pathway choice by CDK-mediated phosphorylation of Yku80.

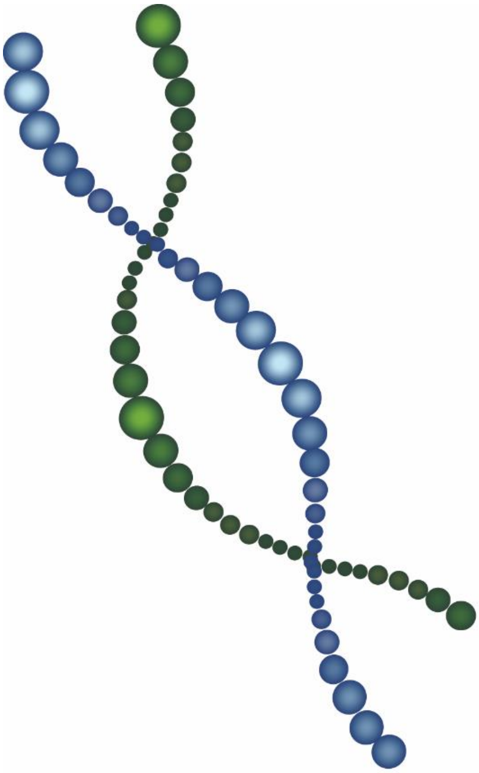

Table of contents

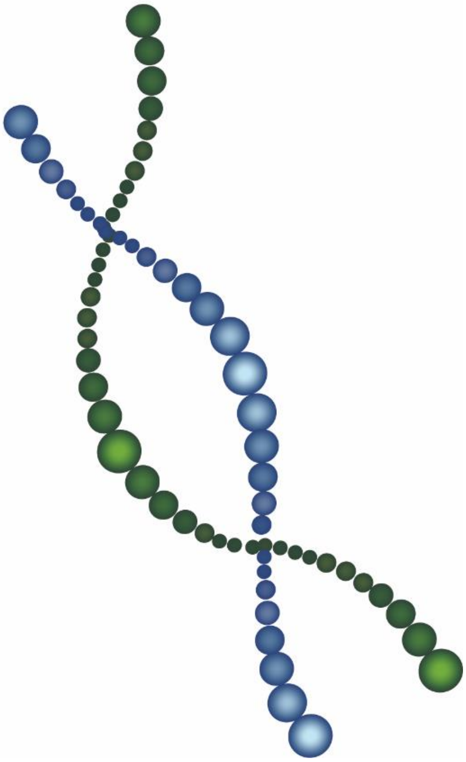

Introduction 1-44

1. *Saccharomyces cerevisiae* as a genetic model 2

2. Genome integrity and DNA repair.......................................4

  2.1 The importance of maintaining genome integrity............4

  2.2. Sources of DNA damage..4

3. DNA repair mechanisms based on the damage 6

  3.1 Excision repair mechanisms..7

    3.1.1 Base excision repair 8

    3.1.2 Nucleotide excision repair.......................................9

    3.1.3 Mismatch repair 9

  3.2 Double-stranded DNA repair mechanisms...................10

    3.2.1 Non-Homologous End Joining 11

    3.2.2 Homologous Recombination.................................11

4. Homologous Recombination...11

  4.1 HR protein core 12

  4.2 DNA resection 13

  4.3 Assembly of Rad51 filament scaffold on ssDNA 15

  4.4 Homology search and strand invasion 16

  4.5 DNA synthesis and ligation 18

5. Non-Homologous End joining 18

  5.1 NHEJ protein core 19

  5.2 End protection and tethering 20

    - 5.3 NHEJ complex assembly, end processing and strand annealing..21
    - 5.4 Ligation and restoration of DNA integrity......................22
- 6. Alternative mechanisms for DSBR.....................................22
    - 6.1 Alternative end-joining pathway 23
    - 6.2 Single-strand annealing..23
- 7. Ku heterodimer complex and DNA repair 24
    - 7.1 Ku structure and evolution...25
    - 7.2 Ku functions 27
        - 7.2.1 Ku and apoptosis...28
        - 7.2.2 Ku and antibody-gene rearrangement 28
        - 7.2.3 Ku and telomere biology 30
        - 7.2.4 Ku and the DNA damage response 32
    - 7.3 Ku in NHEJ..32
- 8. The cell cycle and DNA repair 33
    - 8.1 CDC28 35
    - 8.2 PHO85 36
    - 8.3 Cell cycle checkpoints..37
    - 8.4 DNA repair regulation by the cell cycle.........................40

Objectives 46

Materials and methods 50-84

- 1. Yeast strains, growth conditions and tagging.....................52
    - 1.1 Yeast strains 52

- 1.2 Growth conditions..58
- 1.3 Strains construction and tagging 59

2. Yeast transformation...61

3. Plasmids engineering and DNA cloning.............................61

- 3.1 DNA cloning by homologous recombination.................61
- 3.2 Bacterial transformation 63
- 3.3 Plasmid isolation 63

4. Cell lines and reagents 64

5. Viral cloning and transduction..64

6. Cell synchrony in G1 with α-factor 65

7. Flow cytometry analysis (FACS)..65

- 7.1 Cell-cycle analysis of budding yeast by FACS 65

8.Fluorescence microscopy 66

9. Dot assays...67

10. Cell extract and immunoblot 67

- 10.1 Protein extraction from yeast cells.............................67
- 10.2 Protein extraction from human cell lines.....................68
- 10.3 Western blot 68

11. Recombinant protein purification 70

12. *In vitro* kinase assay 71

13. Yeast genomic DNA isolation and Southern Blot.............72

14. Two-dimensional electrophoresis 74

15. Silencing assay..75

16. DSB plasmid repair assay..76

16.1 NHEJ repair assay 76

16.2 HR repair assay...77

17. NHEJ genomic assay..78

18. HR genomic assay...79

19. NHEJ fidelity assay 80

20. Sensitivity to drugs in asynchronous cultures 81

21. Sensitivity to bleomycin in synchronic cultures 81

23. Statistical analysis 84

Results 86-126

1. Yk80 and the cell cycle 88

2. Yku80 is an *in vitro* substrate of Pcl1-Pho85 88

3. Yku80 bears four consensus sites for CDK phosphorylation 91

4. Yku80 is phosphorylated *in vitro* at Ser623 by Pcl1-Pho8591

5. Yku80 is phosphorylated *in vivo* at Ser623 by Pcl1-Pho85 93

6. The non-phosphorylatable version of Yku80 is viable at 37 degrees..95

7. Protein levels of *yku80*-S623A do not vary compared to the wild-type strain...96

9. Yku80 phosphorylation at Ser623 does not affect transcriptional gene silencing at telomeres and *HML* locus ...98

10. *yku80*-S623A does not present a shortening in telomere length...101

11. *yku80*-S623A shows an increase in NHEJ events 102

12. Repair fidelity is not impaired in *yku80*-S623A...............107

13. Homologous recombination is reduced *in yku80 S623A* mutants 108

14. There are no differences in cell survival rates between *yku80-S623A* and wild-type strains when DNA damage is induced in an asynchronous culture 111

15. *yku80*-S623A shows reduced viability when DNA damage is caused with bleomycin in G2..114

16. Yk80 phosphorylation at the C-terminal domain might be a conserved function..116

17. Overexpression of Ku80^{T629A} increases sensitivity to bleomycin in cancer cell lines 121

Discussion 128-145

1. A cyclin-dependent kinase complex phosphorylates Yku80 130

2. Physiological relevance of Yku80 phosphorylation by Pcl1-Pho85 132

3. An alternative mechanism for DSB repair regulation by the cell cycle machinery..133

  3.1 DNA DSB repair pathway choice 134

  3.2 NHEJ regulation 136

  3.3 Yku80 phosphorylation shifts the balance of the DSB repair towards HR 138

4. Ku regulation might be a conserved function 142

Conclusions...156

Abbreviations 150

Bibliography 164-194

Appendix..196-277

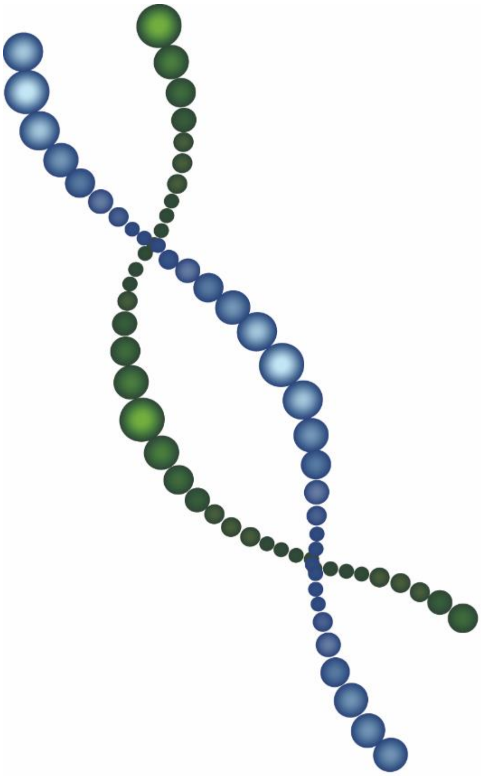

Introduction

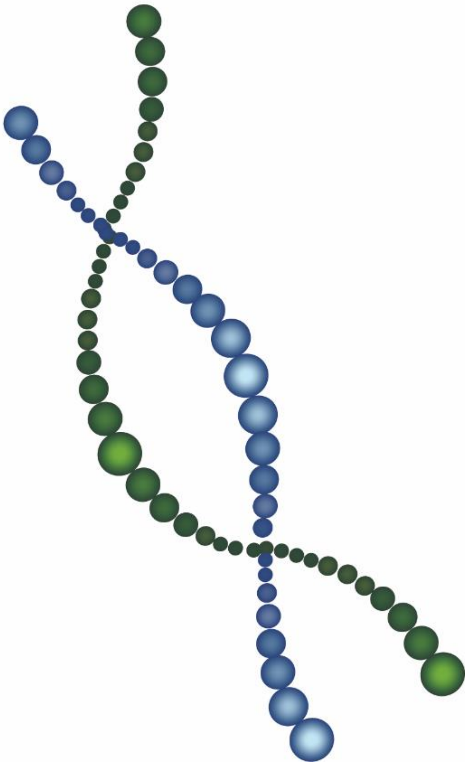

1. *Saccharomyces cerevisiae* as a genetic model

Yeast are eukaryotic microorganisms categorised within the fungi kingdom, where more than 70,000 species have been described. However, high-throughput sequencing techniques have estimated that around 5.1 million fungal species may exist (Blackwell, 2011), proving the high diversity amongst them.

Focusing on yeast cells, they are always unicellular microorganisms with a cell architecture and functional characteristics similar to higher eukaryotes. The main biological processes are also conserved throughout.

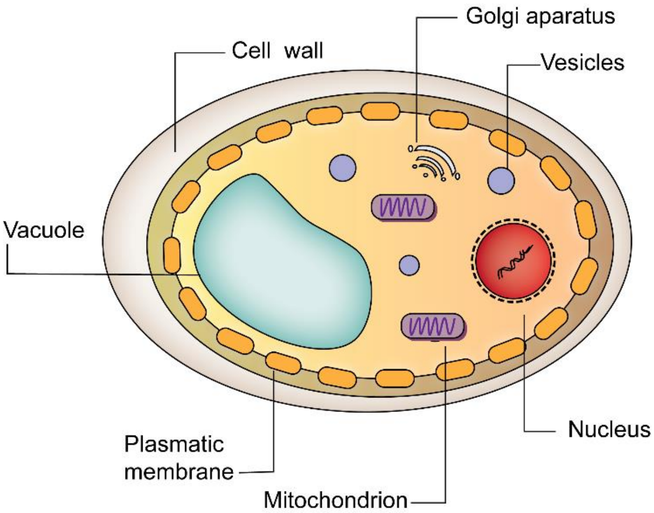

Fig. 1. Schematic diagram of a yeast cell

Some yeast species used mainly for research are *Schizosaccharomyces pombe (S. pombe), Candida albicans (C.albicans), Ashbya gossypii* (*A. gossypii*) and *Saccharomyces cerevisiae (S.cerevisiae).*

Amongst the named species, one of the most popular yeast species used in industry as well as in research laboratories is *Saccharomyces cerevisiae* (*S. cerevisiae*). *S. cerevisiae* was the first eukaryotic organism whose its complete genome was sequenced (16 chromosomes) (Goffeau *et al*. , 1997).

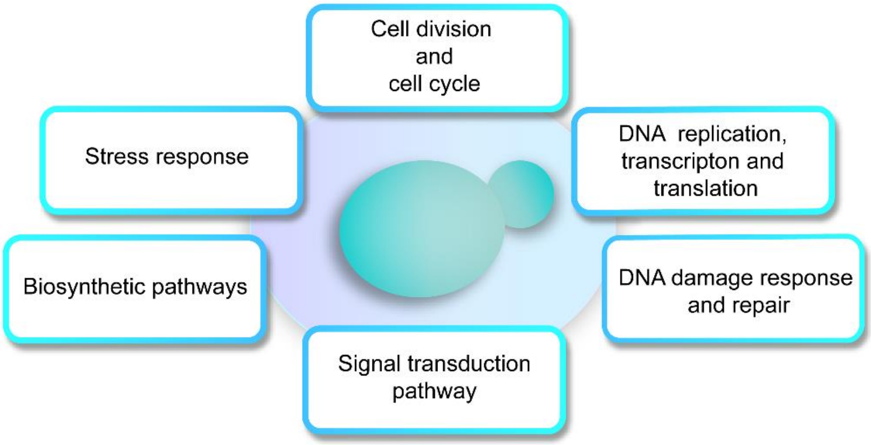
Cell division
and
cell cycle
DNA replication, transcripton and translation
DNA damage response and repair
Signal transduction pathway
Biosynthetic pathways
Stress response

Fig. 2. The main conserved biological processes in yeast.

S. cerevisiae is considered a well-established model organism for all the right reasons: it is a unicellular organism less complex than higher eukaryotes but in which main biological processes such as cell division and cell cycle, DNA replication, recombination and repair and stress response amongst others are conserved. Its genome is smaller than higher eukaryotes and simpler to manipulate. On top of that, yeast can carry drug resistance, auxotrophic markers, and reporter genes, excellent tools for genetic and biochemical studies. Basically, the elegance of yeast genetics and the percentage of homology with higher eukaryotes and the basic cell processes made *S. cerevisiae* a widely recommended model organism for research.

2. Genome integrity and DNA repair

2.1 The importance of maintaining genome integrity

The DNA is the identity of every single organism and preserving its integrity becomes crucial for cell survival and the proper functioning of the cell.

The human genome contains 35,000 genes in approximately three billion base pairs and it is been estimated that a cell can experience up to 10^6 molecular lesions every day (Lindahl and Barnes, 2000). Consequently, cells face genomic instability and so have developed different mechanisms to repair DNA damage.

2.2. Sources of DNA damage

There are several DNA damage agents that can lead to genome instability. The source of this damage can be either endogenous or exogenous. One of the main endogenous sources of DNA damage for the cell is DNA replication. During replication, fork stalling and collapse can occur and as a result, DNA breaks (Branzei and Foiani, 2010). Moreover, the cell can experience the insertion, deletion or mismatch of nucleotides. As endogenous sources of DNA damage, genomic integrity can also be threatened by metabolic bioproducts such as reactive oxygen species (ROS) or reactive nitrogen species (RNS) which can oxidise DNA and generate transversion mutations (De Bont and van Larebeke, 2004).

Probably the most dangerous exogenous factor which induces DNA damage and one to which we are exposed daily is ultraviolet radiation (UV). UV radiation causes pyrimidine dimers and cyclobutene pyrimidine dimers (Yu and Lee, 2017). These modifications result in changes in DNA structure, distorting the DNA double helix. This change of structure has a repercussion in DNA replication and transcription, resulting in DNA mutations or breaks.

The next exogenous DNA damage agent of note is ionising radiation (IR). The energy from this radiation detaches electrons from molecules. Gamma rays and X-rays are classified as IR and both lead to mainly DNA single and double-strand breaks (SSBs and DSBs) (Goodhead, Thacker and Cox, 1993; Dianov, O'Neill and Goodhead, 2001).

Finally, a wide range of drugs can mimic the effect of the DNA agents mentioned above causing induced damage.

4-Nitroquinoline 1-oxide (4-NQO) is considered a UV-mimetic drug. Once 4-NQO is metabolised in the cell, it reacts with the DNA molecule and forms adducts which are responsible for its mutagenicity (Kohda *et al.*, 1991; Arima *et al.*, 2006). Alkylating agents such us methyl-methane sulfonate (MMS) or ethyl-methane sulfonate (EMS) originate nucleobase modifications by adding an alkyl group. Some of the consequences are nucleobases mismatch, blocking of replication machinery and at the time, SSDBs or DSBs.

Finally, hydroxyurea (HU) is another widely used drug which inhibits the ribonucleotide reductase enzyme affecting DNA replication (Singh and Xu, 2016).

4-NQO, MMS and HU are mainly used for research to try and replicate the different damages a cell can undergo on a daily basis.

In addition, there are drugs used as chemotherapeutic treatment for different types of cancer that lead to different DNA lesions with DSBs being the most common. For this reason, they are also assayed in research.

Bleomycin is a chemotherapeutic agent that binds transition metals and oxygen, generating its activated form which interacts with pyrimidine bases causing mainly DSBs (Chen and Stubbe, 2005).

Cross-linking agents like cisplatin when reacting with purine bases cause intra-strand crosslinks and, to a lesser extent inter-strand crosslinks (Basu and Krishnamurthy, 2010). These crosslinks will later interfere with the DNA replication machinery of the cell causing fork stalling and eventually leading to DSBs.

Bearing in mind all the details described above of the different sources and types of DNA damage, it is vitally important for the cells to sense, signal and repair every possible form of DNA damage to avoid compromising cell survival.

If DNA damage is not repaired and accumulates it can cause chromosome fusion, mutations and even loss of physical continuity of the genome which are considered some of the hallmarks of cancer (Hanahan and Weinberg, 2011).

3. DNA repair mechanisms based on the damage

DNA repair mechanisms have evolved to detect and repair every type of damage caused in the molecule. The cell has come up with a variety of mechanisms to repair the damage based on its type and requirements, attempting to avoid any harmful changes in the information stored in the DNA sequence (Fig. 3).

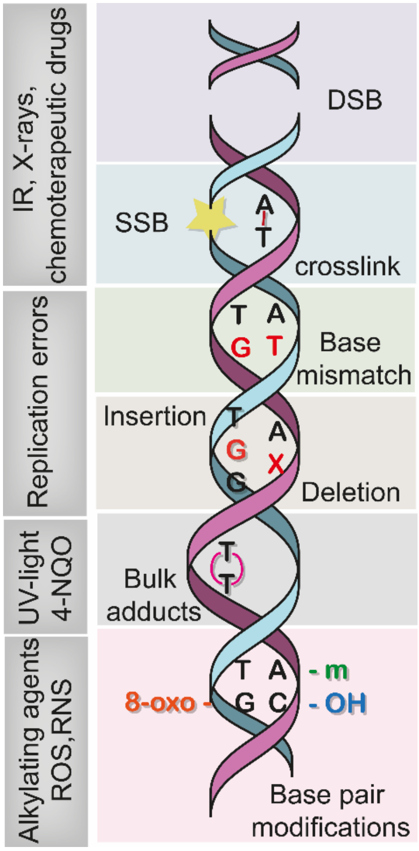
IR, X-rays, chemoterapeutic drugs
Replication errors
UV-light 4-NQO
Alkylating agents ROS,RNS
DSB
SSB
A
T
crosslink
T A
G T
Base mismatch
Insertion
T
G
G
A
X
Deletion
T
T
Bulk adducts
T A
G C
8-oxo -
- m
- OH
Base pair modifications

Fig. 3. Sources of DNA damage and types of DNA lesions.

As previously mentioned, there are different types of DNA damage and even though I will be focusing on DSBs in the following sections, it is worth briefly mentioning all the repair mechanisms intervening in the cell. This is important because DNA repair pathways can be interconnected and the crosstalk between them is crucial to ensure genome integrity.

3.1 Excision repair mechanisms

As I mentioned in the previous sections, there are several toxic metabolites produced by the cell which threaten DNA stability by causing spontaneous damage. Nucleobase oxidation and alkylation are some of the most common consequences of spontaneous damage within the cell and also drug treatment.

The majority of these base modifications are cleared by three excision repair mechanisms: base excision repair (BER), nucleotide excision repair (NER) and mismatch repair (MMR) (Fig.4).

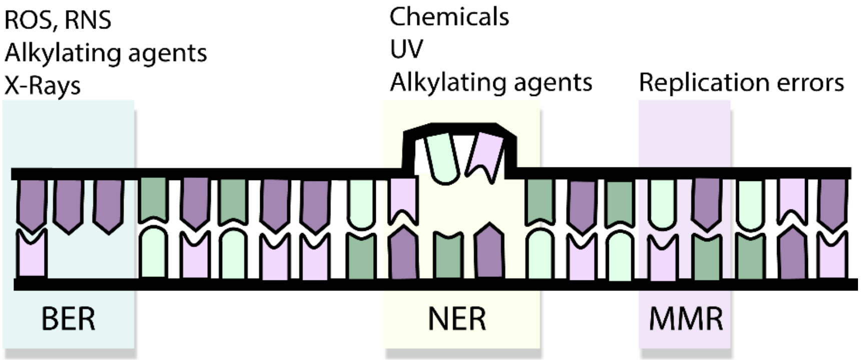

Fig. 4. DNA direct repair mechanisms. Schematic representation of DNA damage sources, the DNA lesions and the DNA direct repair mechanisms that repair the damage: Base Excision Repair (BER), Nucleotide Excision Repair (NR) and Mismatch repair (MMR).

3.1.1 Base excision repair

BER is a process that corrects small DNA lesions that have minorly distorted the DNA helix structure. First, a DNA glycosylase recognises the altered nucleotide and binds selectively to cleave the N-glycosylic bond between the base and the sugar. As a result of the cleavage, an abasic site (AP) is generated and processed straight away by an AP lyase (Eide *et al.*, 1996). An AP endonuclease incises the DNA backbone 5’ leaving a 3’-OH and 5´-deoxyribose-5-phosphate (5’-dRP). Next, the DNA polymerase ε will synthesise the missing nucleotides and Rad27 will remove the 5’-dRP-containing flaps after strand displacement (Wu and Wang, 1999). Finally, Cdc9 ligates the phosphodiester backbone (Wu, Braithwaite and Wang, 1999).

3.1.2 Nucleotide excision repair

NER pathway removes mainly bulky lesions in the DNA caused by environmental sources such as UV radiation and intercalating agents. After the lesion has occurred, DNA damage is recognised by binding factors Rad14, RPA and the Rad4-Rad23 (Guzder *et al.*, 1998). Next, the Transcription Factor IIH (TFIIH) multiprotein complex creates a bubble structure in the helix thanks to its helicase activity (Egly and Coin, 2011). This step is followed by the DNA incision in both sides of the lesion by Rad2 (at 3’-side) and Rad1-Rad10 (at 5’-side) (Habraken *et al.*, 1993; Sung *et al.*, 1993; Tomkinson *et al.*, 1993). This leads to the removal of nucleotides (from approximately 25 to 30 nucleotides) and the subsequent polymerization by pol ε. The final step of the process consists of ligation by Cdc9 (Wu, Braithwaite and Wang, 1999).

3.1.3 Mismatch repair

The mismatch repair pathway is responsible for removing mispaired nucleotides as well as any insertion or deletion that may have occurred during DNA replication and recombination. The MutS complex (Msh2-Msh6 for small insertion/deletion mismatches and Msh2-Msh3 for large insertion/deletion loops) is in charge of recognising the lesions and binding the DNA (Alani *et al.*, 1997; Iaccarino *et al.*, 1998; Marsischky *et al.*, 1999). Upon mismatch recognition, MutS binds to ATP and changes to a conformation with higher affinity for DNA (Hingorani, 2016). The conformational change allows the recruitment of remaining MMR factor such as MutL heterodimer (Mlh1-Pms1) as MutS moves away along the DNA (Gradia *et al.*, 1999). The endonuclease activity of MutL makes a nick in the DNA that is used as an entry point for exonucleases. The excision of the mismatch occurs followed by gap-filling by Polδ (Tran, Gordenin and Resnick, 1999).

3.2 Double-strand DNA repair mechanisms

Double-strand DNA breaks (DSBs) are the most deleterious threat to genome integrity (Malkova and Haber, 2012). DSBs can be induced by several agents as mentioned but can also arise from previous damage not properly repaired (Khan and Ali, 2017). Therefore, the cell has two efficient mechanisms to take care of these types of DNA lesions: Non-Homologous End Joining (NHEJ) and Homologous recombination (HR) (Pannunzio, Watanabe and Lieber, 2018) (Fig. 5).

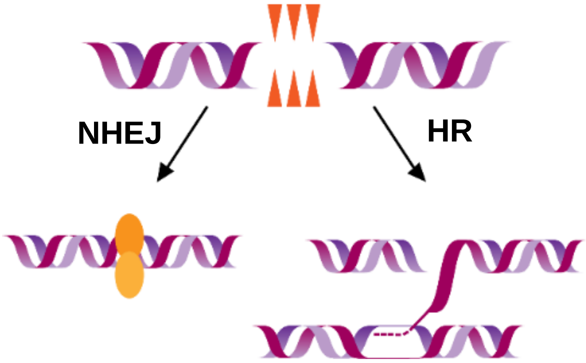

Fig. 5. Mechanisms of DSBs repair. Schematic representation of NHEJ (re-joining of DNA broken ends) and HR (synthesis of the missing information using the homologous strands as a template).

Here I explain the basic concepts of these two mechanisms, though further on I will detail both processes and how they are connected and regulated by the cell cycle.

3.2.1 Non-Homologous End Joining

NHEJ is a process where a set of proteins work together to join and re-ligate the broken DNA ends (Haber and Moore, 1996). It is active throughout the different stages of the cell cycle and is regarded as an error-prone mechanism as it does not use a complementary template to repair the damage (Heidenreich *et al.*, 2003).

3.2.2 Homologous Recombination

HR is a repair mechanism where a homologous DNA sequence is used as a template to repair the missing information (Jasin and Rothstein, 2013; Wright, Shah and Heyer, 2018). HR is considered an error-free mechanism and it takes place only during late S and G2 phases of the cell cycle after DNA is replicated (Aylon, Liefshitz and Kupiec, 2004; Ira *et al.*, 2004).

These two repair pathways are highly conserved in eukaryotes, raising the relevance of these processes as they are crucial to ensuring genomic stability.

4. Homologous Recombination

Homologous recombination is an elegantly orchestrated process designed to achieve DNA repair with high fidelity, ensuring the proper functioning of the cell.

This pathway involves several steps starting with DNA resection, the search for homology followed by DNA strand invasion, synthesis, and DNA ends ligation.

4.1 HR protein core

Yeast proteins involved in HR pathway are listed in table 1 with its correspondent homologue in humans. Of particular relevance is the *RAD52* epistasis group. The genes which belong to this group are: *RAD50, RAD51, RAD52, RAD54, RAD55, RAD57, RAD59, RFA1, MRE11, XRS2 and RDH54* (Pâques and Haber, 1999; Xia *et al.*, 2007). Deletion of these genes or mutations that comprise the function of the proteins leads to a hypersensitivity to IR and various chemical agents (Game and Mortimer, 1974).The proteins encoded by these genes are part of the HR enzymatic core. Especially important are Rad51 and Rad52, two proteins without which HR could not have occurred (Game and Mortimer, 1974; Bai and Symington, 1996; Lim *et al*., 2020).

Table 1: HR proteins

HR role	*S. cerevisiae*	*H. sapiens*
Resection	Sgs1-Top3-Rmi1 Dna2	BLM-TOPOIIIα-RMI1 DNA2
	Mre11-Rad50-Xrs2	MRE11-RAD50-NBS1
	Sae2	CtIP
	Exo1	EXO1
	-	BRCA1

Table 1: HR proteins

HR role	*S. cerevisiae*	*H. sapiens*
Anti-resection	Rad9	53BP1
filament protein	Rad51	RAD51
Positive regulators of filament formation	RPA	RPA
	Rad55-Rad57	RAD51B, RAD51C,RAD51D
		XRCC2, XRCC3
	Rad52	RAD52
	Rad54	RAD54, RAD54B
	-	BRCA1
	-	BRCA2
Negative regulators of filament formation	RPA	RPA
	Srs2	FBH1, PARI
D-loop	Rad54	RAD54, RAD54B
	Sgs1	BLM, RECQ, WRN, RECQ1, RECQ5
	Srs2	FBH1
	Sgs1-Top3-Rmi1	BLM-TOPOIIIα-RMI1
DNA synthesis and annealing	Rad1-Rad10	XFP-ERCC1
	PCNA	PCNA
	RFC	RFC
	Polδ	Polδ
	Rad52, Rad59	RAD52

4.2 DNA resection

The first step required for HR is DNA resection. Unless mentioned otherwise I will be referring to HR proteins from *S. cerevisiae*.

The earliest step in HR is the resection of one of the strands from 5´ to 3´ to produce a terminal 3´OH single-stranded DNA. This process is both complex and flexible.

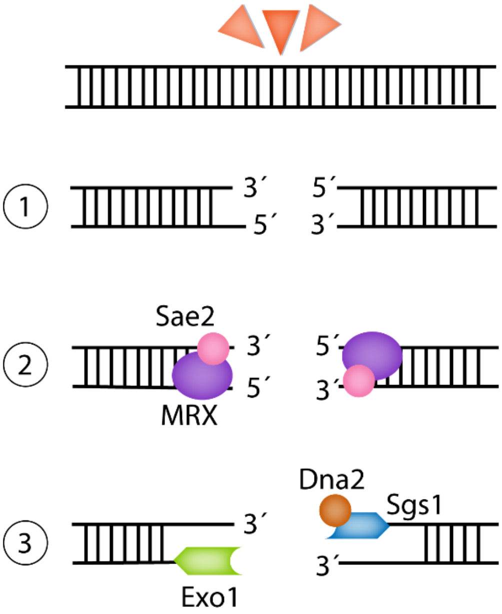

Fig. 6. Mechanisms of DNA resection. Upon DNA damage during S/G2 phases of the cell cycle, MRX recognises DSBs together with Sae2.This complex initiates the resection (2). As a result, ssDNA tails are generated which are a substrate for Dna2-Sgs1 and Exo1 resection (3).

There are two steps to carry out with DNA resection (Mimitou and Symington, 2008). The first one is led by the Mre11-Rad50-Xrs2 (MRX) complex. The MRX complex is responsible for recognising the lesion and initiating resection together with Sae2 (Bressan, Baxter and Petrini, 1999; Lengsfeld *et al.*, 2007) (Fig. 6.2). The endonucleolytic activity of MRX-Sae2 will make an incision to release the 5´ending allowing the 3´OH to be accessible (Paull and Gellert, 1998; Budd and Campbell, 2009). Next, the short 3’-ssDNA tails undergo extensive resection. Long-range resection is carried out by two parallel pathways (Mimitou and Symington, 2008): the first one depends on Exo1 whereas the other is dependent on the Sgs1-Top3-Rmi1 complex with the help of Dna2 nuclease (Bae *et al.*, 1998; Zhu *et al.*, 2008; Budd and Campbell, 2009) (Fig. 6.3).

4.3 Assembly of Rad51 filament scaffold on ssDNA

The single-strand DNA ends generated are susceptible to exonucleases and can form secondary structures that will not allow the continuation of the following steps of HR pathway. The Replication Protein A (RPA) will bind strongly to ssDNA to protect the ssDNA tails (Chen and Wold, 2014) (Fig. 7). However, RPA binding to ssDNA inhibits strand invasion as Rad51 is unable to access and bind the resected DNA ends (Ma *et al.*, 2017). A competition ensues between Rad51 and RPA to join ssDNA. RPA is necessary for removing secondary structures from ssDNA so Rad51 can bind efficiently and extend the filaments (Ma *et al.*, 2017).

To assemble Rad51 on ssDNA, Rad52 will mediate RPA displacement. Rad52 has a high affinity for ssDNA and once ssDNA has wrapped around it, RPA-ssDNA interaction becomes weak and unstable (Sugiyama and Kowalczykowski, 2002; Sugiyama and Kantake, 2009).

This way, Rad52 is promoting the physical interaction between Rad51 recombinase and ssDNA (Sung, 1997; New *et al.*, 1998; Shinohara and Ogawa, 1998).

In humans, the RAD52 role is not completely conserved and there is another complex taking care of RPA displacement. Studies have suggested that the complex BRCA2-DSS1 is critical for RAD51 filament formation (Jensen, Carreira and Kowalczykowski, 2010; Thorslund *et al.*, 2010; Liu *et al.*, 2011). Finally, once Rad51 has bound to ssDNA it starts polymerising on the ssDNA to form a helical nucleoprotein filament and it extends along the DNA (Ogawa *et al.*, 1993; Sung, 1997) (Fig. 7). This structure is named the pre-synaptic complex.

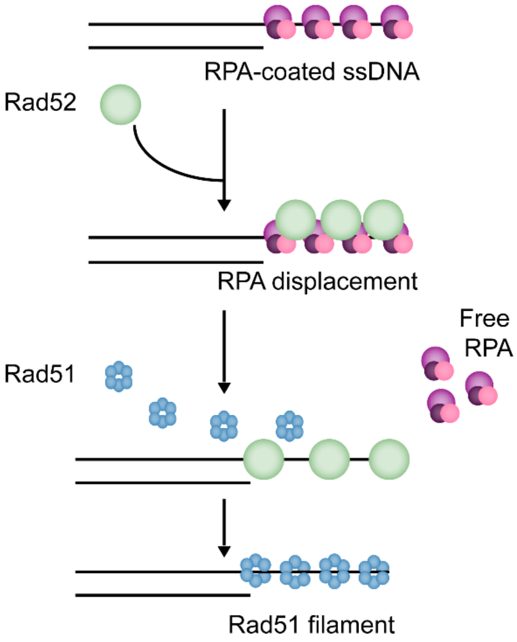

Fig. 7. Rad51 filament formation. After resection, ssDNA tails are recognised and coated by RPA which avoids the formation of secondary structures and further resection. RPA will later be displaced by Rad52 which will promote Rad51 interaction with the DNA allowing Rad51 to further extend the filament.

4.4 Homology search and strand invasion

Up to this point DNA has been resected and Rad51 has extended the filaments, forming a scaffold on ssDNA. Now the pre-synaptic complex searches for homology to initiate DNA synthesis. The pre-synaptic complex has the characteristic to bind transiently as microhomologies of few nucleotides can lead to rapid Rad51 filament extension (Lee *et al.*, 2015; Paoletti *et al.*, 2020). If the sequence is not a match, the pre-synaptic complex can turn over quickly thanks to the transient bond (Liu *et al.*, 2011). During pre-synapsis, Rad54 will help to make Rad51 filaments stable (Ceballos and Heyer, 2011; Renkawitz *et al.*, 2013) (Fig. 8).

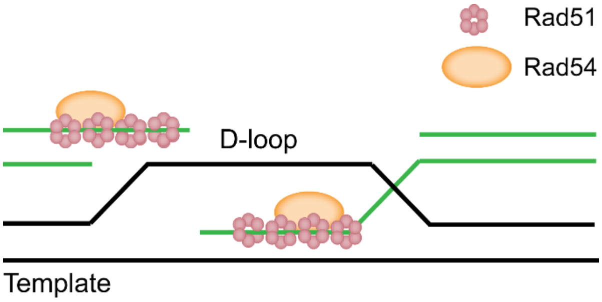

Fig. 8. Schematic representation of the synaptic complex. Rad51 acts together with Rad54 in the search for homology and strand invasion. Once they have found the homology sequence the D-loop is formed. Altogether this leads to the assembly of the synaptic complex to finally perform DNA synthesis and ligation of the two ends.

Once the homologous sequence has been identified, the pre-synaptic complex interacts with the DNA leading to the synaptic complex assemblage (Petukhova *et al.*, 1999). The next step consists of the strand invasion by the 3´-end of the synaptic complex. As a result of the 3´-end joint with its complement, the displacement loop or D-loop is formed (Petukhova, Sung and Klein, 2000; Wright and Heyer, 2014). Rad54 helicase activity has been proposed to have a role during the synapsis, helping Rad51 during strand invasion by disrupting the nucleobases of the donor sequence (Petukhova *et al.*, 1999).

4.5 DNA synthesis and ligation

The D-loop formed after alignment of the 3´-end with its complementary sequence now contains heteroduplex DNA (hDNA) ready for elongation. *In vitro* studies have pointed out Polδ as the polymerase in charge of DNA synthesis (Sebesta *et al.*, 2011). Nevertheless, Pol δ by itself is unable to extend the D-loop and needs the assistance of PCNA and RFC-1 (Li *et al.*, 2009). Pol δ DNA synthesis will be extended to the point that there is enough sequence homology to anneal the new synthesised DNA with the second resected DNA end. Srs2, Mph1 and Sgs1-Top3-Rmi1 are ssDNA translocases that will disrupt the D-loop by dissociation of the Rad51 filaments from DNA (Krejci *et al.*, 2003; Fasching *et al.*, 2015; Piazza *et al.*, 2019). Finally, the DNA is ligated, and DNA integrity is restored.

5. Non-Homologous End joining

In 1996 Moore and Haber used the term non-homologous end joining to describe a process where DSBs are repaired by the re-joining of the two strands without the need of a homologous donor. NHEJ repair mechanism is an iterative process and even though there is an extensive number of studies which help to understand the several steps of the mechanisms, it is not strictly ordered. DNA processing will depend on the type of DNA damage incurred and therefore the recruitment of the core factors may vary. However, three main stages have been proposed. First, end protection and tethering, followed by NHEJ complex assembly, then finally ligation and complex disassembly (Emerson and Bertuch, 2016).

In this section, I will be describing the three main stages of the process and the proteins involved in each of them. As in HR, I will be referring to *S. cerevisiae* NHEJ proteins but for human's homologues see table 2.

5.1 NHEJ protein core

There are several proteins playing a role in the different steps of the NHEJ pathway, the Yku heterodimer comprising Yku70 and Yku80; and the MRX complex as a synaptic factor. To carry out end-processing there is Pol4 which needs to interact with DNA ligase IV that is part of the complex in charge of re-ligating the DNA ends. The ligations factors are DNA ligase IV (Dnl4) and Lif1. Both proteins form a complex where Lif1's role is stabilising DNA ligase IV.

Table 2: NHEJ proteins

NHEJ role	*S. cerevisiae*	*H. sapiens*
End protection and tethering	Yku70/80 - Mre11-Rad50-Xrs2	Ku70/80 DNA-PK MRE11-RAD50-NBS1
Strand annealing	Pol4	Pol µ, Pol λ

Table 2: NHEJ proteins

NHEJ role	*S. cerevisiae*	*H. sapiens*
Ligation	Lig4/Lif1	DNA ligase IV, XRCC4
Other regulation factors	Rad27 Nej1	Fen-1 -

5.2 End protection and tethering

Upon DSBs, the Yku heterodimer recognises and binds the broken ends (Griffith *et al.*, 1992; Getts and Stamato, 1994). The binding of Yku will protect the strands from exonucleases (Mimitou and Symington, 2010) and at the same time, it serves as a signal for the rest of the NHEJ machinery to come (Rathmell and Chu, 1994). The MRX complex is consequently recruited to the DSB (Zhang *et al.*, 2007; Wu, Topper and Wilson, 2008). The function of MRX is to tether the DNA ends(De Jager *et al.*, 2001; Hopfner *et al.*, 2002). Basically, MRX together with Yku heterodimer helps to keep DNA ends in proximity and stable (Hartlerode *et al.*, 2015).

In humans, Ku heterodimer physically interacts with DNA-PK catalytic subunit through the C-terminal domain of Ku80 subunit (Spagnolo *et al.*, 2006; Rivera-Calzada *et al.*, 2007; Hammel *et al.*, 2010). Together, the Ku heterodimer and DNA-PK catalytic subunit form the DNA-PK complex and both proteins will be in charge of keeping DNA ends protected and stabilised (Hammel *et al.*, 2010). In yeast, there is not a homologue for DNA-PK.

5.3 NHEJ complex assembly, end processing and strand annealing

Yku heterodimer act as a scaffold to recruit the DNA ligase IV-Lif1 complex (Herrmann, Lindahl and Schär, 1998; Nick McElhinny *et al.*, 2000). In addition, MRX also promotes NHEJ complex formation as it interacts with Dnl4-Lif (Palmbos *et al.*, 2008).

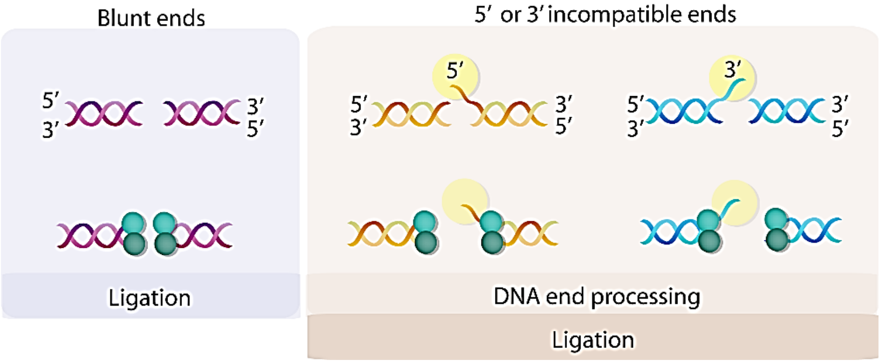

Fig. 9. Various double strand breaks in DNA and NHEJ pathway.

As mentioned above, NHEJ can be a flexible pathway which adapts depending on the processing required to successfully re-join the broken DNA ends. Blunt ends do not need any resection whilst incompatible 5´and 3´-overhangs demand Rad27 nuclease activity (Wu, Wilson and Lieber, 1999) and nucleotide synthesis by Pol4 (Fig. 9). Rad27 physically interacts with the ligase complex and Pol4 (Tseng and Tomkinson, 2002). This interaction ensures the proper processing and optimal filling during DNA repair in NHEJ (Tseng and Tomkinson, 2004). It is important to point out that DNA resection by nucleases in NHEJ are necessary to expose small regions of microhomology, and it differs from the extensive DNA resection required to initiate HR pathway.

5.4 Ligation and restoration of DNA integrity

After DSBs have been processed and DNA ends are compatible, Dnl4 ligates the strands (Tseng and Tomkinson, 2002; Mari *et al.*, 2006). How the core complex disassembles remains unknown. In mammals, Ku80 is removed from DNA by ubiquitin-mediated degradation (Feng and Chen, 2012) but there has not been described a similar mechanism in yeast yet.

complex is disassembled.

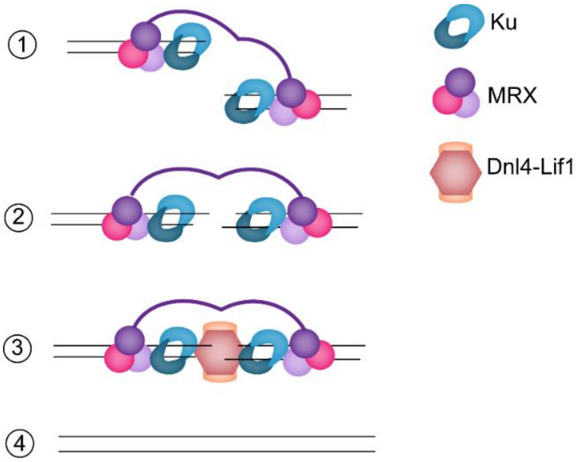

Fig. 10. Sequence of events during NHEJ. Upon DNA damage, Ku70/80 and MRX bind to the DNA ends to protect them and keep them in proximity (1-2). Next, Dnl4-Lif1 complex can recognise the DSB and bind DNA. If the DNA ends are compatible, the complex will proceed to ligate both strands (3). After the ligation reaction the genome integrity is restore and the NHEJ

6. Alternative mechanisms for DSBR

NHEJ and HR are the mechanisms the cell preferably uses to repair DSBs. However, auxiliary pathways exist in case NHEJ, HR or both mechanisms are compromised: alternative-End Joining (a-EJ), Single-Strand Annealing (SSA) and Theta-Mediated End Joining (TMEJ). I will briefly explain these pathways the cell uses to safeguard cell integrity at all cost.

6.1 Alternative end-joining pathway

Boulton and Jackson first described the existence of an alternative DNA end-joining pathway about 20-fold less efficient than NHEJ (Boulton and Jackson, 1996). Even though it is named as a-EJ, this pathway does not rely on the Yku heterodimer and has more in common with SSA than it does with NHEJ. In fact, the loss of the Ku heterodimer increases a-EJ (Ma *et al.*, 2003).

The a-EJ requires a 2-16bp microhomology (Boulton and Jackson, 1996) between the strands, therefore nuclease activities are needed. Nucleolytic processing is initiated by MRX complex and Sae2 to reveal microhomology (Ma *et al.*, 2003; Xie, Kwok and Scully, 2009; Truong *et al.*, 2013). Next, the DNA is subjected to synthesis by Pol 4 or Pol δ. Finally, a-EJ is complete by the ligation of the DNA ends by Dnl4 (Sfeir and Symington, 2015).

6.2 Single-strand annealing

SSA is a Rad52-dependent pathway (Bennardo *et al.*, 2008) that requires resection to reveal the flanking homologous sequence. Whilst NHEJ uses 2-4 bp of microhomology, SSA uses up to 30bp microhomology between both strands (Sugawara, Ira and Haber, 2000). MRX plays a role in SSA pathway initiating resection to generate 3´ ssDNA tails (Ivanov *et al.*, 1996). Next, Sae2 and probably Exo1 will extend resection. Unlike a-EJ, Rad52 binds the resected ssDNA (Ivanov *et al.*, 1996; Tutt *et al.*, 2001) and anneals complementary strands, however, Rad51 is not recruited (Ivanov *et al.*, 1996; Kang and Symington, 2000; Tutt *et al.*, 2001). As this process is Rad51-independent it is considered error-prone and can generate deletions and translocations. The final step is ligation unless there is an unannealed 3´-5´ ssDNA, requiring nucleotide excision (Bhargava, Onyango and Stark, 2016).

6.3 Polymerase Theta-Mediated End Joining

Polymerase Theta-Mediated End Joining (TMEJ) has been recently described as an alternative mechanism for DSBR in higher eukaryotes (Chan, Yu and McVey, 2010; van Schendel *et al.*, 2016; Schimmel *et al.*, 2019). Briefly, this pathway is promoted by Polymerase Thetha (Polθ) and functions independently of HR and NHEJ. It requires short sequence identities in flanking DNA. The annealing at the microhomologous sequence is followed by Polθ-polymerase-mediated ssDNA extension. As a result, small insertions and deletions can occur which are considered hallmarks of TMEJ (Chan, Yu and McVey, 2010; Black *et al.*, 2019; Schimmel *et al.*, 2019).

7. Ku heterodimer complex and DNA repair

The Ku heterodimer composed of Ku70 and Ku80 subunits was identified as an autoantigen in patients with polymyositis-scleroderma overlap syndrome, a rare inflammatory disease (Mimori *et al.*, 1981). In the following sections, I will focus on Ku structure, functions and more specifically in its role during NHEJ.

7.1 Ku structure and evolution

Ku is a highly conserved heterodimer comprised of two subunits: Ku70 and Ku80 (also referred to as Yku70 and Yku80 in *S. cerevisiae*) and it is one of the most abundant DNA end-binding proteins in the cell. Even though the Ku family of proteins are highly conserved through evolution, they are poorly conserved in terms of the amino acids sequence. Despite this, at the secondary level, conserved blocks of domains can be identified through different organisms (Aravind and Koonin, 2001). Each Ku subunit is made up of three domains: the N-terminal domain consisting of a von Willebrand A domain, a DNA binding central core and a diverged C-terminal region (Fig. 11).

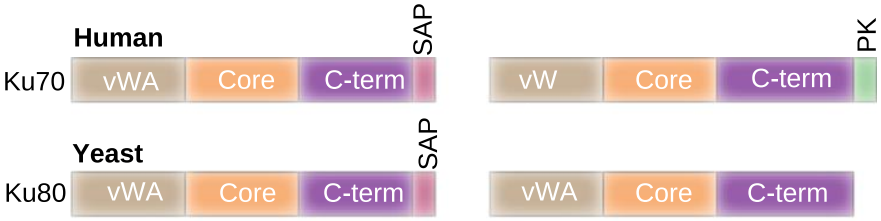

Fig. 11. Domain organization of the human and yeast Ku heterodimer. There are three well differentiated structural domains in Ku proteins: an amino-terminal von Willebrand A domain (vWA), a central DNA-binding core (Core) and a divergent carboxy-terminal domain (C-term). In both Ku70, human and yeast, the C-terminal domain contains a SAP (SAF-A/B, Acinus and Pias) domain. Human Ku80 has a DNA-PK (PK) domain absent in yeast.

The N-terminal domain contributes as a surface for protein-protein interaction (Fell and Schild-Poulter, 2012). The Ku central core domain is important for the dimerization of both subunits and DNA binding.

Ku70 and Ku80 have a helical C-terminal domain. However, it is the most divergent part of both subunits. Ku70 C-terminal region has a SAP (SAF-A/B, Acinus and Pias) domain considered to mediate protein interaction (Schild-Poulter *et al.*, 2001) and Ku80 has a longer C-terminal domain with a disordered region. Exclusively in higher eukaryotes, Ku80 contains a region to interact with DNA-PK. In lower eukaryotes the three differentiated domain organisation remains, but there is not a DNA-PK interaction motif in the sequence. Within vertebrates Ku associates with DNA-PK to phosphorylate targets involved in DNA repair, though lower eukaryotes may use other kinases. However, it has not been reported yet that a CDK-Ku80 interaction occurs *in vivo*.

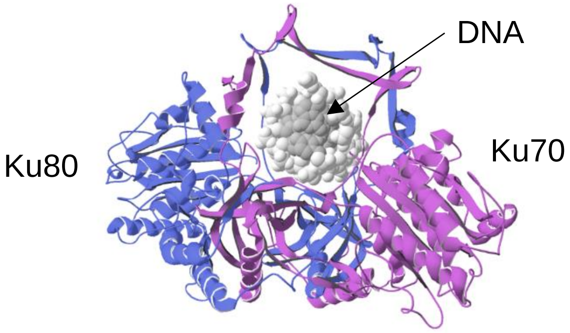

Fig. 12. Structure of Ku-DNA complex. Downward view of the DNA helix (image adapted from Walker, J.K et al 2001). Ku70 is coloured in purple and Ku80 blue. DNA is coloured in grey.

The three-dimensional structure of Ku heterodimer was described by Walker, J.K et al in 2001. The crystal structure showed that Ku70 and Ku80 form an asymmetric ring where the channel comprised of intertwined strands of both subunits accommodates the DNA (Fig. 12). The negatively charged residues from the sugar phosphate backbone of DNA interact with the positively charged channel of Ku’s ring (Walker, Corpina and Goldberg, 2001). It was also observed that the heterodimer does not change conformation upon DNA-binding, which is consistent with the high stability of the heterodimer (Walker, Corpina and Goldberg, 2001).

7.2 Ku functions

Ku heterodimer binds double-stranded DNA in a sequence-independent manner. It is been reported that Ku70/80 can bind several DNA structures (Arosio *et al.*, 2002). The Ku70-Ku80 heterodimer can bind to double-stranded ends with either 3´ or 5´overhangs, blunt ends and double-stranded ends produced by ionizing radiation. It has also been reported that Ku can bind different DNA structures such as nicks, gaps and bubbles in circular double-stranded DNA (Mimori and Hardin, 1986; Griffith *et al.*, 1992; Blier *et al.*, 1993).

Ku participates in many processes thanks to its ability to bind dsDNA through the central ring formed by the interaction of both subunits (Fig. 13). Essentially, Ku function in the different processes where it intervenes is mechanistically related to its role as a DNA-binding factor.

Now, I will briefly introduce Ku´s role in all the processes it participates in. An exclusive section will be dedicated to Ku´s function in NHEJ pathway.

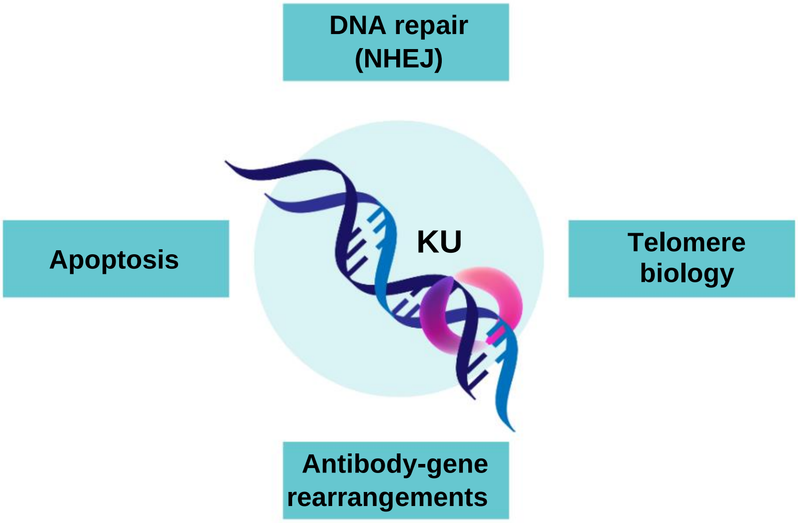

Fig. 13. Ku cellular functions. Ku heterodimer is a protein that´s main characteristic is being able to bind double-stranded DNA with high affinity. Due to its ability to bind DNA, Ku intervenes in all the cellular processes mentioned in the figure.

7.2.1 Ku and apoptosis

Ku localisation is mainly nuclear, however; some studies have nonetheless shown Ku to have a cytosolic localisation during its role in apoptosis (Morio *et al.*, 1999; Sawada *et al.*, 2003). It has been described as a physical interaction between Ku70 subunit and the pro-apoptotic protein BAX. Ku binds BAX inhibiting its re-localization to the mitochondria (Sawada *et al.*, 2003). Ku prevents apoptosis by direct binding to BAX.

7.2.2 Ku and antibody-gene rearrangement

Mammalian cells use a process denominated inmunoglobuline-gene rearrangement to generate diversity among B and T lymphocytes allowing the recognition of a wide variety of antigens. This process, also known as V(D)J recombination (Malu *et al.*, 2012), requires DNA cleavage and repair. Ku has been identified as one of the proteins intervening in the process (Nussenzweig *et al.*, 1996; Zhu *et al.*, 1996).

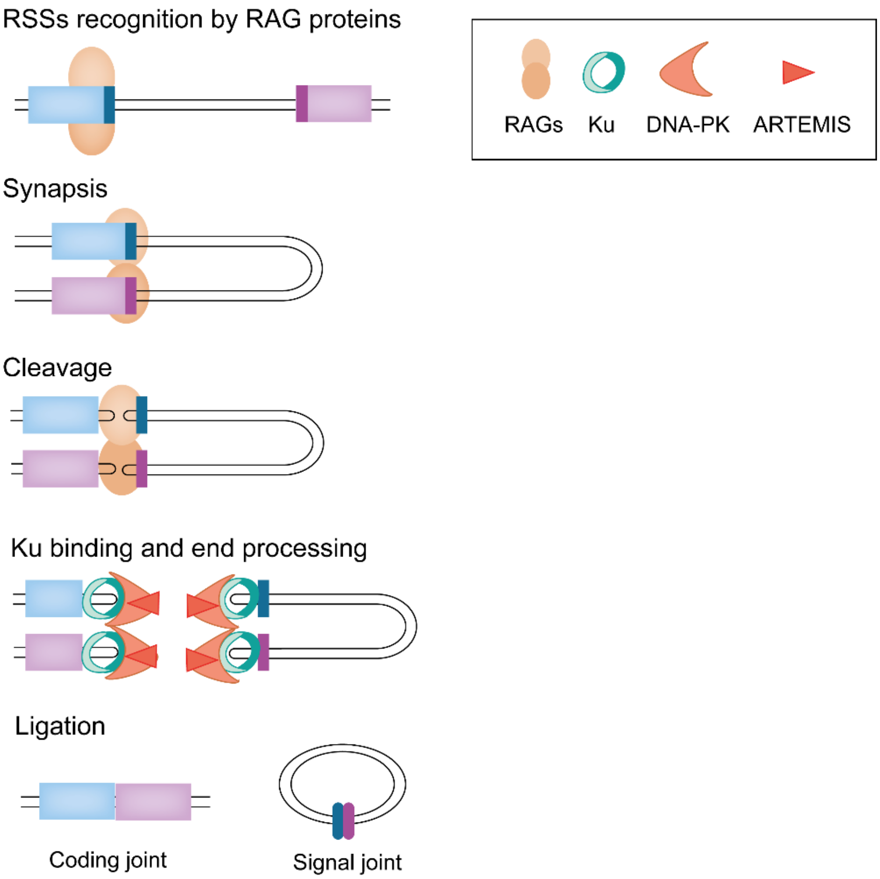
RSSs recognition by RAG proteins
Synapsis
Cleavage
Ku binding and end processing
Ligation
Coding joint
Signal joint
RAGs
Ku
DNA-PK
ARTEMIS

Fig. 14. The V(D)J recombination reaction. RAGs proteins recognise the RSS sequence and initiate the synapsis to snip the DNA. Blunt ends and hairpin coding ends are produced after excision. Ku binds the DNA ends and recruits DNA-PK and the ARTEMIS complex. The active complex cooperates to process DNA ends to form the coding joint and the signal joint.

First, RAG1 and RAG2 (Recombination Active Genes 1 and 2), recognise the conserved recombination signal sequences (RSSs) located between the V, D and J segments and introduce a pair of

DSBs (McBlane *et al.*, 1995; Difilippantonio *et al.*, 1996). A DNA hairpin is thus generated with blunt ends. Ku binds to a hairpin structure and blunt-ended DNA after DNA cleavage by RAGs. Ku also recruits DNA-PK catalytic subunit which bridges the coding ends. Additionally, DNA-PK recruits and activates the ARTEMIS complex.

Upon ARTEMIS COMPLEX phosphorylation by the DNA-PK subunit, the nucleolytic activity of the ARTEMIS complex is activated for hairpin opening and DNA ends processing (Mansilla-Soto and Cortes, 2003; Rooney *et al.*, 2003). The final step requires the action of the DNA-ligase-IV-XRCC4 to ligate the broken DNA ends (Modesti, Hesse and Gellert, 1999; Soulas-Sprauel *et al.*, 2007). The products of the V(D)J recombination are the coding joint; which constitutes the rearranged variable regions of the receptors, and the signals joint; circular molecules that do not have an immune function.

7.2.3 Ku and telomere biology

Telomeres are big nucleoprotein complexes located at the end of linear chromosomes. These structures preserve genome integrity by preventing chromosome fusions, aberrations, and inappropriate activation of the DNA damage response. Ku heterodimer has been shown to play a role in telomere maintenance (Gravel *et al.*, 1998). Ku binds to telomeres to keep their length and protect them from resection and DNA repair mechanisms (Gravel *et al.*, 1998). In *S. cerevisiae* it has been demonstrated that the thermo-sensitivity observed in *yku80Δ* and *yku70Δ* cells was the result of extensive telomeric shortening

(Gravel *et al.*, 1998; Maringele and Lydall, 2002). In humans, Ku heterodimer has an essential role in preventing telomere fusion and loss (Samper *et al.*, 2000; Wang, Ghosh and Hendrickson, 2009). Even though Ku is part of the NHEJ pathway, when binding to the end of telomeres it does not necessarily lead to recruitment of NHEJ machinery to repair the dsDNA. A study showed that Dnl4 deletion, one of the core components of the NHEJ machinery, does not affect either telomere structure or maintenance (Teo and Jackson, 1997), as opposed to how it was described when deleting Ku (Gravel *et al.*, 1998; Maringele and Lydall, 2002).

It has been hypothesised that Ku interaction with telomerase-associated proteins might be contributing to Ku’s ability to differentiate chromosome ends from dsDNA breaks (Gravel *et al.*, 1998). Supporting this hypothesis, Gottschling’s lab described an interaction between Ku80 subunit and the yeast telomerase TLC1 in a 48-nucleotide region required for telomere length regulation (Peterson *et al.*, 2001; Stellwagen *et al.*, 2003). To further support the two-face model of Ku function in DNA repair and telomere maintenance, Bertuch’s lab demonstrated that different phenotypes are observed depending on which Ku subunit and domain are mutated regarding telomere biology or DNA repair (Ribes-Zamora *et al.*, 2007).

In addition to its role as a telomere protector, Ku helps to localise telomeres to the nuclear periphery (Hediger, Dubrana and Gasser, 2002). This leads to the stabilisation and proper localisation of the silent information regulator protein (Sir) resulting in gene silencing and thereby repressing gene transcription (Laroche *et al.*, 1998; Nugent *et al.*, 1998). This occurs thanks to the phenomenon of telomere position silencing also known as TPE. Both Sir and Ku heterodimer are essential in TPE, a process in which genes that are located near the telomere are silenced and so cannot be transcribed. Mutations in Ku80 abrogate telomere silencing (Lopez *et al.*, 2011) and affects the nuclear organization of telomeres (Laroche *et al.*, 1998).

7.2.4 Ku and the DNA damage response

Upon DSB formation, DNA damage sensors Mec1 and Tel1 (ATM and ATR in mammals) promote the activation of cell cycle checkpoints and cell cycle arrest (Longhese, Mantiero and Clerici, 2006). Mec1 and Tel1 are serine/threonine kinases that transduce the DSB alarm, initiating a phosphorylation cascade that results in the modulation of several cellular processes (Banin *et al.*, 1998; Bakkenist and Kastan, 2003). Several studies have shown that Ku prevents the activation of Mec1 and Tel1 (Wang *et al.*, 2002; Iliakis *et al.*, 2003; Corda *et al.*, 2005; Clerici *et al.*, 2008). These results suggested a dual role of Ku as a signal molecule, first promoting repair by NHEJ and relaying signals to the DNA damage response sensors.

7.3 Ku in NHEJ

Ku’s main attribute is to bind dsDNA in a sequence-independent manner. As a result, Ku facilitates the repair of double-stranded broken DNA ends by the NHEJ pathway. Ku´s ability to bind DSBs, allows the heterodimer to have several roles during NHEJ.

First, Ku70/80 recognises the DNA lesion and binds the broken DNA ends. As a result of the binding, it facilitates the second role of KU; protection of overhangs from unwanted or extensive resection. This is important because HR is only active during G2. In fact, when deleting Ku heterodimer in *S. cerevisiae* there is an approximately 2-fold increase in DNA resection (Lee *et al.*, 1998). The third function of Ku heterodimer is to work as a recruitment platform for the rest of the NHEJ machinery. Interaction with MRX ensures that dsDNA ends are stable, and it prevents them drifting apart. Ku will also interact with Dnl4-Lif1, the ligation complex (Nick McElhinny *et al.*, 2000; Mari *et al.*, 2006).

Finally, Ku intervenes in the DNA damage response. Ku DNA recognition and binding prevent cell-cycle checkpoint activation. $Ku80^{-}/^{-}$ cells display a stronger DNA damage response by the two main cell-cycle checkpoints (at S and G2) compared to the wild-type cells (Wang *et al.*, 2002; Zhou *et al.*, 2002).

Lastly, it is worth noting that the different Ku roles described are not mutually exclusive, the cell integrates them all to ensure DNA is repaired successfully.

8. The cell cycle and DNA repair

The cell cycle integrates a group of events whose main function is to replicate the DNA accurately and segregate the copies in two genetically identical daughter cells. It is comprised of four phases: G1, S, G2 and M.

In G1 the cells prepare themselves for DNA duplication. This stage is characterised by cell growth and organisation of structures required for the following phase. During the S phase the genetic information is duplicated and in G2 cells prepare for chromosome segregation. Finally, the M phase consists of cell division.

The relevance of this process makes it a target for extensive regulation. There are several cell division control genes that participate in the regulation of the cell cycle. The progression of the cell through the different phases of the cell cycle is driven by a group of proteins denominated cyclin-dependent-kinases (CDKs). As their name implies, these proteins are regulated by cyclins, proteins that have an oscillatory expression during the different phases of the cell cycle. Together, they form CDK-cyclin complexes which are in charge of controlling the cell cycle. In *S. cerevisiae*, there are two CDKs involved in cell cycle progression: Cdc28 (*CDK1*), and Pho85 (Toh-e *et al.*, 1988) and they will be detailed in the following sections.

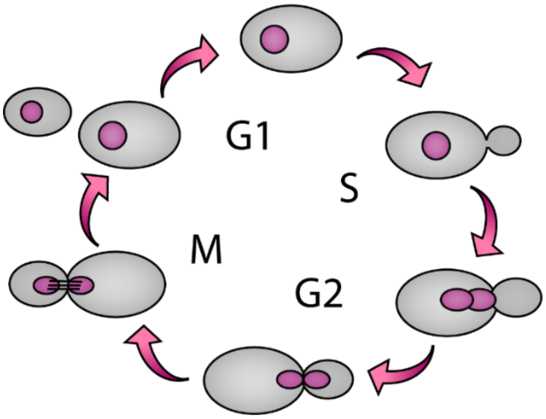

Fig. 15. Schematic representation of the yeast cell cycle. Representation of yeast cell morphology in the different stages of the cell cycle: G1, S, G2 and Mitosis (M)

8.1 CDC28

The CDK Cdc28 was identified as the first central coordinator of the yeast cell cycle thanks to a conditional mutant that arrested cell cycle progression at START (Hartwell *et al.*, 1973; Nurse, Thuriaux and Nasmyth, 1976). Cdc28 activity and specificity are controlled by the interaction with several cyclins and inhibitors at different cell cycle stages.

Cdc28 cyclins are classified into two different groups: G1 cyclins and B-type cyclins. Cln1, Cln2 and Cln3 belong to the G1 cycling group and they are necessary for G1 to S phase transition (Hadwiger *et al.*, 1989; Wittenberg, Sugimoto and Reed, 1990; Uhlmann, Bouchoux and López-Avilés, 2011; Bállega *et al.*, 2018). The B-type cyclins are Clb1, Clb2, Clb3, Clb4, Clb5 and Clb6 and they are necessary for DNA replication, progression through the G2 phase and mitosis. As mentioned, all these cyclins have a cyclic expression throughout the cell cycle where they will be synthesised and eliminated (Mendenhall and Hodge, 1998; Uhlmann, Bouchoux and López-Avilés, 2011 for an extensive review).

Cln1 and Cln2 bind Cdc28 at START (Levine, Oehlen and Cross, 1998). Deletion of both CLN1 and CLN2 leads to a slower growth of the cell and delay of DNA synthesis (Dirick, Böhm and Nasmyth, 1995). Cln3 expression does not oscillate along the cell cycle and it is required for activation of G1 cyclins (Tyers, Tokiwa and Futcher, 1993).

B-type cyclins can be divided into three different categories based on their sequence homology and transcriptional pattern. Clb5 and Clb6 are synthesised at START together with Cln1 and

Cln2 but, they are inhibited by Sic1 until the end of G1 (Schwob and Nasmyth, 1993). Their function is the initiation of the S phase by phosphorylation of the components necessary for DNA replication. Clb3 and Clb4 show up at S phase and contribute to DNA replication and mitotic spindle formation (Richardson *et al.*, 1993). Finally, Clb1 and Clb2 play a role during mitosis promoting the isotropic growth of the bud and chromosome separation (Irniger and Nasmyth, 1997).

8.2 PHO85

Pho85 is a multifunctional CDK which not only has a role in G1 progression in the cell cycle but also intervenes in glycogen and phosphate metabolism as well as in signalling environmental changes (Carroll and O’Shea, 2002). Despite all these functions and in normal laboratory conditions, Pho85 is not essential for cell viability (Measday *et al.*, 1997).

Pho85 is associated with 10 cyclins named after Pcls (Pho85 Cyclins) (Mendenhall and Hodge, 1998) and they are categorized into two different groups based on their sequence homology (Malumbres, 2014).

The first group is comprised of Pcl8, Pcl10, Pho80, Pcl6 and Pcl7 and they are necessary for glycogen and phosphate metabolism and signalling of environmental changes (Measday *et al.*, 1997). The remaining cyclins, Pcl1, Pcl2, Pcl9, Clg1 and Pcl5 are the second group involved in the regulation of the cell cycle.

Interestingly, Pho85-Pcl1,2 complex becomes crucial for cell survival in the absence of Cdc28 (Espinoza *et al.*, 1994; Measday *et al.*, 2000). *PCL1* follows the exact same expression pattern as *CLN1* and *CLN2. PCL2* has been found to be highly expressed after cell exposure to increased temperatures (Bállega *et al.*, 2018). PCL9 is expressed at the end of mitosis and Pcl7 during the S phase. Clg1 has been shown to have a role in regulating Sic1 degradation during G1 (Yang *et al.*, 2010). Lastly, Pcl5 has been shown to be involved in nutrient sensing, a function related to the Pho80 cyclins group despite Pcl5 presenting higher sequence homology with Pcl1,2 cyclin group (Aviram *et al.*, 2008).

Given the wide range of functions Pho85 is implicated in, deletion of the CDK or its cyclin patterns lead to several defects such as glycogen accumulation (*pcl8Δ, plc10Δ)* (Huang, Wilson and Roach, 1997)*,* impaired phosphate metabolism (*pho80Δ*) (Yang *et al.*, 2010)and delay of cell cycle progression amongst others (Espinoza *et al.*, 1994; Hernández-Ortega *et al.*, 2013). Altogether, it highlights the relevance of Pho85 (Jiménez *et al.*, 2013).

In mammalian cells, there is a much higher level of complexity during the cell cycle progression and how it is regulated. Amongst all the CDKs described in mammals, only Cdk1 has been shown to have an essential role (Santamaría *et al.*, 2007; Adhikari *et al.*, 2012; Diril *et al.*, 2012). It is worth mentioning that between all the CDKs reported in mammals, Cdk16 and Cdk5 could be considered as Pho85 putative mammals' homologue (Huang *et al.*, 1999).

8.3 Cell cycle checkpoints

The main purpose of the cell cycle is to pass the hereditary information accurately to the daughter cells. For this reason, it is vitally important for the cell to verify that the hereditary information has not been compromised before committing to the different phases of the cell cycle.

There are several checkpoints distributed along the cell cycle and the crosstalk between the cell cycle and DNA repair mechanisms becomes crucial. Before progressing, cells check for any lesion in the DNA and upon checkpoint activation, the cell cycle will be either delayed or stopped at G1, S or G2 (Johnson and Rao, 1970; Hartwell and Weinert, 1989; Deckbar, Jeggo and Löbrich, 2011).

Coordinating cell size with cell progression is essential to ensure the proper amount of genetic and biosynthetic material in the daughter cells. For this reason, cell size checkpoints occur during key cell cycle transitions (Killander and Zetterberg, 1965; Nurse, Thuriaux and Nasmyth, 1976). There are two cell size checkpoints to guarantee the amount of growth required to proceed to the next phase of the cell cycle. The first one controls cell cycle START and the second one operates before entry into the mitotic phase.

DNA integrity is also examined throughout the cell cycle and lesions in the DNA lead to cell cycle arrest, thereby allowing time for repair pathways to operate and repair the damage before committing to the next cell cycle stage. DNA damage checkpoints are located in G1, S and G2. Finally, the mitotic spindle checkpoint controls the correct attachment of chromosomes to the microtubules prior to the segregation of sister chromatids (Hardwick *et al.*, 1996; Wells and Murray, 1996).

Focusing on the DNA damage checkpoints, despite the different DNA lesions and their specific response for DNA repair, they all activate common checkpoint pathways whose main objective is to inactivate CDK activity and to arrest the cells until the lesions are repaired.

Some key factors have been identified regarding the activation of checkpoint signalling and consequently the cell arrest. In *S. cerevisiae* two members of the phosphatidylinositol 3-kinase-related kinases (PIKK) family are both considered to have a leading role as sensor kinases: Mec1 (Keith and Schreiber, 1995; Carr, 1997) and Tel1 (Greenwell *et al.*, 1995; Morrow *et al.*, 1995). These proteins have a human homologue counterpart which indicates their importance. ATR (Ataxia-Telangiectasia-Mutated and Rad3-related) is Mec1 homologue and ATM (Ataxia-Telangiectasia-Mutated) is Tel1 homologue protein. Mec1 activates in response to different types of lesions with ssDNA. Mec1 forms a complex with Ddc2 and together they will be recruited to the site of damage by interacting with RPA-coated ssDNA (Paciotti *et al.*, 2000; Zou and Elledge, 2003; Falck, Coates and Jackson, 2005; You *et al.*, 2005; Berkovich, Monnat and Kastan, 2007; Shiotani and Zou, 2009). In contrast, Tel1 is recruited in the DNA damage by MRX after a DSB (Nakada, Matsumoto and Sugimoto, 2003; Shiotani and Zou, 2009; Paull, 2015). Even though each pathway initiates after a different stimulus, both lead to the phosphorylation and therefore the activation of checkpoint mediators. These two pathways do not exclude each other, Mec1 and Tel1 work in parallel to make sure the cell does not progress through the cell cycle until the lesions are repaired (Beyer and Weinert, 2014).

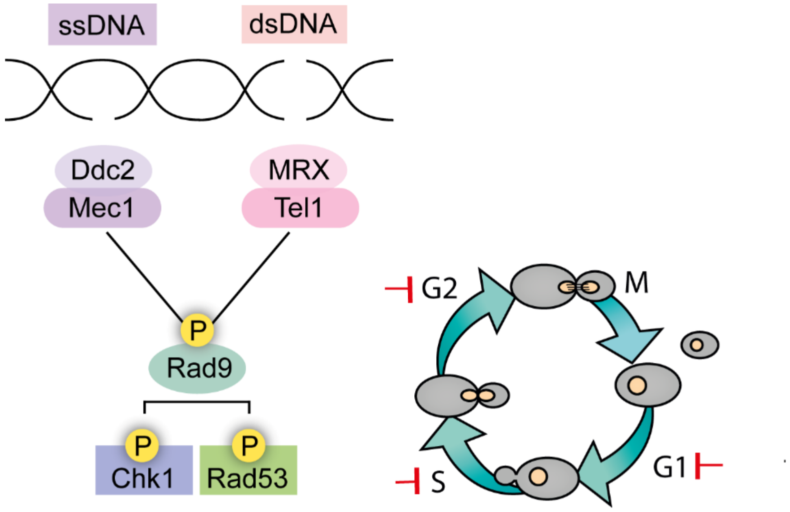

Fig. 16. Schematic representation of the signalling network of yeast DDR Upon DNA damage, signals are transduced from Mec1 and Tel1 to the checkpoint mediator Rad9. Rad9 activation leads to Chk1 and Rad53 phosphorylation resulting in cell arrest at G1, S or G2 phase.

The interaction of Mec1 and Tel1 with the checkpoint mediator Rad9 promotes the full response of the checkpoint proteins Rad53 and Chk1. Through extensive phosphorylation, the kinases Mec1 and Tel1 regulate the activity, stability and localisation of the effector proteins Rad53 and Chk1 which promote cell cycle arrest and DNA repair (Melo and Toczyski, 2002; Branzei and Foiani, 2010; Awasthi, Foiani and Kumar, 2016; Yu, Garcia and Symington, 2019).

8.4 DNA repair regulation by the cell cycle

So far, I have been focusing on describing DNA damage, how the cell senses it and responds based on the DNA lesion produced and the mechanisms the cell has evolved with in order to maintain genomic integrity.

As mentioned above, the cell responds to lesions threatening genomic integrity by activating the DNA damage response (DDR). Several studies in both human cells and yeast have shown that a reduction of Cdk1 activity sensitises cells to DNA damage proving Cdk1 participation in the DDR (Ferreira and Cooper, 2004; Ira *et al.*, 2004; Clerici *et al.*, 2008; Enserink *et al.*, 2009; Prevo *et al.*, 2018) and the coordination between DNA repair mechanisms and the cell's progression through the cell cycle.

Now, I would like to emphasise the importance of regulating the two main processes implicated in double-stranded break repair (DSBR): NHEJ and HR. The choice between NHEJ and HR is extensively regulated through the cell cycle (Shrivastav, De Haro and Nickoloff, 2008).

Cdk1 role in DNA repair was described by Marco Foiani's lab in research where they proved that CDK1 activity is required for DSB-induced homologous recombination (Ira *et al.*, 2004). Cdk1 activation positively regulates DSB end resection that leads to the generation of 3' ssDNA tails which are crucial to undergo HR as the preferred mechanism to repair DSBs (Aylon, Liefshitz and Kupiec, 2004; Ira *et al.*, 2004). The activation of end resection at the beginning of the S phase will lead to a competition between the Ku heterodimer (which bind to DNA ends and protect them from resection) and the nucleases (Aylon, Liefshitz and Kupiec, 2004; Ira *et al.*, 2004; Zhang *et al.*, 2009). Even though NHEJ is not restricted to a specific stage of the cell cycle, it is most active at G1 and its activity is attenuated at G2 due to Cdk1-dependent modulation of DNA ends processing (Clerici *et al.*, 2008; Zhang *et* *al.*, 2009). Cdk1 will promote DNA end resection by a mechanism also conserved in human cells, phosphorylation of an evolutionarily conserved motif of the exonuclease Sae2 (Huertas *et al.*, 2008; Huertas and Jackson, 2009). Sae2 mutation at Ser 267 results in several phenotypes similar to those of *sae2Δ*: hypersensitivity to DSB-inducing agents, a reduction of the recombination events and impaired DNA-end resection (Huertas *et al.*, 2008). In addition to Sae2 phosphorylation, Mre11 and Xrs2, two components of the MRX complex; are phosphorylated by Cdk1 in several residues (Simoneau *et al.*, 2014). Interestingly, the phosphorylation of MRX complex, a major DSB sensor, results in a reduction of the NHEJ events in the cells whilst the non-phosphorylatable mutant increases NHEJ events (Simoneau *et al.*, 2014). This is consistent with the model in previous studies where Sae2 phosphorylation leads to an increase of DNA resection and a reduction of NHEJ events (Clerici *et al.*, 2008; Huertas *et al.*, 2008; Zhang *et al.*, 2009). By MRX and Sae2 phosphorylation, Cdk1 facilitates HR repair. This regulatory mechanism seems to be conserved in humans where a non-phosphorylated version of CtiP (homologue of budding yeast Sae2) or Nbs1 (homologue of budding yeast Xrs2) also results in an increase of NHEJ and hypersensitivity to DSB-generating agents (Huertas and Jackason, 2009; Wohlbold *et al.*, 2012).

Sae2 and the MRX complex are responsible for initiating end resection whilst Exo1 and Dna2 along with the helicase complex Sgs1 are responsible for extensive resection and generating longer ssDNA at DSBs. Dna2 has been also proposed as a target for Cdk1 phosphorylation (Chen *et al.*, 2011). A non-phosphorylatable version of Dna2, where Thr4, Ser17 and Ser237 were mutated; showed no changes in the initiation of resection but a reduction of extensive resection from the break point. In addition, Dna2 phosphorylation by Cdk1 is required for its recruitment at the DSB site (Chen *et al.*, 2011).

Besides the enzymes involved in resection, Cdk1 regulates other DNA damage response proteins. Rad9, a DNA damage response sensor has also been described as a Cdk1 phosphorylation target. The phosphorylation of Rad9 N-terminal residues stimulates Rad9 interaction with Chk1 and therefore the checkpoint activation (Wang *et al.*, 2012; Abreu *et al.*, 2013).

Rad51 and Rad52, the central recombination proteins in HR are positively regulated by Cdk1 (Barlow and Rothstein, 2010; Lim, Chang and Huh, 2020). Recently, Dr Huh laboratory described that both Rad51 and Rad52 are phosphorylated by Cdk1 at G2/M phase. The mutation of Rad51 Ser 125 and Ser 357 residues results in impaired affinity for DNA binding. Moreover, they found out that Rad52 phosphorylation at Thr 412 facilitates the formation of the ring structure that is crucial for its localisation and to promote strand annealing of DSB ends during HR (Plate *et al.*, 2008; Saotome *et al.*, 2018; Lim, Chang and Huh, 2020).

All evidence presented above guarantees an exhaustive regulation of HR. However, there exists some uncertainty about how NHEJ is directly regulated by the cell cycle. So far, it has only been reported a regulatory mechanism involving CDK-mediated phosphorylation of Lif1, a component of the NHEJ machinery in *S. cerevisiae* (Matsuzaki *et al.*, 2012). Lif1 is phosphorylated during the S to G2 phase and is required to coordinate resection and

NHEJ. Hentges (2014) reported the phosphorylation of one of NHEJ core factors in fission yeast, Xlf1 (the ortholog of *S. cerevisiae* Nej1 and human XLF) at the C-terminal domain by Cdc2 (Hentges *et al.*, 2014). Interestingly, the phosphorylation of Xlf1 leads to the downregulation of NHEJ. Regardless of the description of these two regulatory mechanisms in yeast, no more evidence suggests an extensive regulation of NHEJ by the cell cycle in either yeast or humans.

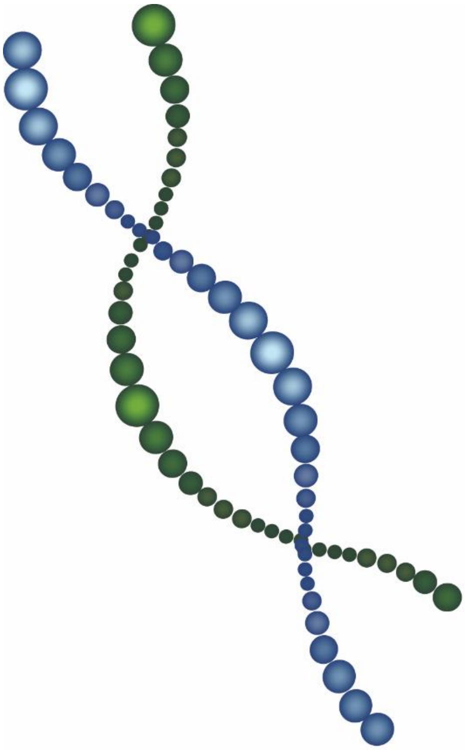

Objectives

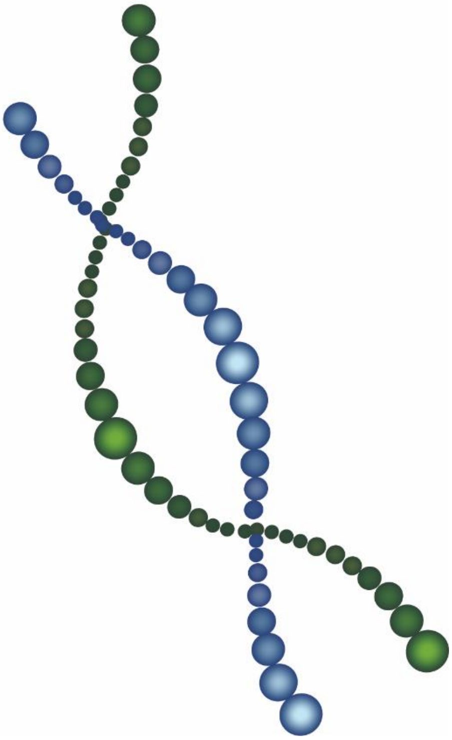

The objectives of my thesis are:

- The identification and characterisation of Yku80 as a phosphorylation target by the Pcl1-Pho85 complex and their validation *in vitro* and *in vivo*.

- Determine the physiological relevance of Yku80 phosphorylation in *Saccharomyces cerevisiae*.

- Investigate the role of Yku80 phosphorylation by Pcl1-Pho85 in DSB repair and the coordination between cell cycle and DNA repair pathway choices.

- Determine if evolutionary conservation is occurring in the identified yeast mechanism and an analysis of Ku80 phosphorylation in mammalian cells.

- Determine the physiological relevance of Ku80 phosphorylation in different cancer cell lines.

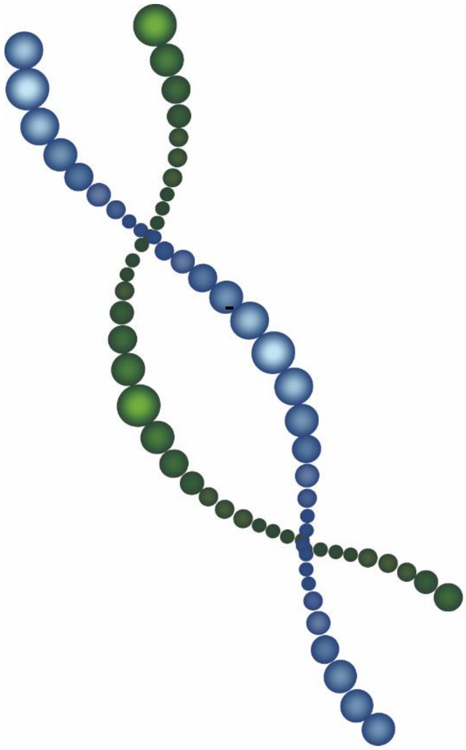

Materials and methods

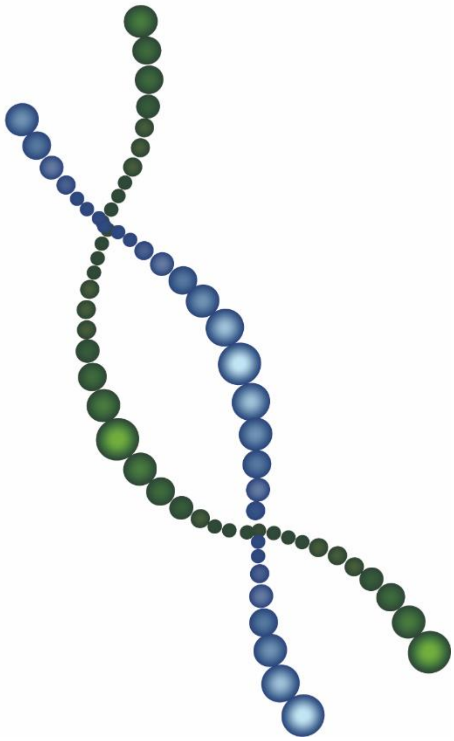

1. Yeast strains, growth conditions and tagging

1.1 Yeast strains

All used strains are listed in table 3 where specific backgrounds are detailed.

Table 3: **Yeast strains**

Name	Genetic details	Relevant genotype	Source
W303-1a	W303-1a	*MATa leu2-3,112 trp1-1 can1-100 ura3-1 ade2-1 his3-11,15*	(Thomas and Rothstein, 1989)
BY4741	BY4741	*MATa his3Δ1 leu2-Δ-200 met15-Δ-0 ura3Δ-0*	(Brachmann *et al.*, 1998)
YBS1058	W303-1a	*yku80::hph*	This study
YBS1071	W303-1a	*YKU80-KanMX*	This study
YBS1066	W303-1a	*yku80-S623A-KanMX*	This study
YBS1061	BY4741	*YKU80-KanMX*	This study
YBS1062	BY4741	*yku80-S623A-KanMX*	This study
YBS1057	BY4741	*yku80::hph*	This study
UCC3505	YPH499	*MATa ura3-52 lys2-801 ade2-101 trp1Δ63 his3Δ200 leu2Δ1 ppr1::HIS3 adh4::URA-TEL DIA5-1*	(Singer and Gottschling, 1994)

UCC3515	YPH499	*MATa ura3-52 lys2-801 ade2-101 trp1Δ63 his3Δ200 leu2Δ1 hml::URA3*	(Singer and Gottschling, 1994)
YBS1015	YPH499	*ppr1::HIS3 adh4::URA-TEL DIA5-1 sir2::KanMX*	This study (derived from UCC3505)
YBS1073	YPH499	*ppr1::HIS3 adh4::URA-TEL Dia5-1 YKU80-KanMX*	This study (derived from UCC3505)
YBS1074	YPH499	*ppr1::HIS3 adh4::URA-TEL Dia5-1 yku80-S623A-KanMX*	This study (derived from UCC3505)
YBS1016	YPH499	*hml::URA3 sir2::KanMX*	This study (derived from UCC3515)
YBS1050	YPH499	*hml::URA3 YKU80*-6HA-*KanMX*	This study (derived from UCC3515)
YBS1051	YPH499	*hml::URA3 yku80-S623A*-6HA-*KanMX*	This study (derived from UCC3515)
YBS1059	YPH499	*ppr1::HIS3 adh4::URA-TEL Dia5-1 yku80::hph*	This study (derived from UCC3505)

YBS1060	YPH499	*hml::URA3 yku80::hph*	This study (derived from UCC3515)
YEB126	BY4741	*Yku80*-TAP-*KanMX*	This study
YEB77	BY4741	*yku80-S623A*-TAP	This study
YBS1039	BY4741	*yku80*-S623A-TAP-*KanMX*	This study
YRC1029	W303-1a	*YKU80*-eGFP-*HIS3*	This study
YRC1031	W303-1a	*yku80-S623A-eGFP-HIS3*	This study
YRC1120	BY4741	*YKU80-KanMX rad52::hph*	This study (derived from YBS1061)
YRC1124	BY4741	*yku80-S623A-KanMX rad52::hph*	This study (derived from YBS1062)
JKM179		*matα HO hml:ADE1 hmr::ADE1 ade1-100 leu2-3, 112 trp::hisG lys5 ura3-52 ade3::GAL::HO*	(Kim and Haber, 2009)
YRC1131		*matα ho hml:ADE1 hmr::ADE1 ade1-100 leu2-3, 112 trp::hisG lys5 ura3-52 ade3::GAL::HO YKU80-KanMX*	This study (derived from JKM179)

YRC1132	*Matα ho hml:ADE1 hmr::ADE1 ade1-100 leu2-3, 112 trp::hisG lys5 ura3-52 ade3::GAL::HO yku80-S623A-KanMX*	This study (derived from JKM179)
YRC1133	*Matα ho hml:ADE1 hmr::ADE1 ade1-100 leu2-3, 112 trp::hisG lys5 ura3-52 ade3::GAL::HO yku80::KanMX*	This study (derived from JKM179)
YJK17	*Matα ho hml:ADE1 hmr::ADE1 ade1-100 leu2-3, 112 trp::hisG lys5 ura3-52 ade3::GAL::HO yku80::KanMX arg5,6::MATa-inc::HPH1*	(Kim and Haber, 2009)
YRC1128	*Matα ho hml:ADE1 hmr::ADE1 ade1-100 leu2-3, 112 trp::hisG lys5 ura3-52 ade3::GAL::HO yku80::KanMX arg5,6::MATa-inc::HPH1 YKU80-KanMX*	This study (derived from YJK17)
YRC1177	*Matα ho hml:ADE1 hmr::ADE1 ade1-100 leu2-3, 112 trp::hisG lys5 ura3-52 ade3::GAL::HO yku80::KanMX arg5,6::MATa-inc::HPH1 yku80-S623A-KanMX*	This study (derived from YJK17)

YRC1178		*Matα ho hml:ADE1 hmr::ADE1 ade1-100 leu2-3, 112 trp::hisG lys5 ura3-52 ade3::GAL::HO yku80::KanMX arg5,6::MATa-inc::HPH1 yku80-S623A-KanMX*	This study (derived from YJK17)
YRC1172		*Matα ho hml:ADE1 hmr::ADE1 ade1-100 leu2-3, 112 trp::hisG lys5 ura3-52 ade3::GAL::HO yku80::KanMX arg5,6::MATa-inc::HPH1 yku80::KanMX*	This study (derived from YJK17)
YRC1167	YPH499	*ppr1::HIS3 adh4::URA-TEL DIA5-1 pho85::KanMX*	This study (derived from UC3505)
YRC1160	YPH499	*ppr1::HIS3 adh4::URA-TEL DIA5-1 pcl1::KanMX*	This study (derived from UC3505)
YRC1150	YPH499	*hml::URA3 pho85::TRP1*	This study (derived from UC351
YRC1165	YPH499	*hml::URA3 pcl1::KanMX*	This study (derived from UC3515)
YW1276		*MAT*α-inc *ade2*::HOSD(+1)::*STE3-MET15 his3*Δ1 *leu2*Δ *met15*Δ *ura3*Δ	(Palmbos, Daley and Wilson, 2005)

YRC1047		*MAT*α-inc *ade2*::HOSD(+1)::*STE3-MET15 his3*Δ1 *leu2*Δ *met15*Δ *ura3*Δ *YKU80-KanMX*	This study (derived from YW1276)
YRC1048		*MAT*α-inc *ade2*::HOSD(+1)::*STE3-MET15 his3*Δ1 *leu2*Δ *met15*Δ *ura3*Δ *YKU80-KanMX*	This study (derived from YW1276)
YRC1051		*MAT*α-inc *ade2*::HOSD(+1)::*STE3-MET15 his3*Δ1 *leu2*Δ *met15*Δ *ura3*Δ *yku80*::*KanMX*	This study (derived from YW1276)
YRC1061		*MAT*α-inc *ade2*::HOSD(+1)::*STE3-MET15 his3*Δ1 *leu2*Δ *met15*Δ *ura3*Δ *yku80-S623A-KanMX*	This study (derived from YW1276)
YEB122	BY4741	*Yku80*-TAP-*KanMX pho85::LEU2*	This study
YRC1063		*MAT*α-inc *ade2*::HOSD(+1)::*STE3-MET15 his3*Δ1 *leu2*Δ *met15*Δ *ura3*Δ *yku80-S623A-KanMX*	This study (derived from YW1276)

YRC1047		*MAT*α-inc *ade2*::HOSD(+1)::*STE3-MET15 his3*Δ1 *leu2*Δ *met15*Δ *ura3*Δ *pcl1::LEU2*	This study
YEB94	BY4741	*Yku80*-TAP-*KanMX* *pcl1::LEU2*	This study

1.2 Growth conditions

In all experiments, to reduce experiment variability; the number of cells inoculated for the overnight cultures was always constant and ranging between $OD_{\lambda 660}$=0.01-0.05 depending on the experiment. Yeasts were grown in water shakers at 30 ºC under vigorous agitation (200 rpm) in the following media:

- YPD medium (1% yeast extract, 2% peptone and 2% glucose)
- Complete synthetic dextrose (SD) medium (0,67% yeast nitrogen base, 0.5% NH_4SO_4, and 2% glucose) supplemented with auxotrophic requirements (15 mg/ml of leucine and uracil, 5 mg/ml of histidine, and 10 mg/ml of tryptophan).
- Galactose-induction medium (0,67% yeast nitrogen base, 3% glycerol, 2% lactate supplemented with auxotrophic requirements (15 mg/ml of leucine and uracil, 5 mg/ml of histidine, and 10 mg/ml of tryptophan).
- 5-FOA plates, SD with all the required amino acids were supplemented with 1 mg/ml 5-FOA, (Thermo Scientific^{TM}) sterilised by filtering, and added to the medium just before plating.

Yeast strain selection was performed by omitting the auxotrophic supplements required or by adding 8 mg/ml geneticin to the medium. To make solid media 2% agar was added to any of the mediums.

1.3 Strains construction and tagging

I performed mutations, deletions and tagging of genes using the tool-box system (Janke *et al.*, 2004).

The tool-box system consists of gene tagging or deletion by chromosomal integration of a PCR amplified cassette from a plasmid. The primers I used to amplify the sequence also carried the flanking homologous sequences of the targeted gene. In the case of *yku80-S623A,* the fact that the residue of interest is located at the end of the sequence allowed me to introduce the mutation with a single step transformation strategy. The forward primer to amplify the tag or antibiotic resistance gene carried the serine to alanine mutation. Proteins were tagged at the C-terminal end (see table 5). For cassettes amplification and mutation confirmation, I amplified DNA with MyCycler^{TM} (Bio-Rad) using Q5 High-Fidelity DNA Polymerase (New England Biolabs$_{Inc}$) and the following reagents at a final concentration of: 1X Buffer Q5 Reaction Buffer 5X, 200 µM dNTPs, 0.5 µM forward primer, 0.5 µM reverse primer and Mili-Q water. PCR conditions are detailed in the following table (annealing and amplification conditions were adapted as required by base pair length and GC-content of the genes):

Table 4: PCR conditions

Cycles	Temperature	Time
1	98°C	5 min
30	98°C	30 s
	55-65°C	30 s - 1 min
	72°C	30 s - 2 min
1	72°C	5 min
1	4°C	5 min

Table 5: Oligonucleotides

*mutation is coloured in red * toolbox system sequence is coloured in blue

Name	Sequence	Purpose
Yku80 F6	TGAAGCGCGGTGAACAACACAGTAGGGGAAGTCCAAACAATAGCAATAATCGTACGCTGCAGGTCGAC	Construction of Yku80 wt by toolbox (Jankee *et al.*, 2004)
Yku80 F6C	TGAAGCGCGGTGAACAACACAGTAGGGGAGCTCCAAACAATAGCAATAATCGTACGCTGCAGGTCGAC	Construction of *yku80*-S623A by toolbox (Jankee *et al*., 2004)
Yku80 R6	TTTAACTGTGGTGACGAAAACATAACTCAAAGGATGTTAGACCTTTTTTAATCGATGAATTCGAGCTCG	Construction of Yku80 wt and *yku80*-S623A by toolbox (Jankee *et al*., 2004)
Yku80 F32	GCAGGACATATGCACAAATAATATATCTCACACCATAATACGTACGCTGCAGGTCGAC	Construction of *yku80*Δ by toolbox (Jankee *et al*., 2004)
Yku80 R32	GTGGTGACGAAAACATAACTCAAAGGATGTTAGACCTTTTATCGATGAATTCGAGCTCG	Construction of *yku80*Δ by toolbox (Jankee *et al.*, 2004)
Pho85 F37	GCGCGGCAAACTGGGCAAACTTGAGCAATACCACGTACGCTGCAGGTCGAC	Construction of *pho85*Δ by toolbox (Jankee *et al*., 2004)
Pho85 R37	CATTATATATACATGGCTACGGTTTTTCGCTGACGGGCTGCGATCGATGAATTCGAGCTCG	Construction of *pho85*Δ by toolbox (Jankee *et al.*, 2004)
Pcl1 F43	CAAAAACAATCAATTATACAAATAACAGTAAAGTAATAAACGTACGCTGCAGGTCGAC	Construction of *pcl1*Δ by toolbox (Jankee *et al.*, 2004)
Pcl1 R43	TCCCACTAAGAGCCCCGTAAGGGCCATCTTGTTTACCACAATCGATGAATTCGAGCTCG	Construction of *pcl1*Δ by toolbox (Jankee *et al.*, 2004)

I confirmed mutations by PCR followed by sequencing and protein tagging by PCR and Western blot or fluorescence microscopy when necessary.

2. Yeast transformation

I transformed yeast cells using the method described in (Hill, Donald and Griffiths, 1991). I inoculated yeast cells in 5 ml of YPD and left them to grow overnight in a shaker at 30°C. I diluted the overnight culture to a final $OD_{\lambda660}$=0.3 in 50 ml of YPD. After yeasts cell reached a mid-log phase of growth at approximately $OD_{\lambda660}$=0.8-1.0 I collected them and centrifuged them at 2000 rpm 3 min. I resuspended the pellet in 1 ml of TELiAc solution (10 mM Tris-HCl pH=7.5, 1mM EDTA pH=8 and 100 mM lithium acetate) and centrifuged it at 3000 rpm for 3 min. Next, I resuspended the pellet in 300 µl of TELiAc. I performed each transformation reaction with 100 µl of the pellet which I resuspended with TELiAc. I added 10 µl of ssDNA (single stranded salmon sperm DNA) and either 10 µl of the transforming cassette or 1-5 µl of the transforming plasmid to the mix. Next, I added 600 µl of PEG 1x (10 mM Tris-HCl pH=7.5, 1mM EDTA pH=8 and 100 mM lithium acetate and 40% PEG-4000) to the transformation, mixed it and left it for 30 min of incubation at 30°C. After incubation, I added 70 µl of DMSO to the tube and proceed to a 15 min heat shock in a 42°C water bath. Finally, I centrifuged yeast cells for 1 min at 3000 rpm and I resuspended the pellet in 100 µl Mili-Q water and finally plated.

3. Plasmids engineering and DNA cloning

3.1 DNA cloning by homologous recombination

All plasmids I used in this work are listed in table 6.

Table 6: List of plasmids

Name	Relevant characteristics	Source
pJC1043	pRS316	(Sikorski and Hieter, 1989)
pJC2287	YIplac211	(Gietz and Sugino, 1988)
pJC1314	pRS415-empty	(Sikorski and Hieter, 1989)
pJC1491	pRS414	(Janke *et al.*, 2004)
pJC2242	pRS414-*YKU80*	This study
pJC2246	pRS414-*yku80-S629A*	This study
pJC1759	pWPI-empty	(#12254, Addgene)
pJC2275	pWPI-Ku80^{wt}	This study
pJC2279	pWPI-Ku80^{T629A}	This study

The genes I amplified in this work were obtained from genomic DNA (gDNA) of yeast strain BY4741. I performed DNA amplification explained in section 1.3. using 0.5 µl of gDNA. After PCR I purified the amplicons using NucleoSpin® Gel and PCR Clean-up kit (Macherey-Nagel).

Before recombination, I performed plasmid enzyme digestion for 1-2 h and I separated cut plasmids by agarose electrophoresis followed by purification with NucleoSpin® Gel and PCR Clean-up kit (Macherey-Nagel). I incubated the digested-plasmid and the gene cassette with the recombinase for 1 h at 50°C using an Infusion HD cloning kit (Takara).

3.2 Bacterial transformation

Subcloning Efficiency™ DH5α™ Competent Cells (Invitrogen) were used for gene cloning. 50 µl of DH5α were incubated with 10 µl of recombination mix in ice for 30 min. Heat-shock was carried out in a 42°C water bath for 1 min and 15 s followed by 1 min of incubation in ice. Later, 1 ml of SOC medium (2% Tryptone**,** 0.5% Yeast Extract, 10 mM NaCl**,** 2.5 mM KCl**,** 10 mM $MgCl_2$**,** 10 mM $MgSO_4$ and 20mM glucose) was added, and cells were incubated for 1 h at 37°C in a shaker under vigorous agitation. Finally, cells were plated in LB-Ampicillin plates and incubated at 37°C for 12-16 h.

3.3 Plasmid isolation

I inoculated colonies from bacteria transformation in 3 ml of LB-Ampicillin for 12-16 h at 37°C in an air shaker under vigorous agitation. I performed plasmid isolation using NucleoSpin® Plasmid EasyPure kit (Macherey-Nagel).

4. Cell lines and reagents

Human embryonic kidney 293 cells (HEK 293) (kindly provided by Ramon Trullas Lab), adenocarcinoma human alveolar basal epithelial cells (A549) (European Collection of Authenticated Cell Cultures), human breast adenocarcinoma cells (MCF-7) (Eucellbank) and MDA-MB-231 (kindly provided by Hospital Clinic).

I cultured all the cell lines in Dulbecco's modified Eagle's medium (Sigma-Aldrich) supplemented with 10% fetal bovine serum (Sigma-Aldrich), 1% GlutaMAX (Biowest, Nuaillé, France) and 1% penicillin/streptomycin (SigmaAldrich). All cells were grown in a humidified atmosphere at 37 °C and 5% CO_2 and mycoplasma contamination were monitored periodically.

5. Viral cloning and transduction.

To clone Ku80 into lentiviral vectors, I amplified the gene from A549 cDNA. I cloned either Ku80^{wt} or Ku80^{T629A} sequences into pWPI lentiviral expression vector (#12254, Addgene) at the *Pme*I restriction site.

For lentivirus production, I seeded HEK293-T cells in 100 mm plates at 70% confluence with 45 µg of lentiviral expression vector. I performed cell transfection using calcium phosphate. First, I vigorously vortexed a mix consisting of the plasmids (45 µg of lentiviral expression vector, 12,9 µg of pMD2G and 29,1 µg of psPAX2), TE 0,1x (1mM Tris-HCl pH=8, 0,1 mM EDTA) and buffered water (2,5 mM HEPES pH=7,3) at the same time I added HeBS 2x (50 mM HEPES, 280 mM NaCl, 1,5 mM Na_2HPO_4-$7H_2O$ pH=7) drop by drop. Then I incubated the mix for 15 min at room temperature and later I added it to the plates drop by drop. 12 h after lentiviral infection, I replaced the medium from the plates for a fresh one. I collected the virus-containing supernatant at 24 h and 48 h post-transduction. I concentrated the virus using the Sartorius VS2042 Vivaspin 20 concentrator (Sartorius) and determined the viral titer. For overexpression studies, I infected MDA-MB-231 and MCF-7 cells with 15 MOI of lentivirus and A549 cells with 5 MOI of lentivirus.

6. Cell synchrony in G1 with α-factor

Yeast cells from an overnight culture were grown exponentially in either YPD or SD to a density of approximately 1×10^7 cells/ml. To synchronize the yeast cells in G_1, I added α-factor (Biomedal) to the culture to a final concentration of 20 µg/ml. After 1 h and 40 min I collected the cells and confirmed the shmoo morphology and the absence of budding structures by microscopy observation, before proceeding to α-factor release. I centrifuged G1 synchronised cells and resuspended them in fresh medium twice for α-factor release.

7. Flow cytometry analysis (FACS)

7.1 Cell-cycle analysis of budding yeast by FACS

I carried out flow cytometry analysis for yeast cells as in (Yaakov *et al.*, 2009). I incubated a volume of 100 µl cells of a culture at $OD_{\lambda 66}$ ranging from 0.7-1.0 with 70% ethanol for 10 min. After cell fixation, I washed cells twice and resuspended the pellet with 500 µl of 50 mM Na-citrate treated with 0.1 mg/ml RNase A. Cells were incubated at 37°C overnight. The next day I stained the cells with 4 µg/ml propidium iodide and slightly sonicated them to disrupt cell aggregates. When it was required, I diluted cells in 50 mM Na-citrate for better detection. I performed FACS analysis in a FACS Calibur flow cytometer (BD Biosciences, San Jose, CA). I analysed 10^4 cells for each time point. Finally, I used Flowing Software (Turku Bioimaging) to analyse the data I obtained from the FACS.

7.2 Lentivirus titer by FACS

I seeded HEK-293 cells to a final density of 10^5 cell/ml and incubated at 37 °C and 5% CO_2 overnight. An extra plate was necessary to count cells and determine the final cell number the next day. After 24 h I infected cells with 10-fold serial dilutions of the viruses. Cells were incubated at 37°C and 5% CO_2 for 12 h and the next day I added 1 ml of fresh medium to each well. After 48 h I trypsinised the cells, centrifuged them at 1000 rpm for 3 min and washed them at least 3 times with PBS 1x. I performed FACS analysis of 10^4 cells as described in section 7.2. I calculated the number of viral particles per ml as follows:

$$\frac{\text{TU}}{\text{ml}} = \frac{\text{\% GFP positive cells x cell number}}{\text{volume of viruses}}$$

8.Fluorescence microscopy

I inoculated yeGFP-tagged cells in SD medium lacking histidine to avoid autofluorescence and left them to grow overnight. The next day, I diluted cells to OD_{660nm} = 0.3 and allowed to a mid-log phase in a water shaker at 30ºC. After 3 h, I centrifuged 100 µl of cells followed by a dilution of the culture to a concentration where single cells could be observed. I obtained the measurement of GFP signal and images using Nikon Ti Eclipse Fluorescence Microscope.

9. Dot assays

I inoculated cells in YPD medium and left them to grow overnight at 30°C. I diluted the overnight culture to $OD_{\lambda 660}$=0.3 and allowed to grow to a mid-log phase for 3 h. Then, I diluted the culture to $OD_{\lambda 660}$=0.05 a sequentially diluted in fresh YPD. I spotted 3 µl of the dilution on the appropriate plates and incubated them for 48 h at the indicated temperature.

10. Cell extract and immunoblot

10.1 Protein extraction from yeast cells

For Western blot analysis, I treated the cells as described elsewhere (Bell *et al.*, 2001)

I incubated 1ml of the yeast cell culture at an $OD_{\lambda 660}$=1.0 with 10M trichloroacetic acid (TCA) to a final concentration of 20% (v/v) for 10 min and centrifuged the mix twice at full speed for 1 min. I dissolved the pellets in 100 µl of 0.5% SDS, 42 mM Tris-HCl at pH 6.8. Next, I prepared cell lysate adding 150 µl of glass beads (Sartorius, BBI-8541701) and bead-beaten three times at maximum force for 60 s using the FastPrep® (MP Biomedicals). Then, I centrifuged the samples and collected the supernatant. I boiled samples at 95°C for 5 min. I used an amount of protein ranging from 40 µg to 60 µg for Western blot analysis.

10.2 Protein extraction from human cell lines.

First, to remove the medium I centrifuged cultured human cell lines and washed them with ice-cold phosphate-buffered saline (PBS). Then, to resuspend the pellet I used 60 µl of lysis buffer, containing 20 mM TRIS, 5 mM EDTA, 1% NP40 (IGEPAL CA-630), 150 mM NaCl pH 7.4, supplemented with Pierce Phosphatase Inhibitor Mini tablets (#88667, Thermo Fisher Scientific) and with Pierce Protease Inhibitor tablets (#88266, Thermo Fisher Scientific). I vortexed the cells for 1 min and then incubated the cell lysate in ice for 1 min. I repeated the previous step five times. Finally, I obtained cell extracts by freezing the samples for 15 min at -20°C following centrifugation at 14,000 rpm for 20 min at 4°C. I collected the supernatants and I quantified protein concentration by Bradford assay (BioRad). I used a total of 30 µg for immunodetection by western blot.

10.3 Western blot

I employed the use of 7.5% either Mini or Midi-PROTEAN® TGX™ Precast Protein Gels (BioRad) for separation of proteins. Using PROTEAN® Tetra Cell, Trans-Blot® Module, and PowerPac™ HC Power Supply (BioRAd) I separated the samples at 100 V-150 V. For protein transfer to PVDF membranes (Immobilon-P; Millipore), I first activated the membranes in 100% methanol. I performed the transfer at 100-150 mA for 1 h and 30 min. Then I incubated membranes with the blocking solution consisting of 1X TBST (Tris Buffered Saline with Tween 20, pH=8) with 5% dry milk for 30 min at room temperature with gentle rocking. The antibodies I used in this work are listed in table 7.

For Phos-tag experiments, I used 4% w/v acrylamide stacking gel and 6% w/v acrylamide separating gel. The stacking gel buffer was 350 mM Bis-Tris (pH 6.8), 0.1% v/v TEMED, 0.05% w/v ammonium persulfate (APS). The separating gel buffer was 350 mM Bis-Tris (pH 6.8), 100 μM Phos-Tag™, 40 μM $Zn(NO_3)_2$, 0.05% v/v TEMED, 0.01% w/v APS. The running buffer consisted of 50 mM Tris-HCl pH=7.5, 50 mM MOPS, 0.1% (w/v) SDS and 5 mM $NaHSO_3$ pH=7.2. Gels were run for 1 h at 100 V for optimal separation of phosphorylated and non-phosphorylated protein species. For proteins transfer I used the following buffer: 25 mM Tris, 192 mM glycine, pH 8.3, 20% w/v methanol, 5mM $NaHSO_3$ pH=7.2 and 2.5mM NaPPi. I transferred proteins to methanol-activated PVDF membranes (Immobilon-P; Millipore) at 20 V and 4°C overnight. Then I incubated the membranes with blocking solution consisting of 1X TBST (Tris Buffered Saline with Tween 20, pH=8) with 5% dry milk for 30 min at room temperature with gentle rocking.

I developed immunoblots using Luminata Forte Western HRP Substrate (Millipore). I took images using GeneSnap (Syngene) and I quantified the amount of protein using Image Studio Lite (Li-Cor).

Table 7: Antibodies

Name	Source	Dilution	Secondary antibody
α-PAP	Sigma (P1291)	1:40,000	-
α-110C (Thiophospate ester)	Acbcam (ab92570)	1:5,000	Rabbit
α-Ku80	Cell Signalling (C48E7)	1:100	Rabbit
α-GFP	Cell Signalling (2956)	1:500	Rabbit
α-GST	CusAb (CSB-MA000021M0M)	1:10,000	Mouse

11. Recombinant protein purification

I expressed GST fusion proteins using *Escherichia coli* strain BL21 (DE3) (Stratagene). I inoculated the cells and allowed them to exponentially grow at 37°C for 5 h. Then, I set the temperature for 18°C to add 200 mM isopropyl β-D-thiogalactopyranoside (IPTG) to induce protein expression for 16 h. I collected cells by centrifugation and resuspended in lysis buffer consisting of 50 mM Tris-HCl pH=7.5, 150 mM NaCl, 5% glycerol, 0.1% Triton X-100, 1 mM EDTA, 1 mM DTT, 100 mM PMSF, 10 mg/ml leupeptin, 1 mg/ml pepstatin and 0.5 M benzamidine. Next, I added 125 µg/ml lysozyme (Sigma), 16.5 µg/ml DNasa I (Panreac) and 16.5 µg/ml RNase A (Roche) to resuspend the pellet. I incubated the mix at 37°C for 10 min. Then, I added STEP buffer 1x (10 mM Tris-HCl pH=8, 100 mM NaCl,1 mM EDTA, 2 mM DTT, 1 mM PMSF, 10 µg/ml leupeptin, 1 µg/ml pepstatin and 1 mM benzamidine) to the mix and I sonicated the cells for 3 min while kept in ice with Hielscher Ultrasonics GmbH.

I removed cell debris by centrifugation of the mix at 8,000 rpm for 10 min at 4°C. To purify the proteins from the supernatant I used glutathione-Sepharose chromatography (GE Healthcare), as described in the manufacturer's protocol. After incubation with rotation for 1 h at 4°C, I collected the beads by centrifugation (1,000 rpm for 1 min at 4°C) and washed them three times with a solution consisting of lysis buffer and STET buffer 10x and twice more with the equilibration buffer (50 mM Tris-HCl pH=8, 150 mM NaCl,1 mM $MgCl_2$, 1 mM DTT). I performed protein elution by adding 10 mM glutathione. To elute the proteins, I left samples rotating for 20 min at 4°C.

12. *In vitro* kinase assay

In vitro phosphorylation assay for yeast proteins was as in (Hernández-Ortega *et al.*, 2013). The method depends on detection of phosphate groups attached to tyrosine, serine and threonine residues in gels by Pro-Q Diamond phosphoprotein gel stain. I assayed GST-proteins in kinase buffer 10x consisting of 500mM Tris-HCl pH=7,5 and 100 mM $MgCl_2$. Protease (100 mM PMSF, 10 µg/ml leupeptin, 0,1 mg/ml pepstatin and 0.5 M benzamidine) and added phosphatase (100mM NaPPi, 1M NaF, 10mM Orthovanadate, 250 mM ß-glycerophosphate) inhibitors to the reaction mix with 20 mM DTT. I incubated the reaction mix at 30°C 1 h. Finally, I added SDS-SB5x to each reaction and boiled the samples before loading them to a gel. I performed western blot as described in section 10.3. After Western blot finished, I washed the gel with Mili-Q water followed by overnight incubation with the fix solution (50% methanol, 10% acetic acid and 40% Mili-Q water). The next day, I washed the gel three times with Mili-Q water prior to 1 h incubation in the dark with Pro-Q staining solution. I removed the staining solution and then washed the gel for 30 min with Pro-Q® Diamond destain solution at least three times. I took images as described in section 10.3.

In vitro kinase assay for human proteins was as in Blethrow et al. 2008. The method is based on the utilisation of ATP-γ-S (adenosine 5'-(gamma-thiotriphosphate) a modified version of the ATP. The kinase uses ATP-γ-S (Axxora, BLG-A060-05) to phosphorylate the substrate of the reaction and this will be consequently labelled with a thiol group. Alkylation of the proteins carrying the thiol group will generate a thiophosphate ester product that will be recognised by a specific antibody.

I assayed GST-proteins in a reaction mix consisting of 2,5 µl of kinase buffer (500 µM HEPES-KOH pH=7,5, 1,5M NaCl, 100 mM $MgCl_2$ and 10 mM DTT), 0,1 µM CDK16-CCNY and 0,2 µM Ku. I incubated the mix at 30°C for 30 min and stopped the reaction with 50 mM EDTA. Alkylation of proteins takes place after addition of 1.8 mM PNBM (p-nitrobenzyl mesylate) and incubation at 25°C for 45 min. Finally, I added SDS-SB 5x to every reaction and I analysed phosphorylation by Western blot using α-110C antibody. I determined the amount of protein by Coomassie staining.

13. Yeast genomic DNA isolation and Southern Blot

I performed isolation of genomic DNA (gDNA) as described by (Hoffman and Winston, 1987). I collected yeast cells from an overnight culture by centrifugation for 1 min at 14.000 rpm and resuspended the pellet in lysis buffer (2% triton X-100, 1% SDS, 100 mM Tris HCl pH=8, 1 mM EDTA pH=8) with 500 µl glass beads (Sartorius, BBI-8541701). I vortexed the cells for 90 s for cell lysis. Next, I added 250 µl of phenol and chloroform and vortexed again for 90 s. I centrifuged the mix at 14.000 rpm 3 min and transferred the aqueous phase to another tube. For DNA precipitation, I added 1 volume of isopropanol. I placed the tube in ice for 15 min followed by centrifugation at 14.000 rpm 20 min. I discarded the supernatant and washed the samples with 70% ethanol. After centrifugation at 14.000 rpm for 5 min, I resuspended the pellet in Mili-Q water and RNasa 10 µl/ml and incubated the tubes at 37°C for 3 h before gDNA quantification.

For southern hybridization, I first digested DNA samples with *Xho*I for 1 h and separated them on a 1% agarose gel. Then, I treated the agarose gel with denaturation buffer (0,5N NaOH, 1,5M NaCl) followed by 30 min incubation with neutralization buffer (0,5M Tri-HCl, 1,5M NaCl pH=7,5). I transferred the DNA from the gel to *Amersham*™ Protran™ NC *Nitrocellulose Membranes* (10600001) in the presence of 20x SSC (3M NaCl, 0,3M tri-sodium citrate, pH=7). After 5 h, I washed the membrane with Mili-Q water. The following step was the pre-hybridisation with 10 ml of DIG Easy Hyb Granules (Roche Applied Science) pre-heated at 56,7°C in the hybridisation oven. Before hybridisation, I pre-heated the probe at 95°C 5 min and placed it immediately in ice for 2 min. I incubated the membrane with the DIG labelled telomere probe: 5'-TGTGGGTGTGGTGTGTGGGG TGGTG-3' (Boulton and Jackson, 1996) at 56,7°C overnight.

After hybridisation, I washed the membrane twice with washing buffer (0,1M acetic acid, 0,15M NaCl and 0,3% Triton) at room temperature. Next, I incubated the membrane with blocking buffer 1x (blocking buffer 10x and Maleic acid buffer (100mM Maleic acid, 150mM NaCl, pH=7,5)) for 1 h at room temperature with gentle rocking. For probe detection, I used anti-digoxigenin-AP, Fab fragments (Roche Applied Science, 11175033910).

14. Two-dimensional electrophoresis

I collected a total cell amount of 15 $O.D_{600}$ from an exponential growth culture. For protein extraction, I incubated cells with 10M trichloroacetic acid (TCA) to a final concentration of 20% (v/v) for 10 min. Next, I washed the samples twice with Mili-Q water and resuspended the pellet with 10% TCA (v/v) followed by 1 h incubation at 4°C. I centrifuged cell lysates at 14.000 rpm 30 min at 4°C and resuspended the pellet with 90% acetone. I centrifuged the mix at 14.000 rpm 30 min at 4°C and resuspended the pellet in UTC buffer consisting of 7 M urea, 2 M thiourea and 2% CHAPS (a detergent to break protein-protein interaction) to denature proteins. I used up to 50 µg of protein. In addition, I added to the samples resuspended in UCT buffer: 1M DTT, a mix of ampholytes and a tip of blue bromophenol solution.

I isoelectrically focused proteins in the first dimension using 11 cm Ready Strips^{TM} IPG (pH 3.0–10.0; Bio Rad) in an Ettan IPGphor II (Amersham Biosciences) system following the indications of the manufacturer. The conditions were: 250 V for 30 min, 1000 V for 30 min and 5000 V 70 min at 20°C.

I incubated the strips in equilibrium buffer (1,5 M Tris-HCl pH=8,8, 6 M urea, 30% glycerol, 2% SDS, 64 mM DTT and blue bromophenol) for 15 min with gentle rocking. After that, I incubated the strips for 30 s in running buffer.

For resolving proteins in the second dimension, I used SDS-PAGE 4-15% gradient acrylamide gels. Proteins were transferred to PVDF membranes (Immobilon-P; Millipore) at 20 V and 4°C overnight. I performed the Western blot as described in section 10.3.

15. Silencing assay

I performed silencing assay as described in Singer (1994). The system is based on the ability of cells to grow either in ura- or *5-FOA* selective plates. All yeasts strains are derived from UCC3505 (MATa *ura3-52 lys2-801 ade2-101 trp1Δ63 his3Δ200 leu2Δ1 ppr1::HIS3 adh4::URA-TEL DIA5-1*) and UCC3515 (MATa *ura3-52 lys2-801 ade2-101 trp1Δ63 his3Δ200 leu2Δ1 hml::URA3*). UCC3505 and UCC3515 harbour a *URA3* reporter gene at either the telomeres or *HML* region. *URA3* gene encodes for orotine-5'-monophosphate decarboxylasa that convert 5-FOA (5-Fluoroorotic acid) to a toxic metabolite for the cells. Therefore, only cells silencing *URA3* reporter can grow in 5-FOA medium but cannot in ura- selective plates.

I diluted overnight cultures to $OD_{\lambda 660}$=0.3 and allowed them to grow to a mid-log phase. After 3 h, I adjusted cell suspensions to $OD_{\lambda 660}$=0.05. I spotted 10-fold serial dilutions of every culture onto ura- or 5-FOA (Thermo Scientific^{TM}) plates and incubated at 30°C for 3-4 days.

16. DSB plasmid repair assay

16.1 NHEJ repair assay

The non-homologous end-joining (NHEJ) repair assay was as in Bertuch and Lundblad (2003). This assay is based on the capacity of cells to re-ligate the plasmid by NHEJ. pRS316 was digested with *Bam*HI which cuts within the multicloning site of the plasmid, therefore there is not a homologous sequence available in the cell's genome to repair the damage by HR. I purified *Bam*HI digested pRS16 in an agarose gel. I diluted yeast cells from an overnight culture to $OD_{\lambda660}$= 0,3 in 50 ml. After 3 h of exponential growth, I collected the cells for yeast transformation and adjusted the $OD_{\lambda660}$ to 0,7 in the different strains. I used 300-350 ng of *Bam*HI digested pRS316 and 50-100 ng of uncut pRS415 for yeast transformation by lithium acetate/single-stranded carrier DNA/polyethylene glycol method (for details see section 2).

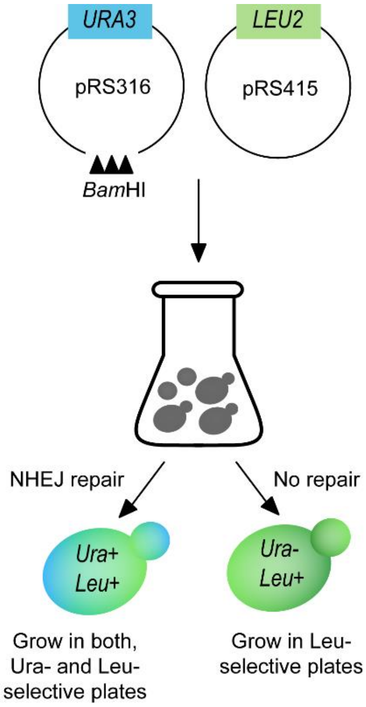
URA3
LEU2
pRS316
pRS415
BamHI
NHEJ repair
No repair
Ura+
Leu+
Ura-
Leu+
Grow in both, Ura- and Leu- selective plates
Grow in Leu- selective plates

Fig. 17. NHEJ repair assay.

Non-digested pRS415 plasmid was used to control yeast transformation efficiency from every culture. Cells were plated in Ura- and Leu- selective plates and incubated at 30°C for 48 h. Cells were counted and NHEJ efficiency was calculated as the ratio of uracil prototrophic growing colonies to leucine prototrophic growing colonies.

16.2 HR repair assay

The homologous recombination (HR) repair assay was performed as described in Hentges (2014). The system is based on genome integration of the *URA3* marker gene from an integrative plasmid. As integrative plasmids are unable to replicate in their hosts, it must integrate into the genome. I digested YIpLac211 with *Eco*RV which makes a cut inside the *URA3* marker gene. I purified the *Eco*RV digested plasmid in an agarose gel. I diluted an overnight culture of yeast cells bearing a mutated version of *URA3* in their genome, to $OD_{\lambda 660}$=0,3. After 3 h of exponential growth, I collected the cells and the $OD_{\lambda 660}$ of each culture was adjusted to 1,0.

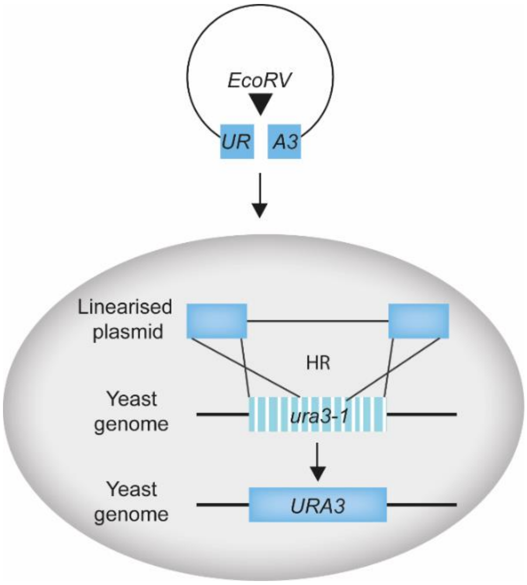

Fig. 18. Homologous recombination in HR repair assay

The next steps for yeast transformation are detailed in section 2. I used 500 ng *Eco*RV digested YIpLac211 and 50-100 ng of uncut pRS415 to transform each strain. Again, I used pRS415 as a control for transformation efficiency. I plated cells in Ura- and Leu- plates and incubated them at 30°C for 48 h. I counted the cells and calculated HR efficiency as the ratio of uracil prototrophic growing colonies which have successfully integrated the *URA3* gene.

17. NHEJ genomic assay

I used two different systems to evaluate NHEJ events. The suicide deletion assay was described in Palmbos, Daley and Wilson (2005). The strains I used in this assay derived from YW1276 (*MAT*α-inc *ade2*::*HOSD*(+1)::*STE3-MET15* *his3*Δ1 *leu2*Δ *met15*Δ *ura3*Δ). This system consists of a yeast strain bearing two HO cleavage sites flanking the endonuclease gene which is under the control of a *GAL1* promoter (Fig. 19). There is no homologous sequence available for the cells to perform HR, therefore once HO has been induced with galactose, the endonuclease snips the genome and the DSB is repaired by re-ligation of DNA ends (NHEJ). I inoculated cells at a final $OD_{\lambda 660}$=0,1 in 5 ml of SD supplemented with 120 µg/ml

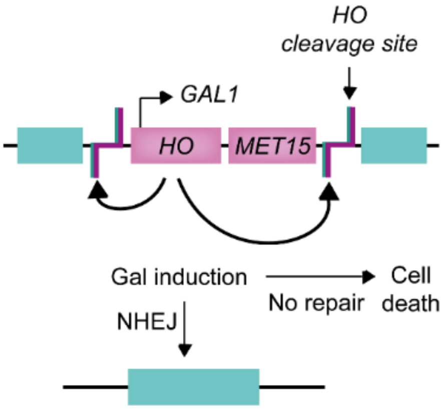

Fig. 19. Schematic representation of the suicide deletion assay. Adapted from Palmbos, Daley and Wilson (2005).

adenine and left to grow overnight. After 16 h, I collected them and adjusted the $OD_{\lambda 660}$ to 0,3. When cells reached a mid-log phase, I plated them in either 2% glucose or 2% galactose plates and incubated them at 30ºC for 3-4 days. Then, I counted the number of cells and calculated the frequency of DSB repair by NHEJ as the ratio of colonies formed on galactose plates compared to the glucose plates.

The second assay was described by Dr Haber's lab (Kim and Haber, 2009). All strains used are derived from JKM179 (*MATα ho hml::ADE1 hmr::ADE1 ade1-100 leu2-3,112 trp::hisG lys5 ura3-52 ade3::GAL::HO*). Induction of HO endonuclease by galactose generates a single cut at the ChIII yeast genome. As cells lack both, *HML* and *HMR* which have the homologous sequence to MAT, the DSB will be repaired by NHEJ. I inoculated yeast cells at an $OD_{\lambda 660}$=0,05 in 5 ml of SD 2% raffinose for an overnight culture. The next day, I obtained a mid-log phase culture of an $OD_{\lambda 660}$ ranging from 0,6-0,8. Next, I plated the cells in either 2% glucose or 2% galactose SD plates and incubated at 30°C.

After 48h, I counted the cells, and I calculated the frequency of DSB repair by NHEJ as the ratio of colonies formed on galactose plates compared to the glucose plates.

18. HR genomic assay

The HR genomic assay was as in Kim and Haber (2009). This system consists of a genetically modified strain (YJK17) where a single cut takes place in the yeast genome after HO is induced by galactose.

HO snips the genome at the *MAT*α locus (ChIII) and, as intrachromosomal homologous sequence was deleted, the recombination occurs with the homologous sequence at *MAT*a locus (ChV) (Fig. 20). The endonuclease will not be able to cut the genome again because the homologous sequence at *MAT*a locus has a mutated version of the HO recognition site. All the strains I used for this experimental procedure are derived from YJK17 (*MATα ho hml::ADE1 hmr::ADE1 ade1-100 leu2-3,112 trp::hisG lys5 ura3-52 ade3::GAL::HO arg5,6::MATa-inc::HPH1*).

I inoculated yeast cells at an $OD_{\lambda 660}$=0,05 in 5 ml of SD 2% raffinose for an overnight culture. After 16 h, the overnight culture reached a mid-log phase of an $OD_{\lambda 660}$ ranging from 0,6-0,8. Next, I plated the cells in either 2% glucose or 2% galactose SD plates and incubated at 30° for 72 h. Finally, I counted the cells, and I calculated the frequency of DSB repair by HR as the ratio of colonies formed on galactose plates compared to the glucose plates.

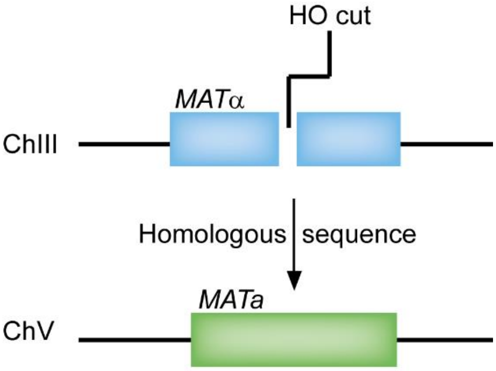

Fig. 20. Schematic representation of the HR genomic assay. Adapted from Kim and Haber (2009)

19. NHEJ fidelity assay

The fidelity in the NHEJ process was measured as follows: I used 200-300 ng of *Nco*I digested pJC2170 plasmid to transform the pertinent strains. pJC2170 plasmid is based on pRS415 in which I cloned the *URA3* marker gene between *Hin*dIII and *Bam*HI restriction site. *Nco*I site is in the *URA3* sequence. Consequently, Leu+ colonies are those that were able to repair the plasmid, and Ura+ those that repaired maintaining the *URA3* intact. I measured fidelity as the ratio between the number of uracil prototrophic colonies to leucine prototrophic colonies.

20. Sensitivity to drugs in asynchronous cultures

For dose-response assays, I diluted the overnight cultures to an $OD_{\lambda 660}$=0,3. After 3 h of exponential growth, I treated cells with either MMS (Sigma) or bleomycin (Abcam). The MMS concentrations I used were: 0,01%, 0,033% and 0,1% and cells were incubated with MMS for 60-, 120-, 180- or 240-min. Bleomycin concentrations I assayed were 3, 30 and 300 µg/ml and cells were incubated for 30, 60, 90 or 120 min.

After drug treatment, I plated cells onto 2% glucose plates and incubated at 30ºC for 2 days. I calculated the percentage of survival as the ratio of non-treated to treated cells grown in glucose plates.

21. Sensitivity to bleomycin in synchronic cultures

For sensitivity assays in synchronic cultures first, I synchronised cells in G_1 as detailed in section 6. 70 min after α-factor released, I added 300 µg/ml of bleomycin (Abcam) to the culture to induce specifically in the G_2 phase the double strand breaks and incubated with bleomycin for 30 min in a water shaker at 30ºC. After that, I plated cells on 2% glucose plates and incubated at 30ºC for 2-3 days. Finally, I counted the number of cells and calculated the percentage of survival as the ratio of non-treated cells to bleomycin-treated cells grown in glucose plates.

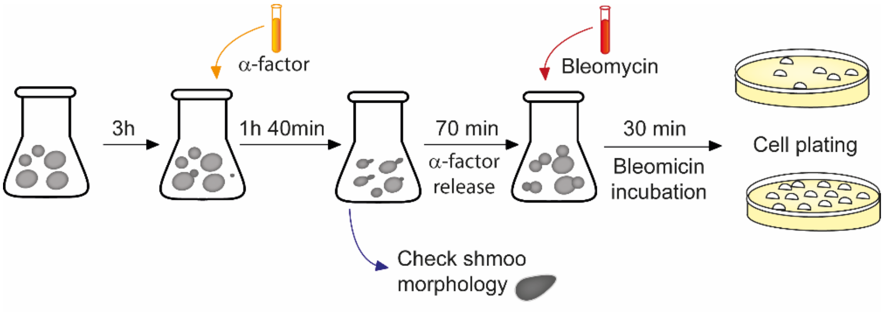

Fig. 21. Schematic representation of the experimental procedure for bleomycin treatment in a synchronic culture.

22. Colony formation assay in cancer cell lines

I seeded the cells and infected them with lentiviral vectors: pWPI-Ku80^{wt}, pWPI-Ku80^{T629A} and pWPI-empty in 24-well plates. 48h post-infection, I incubated cells 2 h with either one of the following bleomycin concentrations: 0,05, 0,1, 0,5, 1 or 5 µg/ml. After bleomycin treatment, I trypsinised cells, washed them and counted them. A total density of 1200 (A549), 2500 (MCF-7) and 1200 (MDA-MB-231) cells were seeded in 6-well plates. After 2 weeks colonies became visible (Fig. 21A). I removed the medium was removed and fixed cells with 1 ml of 100% methanol at -20°C for 5 min. Next, I washed cells twice with PBS and stained them with 0.1% crystal violet for 30 min at room temperature in the dark. Later, I performed 3-4 washes with PBS. To analyse cell viability first, I counted the cell number. Moreover, for a more accurate analysis of cell viability, I measured the absorbance at 570nm after dissolving crystal violet with acetic acid (Fig. 21B). In both cases, I calculated the percentage of cell survival as the ratio of cells treated with bleomycin versus the control.

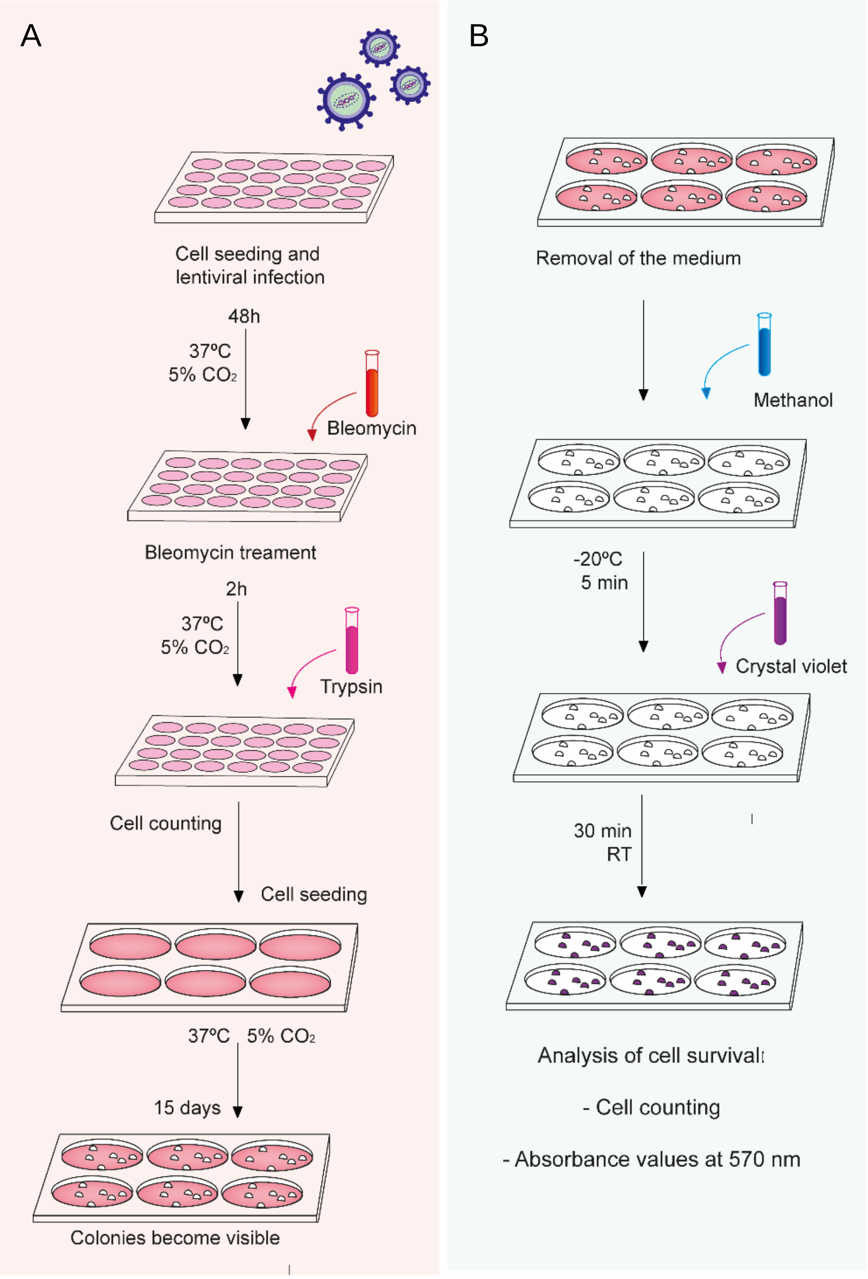
A
Cell seeding and lentiviral infection
48h
37ºC
5% CO₂
Bleomycin
Bleomycin treament
2h
37ºC
5% CO₂
Trypsin
Cell counting
Cell seeding
37ºC 5% CO₂
15 days
Colonies become visible
B
Removal of the medium
Methanol
-20ºC
5 min
Crystal violet
30 min
RT
Analysis of cell survival
- Cell counting
- Absorbance values at 570 nm

Fig. 22. Schematic representation of the experimental procedure bleomycin treatment in cancer cell lines. A. Colony formation assay. Measurement of cell viability.

23. Statistical analysis

I expressed data as standard error of the mean (mean±SD). I determined the statistical significance using the paired sample t-test. I considered a *p value < 0.05, **p value >0.005 and ***p value >0.001 significant.

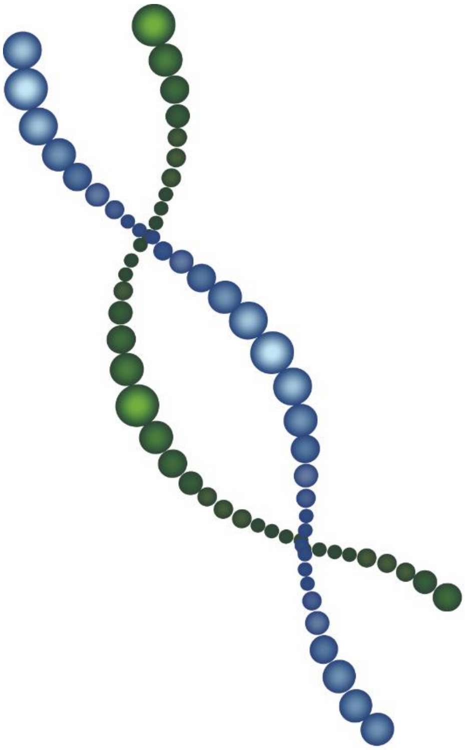

Results

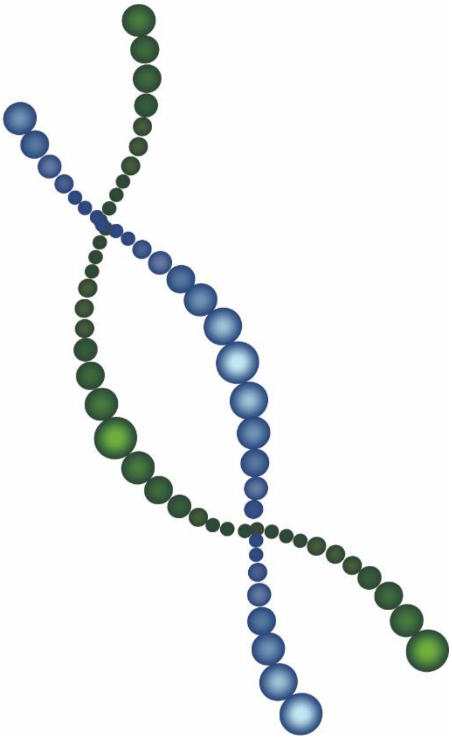

1. Yk80 and the cell cycle

It has been previously demonstrated that *pho85Δ* cells are sensitive to different types of DNA damaging agents such as bleomycin (Kapitzky *et al.*, 2010), methyl methane sulphonate (Chang *et al.*, 2002) and hydroxyurea (Hartman IV, 2007) amongst others. As described, these chemical compounds when either reacting with the DNA or interfering with the replication process, lead to DSBs which are repaired by the HR or NHEJ pathway.

A genome-wide search to look for protein-protein interaction events within *S. cerevisiae* was carried out at Dr Tyers lab (Ho *et al.*, 2002). Interestingly, one of the interactions they described was between CDK Pho85 and Yku80, as mentioned in the introduction, one of the main proteins involved in DSBs repaired by NHEJ. In addition to this study, another genome-wide search experiment was performed at Dr McEachern lab to identify *S. cerevisiae* deletion mutants which have an effect on telomere length (Askree *et al.*, 2004), a function where Yku80 plays an important role.

These facts lead me to consider there might be a connection between cell cycle machinery (Pho85) and DNA repair (Yku80).

2. Yku80 is an *in vitro* substrate of Pcl1-Pho85

As mentioned earlier, an interaction between Yku80 and Pho85 has been described (Ho *et al.*, 2002; Askree *et al.*, 2004). However, this evidence came from genome-wide experiments and to date Yku80 phosphorylation by Pho85 has not yet been reported.

To assess if any of the two different enzymatic forms of Pho85 can phosphorylate Yku80, I performed an *in vitro* phosphorylation assay. First, I produced and purified Yku80, Pho85 and Pcl1 proteins from *E. coli* and I performed the *in vitro* kinase assay as described in (Jeffery *et al.*, 2001). The reason I selected Pcl1 as the cyclin partner of Pho85 is because Pcl1 activates Pho85 during late G1 and S phase of the cell cycle.

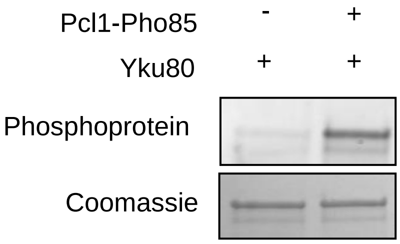

Fig. 23. Yku80 is phosphorylated by Pcl1-Pho85 *in vitro*.
Bacteria produced recombinant GST-Pho85 and GST-Pcl1 were assayed with GST-Yku80. Phosphorylated proteins were detected using the Pro-Q Diamond phosphoprotein gel stain kit (Invitrogen). Coomassie staining of the membrane is presented as a load control.

Pro-Q Diamond phosphoprotein gel stain allowed me the direct in-gel detection of phosphate groups attached to tyrosine, serine, or threonine residues. The kinase assay shows a signal corresponding to phosphorylated Yku80 where both, Pcl1-Pho85 complex and Yku80 were assayed together (Fig. 23). This result indicates that Yku80 is phosphorylated by Pcl1-Pho85 *in vitro*.

In the introduction, I explained how Pho85 can interact with two families of cyclins: Pcls or Pho80 family. Pho85 function depends on the cyclin it binds to. Pho80-Pho85 complex participates in the phosphate metabolism and one of their known targets is Pho4 (Kaffman *et al.*, 1994; Lee *et al.*, 2008)

To find out whether Yku80 phosphorylation takes place strictly when Pho85 is activated by Pcl1, Pho80 or both, I performed another *in vitro* kinase assay now with Yku80, Pho85 and Pho80. These proteins were also produced and purified from *E. coli.*

As shown in Fig 24, there is no signal corresponding to Yku80 phosphoprotein when Pho80-Pho85 were assayed with Yku80.

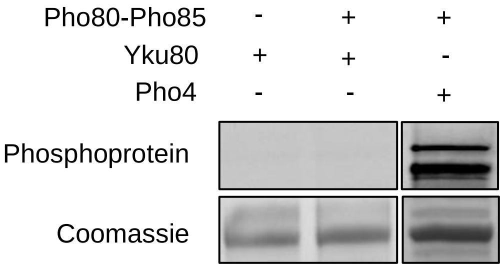

Fig. 24. Yku80 is not phosphorylated by Pho80-Pho85 *in vitro*. Bacteria produced recombinant GST-Pho85 and GST-Pho80 were assayed with GST-Yku80 and GST-Pho4. Phosphorylated proteins were detected using the Pro-Q Diamond phosphoprotein gel stain kit (Invitrogen). Coomassie staining of the membrane is presented as a load control.

This result indicates that Yku80 might be a specific substrate for Pcl1-Pho85 complex. Pho80-Pho85 were unable to phosphorylate Yku80 *in vitro*. However, the complex is active as Pho4 was successfully phosphorylated (Kaffman *et al.*, 1994). Taking into consideration that Pcl1 is involved in cell cycle progression, this result indicates that Yku80 function regarding this phosphorylation by Pcl1-Pho85 could be related to cell cycle.

3. Yku80 bears four consensus sites for CDK phosphorylation

Yku80 protein from *S. cerevisiae* has 629 amino acids. Three different domains can be defined within the sequence: an amino-terminal von Willebrand A domain (vWA), a central core domain which binds to the DNA and a disorganised carboxyl-terminal domain (Harris *et al.*, 2004). Analysing the sequence searching for consensus sequence for CDK phosphorylation, I identified four S/TP motifs distributed amongst the different domains. The first SP motif is at the beginning of the amino acid sequence in the N-terminal domain (S19), the next one is located in the DNA binding core (S200) and the two SP motifs left are located at the disordered region of the C-terminal domain (S567 and S623) (Fig.25).

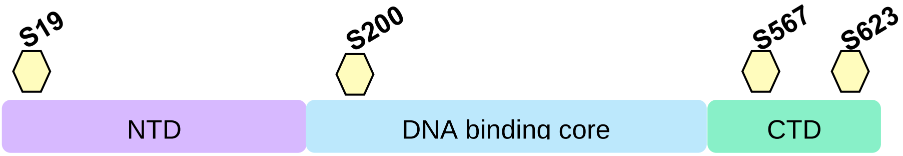

Fig. 25. Schematic diagram of the Yku80 protein and its domains. Numbers on top indicate the different SP CDK consensus sites. The three domains, represented in different colours, are NTD (N-terminal domain), DNA binding core and CTD (C-terminal Domain).

4. Yku80 is phosphorylated *in vitro* at Ser623 by Pcl1-Pho85

As mentioned above, Yku80 amino acids sequence has four SP consensus sites for CDK phosphorylation (Fig. 22). The following question was which residue, if not the four of them, is phosphorylated by the CDK/cyclin complex?

For this, I mutated all serines from the SP motifs to alanines and made different combinations to identify the residue targeted by Pho85.

YKU80 was amplified from BY4741 yeast background by PCR and was used as a template to synthesise also by PCR, the different versions of *YKU80* mutants with primers carrying the mutation. Next, genes were cloned by ligation in a pGEX-6P-1 for *E. coli* protein expression and purification (see Materials and methods section 1 and 3). An *in vitro* kinase assay was performed with purified proteins from *E. coli*.

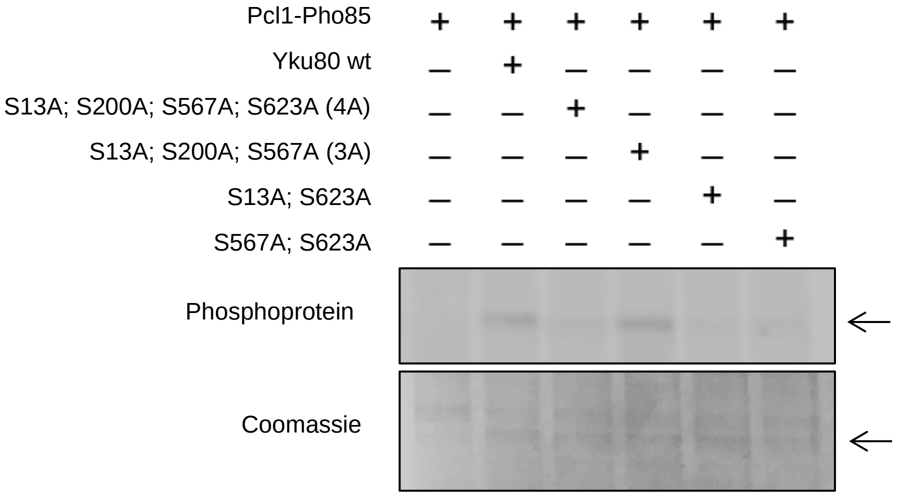
Pcl1-Pho85 + + + + + +
Yku80 wt – + – – – –
S13A; S200A; S567A; S623A (4A) – – + – – –
S13A; S200A; S567A (3A) – – – + – –
S13A; S623A – – – – + –
S567A; S623A – – – – – +
Phosphoprotein
Coomassie

Fig. 26. Yku80 is phosphorylated *in vitro* by Pcl1-Pho85 at Ser623. The indicated mutant versions of Yku80 protein were obtained and assayed as explained in Fig 24. Arrows indicate Yku80.

As shown in all Yku80 mutant versions in which Ser623 has been substituted by an alanine, there is not a signal corresponding to the phospho-protein (Fig. 26). This result suggested that Ser623 may be the residue targeted by Pcl1-Pho85 complex as all Yku80 versions where Ser623 has been substituted by an alanine residue, if compared with Yku80 wild type in lane 2, do not show Yku80 phosphoprotein.

5. Yku80 is phosphorylated *in vivo* at Ser623 by Pcl1-Pho85

The coming step was to check if this phosphorylation also occurs *in vivo*. First, I produced strains where *YKU80* was tagged with a TAP-tag at the C-terminal domain in the wild-type strain, Ser623 to Ala mutant (from now on S623A), *pho85Δ* and *pcl1Δ* mutants (see materials and methods section 1).

To assess in vivo phosphorylation, I used two different methods: two-dimensional electrophoresis and Phos-Tag gel. I analyse Yku80 phosphorylation by Phos-Tag gels. Phos-Tag gel is a technique which helps to dissect the phosphorylated state of proteins based on a shift in the electrophoretic mobility (Kinoshita *et al.*, 2006). When a protein is phosphorylated it will migrate slower in the gel.

I analysed cell extracts from two different clones. As a positive control, I incubated one of the wild-type strains with alkaline phosphate (AP) at 37ºC 30 min before they were analysed by Phos-Tag gels (Fig. 27 A).

There is a shift in mobility between the wild-type and *yku80*-S623A mutant (Fig. 27 A). The same shift took place when the wild-type strain was previously treated with AP (Fig. 27 A).

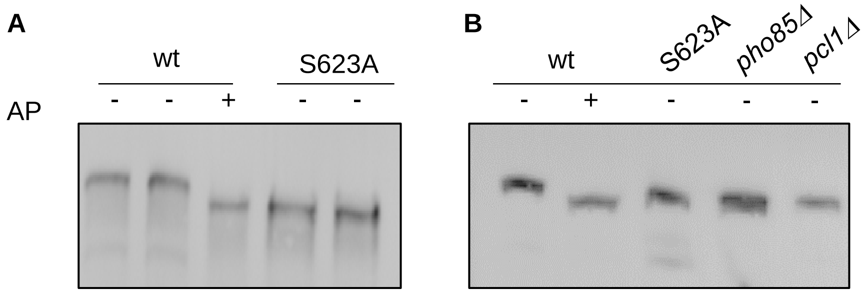

Fig. 27. Yku80 is phosphorylated *in vivo* at Ser623. Two different Phos-tag gel experiment in which cell extracts from A) genomic *YKU80*-TAP and *yku80*-S623A-TAP from two different clones and B) genomic *YKU80*-TAP, *yku80*-S623A-TAP, *pho85Δ YKU80*-TAP and pcl1Δ *YKU80*-TAP were analysed. In both experiments, one of the wild-type cell extracts were treated with alkaline phosphatase (AP) before being electrophoretically separated. Proteins were detected with an α-TAP antibody.

To assess if Pcl1-Pho85 complex is responsible for Yku80 phosphorylation *in vivo*, I performed another Phos-Tag assay with strains where either *PHO85* or *PCL1* was deleted. As shown in Fig. 27 B, there is a difference in protein migration of S623A, *pho85Δ* and *pcl1Δ* mutants compared to the wild-type strain. Moreover, the faster migration of Yku80 in the mutant strains match with the migration pattern of the wild type previously treated with AP which ensures the non-phosphorylated state of Yku80.

These results are suggesting that Pcl1-Pho85 is the cyclin-CDK complex responsible for Yku80 phosphorylation at Ser623.

To further support that Yku80 is phosphorylated at Ser623, I performed a two-dimensional electrophoresis (2D electrophoresis). The 2D electrophoresis is a technique where proteins in a complex mixture are separated based on their isoelectric point (pI) value in the first dimension and their relative molecular weight in the second dimension. As protein phosphorylation changes the pI value of proteins due to the negative charges of phosphate groups, it is possible to differentiate two main populations corresponding to phosphorylated and non-phosphorylated proteins. I analysed cell extracts from an exponentially growing culture of the aforementioned strains. The electrophoretic profile of the wild-type strain is represented by two well-defined dots which is consistent with the presence of the two states of the protein: phosphorylated and non-phosphorylated. However, this pattern changes in the *yku80*-S623A where I can only identify a single dot, the non-phosphorylated population (Fig. 28).

These results show that Yku80 is phosphorylated at Ser623 *in vivo* by Pcl1-Pho85.

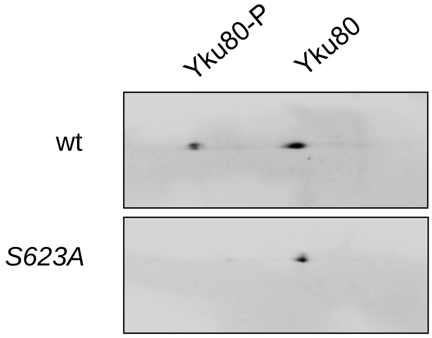

Fig. 28. Yku80 is phosphorylated *in vivo* at Ser623. 2-D electrophoresis analysis of the previous genomic TAP-tag.

6. The non-phosphorylatable version of Yku80 is viable at 37 degrees

Next, I checked if the mutation had an effect on the functionality of the protein. To accomplish this, I began to examine the ability of *yku80*-S623A to grow at 37ºC. The reason to perform this viability assay comes from the fact it has already been described that *YKU80 knockout* cells are unable to grow at 37ºC (Boulton and Jackson, 1996; Gravel and Wellinger, 2002).

The spot assay shows the expected growing defect of *yku80Δ* cells. However, *yku80*-S623A growth is the same as the wild type presents (Fig. 29). *yku80*-S623A viability at 37ºC suggests that the protein is functional despite the mutation at Ser623.

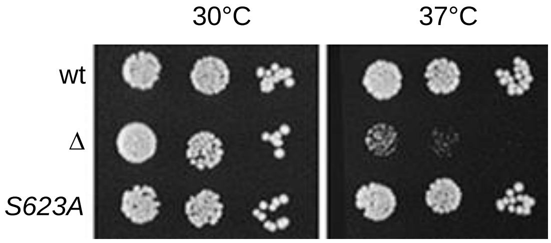

Fig. 29. *yku80*-S623A genomic mutant restores the high temperature growing defect of *yku80Δ* cells. Spot assay of Yku80 wild type, *yku80*Δ and *yku80-S623A* at 30°C and 37°C for 48h. 3 µl of three-fold sequential dilutions were spotted onto YPD plates starting from OD $_{\lambda 660}$ = 0.05.

7. Protein levels of *yku80*-S623A do not vary compared to the wild-type strain

Afterwards, I determined the amount of protein from an asynchronous culture after 3 h of exponential growth.

As shown in Fig. 30, there is a slight decrease in the amount of protein regarding the *yku80*-S623A mutant. Nevertheless, the statistical analysis showed a p value > 0,05 (p value = 0,663) meaning the small reduction in the amount of *yku80*-S623A is not statistically significant.

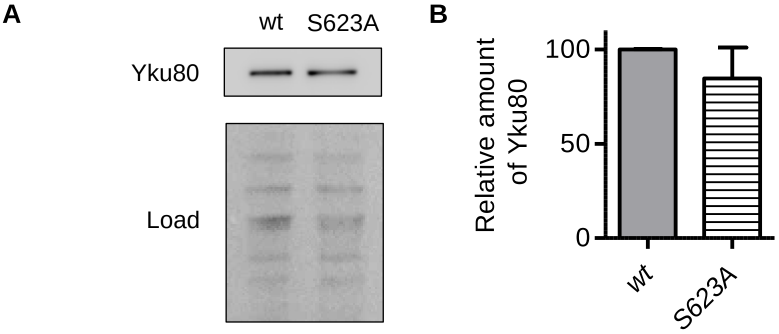

Fig. 30. Yku80 protein amount is not altered by the *yku80*-S623A mutation. A. Western blot of 0.1 OD $_{\lambda 660}$ TAP-tagged wild-type and *yku80*-S623A cultures are presented in the upper panel. Cells from an overnight culture were grown exponentially to an OD $_{\lambda 660}$ ranging from 0.7 to 1.0. Ponceau staining was used as loading control. B. Quantification of the amount of protein is represented in the bar graph as the average and SD of 10 independent experiments. The P value was calculated by two-tailed paired t-test. Values were normalised to wild type = 100.

8. *yku80-S623A* is properly localised in the nucleus

To this point, I have confirmed that *yku80*-S623A is a functional protein and its amount does not vary compared to the wild type. Next, I looked at the localisation of the protein. It has been described that Yku80 has a nuclear localisation (Laporte *et al.*, 2016), that is why the next step was to determine if *yku80*-S623A is also localised within the cells' nucleus.

For this, I decided to generate genomic yeGFP-tag versions of *YKU80* and *yku80*-S623A using the toolbox method explained before (Janke *et al.*, 2004). I analysed cultures after 3h of exponential growth and as shown in Fig. 31., the localisation pattern of either Yk80 wt and *yku80*-S623A is the same and compatible with nuclear localization.

Altogether, this suggests that the S623A mutation produces a functional protein and that the phenotypes I am describing in the following sections are not due to a non-functional, poorly expressed, or delocalised protein.

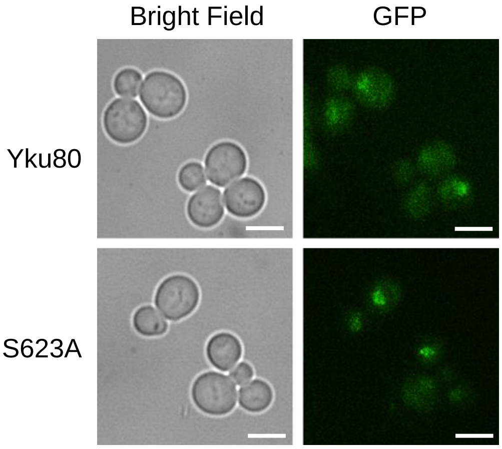

Fig. 31. *yku80-S623A* is localised in the nucleus. Yku80-yeGFP and *yku80*-S623A-yeGFP strains were grown in SD at 30 °C. After 3h of exponentially growing, cells were collected and diluted prior to microscope observation with Nikon Ti Eclipse Fluorescence Microscope. Size bar represents 10 µM.

9. Yku80 phosphorylation at Ser623 does not affect transcriptional gene silencing at telomeres and *HML* locus

Henceforth, my research is focused on establishing the physiological relevance of Ser623 phosphorylation.

In budding yeast, there is an absence of compacted heterochromatin regions to repress gene transcription compared to higher eukaryotes. Silent chromatin represents less than 1% of the genome in budding yeast whilst in humans it is more than 55% (Perrod and Gasser, 2003). However, *S. cerevisiae* has three different chromosomal regions conferring epigenetic silencing on otherwise functional promoters: the homothallic mating-type locus left (*HML*) and right (*HMR*), telomeres and ribosomal DNA array (rDNA). Genes located in these domains or nearby are repressed for transcription.

Earlier in the introduction, I explained Yku80 is involved in gene silencing at both telomeres and *HML/R* locus (Mishra and Shore, 1999; Roy *et al.*, 2004). To determine if gene silencing is impaired in *yku80*-S623A mutants, I used a system described in (Singer and Gottschling, 1994) and (Clément *et al.*, 2006). The system consists of yeast strains UCC3505 and UCC3515 harbouring a *URA3* reporter gene at either the telomeres or *HML* region. To assess whether *yku80*-S623A can silence *URA3* reporter, I checked the capacity of these strains to grow in 5-FOA medium. 5-FOA kills cells expressing the *URA3* reporter gene, therefore only strains silencing *URA3* will be able to grow.

I generated Yku80 wt*, yku80*-S623*, sir2::KanMX, pho85::KanMX* and *pcl1::LEU2* by chromosomal integration using the toolbox system previously described in (Janke *et al.*, 2004).

Silent information regulator (SIR) proteins are essential for gene silencing (Rine and Herskowitz, 1987). These proteins are found at the silent mating type loci, telomeres, and at the rDNA locus repressing gene expression (Kueng, Oppikofer and Gasser, 2013). For this reason, I used yeast cells lacking one of the SIR proteins, Sir2, as a control for gene transcription (Singer and Gottschling, 1994; Chou, Li and Gartenberg, 2008). Additionally, I assayed the original strains UCC3505 and UCC3515 to make sure the tagging at the C-terminus does not interfere with Yku80 function at the telomeres or *HML* locus for gene silencing.

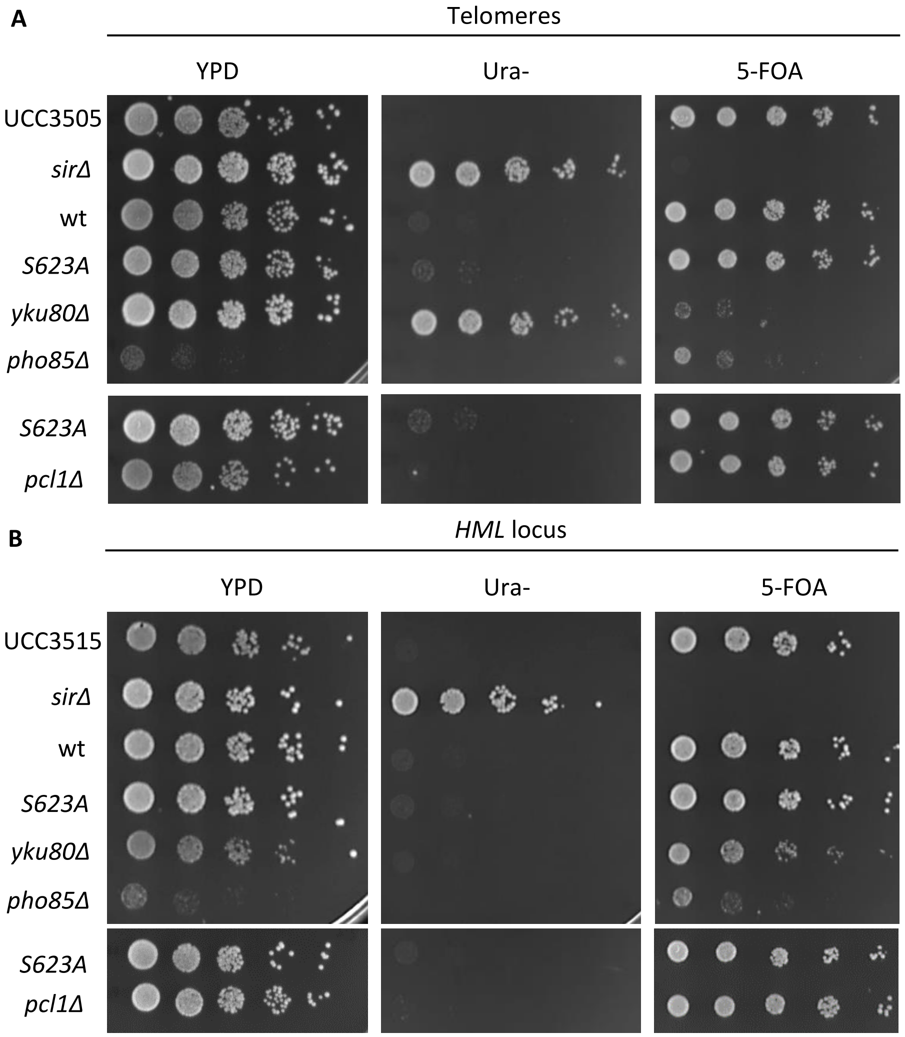
A
Telomeres
YPD
Ura-
5-FOA
UCC3505
sirΔ
wt
S623A
yku80Δ
pho85Δ
S623A
pcl1Δ
B
HML locus
YPD
Ura-
5-FOA
UCC3515
sirΔ
wt
S623A
yku80Δ
pho85Δ
S623A
pcl1Δ

Fig. 32. *yku80-S623A* genomic mutation does not interfere with gene silencing, neither at telomeres nor at *HML* locus. 10-fold serial dilutions of the exponentially growing noted strains were spotted on the indicated plates at an initial OD $_{\lambda 660}$ = 0.05. A. UCC3505 and B. UCC3515 are the original strains provided by Dr Belhumeur where *YKU80* has not been tagged with *KanMX* at the C-terminal end.

The silencing assay shows that the non-phosphorylatable mutant is unable to grow in an Ura- selective medium but capable of surviving in 5-FOA plates meaning that *yku80*-S623A fully silences *URA3* at both locations, the telomeres (Fig. 32 A) and the *HML* locus (Fig. 32 B).

sir2Δ cells perfectly grew in Ura- plates indicating the reduction of transcriptional gene repression already described in the literature (Chou, Li and Gartenberg, 2008).

Additionally, *pho85Δ* and *pcl1Δ* cells grow to the same extent both in YPD and 5-FOA but they are unable to grow in Ura-selective medium showing the same phenotype that *yku80*-S623A presents. Interestingly, *yku80Δ* cells are able to silence the *URA3* reporter gene when it is located in the *HML* locus but not at the telomeres where it shows the same phenotype as *sirΔ* cells do.

This result indicates that S623A mutation does not have an effect on Yku80 role in transcriptional gene repression at either the *HML* locus or telomeric region.

10. *yku80*-S623A does not present a shortening in telomere length

One of the mainly described functions of Yku80 is its role in telomere maintenance. Telomeres are the physical ends of chromosomes and its structure includes a 3’ single strand G-tail and the subtelomeric X and Y´ elements.

To check whether Yku80 phosphorylation at Ser623 has a role in protecting telomere length, I performed a southern blot to detect a Y´ specific sequence of yeast telomeres. As in Fig. 33, there has been reported in the literature a shorter telomeric length in cells lacking Yku80 (Boulton and Jackson, 1996; Gravel *et al.*, 1998; Nugent *et al.*, 1998). Moreover, the lethality of Yku80-deficient cells when exposed to 37ºC as the growth temperature was shown to be the result of telomeric shortening (Gravel and Wellinger, 2002). Similar telomere length is displayed by the wild type and S623A (Fig. 30).

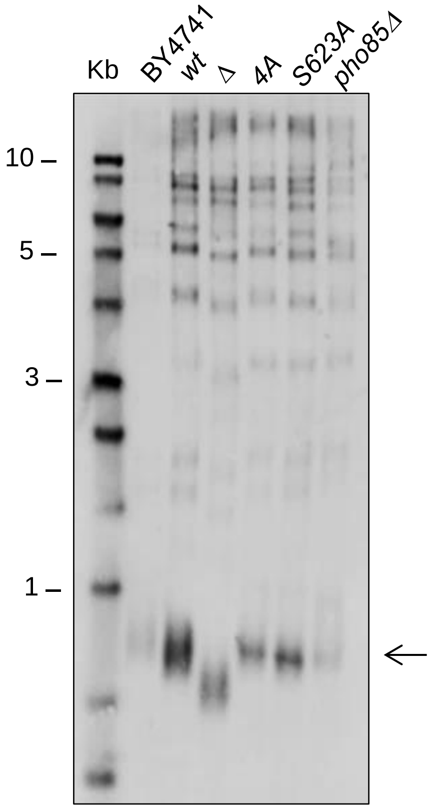

Fig. 33. *yku80-S623A* displays normal telomere length. Southern blot of *Xho*I-digested genomic DNA probed with Y′ specific sequences of yeast telomeres from the noted strains. Arrow indicate the specific fragment detected by the probe.

This result confirms that the phosphorylation of Yku80 at Ser623 is not involved in the regulation of telomere length.

11. *yku80*-S623A shows an increase in NHEJ events

The next Yku function I checked was Yku80's role in DNA repair. Aside from telomere maintenance and gene silencing, Yku proteins are involved in a DNA repair pathway called NHEJ. As HR is restricted to the S/G2 phase of the cell cycle where DNA has been replicated, NHEJ is the main mechanism in charge of DSB repair during G1 even though it is active throughout the cell cycle.

To determine whether the phosphorylation at S623 has a role in NHEJ, I used a method first described in Milne (1996). Briefly, the replicating yeast plasmid pRS416 (*URA3*) was *Bam*HI-digested and separated by DNA electrophoresis. This step allows enhancement of the isolation of mainly *Bam*HI-linearised pRS416 which was transformed into Yku80, *yku80-S623A* and *yku80Δ* cells. Only those cells which re-ligate the plasmid will grow in an Ura- selective medium. To control yeast transformation efficiency, non-digested pRS415 (*LEU2*) was transformed together with *Bam*HI-linearised pRS416. Cells were plated on Ura- and Leu- plates and incubated at 30ºC for 48h. NHEJ efficiency was calculated as the ratio of Ura+ to Leu+ colonies.

As described in the literature, there is a decrease in the number of re-ligated plasmids by *yku80Δ* cells when comparing with the wild type (Boulton and Jackson, 1996). In addition, I observed an interesting 2.5-fold increase of NHEJ events in *yku80*-S623A (Fig. 34).

To further support this result, I performed another assay to evaluate DNA repair by NHEJ described in Kim and Haber (2009). This method consists of a genetically modified strain bearing a single HO cleavage site the *MATα* locus (ChIII). In addition, the intrachromosomal homologous sequence was deleted so DNA damage cannot be repaired by HR. HO expression is induced by galactose (Fig. 35 A).

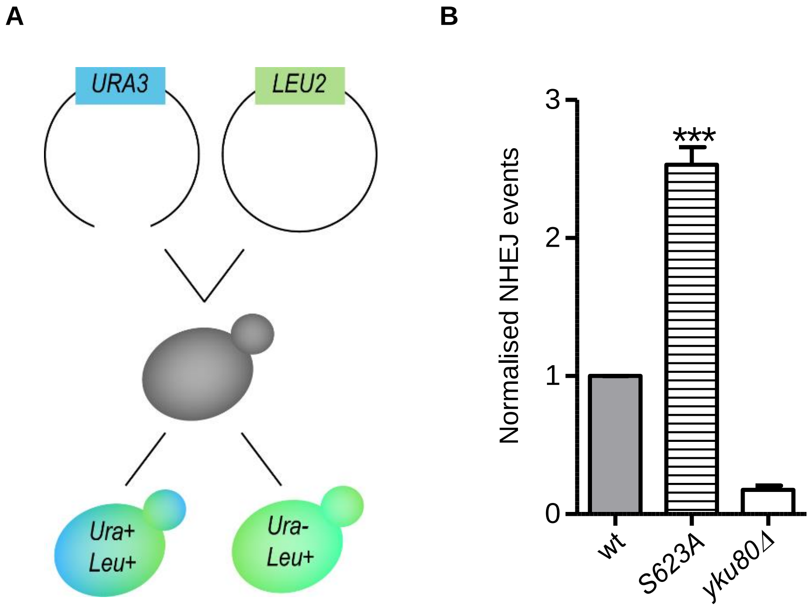

Fig. 34. *yku80*-S623A mutant cells display enhanced NHEJ. A. Schemati representation of the experiment. Cells were transformed with *BamHI*-digeste pRS416 (*URA3*) and with non-digested pRS415 (*LEU2*) and incubated at 30º for 48h. B. Quantification of NHEJ events calculated as the ratio of Ura + to Le + colonies. The bar graph shows the average and SD of four independen experiments with two internal duplicates. P value was calculated by two-taile paired t-test*.* (***)*p*< 0.0001. Values were normalised to wild type = 1.

I plated cells from an exponentially growing culture in either 2% glucose or 2% galactose SD plates and incubated at 30° for 72 h. I observed an interesting 0.5-fold increase of NHEJ events in *yku80*-S623A compared to the wild-type strain (Fig. 35 B).

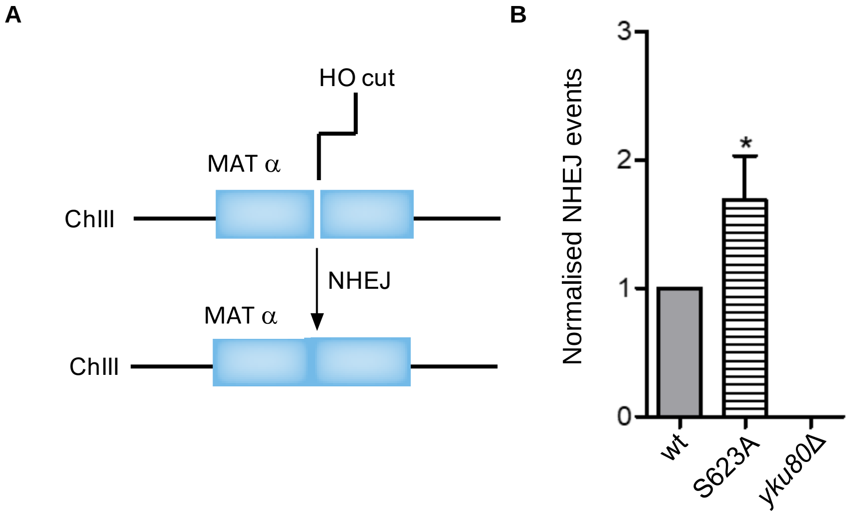

Fig. 35. *yku80*-S623A cells present enhance NHEJ. A. Schematic representation of the assay. B Quantification of NHEJ repair events was measured as the ratio of colonies grown in galactose (where HO is induced) to colonies on glucose plates. The bar graph represents the average and SD of four independent experiments with two internal duplicates. P value was calculated by two-tailed paired t-test. (*)$p< 0.05$ Values were normalised to wild type = 1.

In addition to the two previous systems, I performed another assay named ‘‘suicide system’’ (Palmbos, Daley and Wilson, 2005). Here, DNA damage is also caused directly in a cell’s genome. The suicide deletion method is based on strains bearing two HO cleavage sites flanking the endonuclease gene which is under the control of a GAL promoter. Once HO is induced, the endonuclease snips the genome of the cells and a fragment is excised (Fig. 36 A). The main mechanism to repair the DNA damage caused by the HO is NHEJ as there is not an available homologous sequence to recombine.

I obtained a 50-fold increase of NHEJ events in the non-phosphorylatable version of Yku80 (Fig. 36 B). I performed the assay with two different mutant and wild-type clones and, as shown in Fig. 36 B the difference achieved is clone independent.

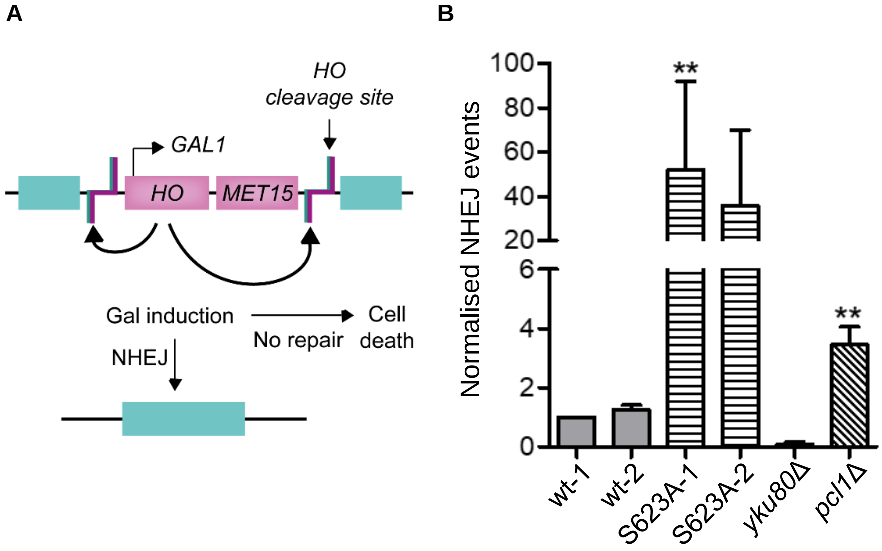

Fig. 36. *yku80*-S623A cells display increased NHEJ. A. Schematic representation of suicide deletion system modified from (Palmbos, Daley and Wilson, 2005). B Quantification of NHEJ repair events was measured as the ratio of colonies grown in galactose (where HO is induced) to colonies on glucose plates. The bar graph represents the average and SD of at least three independent experiments with two internal duplicates. P value was calculated by two-tailed paired t-test. (**)$p< 0.005$ Values were normalised to wild type = 1.

Moreover, I checked if *PHO85* deletion also increases NHEJ but *pho85Δ* cells were not able to grow on galactose. Because *pho85Δ* cells grow poorly on glucose, have aberrant morphologies, and are larger than wild-type *cells* (Measday *et al.*, 1997), I decided to perform the experiment with the activating cyclin of Pho85, Pcl1. *pcl1Δ* cells also grow poorly on galactose plates, but I was able to determine that they show more NHEJ that the wild-type cells (Fig. 36 B).

The three approaches have led to the same conclusion: the non-phosphorylatable version of Yku80 shows an increase in the number of NHEJ events performed by the cells compared to the wild type.

12. Repair fidelity is not impaired in *yku80*-S623A

NHEJ is considered an error-prone DNA repair system employed to repair DSBs. Since NHEJ does not use a homologous template, it can result in DNA mutations.

To evaluate whether yku80-S623A has an effect on DNA repair fidelity, I used a modified version of pRS415 (*LEU2 marker*) I engineered (Fig. 37 A). *URA3* marker was cloned in pRS415 multicloning site and later, the plasmid containing both genes *LEU2* and *URA3* was digested with *Nco*I (which can only cleavage inside *URA3* marker). *Nco*I-digested modified version of pRS415 were transformed and DNA repair fidelity was measured as the ratio Ura+ to Leu+ colonies. Only colonies which have performed error-free NHEJ events will be able to grow in uracil auxotrophic plates. As presented in Fig. 37 B, there is less than a 0.5-fold increase in yku80-S623 compared to the wild-type version; however, it is not statistically significant.

Moreover, *yku80Δ* shows a decrease of DNA repair fidelity, probably due to its inability to repair the *Nco*I-digested plasmid by NHEJ pathway and the use of alternative, less efficient DNA repair mechanisms.

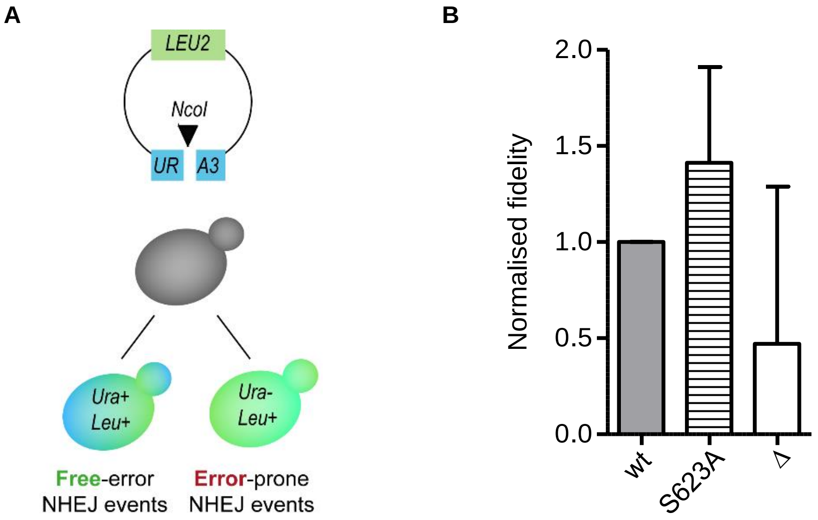

Fig 37. Plasmid repair fidelity is independent of Yku80 phosphorylation at Ser623. A. Schematic representation of the experimental procedure. Cells were transformed with *Nco*I-digested modified-pRS415 and incubated at 30ºC for 48h. B. Repair fidelity was calculated as the ratio of Ura+ to Leu+ cells. The bar graph shows the average and SD of three independent experiments with two internal duplicates. P value was calculated by two-tailed paired t-test. Values were normalised to wild type = 1.

13. Homologous recombination is reduced *in yku80-S623A* mutants

As previously explained in the introduction, there is a balance between NHEJ and HR through the different phases of the cell cycle. Here, I have described an increase in NHEJ events when Yku80 cannot be phosphorylated at Ser623. Next, I wondered if the increase in NHEJ repair is followed by a reduction in HR. To test this hypothesis, I performed an assay described in Hentges (2014) based on genome integration of a *URA3* marker gene from an integrative plasmid (YIplac211). Integrative plasmids, also called suicide vectors, are unable to replicate in the destination host and therefore must integrate into the genome. Briefly, *Eco*RV-disgested integrative YIpac211 plasmid was transformed together with non-digested pRS415 (*LEU2*) to control yeast transformation efficiency. The *URA3* integration rate was measured as the proportion of Ura+ to Leu+ colonies (Fig. 38 A). There are less than half of the HR events taking place in the *yku80*-S623A mutant compared to the wild-type strain (Fig. 38 B).

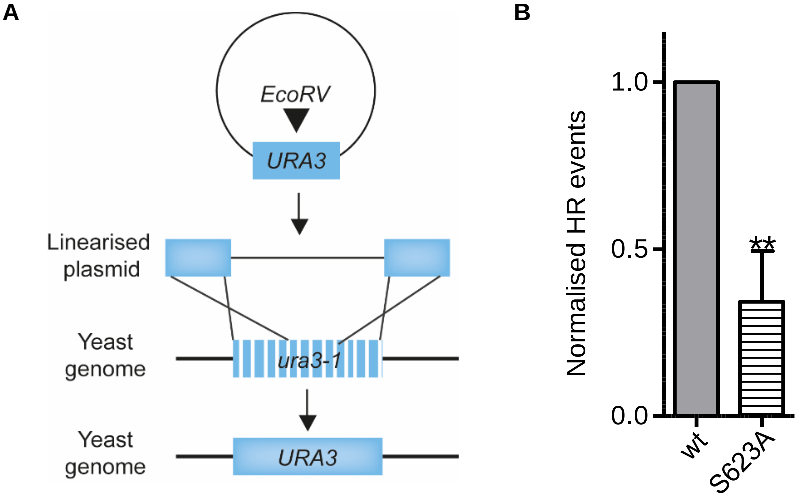

Fig. 38. *yku80*-S623A strain shows reduced HR plasmid repair events. A. Schematic representation of the experimental procedure. First, YIplac211 plasmid is linearised with *Eco*RV and transformed in yeast cells together with non-digested pRS415. B. Relative repair efficiency was measured as the ratio of Ura + to Leu + colonies. The bar graph represents the average and SD of four independent experiments with two internal duplicates. P value was calculated by two-tailed paired t-test. (**)*p*<0,005. Values were normalised to wild type = 1.

As I did with NHEJ experiments, to further support this result, I employed another method described in (Kim and Haber, 2009) where DNA damage is induced in the yeast genome.

This new method consists of a genetically modified strain where a single cut takes place in the genome at the *MATα* locus (ChIII) after HO expression is induced by galactose (Fig. 39 A). The intrachromosomal homologous sequence was deleted so the recombination occurs with homologous sequence at *MATa* (ChV). In addition, the HO recognition site at *MATa* was mutated and the HO endonuclease cannot cleavage the DNA again.

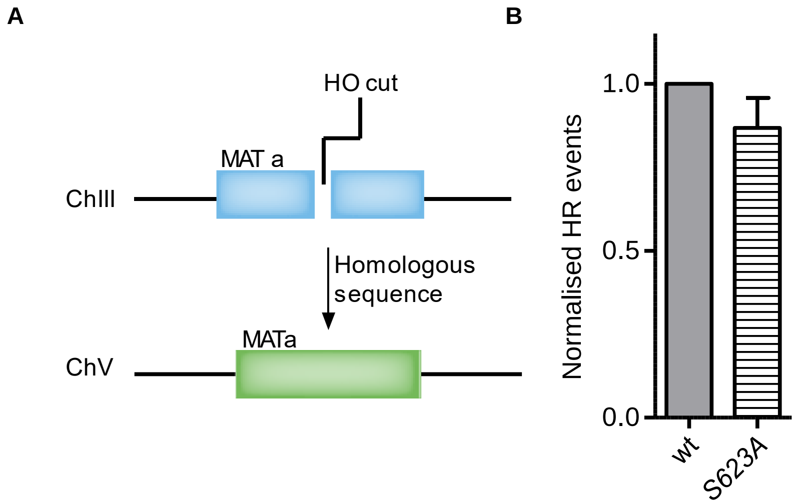

Fig 39. *yku80*-S623A strain shows reduced HR events in the DSB-induce genome system. A. Schematic representation of DSB-induced genom system adapted from Kim and Haber (2009). The DSB is repaired by ectopi homologous recombination using MATa sequence on ChV as a template. MAT carries a mutated HO recognition site that cannot be cleavage by th endonuclease. B. Exponentially growing cells were plated onto either galactos or glucose plates. Relative repair efficiency was calculated as the ratio galactose to glucose colonies. The bar graph represents the average and S of four independent experiments with two internal duplicates. Values wer normalised to wild type = 1.

There is an approximately 20% reduction in HR event performed in the non-phosphorylatable mutant when compared to wild-type cells (Fig 39 B). However, the reduction is not statistically significant. Nevertheless, both approaches have shown a decrease in HR events which correlates with the higher NHEJ activity in *yk80*-S623A *cells.*

14. There are no differences in cell survival rates between *yku80-S623A* and wild-type strains when DNA damage is induced in an asynchronous culture

Until now I have examined DSBs repair by three artificial systems: digested plasmids (Fig. 34, 35 and 36) or genome cuts (one or two) by the HO endonuclease (Fig 38 and 39). Next, I wanted to evaluate cell viability by causing DNA damage with two chemical agents which mimic X-ray and IR radiation. I tested MMS and bleomycin at different concentration and incubation times to see how cells respond to the damage. As *yku80*-S623A has NHEJ enhance, I expected to see some differences in cell survival amongst the wild type and the mutant.

MMS is an alkylating and carcinogenic agent considered an X-ray mimetic (Miyamae *et al.*, 1997). This compound methylates DNA leading to bulky lesions and distortion of the DNA helix which can cause DSBs. First, I tested the cell response to 0,01, 0,03 and 0,1% of MMS at different incubation times (60, 120, 180 and 240 mins). An approximately 70% survival rate was obtained when Yku80 wild type was incubated with 0,01% MMS for 120 min. Higher concentrations of MMS at the same time triplicates cell death and at longer incubation times the rate of mortality is even higher which might make it difficult to see differences between the wild-type and the non-phosphorylatable mutant.

Yku80 wild type and *yku80*-S623A cells from mid-log phase asynchronous cultures were incubated with 0,01% MMS for 120 min. Interestingly, there was not a statistically significant difference in cell survival rates amongst the wild-type and non-phosphorylatable mutant (Fig. 40). A possible explanation for this behaviour might be that MMS is not causing enough DSBs to see any differences. Perhaps, as MMS does not provoke DSBs lesions straight away, 0,01% MMS and 120 min is not enough to lead to DSBs and DNA lesions are first repaired by other types of DNA repair mechanisms (BER, NER…).

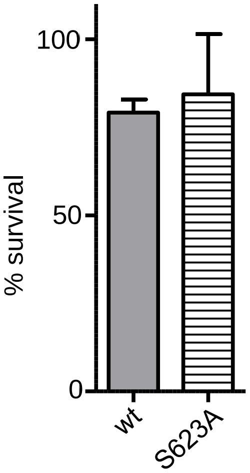

Fig. 40. *yku80*-S623A cell viability is not affected after MMS treatment in an asynchronous culture compared to the wild-type strain. Yku80 and *yku80*-S623A mid-log phase culture were incubated with 0,01% MMS for 120 min. Right after MMS treatment cells were plated onto glucose plates and incubated at 30ºC for 48h. Percentage of survival was measured as the number of colonies after MMS treatment relative to the non-treated cells. The bar graph represents the average and SD of three independent experiments with two internal duplicates.

As I hypothesised that the reason why I did not find any differences in cell survival rates after MMS treatment was due to 0,1% MMS not being able to cause DBSs, I decided to try another chemical agent, bleomycin. Bleomycin is an IR-mimetic agent which binds transition metals and oxygen and once interacting with the DNA results in the formation of DSBs. For this reason, bleomycin might be a more suitable drug to cause several DSBs in the DNA.

Once more, I tested the cell response to different concentrations (3, 30 and 300 µg/ml) and incubation times (30, 60, 90 and 120 mins) of the drug. Smaller concentration of bleomycin did not have any effect on cell survival. After 30 min incubation with either 30 or 300 µg/ml of bleomycin, cell survival was reduced. However, only a 20% mortality rate was found when incubating cells with 30 µg/ml of bleomycin compared to more than 50% with the highest bleomycin concentration, 300 µg/ml. Since a low cell mortality did not allow me to identify any differences after MMS treatment, I picked 300 µg/ml of bleomycin and 30 min as the concentration and time to test cell response in both the wild-type and *yku80*-S623A mutant.

Again, there was a similar cell survival rate in both the wild-type and the non-phosphorylatable Yku80 mutant (Fig. 41).

A possible reason why I did not observe any differences in cell viability might be related to inducing DNA damage in a mid-log phase asynchronous culture. From the literature I know that depending on the cell cycle phase the cells are, a different repair mechanism intervenes to repair the DSBs. Considering this, any phenotypic difference between the wild-type and non-phosphorylatable mutant might be hidden and underestimated in an asynchronous culture.

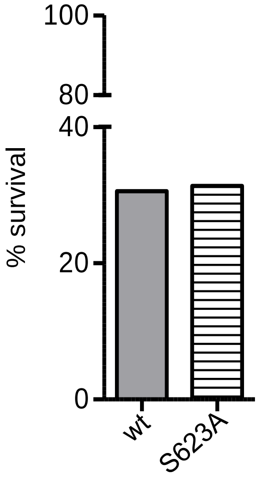

Fig 41. *yku80*-S623A viability is not affected after Bleomycin treatment in an asynchronous culture compared to the wild-type strain. Yku80 and *yku80*-S623A mid-log phase culture were incubated with 300 µg/ml for 30 min. In both cases after bleomycin treatment, cells were plated onto glucose plates and incubated at 30ºC for 48h. The bar graph represents a single experiment with three internal replicates.

15. *yku80*-S623A shows reduced viability when DNA damage is caused by bleomycin in G2

As I explained in the introduction, NHEJ is the only pathway operating in G1 to repair DSBs. For this reason, the next approach consisted of inducing DNA damage to G_1 and G2 synchronised cells with bleomycin. Even though I did not observe differences with either MMS or bleomycin in asynchronous cultures, I decided to move forward with bleomycin as the DSB DNA-damage agent as it is widely used in the literature to induce DSBs in cells (Olive and Banáth, 1993; Boger and Cai, 1999; He *et al.*, 2001; Tounekti *et al.*, 2001; Aouida *et al.*, 2004). First, I synchronised cells in G1 with α-factor. Ten min after α-factor release, I added 300µg/ml of bleomycin to the culture and incubated cells with bleomycin for 30 min.

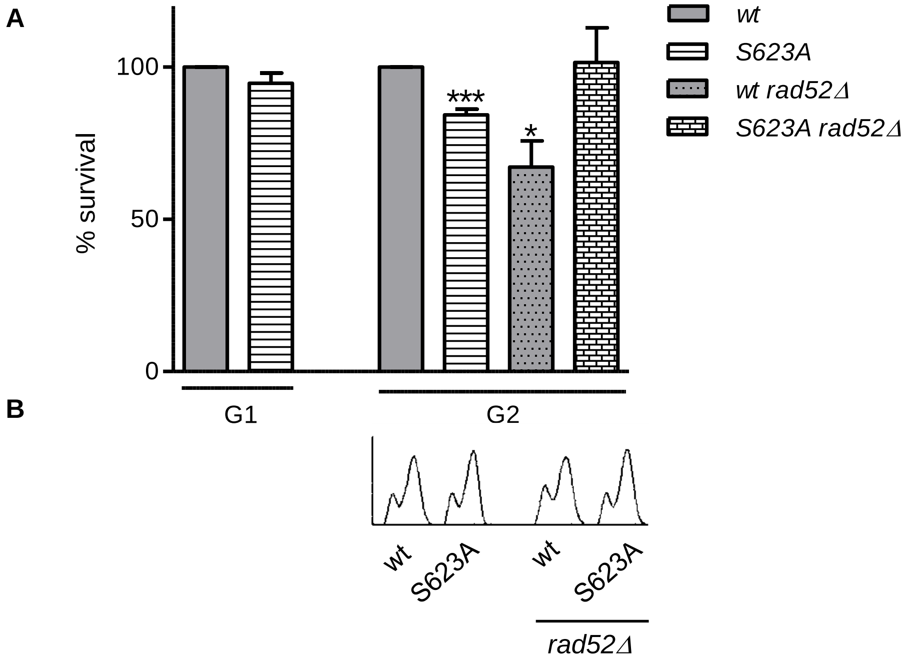

Fig 42. *yku80*-S623A shows reduced viability in G2 after bleomycin treatment. A. Cells were synchronised in G_1 with α-factor. Cell release and DNA damage was produced after 10 min (G_1) and 70 min (G_2). DSBs were induced with 300 µg/ml of bleomycin for 30 min. After DNA damage induction, cells were plated on glucose plates and incubated at 30ºC for 2 days. Percentage of survival was measured as the number of colonies after bleomycin treatment relative to the non-treated cells. The bar graph represents the mean±SD of a minimum of three independent experiments with internal duplicates. P value was calculated by two-tailed paired t-test. (*)p<0,05 and (***)p<0,0001 were considered statistically significant. Values were normalised to wild type = 1. B. FACS analysis from cells 70 min after α-factor release right before inducing DNA damage with 300 µg/ml of bleomycin for 30 min.

I observed a similar survival rate between the wild type and *yku80*-S623A (Fig. 42 A) as it happened when I induced DNA damage in an asynchronous culture (Fig. 41). However, when DNA damage was induced at the moment where most cell population was in G2 (where HR takes place) (Fig. 42 B), there was a 20% reduction of cell survival in *yku80*-S623A cells (Fig. 42 A).

To confirm whether this reduction of cell survival is related to the decrease of HR events in *yku80*-S623A, I deleted *RAD52* gene. Rad52 is a protein with an essential role in HR. It promotes strand exchange by recruiting Rad51 to the damaged area. Using the same experimental design, I induced DNA damage with bleomycin when there were a majority of cells in G_2. As expected, there is a reduction in *rad52Δ* Yku80 wild type viability since the mutation of *RAD52* interferes with HR process (Fig. 42 A). Moreover, *yku80*-S623A viability is not affected by RAD52 deletion probably by the increase of NHEJ repair described earlier (Fig. 34, 35 y 36).

16. Yk80 phosphorylation at the C-terminal domain might be a conserved function

Ku proteins are highly conserved among all organisms, however, in terms of aminoacidic sequence, they show a modest level of similarity. Nevertheless, it has been described that Ku80 proteins are well conserved functionally and structurally (Doherty, Jackson and Weller, 2001; Jones, Gellert and Yang, 2001; Walker, Corpina and Goldberg, 2001; Krishna and Aravind, 2010).

As mentioned in section 2, Ku80 has 3 well differentiated domains and the phosphorylation site found was located at the C-terminal part of the yeast protein in a disordered region.

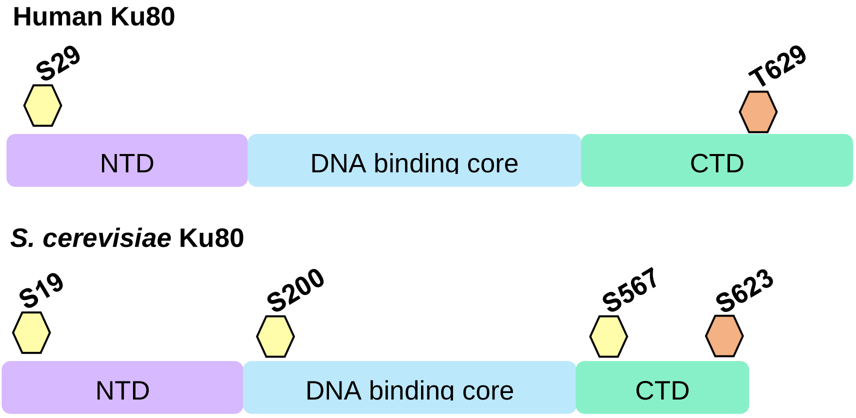

Fig 43. Schematic representation of Ku80 domains among species. hKu80 and Yku80 domains are represented in different colours. S/TP CDK consensus phosphorylation sites are specified on top of the hexagon.

Human Ku80 (hKu80) also has 3 protein domains and only 2 consensus phosphorylation sites for CDK among the sequence (Fig. 43). The first consensus phosphorylation site for CDK in human Ku80 sequence is in the N-terminal domain and the second one happens to be in a disordered region within the C-terminal domain. Even though the TP motif is not exactly in the same position, the modest degree of conservation leads me to wonder if the mechanism might be conserved.

CDK5 is considered the Pho85 ortholog but this CDK is activated by non-cyclin proteins (Humbert, Dhavan and Tsai, 2000; Tarricone *et al.*, 2001). However, there are other members of the CDK5 family which are activated by cyclins. This is the case of CDK16 which is known to interact with cyclin Y (Mikolcevic *et al.*, 2012). Cyclin Y happens to be the closest related cyclin to yeast Pcl1/2 (Mikolcevic, Rainer and Geley, 2012; Malumbres, 2014), therefore it would be the best candidate to assay whether it can phosphorylate hKu80.

To produce hKu80, *KU80* was amplified from A549 cDNA by PCR and I cloned *KU80* in a pGEX vector. I purified hKu80 from bacteria to perform an *in vitro* kinase assay using CDK16. However, the amount of protein purified was insufficient to perform an *in vitro* kinase assay and the little amount I obtained degraded very rapidly (data not shown). For this reason, I was unable to carry out the assay.

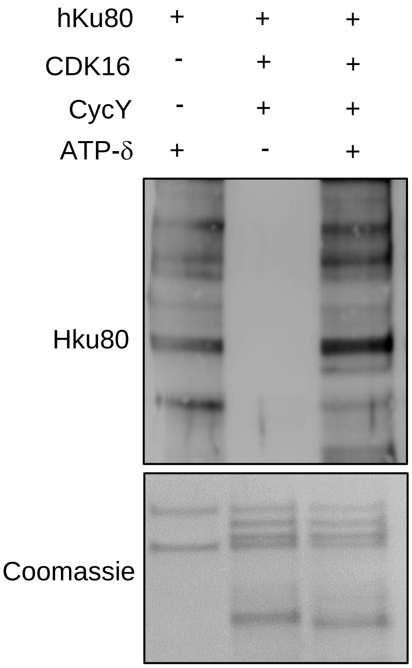

Fig. 44. Recombinant HIS-hKu shows a contaminant kinase activity *in vitro*. Western blot of the *in vitro* kinase assay. Bacteria produced recombinant GST-CDK16 and GST-cyclinY (CycY) were assayed with insect-cells recombinant HIS-hKu80. Coomassie staining of the membrane is presented as a load control.

Nevertheless, the group of Dr Jean-Yves Masson provided me with Ku heterodimer purified from insect cells. As shown in the first line of the Coomassie staining in Fig.44, the amount of hKu to perform the *in vitro* phosphorylation assay is not limiting.

The *in vitro* phosphorylation assay showed a phosphorylation activity in the first line where Ku heterodimer was exclusively incubated with ATP-δ without the CDK-cyclin complex (Fig.44). In fact, the first lane shows the same phosphorylation pattern obtained when hKu was incubated with the CDK-cyclin (Fig. 44). There is no phosphorylation in the second lane where hKu was incubated with the CDK-cyclin complex without ATP-δ.

One possibility that might explain why there is phosphorylation activity in the absence of the CDK-cyclin complex is the presence of an additional protein apart from the Ku. It is highly possible that the 6xHIS tag system used to purify hKu also pulled down a protein that interacts with hKu and most likely has kinase activity.

I pursued different approaches to try and eliminate this contaminant kinase activity. The first approach was boiling the protein at 95ºC for 5 min to try and denature the protein and the second was to incubate the protein with a DNA-PK inhibitor called NU7441. hKu was boiled at 95ºC for 5 min prior to incubation with the rest of the proteins to perform the phosphorylation assay.

The second line of the western blot shows boiled hKu incubated with ATP-δ. The kinase activity observed in the first line where hKu80 has not been boiled at 95ºC has disappeared in the second line (Fig. 45). However, the phosphorylation pattern also vanished when hKu was incubated with ATP-δ and the CDK-cyclin complex. This could mean that I might not only denature the contaminant protein but also hKu. Unfortunately, this approach did not work, and I was not able to eliminate the contaminant kinase activity without affecting the hKu heterodimer.

There are many possible kinases that could have been purified together with the heterodimer, but it is most likely to be DNA-PK. As explained in the introduction, DNA-PK is a kinase requires for NHEJ in human cells and it is known to interact with Ku heterodimer and form a complex.

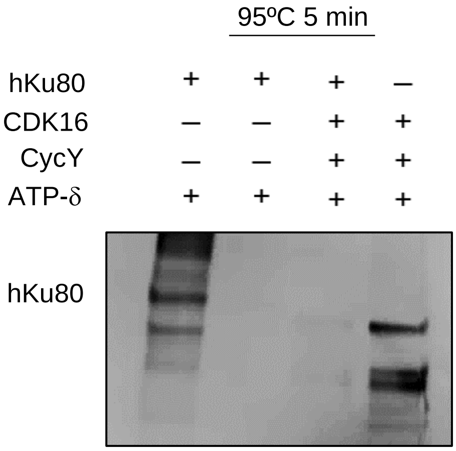

Fig. 45. Denaturation of recombinant 6xHis-hKu80 results in missing phosphorylation *in vitro* activity. Western blot of the *in vitro* kinase assay. GST-CDK16 and GST- (CycY) were assayed with insect-cells recombinant HIS-hKu. hKu was cyclinY boiled at 95ºC for 5 min prior to *in vitro* phosphorylation assay.

The next strategy was to use a DNA-PK inhibitor, NU7441. NU7441 has been described as a highly specific inhibitor of the DNA-PK (Leahy *et al.*, 2004). NU7441 is an ATP-competitive inhibitor that binds to the ATP-binding cleft of the kinase.

I tried three different concentrations of NU7441 and as shown in Fig. 46 none were able to eliminate the contaminant phosphorylation activity. Unfortunately, none of the approaches solved the artefact and I was unable to assess whether any of the likely CDKs are able to phosphorylate hKu80.

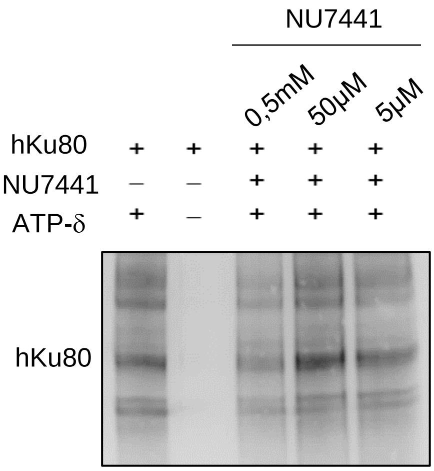

Fig. 46. NU7441 DNA-PK inhibitor is not able to disrupt kinase contaminant activity from purified recombinant hKu80. Western blot of the *in vitro* kinase assay. Insect-cells recombinant HIS-hKu80 was incubated at the indicated concentrations of NU7441 for 1 h before later incubation with ATP-δ at 37°C 1h.

17. Overexpression of Ku80^{T629A} increases sensitivity to bleomycin in cancer cell lines

Despite being unable to perform an *in vitro* hKu80 phosphorylation assay, I decided to study if there were any phenotypic relationship which would suggest the hKu80 phosphorylation function could be conserved. For this reason, the following strategy I pursued was to test the possible influence of KU80^{T629A} mutation on cell viability after bleomycin induced DSBs in different cancer cell lines available in the laboratory.

To analyse bleomycin sensitivity, I used pulmonary adenocarcinoma cell line (A549) and breast adenocarcinoma cell line MCF-7. First, I tested how non-infected cell lines responded to different concentrations of bleomycin to choose a concentration to perform the viability test. To analyse viability, I used the colony formation assay, an *in vitro* assay based on the ability of single cells to grow into colonies.

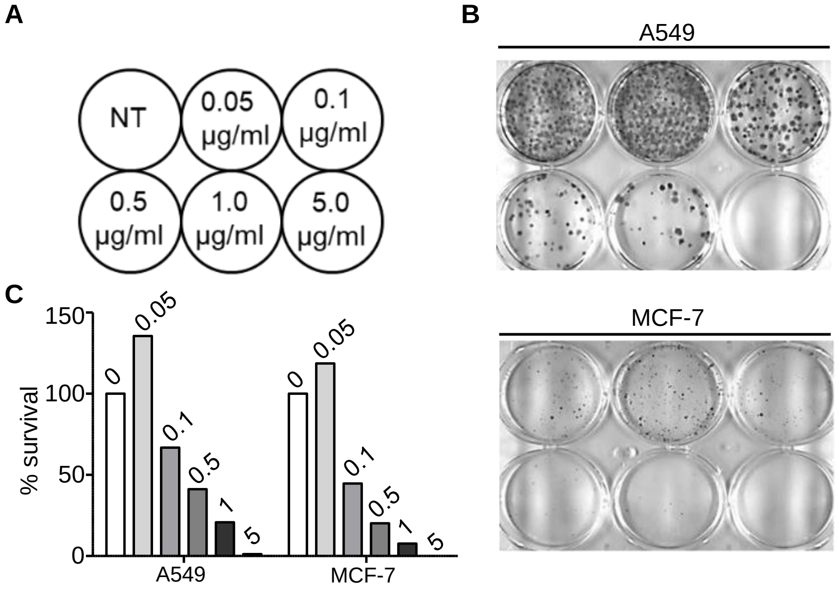

Fig. 47. A549 and MCF-7 cancer cell lines show a dose response effect to different concentrations of bleomycin. A. Schematic representation of the order in which concentrations were assayed. B. Cells were incubated at the indicated concentrations of bleomycin for 2h (A). Afterwards, cells were trypsinised, counted and seeded in 6-well plates at a density of: 1200 (A549) and 2500 (MCF-7). After 2 weeks incubation at 37°C cells were fixed and stained with crystal violet. C. Cells were counted, and cell survival was calculated as the ratio of bleomycin treated cells to non-treated cells. The bar graph represents cell survival from a single experiment. Bleomycin concentration corresponding to each percentage of cell survival is on top of each bar.

The smaller concentration of bleomycin (0.05 µg/ml) does not affect cell survival but when increasing the concentration to 0.1 µg/ml or higher, cell death raises in either A549 or MCF-7 (Fig. 47). I decided to use 0.1 µg/ml of bleomycin as the concentration to test Ku80^{wt} and Ku80^{T629A} cell viability because in both cell lines I obtained approximately a 50% rate of cell survival (Fig.47).

KU80 wild type was amplified from A549 cDNA. Mutation at threonine 629 was achieved by PCR using reverse primers carrying the mutation. KU80 wild type and T629A were cloned into the *Pme*I site in pWPI lentiviral vector. There is an overexpression of 25 to 50% of both Ku80^{wt} and Ku80^{T629A} in either A549 or MCF-7. This might be due to the low efficiency of lentiviral infection in the cells as shown by the α-GFP in Fig. 48.

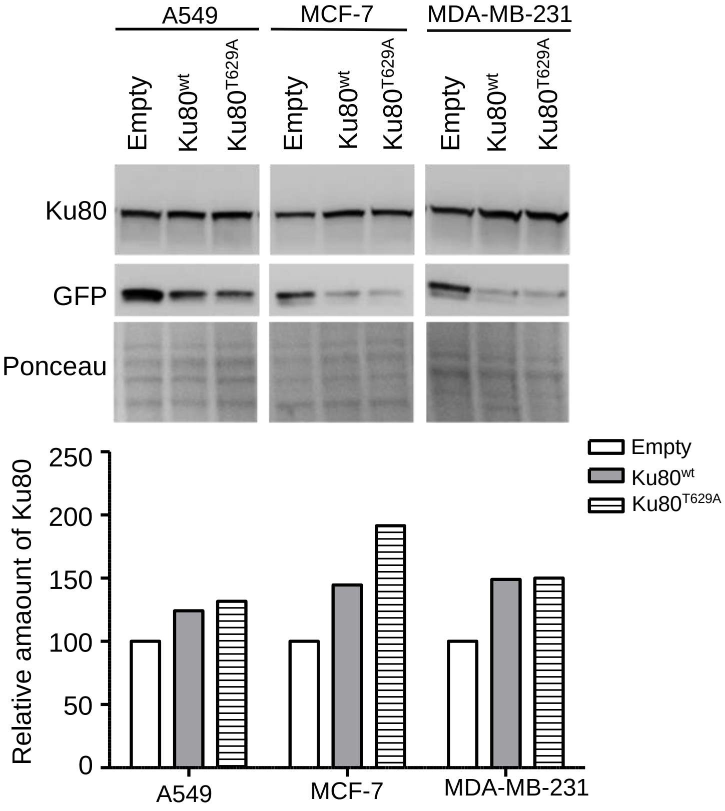

Fig. 48. Overexpression of Ku80^{wt} and Ku80^{T629A} in cancer cell lines. A. Western blot of the overexpression of Ku80^{wt} and Ku80^{T629A} in A549, MCF-7 and MDA-MB-231. The amount of Ku80 is detected by α-Ku80, α-GFP represents transfected cells and Ponceau staining of the membrane is shown as loading control. The bar graph shows quantification of the amount of protein detected in the western blot. Relative amount of protein was calculated as the ratio of Ku80 to the total amount of protein (Ponceau).

Next, I checked if the amount of overexpressed protein is enough to see a phenotypical difference amongst the wild-type and T629A mutant. Performing the same experimental procedure described earlier, I tested cell viability by colony formation assay. 48 h after cell infection, cells were incubated with 0.1µg/ml of bleomycin for 2 h. Afterwards, cells were washed, counted and seeded in 6-well plates as earlier described. Two weeks later cells were fixed and stained with crystal violet. To measure cell viability, I used two approaches. At first, I counted the number of cells in each well. However, sometimes I observed the same number of colonies but a difference in the size of them. The second strategy consisted of dissolving the crystal violet-stained cells with acetic acid and measuring the OD at 570 nm.

Overexpression of Ku80^{T629A} results in an increase of bleomycin sensitivity in A549 (Fig. 49 A). There is 20% more cell death when overexpressing Ku80^{T629A} than Ku80. MCF-7 cells show a similar tendency as the one I observed in A549 cells. Cells overexpressing Ku80^{T629A} survive 10% less than the ones overexpressing the wild-type version of Ku80 (Fig. 49 B). Even though I observed a difference, this one is not statistically different (Fig. 49 B).

As I had another breast cancer cell line available in the lab, I decided to check bleomycin sensitivity. MDA-MB-231 is breast adenocarcinoma cancer cell line. The main difference with MCF-7 cell line is that MDA-MB-231 is a triple-negative breast cancer cell line. This means that it lacks oestrogen (ER), progesterone (PR) and human epidermal growth factor 2 (HER2) receptors. On the other side, MCF-7 is ER+, PR+ and HER2-. This variation translates into the requirement of different drug treatments for effectiveness.

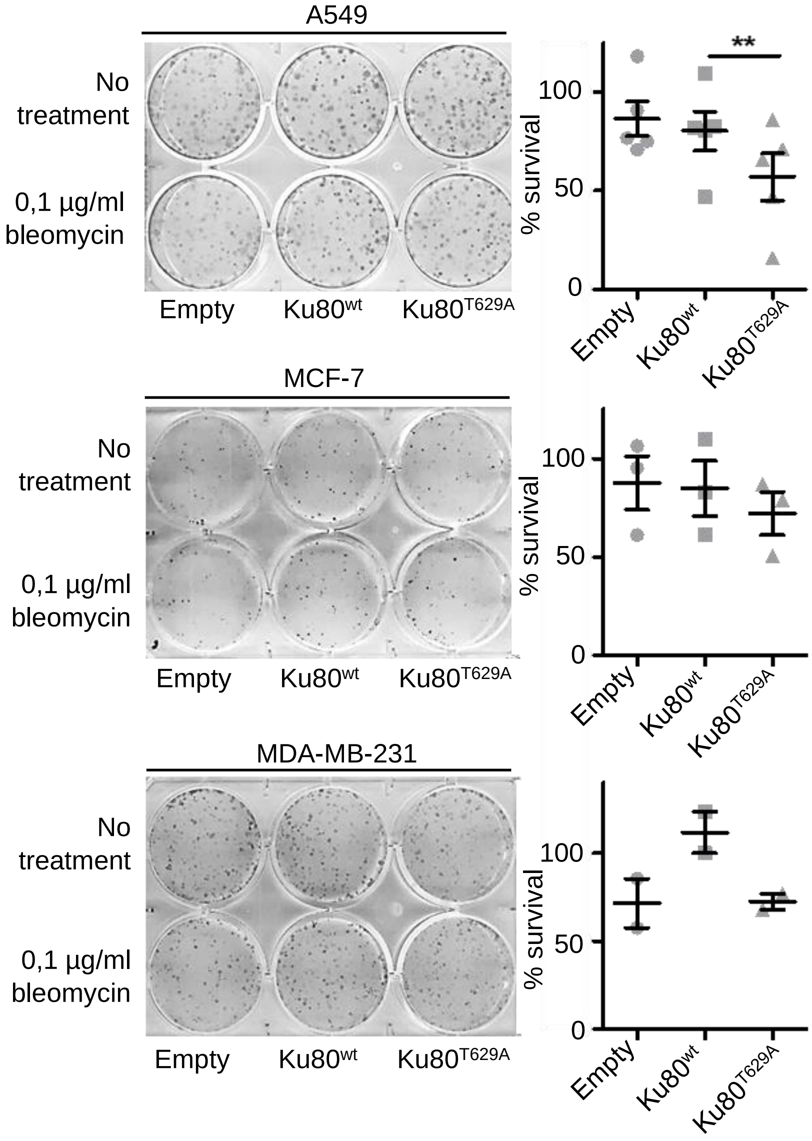

Fig. 49. Overexpression of human KU80^{T629A} increases sensitivity to bleomycin in cancer cell lines. Cancer cells lines A549 (A), MCF-7 (B) and MDA-MB-321 (C) were infected with pWPI bearing the construct Ku80^{wt} or Ku80^{T629A}. 48h after lentiviral infection, DNA damage was induced with 0,1µg/ml of bleomycin for 2h. Survival rate was calculated as the ratio OD$_{\lambda570}$ of colonies formed after bleomycin treatment to non-treated (nt) cells. The graphs represent

the mean±SD of 2-4 independent experiments with 2 internal duplicates. P value was calculated by two-tailed paired t-test and (**)*p*<0,005 was considered statistically significant.

I overexpressed Ku80^{wt} and Ku80^{T629A} in MDA-MB-231 and as it happens with A549 and MCF-7 I achieved approximately 50% of overexpression (Fig. 48) again, due to the little lentiviral infection of cells. Interestingly, overexpression of Ku80^{T629A} cells results in over 20% more cell death compared to the wild type that is not affected by bleomycin treatment (Fig. 49 C).

Overexpression of Ku80^{T629A} results in a slight increase of bleomycin sensitivity in different cancer cell lines. Moreover, A549 and MDA-MB-231 show a similar percentage of cell death (approximately 20%) (Fig.49 A y C) while MCF-7, even though it shows the same tendency, presents less cell death (10%) (Fig. 49 B).

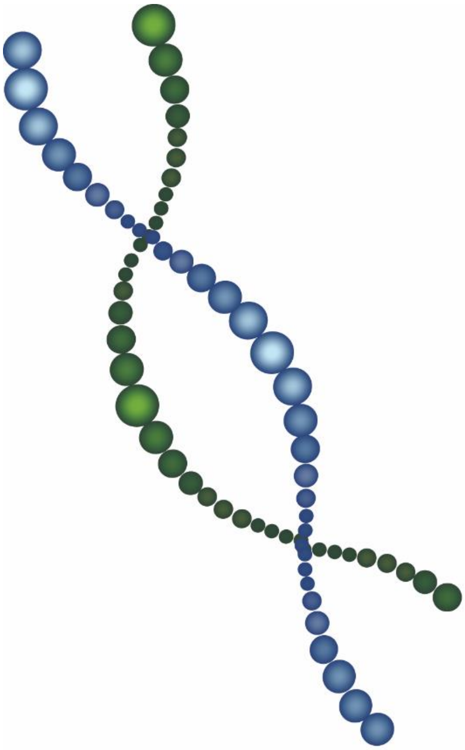

Discussion

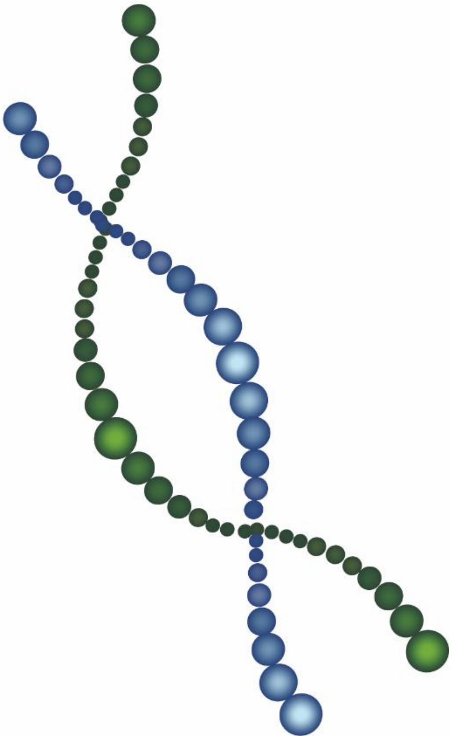

The DNA contains the genetic information in the cells to build and maintain each living organism. It is essential for a faithful cell duplication and therefore for life, to keep intact the integrity and stability of the genome (Krenning, van den Berg and Medema, 2019). However, the DNA is exposed to an extensive variety of damaging agents which can lead to DSBs, the most deleterious DNA lesions (De Bont and van Larebeke, 2004; Branzei and Foiani, 2010). For this reason, several DNA repair pathways exist and are active throughout the different stages of the cell cycle, permitting the cells to repair any possible damage which could end up compromising genomic integrity and cell viability (Krenning, van den Berg and Medema, 2019).

DNA repair mechanisms are tightly regulated and interconnected with the cell cycle (Hakem, 2008). The CDKs are the proteins responsible for coordinating, amongst other processes; the DNA repair pathways such as NHEJ and HR, according to the cell-cycle stage (Zhao *et al.*, 2017). In this study, I suggest a possible mechanism by which the cell cycle machinery regulates the activity of one of the key proteins of NHEJ, Yku80.

1. A cyclin-dependent kinase complex phosphorylates Yku80

Yku80 is a protein with four S/TP consensus motifs for CDK phosphorylation (Fig. 25). However, phosphorylation has not been described as a post-translational modification

(PTM) to control Yku80 function. The *in vitro* phosphorylation assay I performed showed that the Pcl1-Pho85 complex is capable of phosphorylating Yk80 (Fig. 24). The evidence presented in both the *in vitro* (Fig. 26) and *in vivo* phosphorylation assay by either Phostag (Fig. 27) gel or 2D-electrophoresis (Fig. 28), confirmed the Ser623 as the residue phosphorylated in the Yku80 protein. I described Yku80 *in vitro* and *in vivo* phosphorylation by Pho85 however there is another CDK involved in the cell cycle progression in Yeast, Cdc28. Even though I have not checked if Cdc28 is able to phosphorylate Yku80, the result presented in the *in vivo* phosphorylation assay, where *pho85Δ*, *yku80*-S623A and wild type alkaline phosphates treated cell extracts showed the same migration pattern, suggests Pho85 might be the CDK responsible for Yku80 phosphorylation.

The possibility that Yku80 could be a specific substrate of Pho85 raises awareness of the importance of this CDK, which was previously considered to have a specific role in the cell cycle regulation (Jiménez *et al.*, 2013). There is evidence that most of the Pho85 substrate that plays a role in the transition from G1 to S phase are also substrates of Cdc28 (Nishizawa *et al.*, 1998; Measday *et al.*, 2000; Jackson, Reed and Haase, 2006; Huang, Friesen and Andrews, 2007). However, recent studies have shown a more specific role of Pho85. The group of Dr Stephen J. Kron demonstrated that Pho85 has a specific role in the regulation of G1 checkpoint response after DNA damage by Sic1 phosphorylation (Wysocki *et al.*, 2006). The Cln3 cyclin was described as a molecular target of Pho85 (Truman *et al.*, 2012; Menoyo *et al.*, 2013). By Pho85 phosphorylation, Cln3 is protected from proteasome degradation which is essential for Cln3 accumulation before resuming cell cycle progression after phosphate starvation (Menoyo *et al.*, 2013). Another example of Pho85 specificity was recently described in Mirallas et al 2018 where Ran-GTPase Gsp1, a component of nuclear pore complexes required for the exchange of molecules between the nucleus and cytoplasm, was described as a Pho85 substrate (Mirallas *et al.*, 2018). All this evidence demonstrates that even though Pho85 shares some substrates with Cdc28 its function is different and, in some scenarios Pho85 has been shown to play an essential role.

2. Physiological relevance of Yku80 phosphorylation by Pcl1-Pho85

Yku80 is a subunit of the Ku heterodimer that binds double-stranded DNA with high affinity (Arosio *et al.*, 2002). The Ku heterodimer participates in many processes thanks to its ability to bind dsDNA in a sequence independent manner (see introduction section 7.2). I analysed the possible physiological relevance of Yku80 phosphorylation in most of the processes where the Ku heterodimer participates. First, I determined that S623A mutation does not interfere with the amount of Yku80 protein produced (Fig.30), its localization (Fig.31) and functionality (Fig.29). Based on the results obtained, I can conclude that the mutation at Ser 623 produces a functional protein that shows the same localisation pattern as the wild-type strain.

Telomere maintenance is one of the main functions of the Ku heterodimer. Ku binds to telomeres to prevent telomere fusion and loss (Samper *et al.*, 2000), DNA resection and to protect telomeres from DNA repair mechanisms (Gravel *et al.*, 1998). By southern blot analysis, I evaluated telomere length in *yku80*-S623A. The non-phosphorylatable mutant showed similar telomere length to the wild type (Fig. 33). As previously described in the literature, *yku80Δ* presented shorter telomeres (Mozdy, Podell and Cech, 2008) compared to the wild-type strain suggesting that the phosphorylation of Yku80 by Pho85 does not regulate Yku80 function in telomere maintenance.

The Ku heterodimer is also involved in gene silencing at the telomeres (Mishra and Shore, 1999; Roy *et al.*, 2004). It has been described that mutations in Ku80 interfere with its function in telomere silencing (Lopez *et al.*, 2011). I found no differences in gene silencing between the wild-type strain and the non-phosphorylatable mutant (Fig. 32). *yku80*-S623A is capable of fully silencing the *URA3* gene in both loci. This result indicates that Yku80 phosphorylation at Ser623 does not regulate Yku80 function in gene silencing. All the points discussed above suggest that Yku80 phosphorylation by Pcl1-Pho85 does not regulate Yku80 function in either telomere protection and maintenance or gene silencing.

3. An alternative mechanism for DSB repair regulation by the cell cycle machinery

There are two major pathways to repair DSBs in the cells: HR and NHEJ. In the early ‘80s Szostak and colleagues described HR as a mechanism for DSBR by which a double-strand gap in the DNA can be repaired using a homologous sequence as a template to retrieve the sequence information that was lost at the break point (Orr-Weaver, Szostak and Rothstein, 1981; Orr Weaver and Szostak, 1983). Moreover, they hypothesised that the DNA flanking regions of the gap might define the mechanism for DNA repair. Only a few years later, Moore and Haber introduced the term of NHEJ to refer to a process where both ends of the DSB are re-joined with no regard for homology (Haber and Moore, 1996). As NHEJ does not require a homologous sequence for DNA repair, it operates throughout the cell cycle while HR is restricted to the S and G2 phases where the homologous sequence is available (Takata *et al.*, 1998). Both mechanisms play an important role in DSBR and the balance between both pathways is essential for genomic stability and integrity.

3.1 DNA DSB repair pathway choice

The cell cycle phase determines the availability of HR. However, it is not clearly understood how the repair choice is made in the cell cycle phases where both mechanisms can operate. DNA resection has been described as one of the key elements to select the mechanism for DNA repair (Aylon, Liefshitz and Kupiec, 2004; Ira *et al.*, 2004; Huertas *et al.*, 2008). As a consequence of end resection activation by CDKs at the beginning of the S phase (Caspari, Murray and Carr, 2002; Aylon, Liefshitz and Kupiec, 2004; Ira *et al.*, 2004; Huertas *et al.*, 2008; Chen *et al.*, 2011; Tomimatsu *et al.*, 2014; Luo *et al.*, 2015; Makharashvili and Paull, 2015; Yu, Garcia and Symington, 2019) NHEJ activity is attenuated at S/G2. The phosphorylation of proteins responsible for initiating end resection (Clerici *et al.*, 2008; Huertas *et al.*, 2008; Zhang *et al.*, 2009), generating longer ssDNA (Chen *et al.*, 2011) and promoting the strand annealing of DSB ends (Plate *et al.*, 2008; Barlow and Rothstein, 2010; Saotome *et al.*, 2018; Lim, Chang and Huh, 2020), results in an increase of HR events and it is a mechanism conserved in humans (Huertas and Jackson, 2009; Wohlbold *et al.*, 2012).

Interestingly, all the mechanisms described so far ensure the regulation of HR to activate the pathway at the appropriate stage of the cell cycle. Matsuzaki (2012) described the Cdc28-mediated phosphorylation of Lif1 a regulatory subunit of the DNA ligase IV complex in *S. cerevisiae* (Matsuzaki *et al.*, 2012). They reported that Lif1 phosphorylation takes place during the S/G2 phases and it is required to coordinate resection and NHEJ during G2. This is interesting as it suggests that Pho85 and Cdc28 may play different roles in DSBR regulation. However, it seems that this regulatory mechanism is not involved in DSBR pathway choice. Additionally, Hentges (2014) reported the regulation of NHEJ by the cell cycle in *S. pombe*. A key component of the NHEJ pathway Xlf1, the ortholog of budding yeast Nej1 and human XLF/Cernunnos protein, is phosphorylated by Cdc2 at the S phase leading to the downregulation of the NHEJ in fission yeast (Hentges *et al.*, 2014). This mechanism could be relevant to ensure that NHEJ does not interfere with the HR pathway in those stages of the cell cycle where there exists a homologous sequence to repair the DNA without compromising the genetic information. This regulatory mechanism represents an advantage to the cell, and it is probable that a similar mechanism might be conserved in other organisms.

3.2 NHEJ regulation

The work I presented in this study unveiled a possible regulatory mechanism for NHEJ. Using different systems, I evaluated NHEJ in the non-phosphorylatable mutant of Yku80, *yku80*-S623A *(*Fig. 34 A, 35 A and 36 A*)*. The first method (Milne *et al.*, 1996) shows the ability of cells to re-ligate enzyme-digested plasmids (Fig. 34). The second (Kim and Haber, 2009) (Fig. 35) and third (Palmbos, Daley and Wilson, 2005) (Fig. 36) method are based on genetically modified strains where DSBs are caused in the yeast genome with galactose-inducible HO. The lack of a homologous sequence in the three systems does not allow the cells to repair DNA damage by HR. The three approaches showed a statistically significant increase in the number of NHEJ events when Yku80 cannot be phosphorylated at Ser623 compared to the wild type (Fig. 34 B, 35 B and 36 B). These results reveal a mechanism where the phosphorylation of Yku80 hampers NHEJ. However, there is a difference regarding the fold-increase of NHEJ events presented in each system which ranges from 2 to 50 times higher. A possible explanation for the differences observed between the systems used for measuring NHEJ may rely on how cells respond to DSBs induced in their genome or naked DNA transformed by lithium acetate / single-stranded carrier DNA / polyethylene glycol method. Due to some microhomologies being available in the sequence after DNA damage induction and the length of those microhomologies, alternative mechanisms such as alt-NHEJ and SSA can intervene resulting in viable cells. These alternative mechanisms are independent of Yku heterodimer and rely on pre-existing microhomologies around the break point to repair DSBs (Boulton and Jackson, 1996; Bennardo *et al.*, 2008). It has been reported that DSBs created by HO endonuclease induction are not exclusively repaired by NHEJ (Kramer *et al.*, 1994). In contrast to recircularisation of linearised plasmids where DNA ends are re-ligated without any homology or with only few nucleotides of homology (Roth and Wilson, 1986; Kramer *et al.*, 1994), it has been shown that HO-induced DSBs can undergo 5’ to 3’ exonucleolytic degradation to expose larger single-stranded regions of homology required for both, alt-NHEJ or SSA (McVey and Lee, 2008; Villarreal *et al.*, 2012). The length of homology required for each pathway varies as do their repaired products which may contain, inserted nucleotides or variable-size deletions. Aside from the quantitative differences, the three strategies display an increase of NHEJ events in *yku80*-S623A*.* This suggests that Yku80 phosphorylation by Pcl1-Pho85 at Ser623 downregulates the NHEJ pathway. Since Pcl1 is expressed during the G1 to S-phase transition, Yku80 phosphorylation at the end of G1 could represent an advantage for the cells that would primarily repair DSBs by HR at the cell cycle phases where a homologous sequence is available ensuring DNA repair without compromising genetic information.

The results from the *in vitro* and *in vivo* phosphorylation assays highlighted Pcl1-Pho85 as the cyclin-CDK complex responsible for Yku80 phosphorylation. For this reason, I checked whether a *pho85Δ* mutant, where presumably Yku80 will not be phosphorylated, shows an increase in the number of NHEJ events by the suicide method (Fig. 36). Unfortunately, *pho85Δ* cells were not able to grow in galactose plates. Alternatively, I used *pcl1Δ*.

Pcl1 is the activating cyclin of Pho85 and therefore the deletion of Pcl1 most likely leads to the same phenotype due to the inability of Pho85 to phosphorylate Yku80. Even though *pcl1Δ* also grows poorly in galactose plates, it showed more NHEJ events than the wild-type cells (Fig 36 B). This result suggests, together with the phosphorylation assays, that Yku80 phosphorylation is Pcl1-Pho85-dependent and it results in NHEJ downregulation.

NHEJ has been long considered an error-prone mechanism (Bétermier, Bertrand and Lopez, 2014) as small insertions and deletions can occur when re-ligating the broken ends to repair the DSBs. I examined whether the mutation of Yku80 at Ser623 has any impact on the fidelity of NHEJ. I found no statistically significant differences between the wild-type and the non-phosphorylatable mutant meaning that the phosphorylation of Yku80 by Pho85 does not interfere with the accuracy of the process.

3.3 Yku80 phosphorylation shifts the balance of the DSB repair towards HR

After a DSB is created the cell has a choice to make: NHEJ or HR? My work has shown that the Cyclin-CDK complex Pcl1-Pho85 is able to phosphorylate Yku80 at Ser623. This phosphorylation seems to hamper the NHEJ pathway. As I showed by three different approaches, the non-phosphorylatable mutant displays an increase of NHEJ events. To repair DSB by NHEJ, Yku80 needs to bind the DNA to protect the DNA ends (Mimori and Hardin, 1986) and consequently the HR machinery cannot access the broken ends to resect the DNA tails and initiate the pathway. By two different assays described in Hentges (2014) and Kim and Haber (2009) I found a decrease in the number of HR events (Fig. 38) in the non-phosphorylatable mutant, *yku80*-S623A*.* There exists a difference in the reduction obtained in both methods that could be explained by error-prone NHEJ events at the MATα locus that modify the HO-cut sequence, thereby contributing to an increase in the number of viable colonies in *yku80*-S623A*.* Nevertheless, I would like to emphasise that the increase described in NHEJ seems to go with a reduction in HR in both systems. The group of Dr Doherty described a similar mechanism to the one I propose but in *S. pombe* (Hentges *et al.*, 2014). They published a study involving the phosphorylation by Cdc21 of Xlf1, one of the core factors in NHEJ. Xlf1 is the ortholog of budding yeast Nej1 and human XLF, a protein that binds to the DNA and promotes end-joining (Hentges *et al.*, 2006; Cavero, Chahwan and Russell, 2007). Interestingly, they described that the phosphorylation of Xlf1 by the CDK inhibits NHEJ. They also reported that the loss of Xlf1 regulation by CDK phosphorylation is accompanied by the inactivation of HR becoming NHEJ the predominant mechanism to repair DSBs.

By the direct phosphorylation of Yku80 the cell cycle would be able to shift the predominant mechanism for DSBR from NHEJ to HR at the times it represents an advantage for the cells. In *S. cerevisiae*, HR is the dominant mechanism of DSB repair (Resnick and Martin, 1976; Budd and Mortimer, 1982; Sugawara and Haber, 1992) unlike in mammalian cells where NHEJ is thought to be the predominant and most efficient pathway for DSBR (Shibata *et al.*, 2011; Brandsma and Gent, 2012). I evaluated the biological significance regarding the increase of NHEJ events when Yku80 cannot be phosphorylated at Ser623 by assessing cell viability after inducing DNA damage with different chemical compounds in asynchronous cultures. I found no differences in viability between the wild type and *yku80*-S623A (Fig. 40 and 41). In an asynchronous culture there are different cell populations at different stages of their cycle, and this could be the reason why I was unable to observe any differences in cell viability. Considering that the increase of NHEJ goes with a reduction of HR events, I analysed the effect of the mutation at Ser623 after inducing DNA damage specifically in G1 an G2. Similar to what I observed in asynchronous cultures, when I insulted cells synchronised in G1 with bleomycin, I observed no differences between the wild-type and the non-phosphorylatable mutant (Fig. 42 A). When DNA damage was caused in G2 at the point where most cells have their genome replicated (Fig. 42 B), *yku80*-S623A cells showed a reduction in cell viability (Fig. 42 B). This reduction might have occurred as the result of increased NHEJ in G2 due to the cell’s inability to phosphorylate Yku80 at Ser623. As mentioned earlier, NHEJ is less accurate than HR and the DNA damage induced by bleomycin may require end-processing to successfully repair the DNA, as a consequence; *yku80*-S623A showed a lower rate of survival compared to wild-type cells. It is important to note that even though the decrease in cell survival is consistent and statistically significant, it is limited. Likely, alternative mechanisms of NHEJ might be contributing to the increasing number of viable cells. By deleting *RAD52,* a key component of the HR machinery that plays a role in DNA strand exchange (Sung, 1997; New *et al.*, 1998; Shinohara and Ogawa, 1998), I observed the expected reduction in *rad52Δ* Yku80 wt strain survival rate compared to the *RAD52* Yku80 wt and *yku80*-S623A *(*Fig. 42 B*)*. Moreover, I observed the recovery of viability in *rad52Δ yku80*-S623A which presents approximately the same survival rate as *RAD52* Yku80 wt (Fig. 42 B). This result is interesting as at first, I did not consider that the deletion of *RAD52* would have a positive effect on *RAD52Δ yku80*-S623A survival. It is possible that the mere fact that the Yku heterodimer does not need to compete with the HR machinery to repair DSBs makes it more efficient. Also, as I suggested earlier, it is likely that alternative mechanisms are contributing to the number of viable cells. Rad52 promotes the annealing of complementary DNA sequences in the alternative mechanism SSA (Bhargava, Onyango and Stark, 2016). Perhaps, the impairment of SSA due to *RAD52* deletion is also contributing to the increase of viable cells in *rad52Δ yku80*-S623A. The evidence presented in the viability assay suggests that during G2 when HR is active and can take place, Yku80 phosphorylation hampers NHEJ and so promotes DSB repair by HR, ensuring faithful repair.

The results that I have presented in this work suggests a regulatory mechanism for the balance of NHEJ and HR through Yku80 phosphorylation by the cell cycle. The cyclin-CDK complex Pcl1-Pho85 phosphorylates Yku80 at Ser623. Pcl1, the cyclin responsible for Pho85 activation, is only present during late G1 and S phase of the cell cycle. This is relevant since it suggests that Yku80 might be inactivated through G1 to S-phase transition allowing HR to become the predominant mechanism for DSBR. The Ser623 residue I identified as the target for Pcl1-Pho85 phosphorylation is in the C-terminal domain of Yku80 which has been proven to be specifically required for NHEJ (Palmbos, Daley and Wilson, 2005). It is possible that as a consequence of Yku80 phosphorylation at Ser623, the conformation of Yku80 C-terminal domain changes. This could be interesting as there has been described a physical interaction between Yku80 and Dnl4, the DNA ligase required for NHEJ (Palmbos, Daley and Wilson, 2005; Palmbos *et al.*, 2008). The conformational changes of Yku80 C-terminal could lead to the loss of Yku80-Dnl4 interaction hampering DNA repair by NHEJ. In the future, it would be interesting to analyse if there are any differences in the cross-linked DNA-protein complexes in the wild-type strain and the non-phosphorylatable mutant. It would help to unveil the molecular mechanism behind the decrease of NHEJ activity due to Yku80 phosphorylation.

4. Ku regulation might be a conserved function

Ku proteins are highly conserved amongst all organisms and even though its primary sequence has diverged, they are similar in size, domains, and subunit structure (Dynan and Yoo, 1998). The Ser623 residue I identified as the target for Pcl1-Pho85 phosphorylation is located at the C-terminus domain, more specifically in the structurally disordered region within the C-terminus domain (Fig. 43). Analysing human KU sequence, I found a S/TP motif for CDK phosphorylation localised in the poorly organised region at the C-terminus domain of Ku80: T629. Its localisation and the already described preference of CDK for disorganised domain (Amata, Maffei and Pons, 2014) made me consider Thr 629 as a possible target for CDK phosphorylation in humans to regulate its function in DNA repair. Unfortunately, I was unable to evaluate if hKu80 is phosphorylated by CCNY/CDK16 (human ortholog of Pcl1-Pho85).

To skip this difficulty and gain insight into the possible relevance of Ku80 phosphorylation in mammalian cells, I moved to a more physiological context and decided to analyse viability in cancer cell lines overexpressing Ku80^{T629A} in asynchronous cultures. I observed a reduction in the capacity to form colonies of the cells overexpressing Ku80^{T629A} compared to Ku80^{wt} (Fig. 48). The phenotype obtained differs from the one I described in *S. cerevisiae* where there were not any differences between the wild-type and non-phosphorylatable mutant in an asynchronous culture. This could be explained by the preference of higher eukaryotes for NHEJ as the mechanism to repair DSBs, contrary to what happens in yeasts where the predominant mechanism is HR (Mao *et al.*, 2008; Shibata *et al.*, 2011; Brandsma and Gent, 2012). The presence of large repetitive sequences in the DNA of higher eukaryotes is thought to be the reason why the cells prefer to repair DSBs by NHEJ therefore avoiding possible misalignments of sequences. Also, the reduction in cell viability is not consistent with the increase of NHEJ I identified in yeast when Yku80 cannot be phosphorylated. This result suggests that Ku80 phosphorylation might be conserved and have a role in the regulation of DSB repair in mammalian cells. However, based on the results from the viability assay the function of Ku80 phosphorylation seems to differ from the one I proposed in yeasts. For this reason, it would be interesting to evaluate if Ku80 phosphorylation in mammalian cells shifts the balance between NHEJ and HR. Establishing if Ku80 phosphorylation increases or decreases the number of NHEJ events and how this affects to the HR pathway may help to unveil whether Ku80 phosphorylation has a conserved function or it contributes in a different manner to the regulation of DSB repair pathway choice and balance in mammalian cells.

5. Model for the balance regulation of NHEJ and HR throughout the cell cycle by Pcl1-Pho85 dependent phosphorylation of Yku80

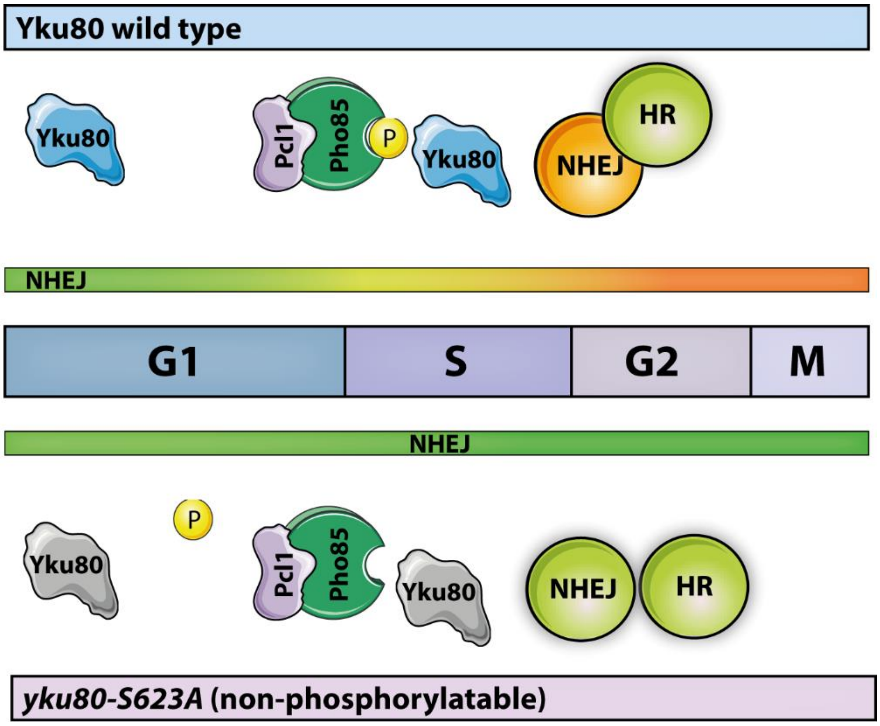
Yku80 wild type
Yku80
Pcl1
Pho85
P
Yku80
HR
NHEJ
NHEJ
G1
S
G2
M
NHEJ
P
Yku80
Pcl1
Pho85
Yku80
NHEJ
HR
yku80-S623A (non-phosphorylatable)

Fig. 50. Working model for Yku80 phosphorylation.

The working model I proposed is graphically represented in Fig. 50. Briefly, Pcl1-Pho85 phosphorylates Yku80 at Ser623 at the end of G1. The Yku80 phosphorylation leads to the downregulation of NHEJ promoting DSBR by HR in G2. NHEJ in the non-phosphorylatable mutant *yk80*-S623A remains active throughout the entire cell cycle competing with HR to repair DSB.

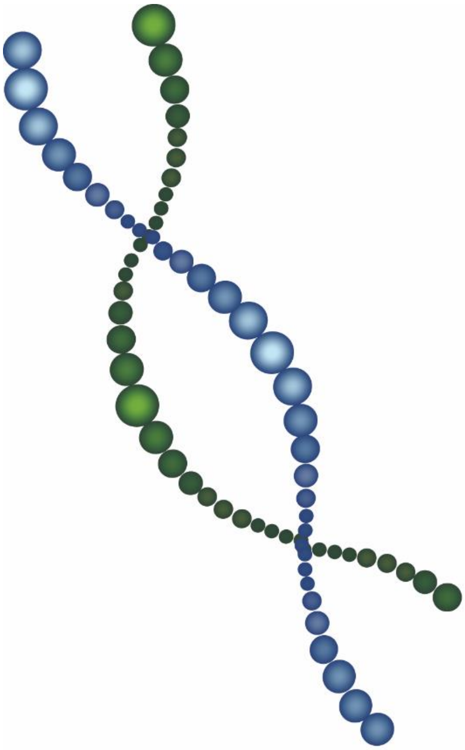

Conclusions

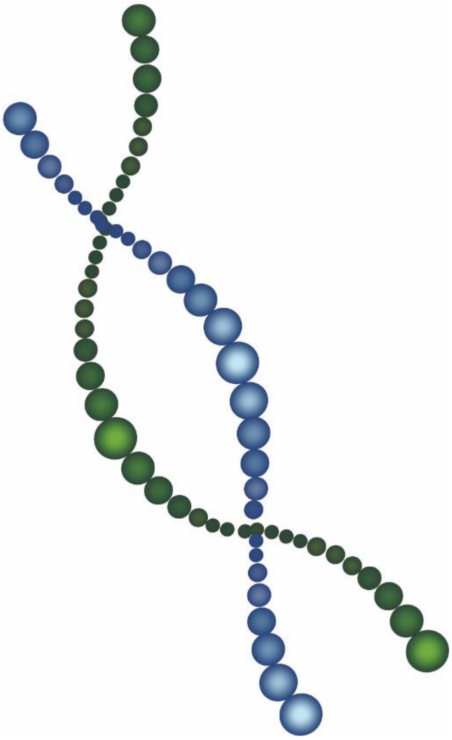

1. Yku80 is phosphorylated at Ser623 by Pcl1-Pho85 *in vitro* and *in vivo*.

2. Yku80 phosphorylation at Ser623 reduces NHEJ activity and increases HR suggesting a regulatory mechanism where Yku80 phosphorylation hampers NHEJ. The downregulation of NHEJ would allow HR to be the preferred mechanism for DSBR during S/G2 phases of the cell cycle.

3. Yku80 phosphorylation at Ser623 decreases sensitivity to bleomycin at the G2 phase of the cell cycle in *S. cerevisiae* probably as the result of an increase in HR.

4. Phosphorylation of human Ku80 decreases bleomycin sensitivity in cancer cell lines suggesting that Ku80 phosphorylation might be a conserved mechanism among different organisms.

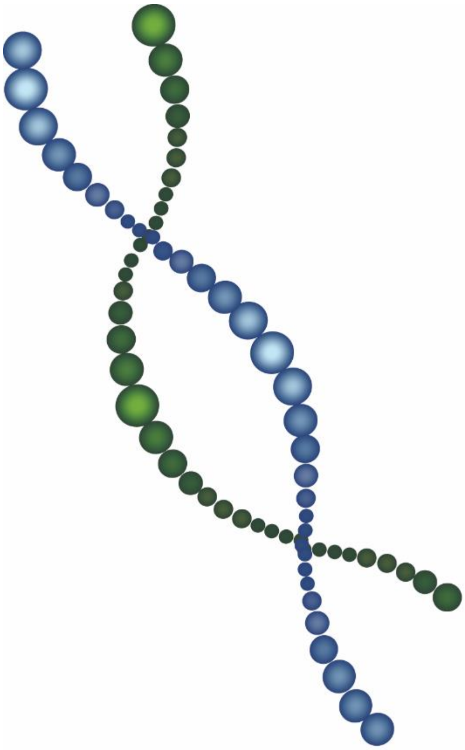

Abbreviations

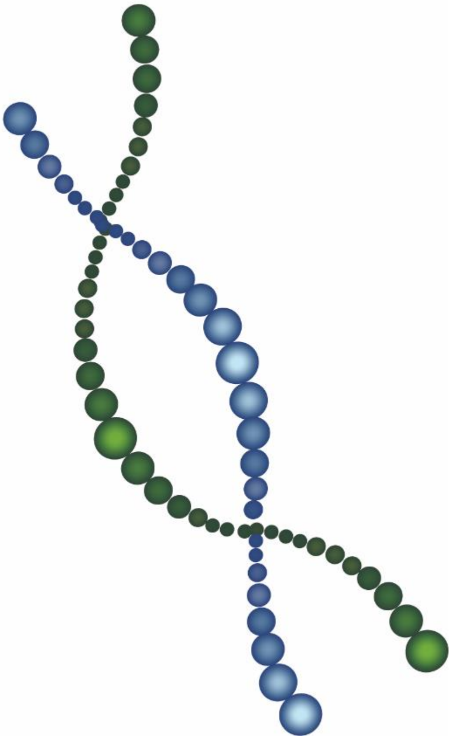

4-NQO 4-Nitroquinolina 1-oxide

5’-dRP 5´-deoxyribose-5-phosphate

a-EJ Alternative end joining

ATM Ataxia-Telangiectasia-Mutated

ATR Ataxia-Telangiectasia-Mutated and Rad3-related

BER Base excision repair

C. albicans *Candida albicans*

CCN Cyclin

CDK Cyclin Dependent Kinase

C-term Carboxy-terminal domain

D-loop Displacement loop

DSBs Double-stranded breaks

DSBR Double-stranded break repair

EMS ethyl-methane sulfonate

HR Homologous recombination

hKu80 Human Ku80

HU Hydroxyurea

IR Ionizing radiation

Leu Leucine

NER Nucleotide excision repair

N-term Amino terminal domain

MMR Mismatch repair

MMS Methyl-methane sulfonate

NHEJ Non-homologous end joining

PIKK phosphatidylinositol 3-kinase-related kinases

RAG Recombination Active Genes

ROS Reactive Oxygen species

RNS Reactive Nitrogen species

RSSs recombination signal sequences

SAP SAF-A/B, Acinus and Pias

SSA Single-stranded annealing

Ser Serine

S. pombe *Schizosaccharomyces pombe*

S. cerevisiae *Saccharomyces cerevisiae*

SSBs Single-strand breaks

TMEJ Polymerase Theta-Mediated End Joining

Thr Threonine

vWA von Willebrand domain

UV Ultraviolet radiation

Ura Uracil

Yku80 Yeast ku80

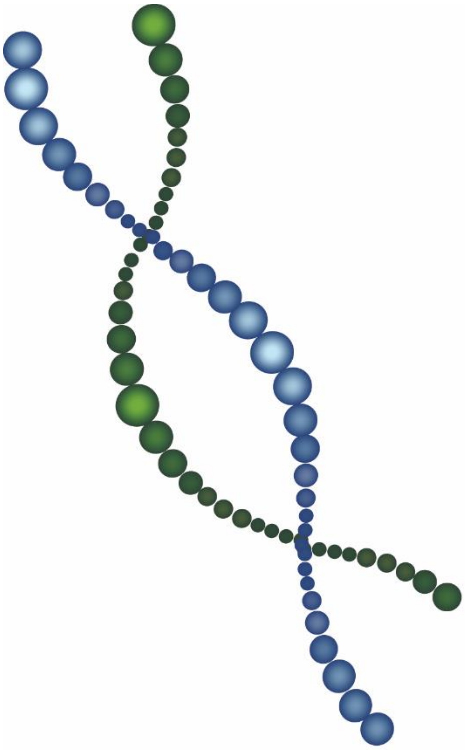

Bibliography

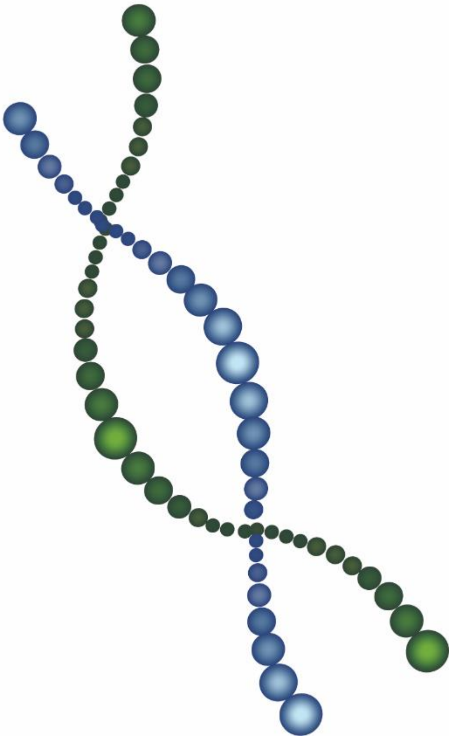

Abreu, C. M. *et al.* (2013) ‘Site-Specific Phosphorylation of the DNA Damage Response Mediator Rad9 by Cyclin-Dependent Kinases Regulates Activation of Checkpoint Kinase 1’, *PLoS Genetics*, 9(4), pp. 16–22. doi: 10.1371/journal.pgen.1003310.

Adhikari, D. *et al.* (2012) ‘Cdk1, but not Cdk2, is the sole Cdk that is essential and sufficient to drive resumption of meiosis in mouse oocytes’, *Human Molecular Genetics*, 21(11), pp. 2476–2484. doi: 10.1093/hmg/dds061.

Alani, E. *et al.* (1997) ‘Genetic and biochemical analysis of Msh2p-Msh6p: role of ATP hydrolysis and Msh2p-Msh6p subunit interactions in mismatch base pair recognition’, *Molecular and Cellular Biology*, 17(5), pp. 2436–2447. doi: 10.1128/mcb.17.5.2436.

Amata, I., Maffei, M. and Pons, M. (2014) ‘Phosphorylation of unique domains of Src family kinases’, *Frontiers in Genetics*, 5(JUN), pp. 1–6. doi: 10.3389/fgene.2014.00181.

Aouida, M. *et al.* (2004) ‘Isolation and characterization of Saccharomyces cerevisiae mutants with enhanced resistance to the anticancer drug bleomycin’, *Current Genetics*, 45(5), pp. 265–272. doi: 10.1007/s00294-004-0492-x.

Aravind, L. and Koonin (2001) ‘Prokaryotic homologs of the eukaryotic DNA-end-binding protein Ku, novel domains in the Ku protein and prediction of a prokaryotic double-strand break repair system’, *Genome Research*, 11(8), pp. 1365–1374. doi: 10.1101/gr.181001.gions.

Arima, Y. *et al.* (2006) ‘4-Nitroquinoline 1-oxide forms 8-hydroxydeoxyguanosine in human fibroblasts through reactive oxygen species’, *Toxicological Sciences*, 91(2), pp. 382–392. doi: 10.1093/toxsci/kfj161.

Arosio, D. *et al.* (2002) ‘Studies on the mode of Ku interaction with DNA’, *Journal of Biological Chemistry*, 277(12), pp. 9741–9748. doi: 10.1074/jbc.M111916200.

Askree, S. H. *et al.* (2004) ‘A genome-wide screen for Saccharomyces cerevisiae deletion mutants that affect telomere length’, *Proceedings of the National Academy of Sciences of the United States of America*, 101(23), pp. 8658–8663. doi: 10.1073/pnas.0401263101.

Aviram, S. *et al.* (2008) ‘Autophosphorylation-Induced Degradation of the Pho85 Cyclin Pcl5 Is Essential for Response to Amino Acid Limitation’, *Molecular and Cellular Biology*, 28(22), pp. 6858–6869. doi: 10.1128/mcb.00367-08.

Awasthi, P., Foiani, M. and Kumar, A. (2016) ‘Correction to ATM and ATR signaling at a glance’, *Journal of Cell Science*, 128, pp. 4255–4262. doi: 10.1242/jcs.188631.

Aylon, Y., Liefshitz, B. and Kupiec, M. (2004) ‘The CDK regulates repair of double-strand breaks by homologous recombination during the cell cycle’, *EMBO Journal*, 23(24), pp. 4868–4875. doi: 10.1038/sj.emboj.7600469.

Bae, S. H. *et al.* (1998) ‘Dna2 of Saccharomyces cerevisiae possesses a single-stranded DNA- specific endonuclease activity that is able to act on double-stranded dna in the presence of ATP’, *Journal of Biological Chemistry*, 273(41), pp. 26880–26890. doi: 10.1074/jbc.273.41.26880.

Bai, Y. and Symington, L. S. (1996) ‘A Rad52 homolog is required for RAD51-independent mitotic recombination in Saccharomyces cerevisiae’, *Genes and Development*, 10(16), pp. 2025–2037. doi: 10.1101/gad.10.16.2025.

Bakkenist, C. J. and Kastan, M. B. (2003) ‘DNA damage activates

ATM through intermolecular autophosphorylation and dimer dissociation', *Nature*, 421(6922), pp. 499–506. doi: 10.1038/nature01368.

Bállega, E. *et al.* (2018) 'Comprehensive and quantitative analysis of G1 cyclins. A tool for studying the cell cycle', *PLoS ONE*, 14(6), pp. 1–24. doi: 10.1371/journal.pone.0218531.

Banin, S. *et al.* (1998) 'Enhanced Phosphorylation of p53 by ATM in Response to DNA Damage', 281, pp. 1674–1677. doi: 10.1126/science.281.5383.1674.

Barlow, J. H. and Rothstein, R. (2010) 'Timing is everything: cell cycle control of Rad52', *Cell Division*, 5, pp. 29–31. doi: 10.1186/1747-1028-5-7.

Basu, A. and Krishnamurthy, S. (2010) 'Cellular responses to cisplatin-induced DNA damage', *Journal of Nucleic Acids*, 2010, pp. 1–16. doi: 10.4061/2010/201367.

Bell, M. *et al.* (2001) 'Isolation of Hyperactive Mutants of the MAPK p38/Hog1 that are Independent of MAPK Kinase Activation', *Journal of Biological Chemistry*, 276(27), pp. 25351–25358. doi: 10.1074/jbc.M101818200.

Bennardo, N. *et al.* (2008) 'Alternative-NHEJ is a mechanistically distinct pathway of mammalian chromosome break repair', *PLoS Genetics*, 4(6). doi: 10.1371/journal.pgen.1000110.

Berkovich, E., Monnat, R. J. and Kastan, M. B. (2007) 'Roles of ATM and NBS1 in chromatin structure modulation and DNA double-strand break repair', *Nature Cell Biology*, 9(6), pp. 683–690. doi: 10.1038/ncb1599.

Bertuch, A. A. and Lundblad, V. (2003) 'Which end: Dissecting Ku's function at telomeres and double-strand breaks’, *Genes and Development*, 17(19), pp. 2347–2350. doi: 10.1101/gad.1146603.

Bétermier, M., Bertrand, P. and Lopez, B. S. (2014) ‘Is Non-Homologous End-Joining Really an Inherently Error-Prone Process?’, *PLoS Genetics*, 10(1). doi: 10.1371/journal.pgen.1004086.

Beyer, T. and Weinert, T. (2014) ‘Mec1 and Tel1: An arresting dance of resection’, *EMBO Journal*, 33(3), pp. 176–178. doi: 10.1002/embj.201387440.

Bhargava, R., Onyango, D. O. and Stark, J. M. (2016) ‘Regulation of Single-Strand Annealing and its Role in Genome Maintenance’, *Trends in Genetics*, 32(9), pp. 566–575. doi: 10.1016/j.tig.2016.06.007.

Black, S. J. *et al.* (2019) ‘Molecular basis of microhomology-mediated end-joining by purified full-length Polθ’, *Nature Communications*, 10(1). doi: 10.1038/s41467-019-12272-9.

Blackwell, M. (2011) ‘The fungi: 1, 2, 3 ... 5.1 million species?’, *American Journal of Botany*, 98(3), pp. 426–438. doi: 10.3732/ajb.1000298.

Blier, P. R. *et al.* (1993) ‘Binding of Ku protein to DNA. Measurement of affinity for ends and demonstration of binding to nicks’, *Journal of Biological Chemistry*, 268(10), pp. 7594–7601. doi: 10.1016/S0021-9258(18)53216-6.

Boger, D. L. and Cai, H. (1999) ‘Bleomycin: Synthetic and Mechanistic Studies’, *Angewandte Chemie*, 38, pp. 448–476. doi: 10.1002/(SICI)1521-3773(19990215)38:4<448::AID-ANIE448>3.0.CO;2-W.

De Bont, R. and van Larebeke, N. (2004) ‘Endogenous DNA damage in humans: A review of quantitative data’, *Mutagenesis*, 19(3), pp.

169–185. doi: 10.1093/mutage/geh025.

Boulton, S. J. and Jackson, S. P. (1996) ‘Saccharomyces cerevisiae Ku70 potentiates illegitimate DNA double-strand break repair and serves as a barrier to error-prone DNA repair pathways’, *EMBO Journal*, 15(18), pp. 5093–5103. doi: 10.1002/j.1460-2075.1996.tb00890.x.

Brachmann, C. B. *et al.* (1998) ‘Designer deletion strains derived from Saccharomyces cerevisiae S288C: A useful set of strains and plasmids for PCR-mediated gene disruption and other applications’, *Yeast*, 14(2), pp. 115–132. doi: 10.1002/(SICI)1097-0061(19980130)14:2<115::AID-YEA204>3.0.CO;2-2.

Brandsma, I. and Gent, D. C. (2012) ‘Pathway choice in DNA double strand break repair: Observations of a balancing act’, *Genome Integrity*, 3(1), p. 1. doi: 10.1186/2041-9414-3-9.

Branzei, D. and Foiani, M. (2010) ‘Maintaining genome stability at the replication fork’, *Nature Reviews Molecular Cell Biology*, 11(3), pp. 208–219. doi: 10.1038/nrm2852.

Bressan, D. A., Baxter, B. K. and Petrini, J. H. J. (1999) ‘The Mre11-Rad50-Xrs2 Protein Complex Facilitates Homologous Recombination-Based Double-Strand Break Repair in Saccharomyces cerevisiae’, *Molecular and Cellular Biology*, 19(11), pp. 7681–7687. doi: 10.1128/mcb.19.11.7681.

Budd, M. E. and Campbell, J. L. (2009) ‘Interplay of Mre11 nuclease with Dna2 plus Sgs1 in Rad51-dependent recombinational repair’, *PLoS ONE*, 4(1). doi: 10.1371/journal.pone.0004267.

Budd, M. and Mortimer, R. K. (1982) ‘REPAIR OF DOUBLE-STRAND BREAKS IN A TEMPERATURE CONDITIONAL RADIATION-SENSITIVE MUTANT OF Saccharomyces cerevisiae’, *Mutation*

Research - Genetic Toxicology and Environmental Mutagenesis, 103, pp. 19–24. doi: 10.1016/0165-7992(82)90080-x.

Carr, A. M. (1997) ‘Control of cell cycle arrest by the Mec1sc/Rad3sp DNA structure checkpoint pathway’, *Current Opinion in Genetics and Development*, 7(1), pp. 93–98. doi: 10.1016/S0959-437X(97)80115-3.

Carroll, A. S. and O’Shea, E. K. (2002) ‘Pho85 and signaling environmental conditions’, *Trends in Biochemical Sciences*, 27(2), pp. 87–93. doi: 10.1016/S0968-0004(01)02040-0.

Caspari, T., Murray, J. M. and Carr, A. M. (2002) ‘Cdc2-cyclin B kinase activity links Crb2 and Rqh1-topoisomerase III’, *Genes and Development*, 16(10), pp. 1195–1208. doi: 10.1101/gad.221402.

Cavero, S., Chahwan, C. and Russell, P. (2007) ‘Xlf1 is required for DNA repair by nonhomologous end joining in Schizosaccharomyces pombe’, *Genetics*, 175(2), pp. 963–967. doi: 10.1534/genetics.106.067850.

Ceballos, S. J. and Heyer, W. D. (2011) ‘Functions of the Snf2/Swi2 family Rad54 motor protein in homologous recombination’, *Biochimica et Biophysica Acta - Gene Regulatory Mechanisms*, 1809(9), pp. 509–523. doi: 10.1016/j.bbagrm.2011.06.006.

Chan, S. H., Yu, A. M. and McVey, M. (2010) ‘Dual roles for DNA polymerase theta in alternative end-joining repair of double-strand breaks in Drosophila’, *PLoS Genetics*, 6(7), pp. 1–16. doi: 10.1371/journal.pgen.1001005.

Chang, M. *et al.* (2002) ‘A genome-wide screen for methyl methanesulfonate-sensitive mutants reveals genes required for S phase progression in the presence of DNA damage’, *Proceedings of the National Academy of Sciences of the United States of America*, 99(26), pp. 16934–16939. doi: 10.1073/pnas.262669299.

Chen, J. and Stubbe, J. A. (2005) ‘Bleomycins: Towards better therapeutics’, *Nature Reviews Cancer*, 5(2), pp. 102–112. doi: 10.1038/nrc1547.

Chen, R. and Wold, M. S. (2014) ‘Replication protein A: Single-stranded DNA’s first responder’, *BioEssays*, 36(12), pp. 1156–1161. doi: 10.1002/bies.201400107.

Chen, X. *et al.* (2011) ‘Cell cycle regulation of DNA double-strand break end resection by Cdk1-dependent Dna2 phosphorylation’, *Nature Structural and Molecular Biology*, 18(9), pp. 1015–1019. doi: 10.1038/nsmb.2105.

Chou, C. C., Li, Y. C. and Gartenberg, M. R. (2008) ‘Bypassing Sir2 and O-Acetyl-ADP-Ribose in Transcriptional Silencing’, *Molecular Cell*, 31(5), pp. 650–659. doi: 10.1016/j.molcel.2008.06.020.

Clément, M. *et al.* (2006) ‘The nuclear GTPase Gsp1p can affect proper telomeric function through the Sir4 protein in Saccharomyces cerevisiae’, *Molecular Microbiology*, 62(2), pp. 453–468. doi: 10.1111/j.1365-2958.2006.05374.x.

Clerici, M. *et al.* (2008) ‘The Yku70-Yku80 complex contributes to regulate double-strand break processing and checkpoint activation during the cell cycle’, *EMBO Reports*, 9(8), pp. 810–818. doi: 10.1038/embor.2008.121.

Corda, Y. *et al.* (2005) ‘Inactivation of Ku-Mediated End Joining Suppresses mec1Δ Lethality by Depleting the Ribonucleotide Reductase Inhibitor Sml1 through a Pathway Controlled by Tel1 Kinase and the Mre11 Complex’, *Molecular and Cellular Biology*, 25(23), pp. 10652–10664. doi: 10.1128/mcb.25.23.10652-10664.2005.

Deckbar, D., Jeggo, P. A. and Löbrich, M. (2011) ‘Understanding the limitations of radiation-induced cell cycle checkpoints’, *Critical Reviews* *in Biochemistry and Molecular Biology*, 46(4), pp. 271–283. doi: 10.3109/10409238.2011.575764.

Dianov, G. L., O’Neill, P. and Goodhead, D. T. (2001) ‘Securing genome stability by orchestrating DNA repair: Removal of radiation-induced clustered lesions in DNA’, *BioEssays*, 23(8), pp. 745–749. doi: 10.1002/bies.1104.

Difilippantonio, M. J. *et al.* (1996) ‘RAG1 mediates signal sequence recognition and recruitment of RAG2 in V(D)J recombination’, *Cell*, 87(2), pp. 253–262. doi: 10.1016/S0092-8674(00)81343-4.

Dirick, L., Böhm, T. and Nasmyth, K. (1995) ‘Roles and regulation of Cln-Cdc28 kinases at the start of the cell cycle of Saccharomyces cerevisiae’, *EMBO Journal*, 14(19), pp. 4803–4813. doi: 10.1002/j.1460-2075.1995.tb00162.x.

Diril, M. K. *et al.* (2012) ‘Cyclin-dependent kinase 1 (Cdk1) is essential for cell division and suppression of DNA re-replication but not for liver regeneration’, *Proceedings of the National Academy of Sciences of the United States of America*, 109(10), pp. 3826–3831. doi: 10.1073/pnas.1115201109.

Doherty, A. J., Jackson, S. P. and Weller, G. R. (2001) ‘Correspondence Identification of bacterial homologues of the Ku DNA repair proteins’, 500(Jun), pp. 186–188.

Dynan, W. S. and Yoo, S. (1998) ‘Interaction of Ku protein and DNA-dependent protein kinase catalytic subunit with nucleic acids’, *Nucleic Acids Research*, 26(7), pp. 1551–1559. doi: 10.1093/nar/26.7.1551.

Egly, J. M. and Coin, F. (2011) ‘A history of TFIIH: Two decades of molecular biology on a pivotal transcription/repair factor’, *DNA Repair*, 10(7), pp. 714–721. doi: 10.1016/j.dnarep.2011.04.021.

Eide, L. *et al.* (1996) ‘Base excision of oxidative purine and pyrimidine DNA damage in Saccharomyces cerevisiae by a DNA glycosylase with sequence similarity to endonuclease III from Escherichia coli’, *Proceedings of the National Academy of Sciences of the United States of America*, 93(20), pp. 10735–10740. doi: 10.1073/pnas.93.20.10735.

Emerson, C. H. and Bertuch, A. A. (2016) ‘Consider the workhorse: Nonhomologous end-joining in budding yeast’, *Biochemistry and Cell Biology*, 94(5), pp. 396–406. doi: 10.1139/bcb-2016-0001.

Enserink, J. M. *et al.* (2009) ‘Cdc28/Cdk1 positively and negatively affects genome stability in S. cerevisiae’, *Journal of Cell Biology*, 185(3), pp. 423–437. doi: 10.1083/jcb.200811083.

Espinoza, F. H. *et al.* (1994) ‘Cell cycle control by a complex of the cyclin HCS26 (PCL1) and the kinase PHO85’, *Science*, 266(5189), pp. 1388–1391. doi: 10.1126/science.7973730.

Falck, J., Coates, J. and Jackson, S. P. (2005) ‘Conserved modes of recruitment of ATM, ATR and DNA-PKcs to sites of DNA damage’, *Nature*, 434(7033), pp. 605–611. doi: 10.1038/nature03442.

Fasching, C. L. *et al.* (2015) ‘Top3-Rmi1 dissolve Rad51-mediated D loops by a topoisomerase-based mechanism’, *Molecular Cell*, 57(4), pp. 595–606. doi: 10.1016/j.molcel.2015.01.022.

Fell, V. L. and Schild-Poulter, C. (2012) ‘Ku Regulates Signaling to DNA Damage Response Pathways through the Ku70 von Willebrand A Domain’, *Molecular and Cellular Biology*, 32(1), pp. 76–87. doi: 10.1128/mcb.05661-11.

Feng, L. and Chen, J. (2012) ‘The E3 ligase RNF8 regulates KU80 removal and NHEJ repair’, *Nature Structural and Molecular Biology*, 19(2), pp. 201–206. doi: 10.1038/nsmb.2211.

Ferreira, M. G. and Cooper, J. P. (2004) ‘Two modes of DNA double-strand break repair are reciprocally regulated through the fission yeast cell cycle’, *Genes and Development*, 18(18), pp. 2249–2254. doi: 10.1101/gad.315804.

Game, J. C. and Mortimer, R. K. (1974) ‘A genetic study of x-ray sensitive mutants in yeast’, *Mutation research*, 24, pp. 281–292. doi: 10.1016/0027-5107(74)90176-6.

Getts, R. C. and Stamato, T. D. (1994) ‘Absence of a Ku-like DNA end binding activity in the xrs double-strand DNA repair-deficient mutant’, *Journal of Biological Chemistry*, 269(23), pp. 15981–15984. doi: 10.1016/S0021-9258(17)33960-1.

Gietz, R. D. and Sugino, A. (1988) ‘New yeast-Escherichia coli shuttle vectors constructed with in vitro mutagenized yeast genes lacking six-base pair resection sites’, *Gene*, 14, pp. 527–534. doi: 10.1016/0378-1119(88)90185-0.

Goffeau, A. (1997) ‘The yeast genome directory.’, *Nature*, 387(6632 Suppl), p. 5. doi: 10.1038/387s005.

Goodhead, D. T., Thacker, J. and Cox, R. (1993) ‘Effects of radiations of different qualities on cells: Molecular mechanisms of damage and repair’, *International Journal of Radiation Biology*, 63(5), pp. 543–556. doi: 10.1080/09553009314450721.

Gradia, S. *et al.* (1999) ‘hMSH2-hMSH6 forms a hydrolysis-independent sliding clamp on mismatched DNA’, *Molecular Cell*, 3(2), pp. 255–261. doi: 10.1016/S1097-2765(00)80316-0.

Gravel, S. *et al.* (1998) ‘Yeast Ku as a Regulator of Chromosomal DNA End Structure’, *Science*, 280(5364), pp. 741–744. doi: 10.1126/science.280.5364.741.

Gravel, S. and Wellinger, R. J. (2002) ‘Maintenance of Double-Stranded Telomeric Repeats as the Critical Determinant for Cell Viability in Yeast Cells Lacking Ku’, *Molecular and Cellular Biology*, 22(7), pp. 2182–2193. doi: 10.1128/mcb.22.7.2182-2193.2002.

Greenwell, P. W. *et al.* (1995) ‘TEL1, a Gene Involved in Controlling Telomere Length in S. cerevisiae, Is Homologous to the Human Ataxia Telangiectasia Gene’, *Cell press*, 82, pp. 823–829. doi: 10.1080/713690218.

Griffith, A. J. *et al.* (1992) ‘Ku polypeptides synthesized in vitro assemble into complexes which recognize ends of double-stranded DNA’, *Journal of Biological Chemistry*, 267(1), pp. 331–338. doi: 10.1016/S0021-9258(18)48498-0.

Guzder, S. N. *et al.* (1998) ‘Affinity of yeast nucleotide excision repair factor 2, consisting of the Rad4 and Rad23 proteins, for ultraviolet damaged DNA’, *Journal of Biological Chemistry*, 273(47), pp. 31541–31546. doi: 10.1074/jbc.273.47.31541.

Haber, J. E. and Moore, J. K. (1996) ‘Cell Cycle and Genetic Requirements of Two Pathways of Nonhomologous End-Joining Repair of Double-Strand Breaks in Saccharomyces cerevisiae’, *Molecular and cellular biology*, 16(5), pp. 2164–2173.

Habraken, Y. *et al.* (1993) ‘Yeast excision repair gene RAD2 encodes a single-stranded DNA endonuclease’, *Nature*, 366(6453), pp. 365–368. doi: 10.1038/366365a0.

Hadwiger, J. A. *et al.* (1989) ‘A family of cyclin homologs that control the G1 phase in yeast)’, *Proceedings of the National Academy of Sciences of the United States of America*, 86(16), pp. 6255–6259. doi: 10.1073/pnas.86.16.6255.

Hakem, R. (2008) ‘DNA-damage repair; the good, the bad, and the ugly', *EMBO Journal*, 27(4), pp. 589–605. doi: 10.1038/emboj.2008.15.

Hammel, M. *et al.* (2010) 'Ku and DNA-dependent protein kinase dynamic conformations and assembly regulate DNA binding and the initial non-homologous end joining complex', *Journal of Biological Chemistry*, 285(2), pp. 1414–1423. doi: 10.1074/jbc.M109.065615.

Hanahan, D. and Weinberg, R. A. (2011) 'Hallmarks of cancer: The next generation', *Cell*, 144(5), pp. 646–674. doi: 10.1016/j.cell.2011.02.013.

Hardwick, K. G. *et al.* (1996) 'Activation of the budding yeast spindle assembly checkpoint without mitotic spindle disruption', *Science*, 273(5277), pp. 953–956. doi: 10.1126/science.273.5277.953.

Harris, R. *et al.* (2004) 'The 3D Solution Structure of the C-terminal Region of Ku86 (Ku86CTR)', *Journal of Molecular Biology*, 335(2), pp. 573–582. doi: 10.1016/j.jmb.2003.10.047.

Hartlerode, A. J. *et al.* (2015) 'Recruitment and activation of the ATM kinase in the absence of DNA-damage sensors', *Nature Structural and Molecular Biology*, 22(9), pp. 736–743. doi: 10.1038/nsmb.3072.

Hartman IV, J. L. (2007) 'Buffering of deoxyribonucleotide pool homeostasis by threonine metabolism', *Proceedings of the National Academy of Sciences of the United States of America*, 104(28), pp. 11700–11705. doi: 10.1073/pnas.0705212104.

Hartwell, L. H. *et al.* (1973) 'Genetic control of the cell division cycle in yeast: V. Genetic analysis of cdc mutants', *Genetics*, 74(2), pp. 267–286.

Hartwell, L. H. and Weinert, T. A. (1989) 'Checkpoints: Controls that ensure the order of cell cycle events', *Science*, 246(4930), pp. 629–634. doi: 10.1126/science.2683079.

He, Y. H. *et al.* (2001) ‘Expression of yeast apurinic/apyrimidinic endonuclease (APN1) protects lung epithelial cells from bleomycin toxicity’, *American Journal of Respiratory Cell and Molecular Biology*, 25(6), pp. 692–698. doi: 10.1165/ajrcmb.25.6.4550.

Hediger, F., Dubrana, K. and Gasser, S. M. (2002) ‘Myosin-like proteins 1 and 2 are not required for silencing or telomere anchoring, but act in the Tel1 pathway of telomere length control’, *Journal of Structural Biology*, 140(1–3), pp. 79–91. doi: 10.1016/S1047-8477(02)00533-6.

Heidenreich, E. *et al.* (2003) ‘Non-homologous end joining as an important mutagenic process in cell cycle-arrested cells’, *EMBO Journal*, 22(9), pp. 2274–2283. doi: 10.1093/emboj/cdg203.

Hentges, P. *et al.* (2006) ‘Evolutionary and functional conservation of the DNA non-homologous end-joining protein, XLF/Cernunnos’, *Journal of Biological Chemistry*, 281(49), pp. 37517–37526. doi: 10.1074/jbc.M608727200.

Hentges, P. *et al.* (2014) ‘Cdk1 Restrains NHEJ through Phosphorylation of XRCC4-like Factor Xlf1’, *Cell Reports*, 9(6), pp. 2011–2017. doi: 10.1016/j.celrep.2014.11.044.

Hernández-Ortega, S. *et al.* (2013) ‘Defective in mitotic arrest 1 (Dma1) ubiquitin ligase controls G 1 cyclin degradation’, *Journal of Biological Chemistry*, 288(7), pp. 4704–4714. doi: 10.1074/jbc.M112.426593.

Herrmann, G., Lindahl, T. and Schär, P. (1998) ‘Saccharomyces cerevisiae LIF1: A function involved in DNA double-strand break repair related to mammalian XRCC4’, *EMBO Journal*, 17(14), pp. 4188–4198. doi: 10.1093/emboj/17.14.4188.

Hill, J., Donald, K. A. G. and Griffiths, D. E. (1991) ‘DMSO-enhanced whole cell yeast transformation’, *Nucleic Acids Research*, 19(23), p. 6688. doi: 10.1093/nar/19.23.6688.

Hingorani, M. M. (2016) ‘Mismatch binding, ADP-ATP exchange and intramolecular signaling during mismatch repair’, *DNA Repair*, 38, pp. 24–31. doi: 10.1016/j.dnarep.2015.11.017.

Ho, Y. *et al.* (2002) ‘Systematic identification of protein complexes in Saccharomyces cerevisiae by mass spectrometry’, *Nature*, 415(6868), pp. 180–183. doi: 10.1038/415180a.

Hoffman, C. S. and Winston, F. (1987) ‘A ten-minute DNA preparation from yeast efficiently releases autonomous plasmids for transformaion of Escherichia coli’, *Gene*, 57(2–3), pp. 267–272. doi: 10.1016/0378-1119(87)90131-4.

Hopfner, K. P. *et al.* (2002) ‘The Rad50 zinc-hook is a structure joining Mre11 complexes in DNA recombination and repair’, *Nature*, 418(6897), pp. 562–566. doi: 10.1038/nature00922.

Huang, D. *et al.* (1999) ‘Mammalian Cdk5 is a functional homologue of the budding yeast Pho85 cyclin-dependent protein kinase’, *Proceedings of the National Academy of Sciences of the United States of America*, 96(25), pp. 14445–14450. doi: 10.1073/pnas.96.25.14445.

Huang, D., Friesen, H. and Andrews, B. (2007) ‘Pho85, a multifunctional cyclin-dependent protein kinase in budding yeast’, *Molecular Microbiology*, 66(2), pp. 303–314. doi: 10.1111/j.1365-2958.2007.05914.x.

Huang, D., Wilson, W. A. and Roach, P. J. (1997) ‘Glucose-6-P control of glycogen synthase phosphorylation in yeast’, *Journal of Biological Chemistry*, 272(36), pp. 22495–22501. doi: 10.1074/jbc.272.36.22495.

Huertas, P. *et al.* (2008) ‘CDK targets Sae2 to control DNA-end resection and homologous recombination', *Nature*, 455(7213), pp. 689–692. doi: 10.1038/nature07215.

Huertas, P. and Jackason, S. P. (2009) 'Human CtIP mediates cell cycle control of DNA end resection and double strand break repair', *Journal of Biological Chemistry*, 284(14), pp. 9558–9565. doi: 10.1074/jbc.M808906200.

Humbert, S., Dhavan, R. and Tsai, L. H. (2000) 'P39 Activates Cdk5 in Neurons, and is associated with the actin cytoskeleton', *Journal of Cell Science*, 113(6), pp. 975–983.

Iaccarino, I. *et al.* (1998) 'hMSH2 and hMSH6 play distinct roles in mismatch binding and contribute differently to the ATPase activity of hMutSα', *EMBO Journal*, 17(9), pp. 2677–2686. doi: 10.1093/emboj/17.9.2677.

Iliakis, G. *et al.* (2003) 'DNA damage checkpoint control in cells exposed to ionizing radiation', *Oncogene*, 22(37), pp. 5834–5847. doi: 10.1038/sj.onc.1206682.

Ira, G. *et al.* (2004) 'DNA end resection, homologous recombination and DNA damage checkpoint activation require CDK1', *Nature*, 431(7011), pp. 1011–1017. doi: 10.1038/nature02964.

Irniger, S. and Nasmyth, K. (1997) 'The anaphase-promoting complex is required in G1 arrested yeast cells to inhibit B-type cyclin accumulation and to prevent uncontrolled entry into S-phase', *Journal of Cell Science*, 110(13), pp. 1523–1531.

Ivanov, E. L. *et al.* (1996) 'Genetic requirements for the single-strand annealing pathway of double-strand break repair in Saccharomyces cerevisiae', *Genetics*, 142(3), pp. 693–704.

Jackson, L. P., Reed, S. I. and Haase, S. B. (2006) 'Distinct

Mechanisms Control the Stability of the Related S-Phase Cyclins Clb5 and Clb6', *Molecular and Cellular Biology*, 26(6), pp. 2456–2466. doi: 10.1128/mcb.26.6.2456-2466.2006.

De Jager, M. *et al.* (2001) 'Human Rad50/Mre11 is a flexible complex that can tether DNA ends', *Molecular Cell*, 8(5), pp. 1129–1135. doi: 10.1016/S1097-2765(01)00381-1.

Janke, C. *et al.* (2004) 'A versatile toolbox for PCR-based tagging of yeast genes: New fluorescent proteins, more markers and promoter substitution cassettes', *Yeast*, 21(11), pp. 947–962. doi: 10.1002/yea.1142.

Jasin, M. and Rothstein, R. (2013) 'Repair of strand breaks by homologous recombination', *Cold Spring Harbor Perspectives in Biology*, 5(11), pp. 1–18. doi: 10.1101/cshperspect.a012740.

Jeffery, D. A. *et al.* (2001) 'Multi-site phosphorylation of Pho4 by the cyclin-CDK Pho80-Pho85 is semi-processive with site preference', *Journal of Molecular Biology*, 306(5), pp. 997–1010. doi: 10.1006/jmbi.2000.4417.

Jensen, R. B., Carreira, A. and Kowalczykowski, S. C. (2010) 'Purified human BRCA2 stimulates RAD51-mediated recombination', *Nature*, 467(7316), pp. 678–683. doi: 10.1038/nature09399.

Jiménez, J. *et al.* (2013) 'Redundancy or specificity? the role of the CDK Pho85 in cell cycle control', *International Journal of Biochemistry and Molecular Biology*, 4(3), pp. 140–149.

Johnson, R. . and Rao, P. . (1970) 'Mammalian Cell Fusion: Induction of Premature Chromosome Condensation in Interphase Nuclei', *Nature*, 228, pp. 726–734. doi: doi.org/10.1038/226717a0.

Jones, J. M., Gellert, M. and Yang, W. (2001) 'A Ku bridge over broken

DNA', *Structure*, 9(10), pp. 881–884. doi: 10.1016/S0969-2126(01)00658-X.

Kaffman, A. *et al.* (1994) 'Phosphorylation of the transcription factor PHO4 by a cyclin-CDK complex, PHO80-PHO85', *Science*, 263(5150), pp. 1153–1156. doi: 10.1126/science.8108735.

Kang, L. E. and Symington, L. S. (2000) 'Aberrant Double-Strand Break Repair in rad51 Mutants of Saccharomyces cerevisiae', *Molecular and Cellular Biology*, 20(24), pp. 9162–9172. doi: 10.1128/mcb.20.24.9162-9172.2000.

Kapitzky, L. *et al.* (2010) 'Cross-species chemogenomic profiling reveals evolutionarily conserved drug mode of action', *Molecular Systems Biology*, 6(451), pp. 1–14. doi: 10.1038/msb.2010.107.

Keith, C. T. and Schreiber, S. L. (1995) 'PIK-related kinases: DNA repair, recombination, and cell cycle checkpoints', *Science*, 270(5233), pp. 50–51. doi: 10.1126/science.270.5233.50.

Khan, F. A. and Ali, S. O. (2017) 'Physiological Roles of DNA Double-Strand Breaks', *Journal of Nucleic Acids*, 2017. doi: 10.1155/2017/6439169.

Killander, D. and Zetterberg, A. (1965) 'Quantitative cytochemical studies on interphase growth. I. Determination of DNA, RNA and mass content of age determined mouse fibroblasts in vitro and of intercellular variation in generation time', *Experimental Cell Research*, 38(2), pp. 272–284. doi: 10.1016/0014-4827(65)90403-9.

Kim, J. A. and Haber, J. E. (2009) 'Chromatin assembly factors Asf1 and CAF-1 have overlapping roles in deactivating the DNA damage checkpoint when DNA repair is complete', *Proceedings of the National Academy of Sciences of the United States of America*, 106(4), pp. 1151–1156. doi: 10.1073/pnas.0812578106.

Kinoshita, E. *et al.* (2006) ‘Phosphate-binding tag, a new tool to visualize phosphorylated proteins’, *Molecular and Cellular Proteomics*, 5(4), pp. 749–757. doi: 10.1074/mcp.T500024-MCP200.

Kohda, K. *et al.* (1991) ‘Separation and identification of n-(guanosin-7-yl)-4-aminoquinoline 1-oxide, a novel nucleic acid adduct of carcinogen 4-nitroquinoline 1-oxide’, *Carcinogenesis*, 12(8), pp. 1523–1525. doi: 10.1093/carcin/12.8.1523.

Kramer, K. M. *et al.* (1994) ‘Two different types of double-strand breaks in Saccharomyces cerevisiae are repaired by similar RAD52-independent, nonhomologous recombination events.’, *Molecular and Cellular Biology*, 14(2), pp. 1293–1301. doi: 10.1128/mcb.14.2.1293.

Krejci, L. *et al.* (2003) ‘DNA helicase Srs2 disrupts the Rad51 presynaptic filament’, *Nature*, 423(6937), pp. 305–309. doi: 10.1038/nature01577.

Krenning, L., van den Berg, J. and Medema, R. H. (2019) ‘Life or Death after a Break: What Determines the Choice?’, *Molecular Cell*, 76(2), pp. 346–358. doi: 10.1016/j.molcel.2019.08.023.

Krishna, S. S. and Aravind, L. (2010) ‘The bridge-region of the Ku superfamily is an atypical zinc ribbon domain’, *Journal of Structural Biology*, 172(3), pp. 294–299. doi: 10.1016/j.jsb.2010.05.011.

Kueng, S., Oppikofer, M. and Gasser, S. M. (2013) ‘SIR proteins and the assembly of silent chromatin in budding yeast’, *Annual Review of Genetics*, 47, pp. 275–306. doi: 10.1146/annurev-genet-021313-173730.

Laporte, D. *et al.* (2016) ‘Quiescent Saccharomyces cerevisiae forms telomere hyperclusters at the nuclear membrane vicinity through a multifaceted mechanism involving Esc1, the Sir complex, and chromatin condensation’, *Molecular Biology of the Cell*, 27(12), pp.

1875–1884. doi: 10.1091/mbc.E16-01-0069.

Laroche, T. *et al.* (1998) ‘Mutation of yeast Ku genes disrupts the subnuclear organization of telomeres’, *Current Biology*, 8(11), pp. 653–657. doi: 10.1016/s0960-9822(98)70252-0.

Leahy, J. J. J. *et al.* (2004) ‘Identification of a highly potent and selective DNA-dependent protein kinase (DNA-PK) inhibitor (NU7441) by screening of chromenone libraries’, *Bioorganic and Medicinal Chemistry Letters*, 14(24), pp. 6083–6087. doi: 10.1016/j.bmcl.2004.09.060.

Lee, J. Y. *et al.* (2015) ‘Base triplet stepping by the Rad51/RecA family of recombinases’, *Science*, 350(6260), pp. 977–981. doi: 10.1126/science.aad6940.

Lee, S. E. *et al.* (1998) ‘and RPA Proteins Regulate Adaptation to G2 / M Arrest after DNA Damage’, *Cell*, 94(3), pp. 399–409.

Lee, Y. S. *et al.* (2008) ‘Molecular basis of cyclin-CDK-CKI regulation by reversible binding of an inositol pyrophosphate’, *Nature Chemical Biology*, 4(1), pp. 25–32. doi: 10.1038/nchembio.2007.52.

Lengsfeld, B. M. *et al.* (2007) ‘Sae2 Is an Endonuclease that Processes Hairpin DNA Cooperatively with the Mre11/Rad50/Xrs2 Complex’, *Molecular Cell*, 28(4), pp. 638–651. doi: 10.1016/j.molcel.2007.11.001.

Levine, K., Oehlen, L. J. W. M. and Cross, F. R. (1998) ‘Isolation and Characterization of New Alleles of the Cyclin-Dependent Kinase Gene CDC28 with Cyclin-Specific Functional and Biochemical Defects’, *Molecular and Cellular Biology*, 18(1), pp. 290–302. doi: 10.1128/mcb.18.1.290.

Li, X. *et al.* (2009) ‘PCNA Is Required for Initiation of Recombination-

Associated DNA Synthesis by DNA Polymerase δ', *Molecular Cell*, 36(4), pp. 704–713. doi: 10.1016/j.molcel.2009.09.036.

Lim, G., Chang, Y. and Huh, W. K. (2020) 'Phosphoregulation of Rad51/Rad52 by CDK1 functions as a molecular switch for cell cycle–specific activation of homologous recombination', *Science Advances*, 6(6). doi: 10.1126/sciadv.aay2669.

Lindahl, T. and Barnes, D. E. (2000) 'Repair of endogenous DNA damage', *Cold Spring Harbor Symposia on Quantitative Biology*, 65, pp. 127–133. doi: 10.1101/sqb.2000.65.127.

Liu, J. *et al.* (2011) 'Presynaptic filament dynamics in homologous recombination and DNA repair', *Critical Reviews in Biochemistry and Molecular Biology*, 46(3), pp. 240–270. doi: 10.3109/10409238.2011.576007.

Longhese, M. P., Mantiero, D. and Clerici, M. (2006) 'The cellular response to chromosome breakage', *Molecular Microbiology*, 60(5), pp. 1099–1108. doi: 10.1111/j.1365-2958.2006.05186.x.

Lopez, C. R. *et al.* (2011) 'Ku must load directly onto the chromosome end in order to mediate its telomeric functions', *PLoS Genetics*, 7(8). doi: 10.1371/journal.pgen.1002233.

Luo, K. *et al.* (2015) 'CDK-mediated RNF4 phosphorylation regulates homologous recombination in S-phase', *Nucleic Acids Research*, 43(11), pp. 5465–5475. doi: 10.1093/nar/gkv434.

Ma, C. J. *et al.* (2017) 'Protein dynamics of human RPA and RAD51 on ssDNA during assembly and disassembly of the RAD51 filament', *Nucleic Acids Research*, 45(2), pp. 749–761. doi: 10.1093/nar/gkw1125.

Ma, J.-L. *et al.* (2003) 'Yeast Mre11 and Rad1 Proteins Define a Ku-

Independent Mechanism To Repair Double-Strand Breaks Lacking Overlapping End Sequences’, *Molecular and Cellular Biology*, 23(23), pp. 8820–8828. doi: 10.1128/mcb.23.23.8820-8828.2003.

Makharashvili, N. and Paull, T. T. (2015) ‘CtIP: A DNA damage response protein at the intersection of DNA metabolism’, *DNA Repair*, 32, pp. 75–81. doi: 10.1016/j.dnarep.2015.04.016.

Malkova, A. and Haber, J. E. (2012) ‘Mutations arising during repair of chromosome breaks’, *Annual Review of Genetics*, 46, pp. 455–473. doi: 10.1146/annurev-genet-110711-155547.

Malu, S. *et al.* (2012) ‘Role of non-homologous end joining in V(D)J recombination’, *Immunologic Research*, 54(1–3), pp. 233–246. doi: 10.1007/s12026-012-8329-z.

Malumbres, M. (2014) ‘Cyclin-dependent kinases’, *Genome Biology*, 15(6), pp. 1–10. doi: 10.1186/gb4184.

Mansilla-Soto, J. and Cortes, P. (2003) ‘VDJ recombination: Artemis and its in vivo role in hairpin opening’, *Journal of Experimental Medicine*, 197(5), pp. 543–547. doi: 10.1084/jem.20022210.

Mao, Z. *et al.* (2008) ‘Comparison of nonhomologous end joining and homologous recombination in human cells’, *DNA Repair*, 7(10), pp. 1765–1771. doi: 10.1016/j.dnarep.2008.06.018.

Mari, P. O. *et al.* (2006) ‘Dynamic assembly of end-joining complexes requires interaction between Ku70/80 and XRCC4’, *Proceedings of the National Academy of Sciences of the United States of America*, 103(49), pp. 18597–18602. doi: 10.1073/pnas.0609061103.

Maringele, L. and Lydall, D. (2002) ‘EXO1-dependent single-stranded DNA at telomeres activates subsets of DNA damage and spindle checkpoint pathways in budding yeast yku70Δ mutants’, *Genes and*

Development, 16(15), pp. 1919–1933. doi: 10.1101/gad.225102.

Marsischky, G. T. *et al.* (1999) ''Saccharomyces cerevisiae MSH2/6 complex interacts with Holliday junctions and facilitates their cleavage by phage resolution enzymes', *Journal of Biological Chemistry*, 274(11), pp. 7200–7206. doi: 10.1074/jbc.274.11.7200.

Matsuzaki, K. *et al.* (2012) 'Cyclin-dependent kinase-dependent phosphorylation of Lif1 and Sae2 controls imprecise nonhomologous end joining accompanied by double-strand break resection', *Genes to Cells*, 17(6), pp. 473–493. doi: 10.1111/j.1365-2443.2012.01602.x.

McBlane, J. F. *et al.* (1995) 'Cleavage at a V(D)J recombination signal requires only RAG1 and RAG2 proteins and occurs in two steps', *Cell*, 83(3), pp. 387–395. doi: 10.1016/0092-8674(95)90116-7.

McVey, M. and Lee, S. E. (2008) 'MMEJ repair of double-strand breaks (director's cut): deleted sequences and alternative endings', *Trends in Genetics*, 24(11), pp. 529–538. doi: 10.1016/j.tig.2008.08.007.

Measday, V. *et al.* (1997) 'A family of cyclin-like proteins that interact with the Pho85 cyclin-dependent kinase.', *Molecular and Cellular Biology*, 17(3), pp. 1212–1223. doi: 10.1128/mcb.17.3.1212.

Measday, V. *et al.* (2000) 'Interactions between Pho85 cyclin-dependent kinase complexes and the Swi5 transcription factor in budding yeast', *Molecular Microbiology*, 35(4), pp. 825–834. doi: 10.1046/j.1365-2958.2000.01754.x.

Melo, J. and Toczyski, D. (2002) 'A unified view of the DNA-damage checkpoint', *Current Opinion in Cell Biology*, 14(2), pp. 237–245. doi: 10.1016/S0955-0674(02)00312-5.

Mendenhall, M. D. and Hodge, A. E. (1998) 'Regulation of Cdc28

Cyclin-Dependent Protein Kinase Activity during the Cell Cycle of the Yeast Saccharomyces cerevisiae', *Microbiology and Molecular Biology Reviews*, 62(4), pp. 1191–1243. doi: 10.1128/mmbr.62.4.1191-1243.1998.

Menoyo, S. *et al.* (2013) 'Phosphate-Activated Cyclin-Dependent Kinase Stabilizes G1 Cyclin To Trigger Cell Cycle Entry', *Molecular and Cellular Biology*, 33(7), pp. 1273–1284. doi: 10.1128/mcb.01556-12.

Mikolcevic, P. *et al.* (2012) 'Cyclin-Dependent Kinase 16/PCTAIRE Kinase 1 Is Activated by Cyclin Y and Is Essential for Spermatogenesis', *Molecular and Cellular Biology*, 32(4), pp. 868–879. doi: 10.1128/mcb.06261-11.

Mikolcevic, P., Rainer, J. and Geley, S. (2012) 'Orphan kinases turn eccentric: A new class of cyclin Y-activated, membrane-targeted CDKs', *Cell Cycle*, 11(20), pp. 3758–3768. doi: 10.4161/cc.21592.

Milne, G. T. *et al.* (1996) 'Mutations in two Ku homologs define a DNA end-joining repair pathway in Saccharomyces cerevisiae.', *Molecular and Cellular Biology*, 16(8), pp. 4189–4198. doi: 10.1128/mcb.16.8.4189.

Mimitou, E. P. and Symington, L. S. (2008) 'Sae2, Exo1 and Sgs1 collaborate in DNA double-strand break processing', *Nature*, 455(7214), pp. 770–774. doi: 10.1038/nature07312.

Mimitou, E. P. and Symington, L. S. (2010) 'Ku prevents Exo1 and Sgs1-dependent resection of DNA ends in the absence of a functional MRX complex or Sae2', *EMBO Journal*, 29(19), pp. 3358–3369. doi: 10.1038/emboj.2010.193.

Mimori, T. *et al.* (1981) 'Characterization of a high molecular weight acidic nuclear protein recognized by autoantibodies in sera from patients with polymyositis-scleroderma overlap', *Journal of Clinical Investigation*, 68(3), pp. 611–620. doi: 10.1172/JCI110295.

Mimori, T. and Hardin, J. A. (1986) 'Mechanism of interaction between Ku protein and DNA', *Journal of Biological Chemistry*, 261(22), pp. 10375–10379. doi: 10.1016/S0021-9258(18)67534-9.

Mirallas, O. *et al.* (2018) 'Intertwined control of the cell cycle and nucleocytoplasmic transport by the cyclin-dependent kinase Pho85 and RanGTPase Gsp1 in Saccharomyces cerevisiae', *Microbiological Research*, 206, pp. 168–176. doi: 10.1016/j.micres.2017.10.008.

Mishra, K. and Shore, D. (1999) 'Yeast Ku protein plays a direct role in telomeric silencing and counteracts inhibition by Rif proteins', *Current Biology*, 9(19), pp. 1123–1126. doi: 10.1016/S0960-9822(99)80483-7.

Miyamae, Y. *et al.* (1997) 'Detection of DNA lesions induced by chemical mutagens by the single cell gel electrophoresis (Comet) assay. 1. Relationship between the onset of DNA damage and the characteristics of mutagens', *Mutation Research - Genetic Toxicology and Environmental Mutagenesis*, 393(1–2), pp. 99–106. doi: 10.1016/S1383-5718(97)00090-9.

Modesti, M., Hesse, J. E. and Gellert, M. (1999) 'DNA binding of Xrcc4 protein is associated with V(D)J recombination but not with stimulation of DNA ligase IV activity', *EMBO Journal*, 18(7), pp. 2008–2018. doi: 10.1093/emboj/18.7.2008.

Morio, T. *et al.* (1999) 'Ku in the cytoplasm associates with CD40 in human B cells and translocates into the nucleus following incubation with IL-4 and anti-CD40 mAb', *Immunity*, 11(3), pp. 339–348. doi: 10.1016/S1074-7613(00)80109-0.

Morrow, D. M. *et al.* (1995) 'TEL1, an S. cerevisiae homolog of the human gene mutated in ataxia telangiectasia, is functionally related to the yeast checkpoint gene MEC1’, *Cell*, 82(5), pp. 831–840. doi: 10.1016/0092-8674(95)90480-8.

Mozdy, A. D., Podell, E. R. and Cech, T. R. (2008) ‘Multiple Yeast Genes, Including Paf1 Complex Genes, Affect Telomere Length via Telomerase RNA Abundance’, *Molecular and Cellular Biology*, 28(12), pp. 4152–4161. doi: 10.1128/mcb.00512-08.

Nakada, D., Matsumoto, K. and Sugimoto, K. (2003) ‘ATM-related Tel1 associates with double-strand breaks through an Xrs2-dependent mechanism’, *Genes and Development*, 17(16), pp. 1957–1962. doi: 10.1101/gad.1099003.

New, J. H. *et al.* (1998) ‘Rad52 protein stimulates DNA strand exchange by Rad51 and replication protein A’, *Nature*, 391(6665), pp. 407–410. doi: 10.1038/34950.

Nick McElhinny, S. A. *et al.* (2000) ‘Ku Recruits the XRCC4-Ligase IV Complex to DNA Ends’, *Molecular and Cellular Biology*, 20(9), pp. 2996–3003. doi: 10.1128/mcb.20.9.2996-3003.2000.

Nishizawa, M. *et al.* (1998) ‘Phosphorylation of Sic1, a cyclin-dependent kinase (Cdk) inhibitor, by Cdk including Pho85 kinase is required for its prompt degradation’, *Molecular Biology of the Cell*, 9(9), pp. 2393–2405. doi: 10.1091/mbc.9.9.2393.

Nugent, C. I. *et al.* (1998) ‘Telomere maintenance is dependent on activities required for end repair of double-strand breaks’, *Current Biology*, 8(11), pp. 657–662. doi: 10.1016/s0960-9822(98)70253-2.

Nurse, P., Thuriaux, P. and Nasmyth, K. (1976) ‘Genetic control of the cell division cycle in the fission yeast Schizosaccharomyces pombe’, *MGG Molecular & General Genetics*, 146(2), pp. 167–178. doi: 10.1007/BF00268085.

Nussenzweig, A. *et al.* (1996) ‘Requirement for Ku80 in growth and immunoglobulin V(D)J recombination’, *Nature*, 382(6591), pp. 551–555. doi: 10.1038/382551a0.

Ogawa, T. *et al.* (1993) ‘Similarity of the yeast RAD51 filament to the bacterial RecA filament’, *Science*, 259(5103), pp. 1896–1899. doi: 10.1126/science.8456314.

Olive, P. L. and Banáth, J. P. (1993) ‘Detection of DNA double-Strand breaks through the cell cycle after exposure to x-rays, bleomycin, etoposide and 125idurd’, *International Journal of Radiation Biology*, 64(4), pp. 349–358. doi: 10.1080/09553009314551531.

Orr-Weaver, T. L., Szostak, J. W. and Rothstein, R. J. (1981) ‘Yeast transformation: A model system for the study of recombination’, *Proceedings of the National Academy of Sciences of the United States of America*, 78(10 I), pp. 6354–6358. doi: 10.1073/pnas.78.10.6354.

Orr Weaver, T. L. and Szostak, J. W. (1983) ‘Yeast recombination: The association between double-strand gap repair and crossing-over’, *Proceedings of the National Academy of Sciences of the United States of America*, 80(14 I), pp. 4417–4421. doi: 10.1073/pnas.80.14.4417.

Paciotti, V. *et al.* (2000) ‘The checkpoint protein Ddc2, functionally related to S. pombe Rad26, interacts with Mec1 and is regulated by Mec1-dependent phosphorylation in budding yeast’, *Genes and Development*, 14(16), pp. 2046–2059. doi: 10.1101/gad.14.16.2046.

Palmbos, P. L. *et al.* (2008) ‘Recruitment of Saccharomyces cerevisiae Dnl4-Lif1 complex to a double-strand break requires interactions with Yku80 and the Xrs2 FHA domain’, *Genetics*, 180(4), pp. 1809–1819. doi: 10.1534/genetics.108.095539.

Palmbos, P. L., Daley, J. M. and Wilson, T. E. (2005) ‘Mutations of the Yku80 C Terminus and Xrs2 FHA Domain Specifically Block Yeast

Nonhomologous End Joining', *Molecular and Cellular Biology*, 25(24), pp. 10782–10790. doi: 10.1128/mcb.25.24.10782-10790.2005.

Pannunzio, N. R., Watanabe, G. and Lieber, M. R. (2018) 'Nonhomologous DNA end-joining for repair of DNA double-strand breaks', *Journal of Biological Chemistry*, 293(27), pp. 10512–10523. doi: 10.1074/jbc.TM117.000374.

Paoletti, F. *et al.* (2020) ' Molecular flexibility of DNA as a key determinant of RAD 51 recruitment ', *The EMBO Journal*, 39(7), pp. 1–15. doi: 10.15252/embj.2019103002.

Pâques, F. and Haber, J. E. (1999) 'Multiple Pathways of Recombination Induced by Double-Strand Breaks in Saccharomyces cerevisiae', *Microbiology and Molecular Biology Reviews*, 63(2), pp. 349–404. doi: 10.1128/mmbr.63.2.349-404.1999.

Paull, T. T. (2015) 'Mechanisms of ATM activation', *Annual Review of Biochemistry*, 84, pp. 711–738. doi: 10.1146/annurev-biochem-060614-034335.

Paull, T. T. and Gellert, M. (1998) 'The 3′ to 5′ exonuclease activity of Mre11 facilitates repair of DNA double-strand breaks', *Molecular Cell*, 1(7), pp. 969–979. doi: 10.1016/S1097-2765(00)80097-0.

Perrod, S. and Gasser, S. M. (2003) 'Long-range silencing and position effects at telomeres and centromeres: Parallels and differences', *Cellular and Molecular Life Sciences*, 60(11), pp. 2303–2318. doi: 10.1007/s00018-003-3246-x.

Peterson, S. E. *et al.* (2001) 'The function of a stem-loop in telomerase RNA is linked to the DNA repair protein Ku', *Nature Genetics*, 27(1), pp. 64–67. doi: 10.1038/83778.

Petukhova, G. *et al.* (1999) 'Yeast Rad54 promotes Rad51-dependent homologous DNA pairing via ATP hydrolysis-driven change in DNA double helix conformation’, *Journal of Biological Chemistry*, 274(41), pp. 29453–29462. doi: 10.1074/jbc.274.41.29453.

Petukhova, G., Sung, P. and Klein, H. (2000) ‘Promotion of Rad51-dependent D-loop formation by yeast recombination factor Rdh54/Tid1’, *Genes and Development*, 14(17), pp. 2206–2215. doi: 10.1101/gad.826100.

Piazza, A. *et al.* (2019) ‘Dynamic Processing of Displacement Loops during Recombinational DNA Repair’, *Molecular Cell*, 73(6), pp. 1255-1266.e4. doi: 10.1016/j.molcel.2019.01.005.

Plate, I. *et al.* (2008) ‘Rad52 multimerization is important for its nuclear localization in Saccharomyces cerevisiae’, *DNA Repair*, 7(1), pp. 57–66. doi: 10.1016/j.dnarep.2007.07.016.

Prevo, R. *et al.* (2018) ‘CDK1 inhibition sensitizes normal cells to DNA damage in a cell cycle dependent manner’, *Cell Cycle*, 17(12), pp. 1513–1523. doi: 10.1080/15384101.2018.1491236.

Rathmell, W. K. and Chu, G. (1994) ‘Involvement of the Ku autoantigen in the cellular response to DNA double- strand breaks’, *Proceedings of the National Academy of Sciences of the United States of America*, 91(16), pp. 7623–7627. doi: 10.1073/pnas.91.16.7623.

Renkawitz, J. *et al.* (2013) ‘Monitoring Homology Search during DNA Double-Strand Break Repair In Vivo’, *Molecular Cell*, 50(2), pp. 261–272. doi: 10.1016/j.molcel.2013.02.020.

Resnick, M. A. and Martin, P. (1976) ‘The repair of double-strand breaks in the nuclear DNA of Saccharomyces cerevisiae and its genetic control’, *MGG Molecular & General Genetics*, 143(2), pp. 119–129. doi: 10.1007/BF00266917.

Ribes-Zamora, A. *et al.* (2007) 'Distinct faces of the Ku heterodimer mediate DNA repair and telomeric functions', *Nature Structural and Molecular Biology*, 14(4), pp. 301–307. doi: 10.1038/nsmb1214.

Richardson, H. *et al.* (1993) 'Cyclin-B homologs in Saccbaromyces cerevisiae function in S phase and in G2', *Trends in Genetics*, 9(2), p. 44. doi: 10.1016/0168-9525(93)90181-g.

Rine, J. and Herskowitz, I. (1987) 'Four genes responsible for a position effect on expression from HML and HMR in Saccharomyces cerevisiae.', *Genetics*, 116(1), pp. 9–22.

Rivera-Calzada, A. *et al.* (2007) 'Structural model of full-length human Ku70-Ku80 heterodimer and its recognition of DNA and DNA-PKcs', *EMBO Reports*, 8(1), pp. 56–62. doi: 10.1038/sj.embor.7400847.

Rooney, S. *et al.* (2003) 'Defective DNA repair and increased genomic instability in Artemis-deficient murine cells', *Journal of Experimental Medicine*, 197(5), pp. 553–565. doi: 10.1084/jem.20021891.

Roth, D. B. and Wilson, J. H. (1986) 'Nonhomologous recombination in mammalian cells: role for short sequence homologies in the joining reaction.', *Molecular and Cellular Biology*, 6(12), pp. 4295–4304. doi: 10.1128/mcb.6.12.4295.

Roy, R. *et al.* (2004) 'Separation-of-function Mutants of Yeast Ku80 Reveal a Yku80p-Sir4p Interaction Involved in Telomeric Silencing', *Journal of Biological Chemistry*, 279(1), pp. 86–94. doi: 10.1074/jbc.M306841200.

Samper, E. *et al.* (2000) 'Mammalian Ku86 protein prevents telomeric fusions independently of the length of TTAGGG repeats and the G-strand overhang', *EMBO Reports*, 1(3), pp. 244–252. doi: 10.1093/embo-reports/kvd051.

Santamaría, D. *et al.* (2007) ‘Cdk1 is sufficient to drive the mammalian cell cycle’, *Nature*, 448(7155), pp. 811–815. doi: 10.1038/nature06046.

Saotome, M. *et al.* (2018) ‘Structural Basis of Homology-Directed DNA Repair Mediated by RAD52’, *iScience*, 3, pp. 50–62. doi: 10.1016/j.isci.2018.04.005.

Sawada, M. *et al.* (2003) ‘Ku70 suppresses the apoptotic translocation of bax to mitochondria’, *Nature Cell Biology*, 5(4), pp. 320–329. doi: 10.1038/ncb950.

van Schendel, R. *et al.* (2016) ‘Genomic Scars Generated by Polymerase Theta Reveal the Versatile Mechanism of Alternative End-Joining’, *PLoS Genetics*, 12(10), pp. 1–21. doi: 10.1371/journal.pgen.1006368.

Schild-Poulter, C. *et al.* (2001) ‘The Binding of Ku Antigen to Homeodomain Proteins Promotes Their Phosphorylation by DNA-dependent Protein Kinase’, *Journal of Biological Chemistry*, 276(20), pp. 16848–16856. doi: 10.1074/jbc.M100768200.

Schimmel, J. *et al.* (2019) ‘Templated Insertions: A Smoking Gun for Polymerase Theta-Mediated End Joining’, *Trends in Genetics*, 35(9), pp. 632–644. doi: 10.1016/j.tig.2019.06.001.

Schwob, E. and Nasmyth, K. (1993) ‘CLB5 and CLB6, a new pair of B cyclins involved in DNA replication in Saccharomyces cerevisiae’, *Genes and Development*, 7(7 A), pp. 1160–1175. doi: 10.1101/gad.7.7a.1160.

Sebesta, M. *et al.* (2011) ‘Reconstitution of DNA repair synthesis in vitro and the role of polymerase and helicase activities’, *DNA Repair*, 10(6), pp. 567–576. doi: 10.1016/j.dnarep.2011.03.003.

Sfeir, A. and Symington, L. S. (2015) ‘Microhomology-Mediated End

Joining: A Back-up Survival Mechanism or Dedicated Pathway?', *Trends in Biochemical Sciences*, 40(11), pp. 701–714. doi: 10.1016/j.tibs.2015.08.006.

Shibata, A. *et al.* (2011) 'Factors determining DNA double-strand break repair pathway choice in G2 phase', *EMBO Journal*, 30(6), pp. 1079–1092. doi: 10.1038/emboj.2011.27.

Shinohara, A. and Ogawa, T. (1998) 'Stimulation by Rad52 of yeast Rad51-mediated recombination', *Nature*, 391(6665), pp. 404–407. doi: 10.1038/34943.

Shiotani, B. and Zou, L. (2009) 'Single-Stranded DNA Orchestrates an ATM-to-ATR Switch at DNA Breaks', *Molecular Cell*, 33(5), pp. 547–558. doi: 10.1016/j.molcel.2009.01.024.

Shrivastav, M., De Haro, L. P. and Nickoloff, J. A. (2008) 'Regulation of DNA double-strand break repair pathway choice', *Cell Research*, 18(1), pp. 134–147. doi: 10.1038/cr.2007.111.

Sikorski, R. S. and Hieter, P. (1989) 'A System of Shuttle Vectors and Yeast Host Strains Designed for Efficient Manipulation of DNA in Saccharomyces ceratisiae', *Genetics*, 122(1), pp. 19–27. doi: 10.1080/00362178385380431.

Simoneau, A. *et al.* (2014) 'Cdk1-dependent regulation of the Mre11 complex couples DNA repair pathways to cell cycle progression', *Cell Cycle*, 13(7), pp. 1078–1090. doi: 10.4161/cc.27946.

Singer, M. S. and Gottschling, D. E. (1994) 'TLC1: Template RNA component of Saccharomyces cerevisiae telomerase', *Science*, 266(5184), pp. 404–409. doi: 10.1126/science.7545955.

Singh, A. and Xu, Y. J. (2016) 'The cell killing mechanisms of hydroxyurea', *Genes*, 7(11). doi: 10.3390/genes7110099.

Soulas-Sprauel, P. *et al.* (2007) 'Role for DNA repair factor XRCC4 in immunoglobulin class switch recombination', *Journal of Experimental Medicine*, 204(7), pp. 1717–1727. doi: 10.1084/jem.20070255.

Spagnolo, L. *et al.* (2006) 'Three-Dimensional Structure of the Human DNA-PKcs/Ku70/Ku80 Complex Assembled on DNA and Its Implications for DNA DSB Repair', *Molecular Cell*, 22(4), pp. 511–519. doi: 10.1016/j.molcel.2006.04.013.

Stellwagen, A. E. *et al.* (2003) 'Ku interacts with telomerase RNA to promote telomere addition at native and broken chromosome ends', *Genes and Development*, 17(19), pp. 2384–2395. doi: 10.1101/gad.1125903.

Sugawara, N. and Haber, J. E. (1992) 'Characterization of double-strand break-induced recombination: homology requirements and single-stranded DNA formation.', *Molecular and Cellular Biology*, 12(2), pp. 563–575. doi: 10.1128/mcb.12.2.563.

Sugawara, N., Ira, G. and Haber, J. E. (2000) 'DNA Length Dependence of the Single-Strand Annealing Pathway and the Role of Saccharomyces cerevisiae RAD59 in Double-Strand Break Repair', *Molecular and Cellular Biology*, 20(14), pp. 5300–5309. doi: 10.1128/mcb.20.14.5300-5309.2000.

Sugiyama, T. and Kantake, N. (2009) 'Dynamic Regulatory Interactions of Rad51, Rad52, and Replication Protein-A in Recombination Intermediates', *Journal of Molecular Biology*, 390(1), pp. 45–55. doi: 10.1016/j.jmb.2009.05.009.

Sugiyama, T. and Kowalczykowski, S. C. (2002) 'Rad52 protein associates with replication protein A (RPA)-single-stranded DNA to accelerate Rad51-mediated displacement of RPA and presynaptic complex formation', *Journal of Biological Chemistry*, 277(35), pp.

31663–31672. doi: 10.1074/jbc.M203494200.

Sung, P. *et al.* (1993) ‘Purification and characterization of the Saccharomyces cerevisiae RAD1/RAD10 endonuclease’, *Journal of Biological Chemistry*, 268(35), pp. 26391–26399. doi: 10.1016/S0021-9258(19)74327-0.

Sung, P. (1997) ‘Function of yeast Rad52 protein as a mediator between replication protein A and the Rad51 recombinase’, *Journal of Biological Chemistry*, 272(45), pp. 28194–28197. doi: 10.1074/jbc.272.45.28194.

Takata, M. *et al.* (1998) ‘Homologous recombination and non-homologous end-joining pathways of DNA double-strand break repair have overlapping roles in the maintenance of chromosomal integrity in vertebrate cells’, *EMBO Journal*, 17(18), pp. 5497–5508. doi: 10.1093/emboj/17.18.5497.

Tarricone, C. *et al.* (2001) ‘Structure and regulation of the CDK5-p25nck5a complex’, *Molecular Cell*, 8(3), pp. 657–669. doi: 10.1016/S1097-2765(01)00343-4.

Teo, S. H. and Jackson, S. P. (1997) ‘Identification of saccharomyces cerevisiae DNA ligase IV: Involvement in DNA double-strand break repair’, *EMBO Journal*, 16(15), pp. 4788–4795. doi: 10.1093/emboj/16.15.4788.

Thomas, B. J. and Rothstein, R. (1989) ‘Elevated recombination rates in transcriptionally active DNA’, *Cell*, 56(4), pp. 619–630. doi: 10.1016/0092-8674(89)90584-9.

Thorslund, T. *et al.* (2010) ‘The breast cancer tumor suppressor BRCA2 promotes the specific targeting of RAD51 to single-stranded DNA’, *Nature Structural and Molecular Biology*, 17(10), pp. 1263–1265. doi: 10.1038/nsmb.1905.

Toh-e, A. *et al.* (1988) ‘PHO85, a negative regulator of the PHO system, is a homolog of the protein kinase gene, CDC28, of Saccharomyces cerevisiae’, *MGG Molecular & General Genetics*, 214(1), pp. 162–164. doi: 10.1007/BF00340196.

Tomimatsu, N. *et al.* (2014) ‘Phosphorylation of EXO1 by CDKs 1 and 2 regulates DNA end resection and repair pathway choice’, *Nature communications*, 5, p. 3561. doi: 10.1038/ncomms4561.

Tomkinson, A. E. *et al.* (1993) ‘Yeast DNA repair and recombination proteins Rad1 and Rad1O constitute a single-stranded-DNA endonuclease’, *Nature*, 362(6423), pp. 860–862. doi: 10.1038/362860a0.

Tounekti, O. *et al.* (2001) ‘The ratio of single-to double-strand DNA breaks and their absolute values determine cell death pathway’, *British Journal of Cancer*, 84(9), pp. 1272–1279. doi: 10.1054/bjoc.2001.1786.

Tran, H. T., Gordenin, D. A. and Resnick, M. A. (1999) ‘The 3′→5′ Exonucleases of DNA Polymerases δ and ε and the 5′→3′ Exonuclease Exo1 Have Major Roles in Postreplication Mutation Avoidance in Saccharomyces cerevisiae’, *Molecular and Cellular Biology*, 19(3), pp. 2000–2007. doi: 10.1128/mcb.19.3.2000.

Truman, A. W. *et al.* (2012) ‘CDK-Dependent Hsp70 phosphorylation controls G1 cyclin abundance and cell-cycle progression’, *Cell*, 151(6), pp. 1308–1318. doi: 10.1016/j.cell.2012.10.051.

Truong, L. N. *et al.* (2013) ‘Microhomology-mediated End Joining and Homologous Recombination share the initial end resection step to repair DNA double-strand breaks in mammalian cells’, *Proceedings of the National Academy of Sciences of the United States of America*, 110(19), pp. 7720–7725. doi: 10.1073/pnas.1213431110.

Tseng, H. M. and Tomkinson, A. E. (2002) ‘A physical and functional interaction between yeast Pol4 and Dnl4-Lif1 links DNA synthesis and ligation in nonhomologous end joining’, *Journal of Biological Chemistry*, 277(47), pp. 45630–45637. doi: 10.1074/jbc.M206861200.

Tseng, H. M. and Tomkinson, A. E. (2004) ‘Processing and joining of DNA ends coordinated by interactions among Dnl4/Lif1, Pol4, and FEN-1’, *Journal of Biological Chemistry*, 279(46), pp. 47580–47588. doi: 10.1074/jbc.M404492200.

Tutt, A. *et al.* (2001) ‘Mutation in Brca2 stimulates error-prone homology-directed repair of DNA double-strand breaks occurring between repeated sequences’, *EMBO Journal*, 20(17), pp. 4704–4716. doi: 10.1093/emboj/20.17.4704.

Tyers, M., Tokiwa, G. and Futcher, B. (1993) ‘Comparison of the Saccharomyces cerevisiae G1 cyclins: Cln3 may be an upstream activator of Cln1, Cln2 and other cyclins’, *EMBO Journal*, 12(5), pp. 1955–1968. doi: 10.1002/j.1460-2075.1993.tb05845.x.

Uhlmann, F., Bouchoux, C. and López-Avilés, S. (2011) ‘A quantitative model for cyclin-dependent kinase control of the cell cycle: Revisited’, *Philosophical Transactions of the Royal Society B: Biological Sciences*, 366(1584), pp. 3572–3583. doi: 10.1098/rstb.2011.0082.

Villarreal, D. D. *et al.* (2012) ‘Microhomology Directs Diverse DNA Break Repair Pathways and Chromosomal Translocations’, *PLoS Genetics*, 8(11). doi: 10.1371/journal.pgen.1003026.

Walker, J. R., Corpina, R. A. and Goldberg, J. (2001) ‘Structure of the Ku heterodimer bound to dna and its implications for double-strand break repair’, *Nature*, 412(6847), pp. 607–614. doi: 10.1038/35088000.

Wang, G. *et al.* (2012) ‘Multiple phosphorylation of Rad9 by CDK is required for DNA damage checkpoint activation’, *Cell Cycle*, 11(20), pp. 3792–3800. doi: 10.4161/cc.21987.

Wang, H. *et al.* (2002) ‘Ku affects the ataxia and rad 3-related/CHK1-dependent S phase checkpoint response after camptothecin treatment’, *Cancer Research*, 62(9), pp. 2483–2487.

Wang, Y., Ghosh, G. and Hendrickson, E. A. (2009) ‘Ku86 represses lethal telomere deletion events in human somatic cells’, *Proceedings of the National Academy of Sciences of the United States of America*, 106(30), pp. 12430–12435. doi: 10.1073/pnas.0903362106.

Wells, W. A. E. and Murray, A. W. (1996) ‘Aberrantly segregating centromeres activate the spindle assembly checkpoint in budding yeast’, *Journal of Cell Biology*, 133(1), pp. 75–84. doi: 10.1083/jcb.133.1.75.

Wittenberg, C., Sugimoto, K. and Reed, S. I. (1990) ‘G1-specific cyclins of S. cerevisiae: Cell cycle periodicity, regulation by mating pheromone, and association with the p34CDC28 protein kinase’, *Cell*, 62(2), pp. 225–237. doi: 10.1016/0092-8674(90)90361-H.

Wohlbold, L. *et al.* (2012) ‘Chemical Genetics Reveals a Specific Requirement for Cdk2 Activity in the DNA Damage Response and Identifies Nbs1 as a Cdk2 Substrate in Human Cells’, *PLoS Genetics*, 8(8). doi: 10.1371/journal.pgen.1002935.

Wright, W. D. and Heyer, W. D. (2014) ‘Rad54 Functions as a Heteroduplex DNA Pump Modulated by Its DNA Substrates and Rad51 during D Loop Formation’, *Molecular Cell*, 53(3), pp. 420–432. doi: 10.1016/j.molcel.2013.12.027.

Wright, W. D., Shah, S. S. and Heyer, W. D. (2018) ‘Homologous recombination and the repair of DNA double-strand breaks’, *Journal of Biological Chemistry*, 293(27), pp. 10524–10535. doi: 10.1074/jbc.TM118.000372.

Wu, D., Topper, L. M. and Wilson, T. E. (2008) ‘Recruitment and dissociation of nonhomologous end joining proteins at a DNA double-strand break in Saccharomyces cerevisiae’, *Genetics*, 178(3), pp. 1237–1249. doi: 10.1534/genetics.107.083535.

Wu, X., Braithwaite, E. and Wang, Z. (1999) ‘DNA ligation during excision repair in yeast cell-free extracts is specifically catalyzed by the CDC9 gene product’, *Biochemistry*, 38(9), pp. 2628–2635. doi: 10.1021/bi982592s.

Wu, X. and Wang, Z. (1999) ‘Relationships between yeast Rad27 and Apn1 in response to apurinic/apyrimidinic (AP) sites in DNA’, *Nucleic Acids Research*, 27(4), pp. 956–962. doi: 10.1093/nar/27.4.956.

Wu, X., Wilson, T. E. and Lieber, M. R. (1999) ‘A role for FEN-1 in nonhomologous DNA end joining: The order of strand annealing and nucleolytic processing events’, *Proceedings of the National Academy of Sciences of the United States of America*, 96(4), pp. 1303–1308. doi: 10.1073/pnas.96.4.1303.

Wysocki, R. *et al.* (2006) ‘CDK Pho85 targets CDK inhibitor Sic1 to relieve yeast G1 checkpoint arrest after DNA damage’, *Nature Structural and Molecular Biology*, 13(10), pp. 908–914. doi: 10.1038/nsmb1139.

Xia, L. *et al.* (2007) ‘Identification of genes required for protection from doxorubicin by a genome-wide screen in Saccharomyces cerevisiae’, *Cancer Research*, 67(23), pp. 11411–11418. doi: 10.1158/0008-5472.CAN-07-2399.

Xie, A., Kwok, A. and Scully, R. (2009) ‘Role of mammalian Mre11 in classical and alternative nonhomologous end joining’, *Nature Structural and Molecular Biology*, 16(8), pp. 814–818. doi: 10.1038/nsmb.1640.

Yaakov, G. *et al.* (2009) ‘The Stress-activated Protein Kinase Hog1 Mediates S Phase Delay in Response to Osmostress’, *Molecular Biology of the Cell*, 20, pp. 3572–3582. doi: 10.1091/mbc.E09.

Yang, Z. *et al.* (2010) ‘Positive or Negative Roles of Different Cyclin-Dependent Kinase Pho85-Cyclin Complexes Orchestrate Induction of Autophagy in Saccharomyces cerevisiae’, *Molecular Cell*, 38(2), pp. 250–264. doi: 10.1016/j.molcel.2010.02.033.

You, Z. *et al.* (2005) ‘ATM Activation and Its Recruitment to Damaged DNA Require Binding to the C Terminus of Nbs1’, *Molecular and Cellular Biology*, 25(13), pp. 5363–5379. doi: 10.1128/mcb.25.13.5363-5379.2005.

Yu, S. L. and Lee, S. K. (2017) ‘Ultraviolet radiation: DNA damage, repair, and human disorders’, *Molecular and Cellular Toxicology*, 13(1), pp. 21–28. doi: 10.1007/s13273-017-0002-0.

Yu, T. Y., Garcia, V. E. and Symington, L. S. (2019) ‘CDK and Mec1/Tel1-catalyzed phosphorylation of Sae2 regulate different responses to DNA damage’, *Nucleic Acids Research*, 47(21), pp. 11238–11249. doi: 10.1093/nar/gkz814.

Zhang, Y. *et al.* (2007) ‘Role of Dnl4-Lif1 in nonhomologous end-joining repair complex assembly and suppression of homologous recombination’, *Nature Structural and Molecular Biology*, 14(7), pp. 639–646. doi: 10.1038/nsmb1261.

Zhang, Y. *et al.* (2009) ‘Regulation of repair choice: Cdk1 suppresses recruitment of end joining factors at DNA breaks’, *DNA Repair*, 8(10), pp. 1235–1241. doi: 10.1016/j.dnarep.2009.07.007.

Zhao, X. *et al.* (2017) ‘Cell cycle-dependent control of homologous recombination’, *Acta Biochimica et Biophysica Sinica*, 49(8), pp. 655–668. doi: 10.1093/abbs/gmx055.

Zhou, X. Y. *et al.* (2002) ‘An ATM-independent S-phase checkpoint response involves CHK1 pathway’, *Cancer Research*, 62(6), pp. 1598–1603.

Zhu, C. *et al.* (1996) ‘Ku86-deficient mice exhibit severe combined immunodeficiency and defective processing of V(D)J recombination intermediates’, *Cell*, 86(3), pp. 379–389. doi: 10.1016/S0092-8674(00)80111-7.

Zhu, Z. *et al.* (2008) ‘Sgs1 Helicase and Two Nucleases Dna2 and Exo1 Resect DNA Double-Strand Break Ends’, *Cell*, 134(6), pp. 981–994. doi: 10.1016/j.cell.2008.08.037.

Zou, L. and Elledge, S. J. (2003) ‘Sensing DNA damage through ATRIP recognition of RPA-ssDNA complexes’, *Science*, 300(5625), pp. 1542–1548. doi: 10.1126/science.1083430.

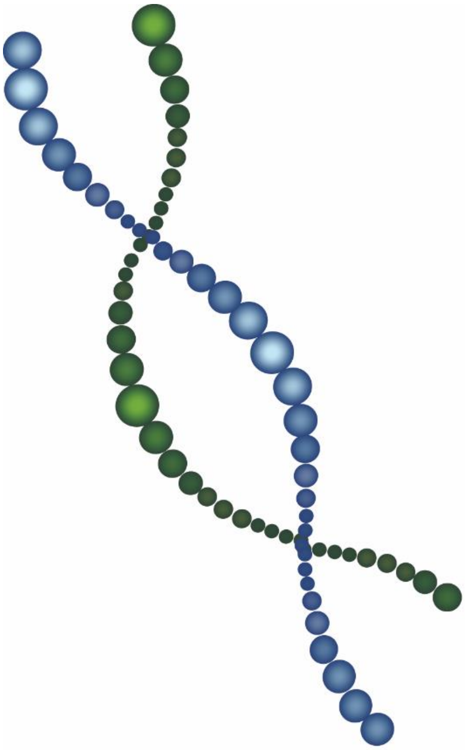

Appendix

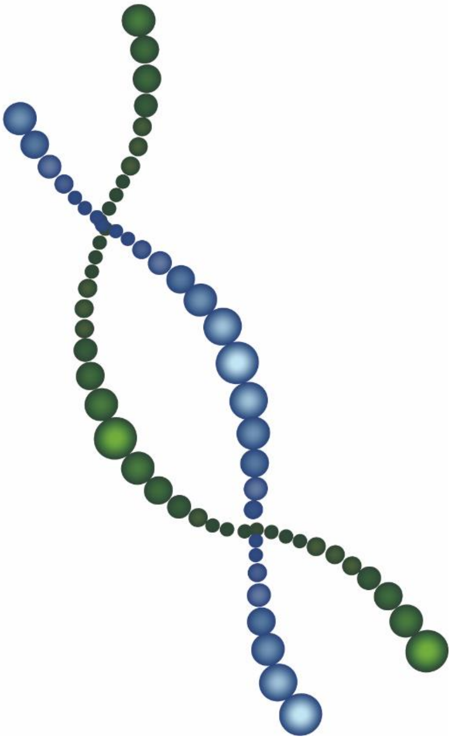

Research Article

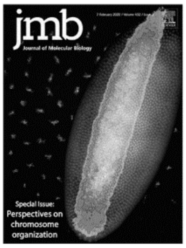

CDK-mediated Yku80 Phosphorylation Regulates the Balance Between Non-homologous End Joining (NHEJ) and Homologous Directed Recombination (HDR)

Reyes Carballar[†] Joan M. Martínez-Láinez[†] Bàrbara Samper, Samuel Bru, Elisabet Bállega, Oriol Mirallas, Natalia Ricco, Josep Clotet[*] and Javier Jiménez[*]

Basic Sciences Department, *Faculty of Medicine and Health Sciences, Universitat Internacional de Catalunya, Barcelona, Spain*

Correspondence to Josep Clotet and Javier Jiménez: *jclotet@uic.cat (J. Clotet), jjimenez@uic.es (J. Jiménez)*

https://doi.org/10.1016/j.jmb.2020.11.014
Edited by M. Yaniv

Abstract

There are two major pathways for repairing DNA double-strand breaks (DSBs): homologous directed recombination (HDR) and non-homologous end-joining (NHEJ). While NHEJ functions throughout the cell cycle, HDR is only possible during S/G_2 phases, suggesting that there are cell cycle-specific mechanisms regulating the balance between the two repair systems. The regulation exerted by CDKs on HDR has been extensively demonstrated, and here we present evidence that the CDK Pho85, in association with the G_1 cyclin Pcl1, phosphorylates Yku80 on Ser 623 to regulate NHEJ activity. Cells bearing a non-phosphorylatable version of Yku80 show increased NHEJ and reduced HDR activity. Accordingly, *yku80*^{S623A} cells present diminished viability upon treatment with the DSB-producer bleomycin, specifically in the G_2 phase of the cell cycle. Interestingly, the mutation of the equivalent residue in human Ku80 increases sensitivity to bleomycin in several cancer cell lines, suggesting that this mechanism is conserved in humans. Altogether, our results reveal a new mechanism whereby G_1-CDKs mediate the choice between HDR and NHEJ repair pathways, putting the error prone NHEJ on a leash and enabling error free HDR in G_2 when homologous sequences are available.

© 2020 Elsevier Ltd. All rights reserved.

Introduction

Maintaining the genome intact after using it to make copies or after its exposure to the wide range of insults able to damage it, is central for the ongoing correct functioning of cells. In addition, defects in DNA repair mechanisms lead to genetic instability which is responsible for several of the hallmarks of cancer.[1] Of the types of damage that DNA can undergo, double strand breaks (DSBs) is the most harmful; when not adequately repaired it can lead to chromosome rearrangements and fusions, aneuploidies, mutations, material loss, etc.[2] Cells can repair DSBs, either in a template-dependent way using homology-directed repair (HDR) pathways,[3] or in a template-independent way using error-prone non-homologous end joining (NHEJ) pathways which consist of binding the two DNA ends independently of the sequence.[4,5] The error-free HDR needs a homologous sequence to take place, which explains why HDR is restricted to the S-G_2 phases of the cell cycle.[6–9] As a result, during G_1 when homologous DNA sequences are not present, NHEJ, a repair system independent from the homologous sequences, is required. With this in mind, NHEJ could be understood as a sort of rescue mechanism functioning throughout the cell cycle but, most importantly, when HDR is inherently absent.[4] Despite the absence of a homologous template, NHEJ is mainly accurate,[10–12] suggesting that NHEJ factors play a role in maintaining fidelity.[13]

Immediately after the DSB the Ku heterodimer composed by human Ku70 and Ku80 proteins (Yku80 and Yku70 in yeast), binds to DNA

0022-2836/© 2020 Elsevier Ltd. All rights reserved.

ends.[14,15] Ku heterodimer assembles in a ring-like structure with the ability to encircle DNA ends.[16] The Ku heterodimer works as a scaffold for the DNA ligase IV, the kinase DNA-PK$_{cs}$ (absent in yeast), XRCC4[17,18] and several other proteins involved in preparing and processing the DNA ends to be joined.[19,20] In yeast, genetic studies showed that the yKu complex rapidly recruits the Mre11-Rad50-Xrs2 (MRX) complex and Sae2 to the DSB site.[21] As well as activating the DNA damage signalling by recruiting Tel1,[22] the MRX complex has two enzymatic activities; on the one hand, it displays clipping activity able to produce a nick in one of the DNA strands and; on the other hand, 3′-5′ exonuclease activity,[23] regulated by Sae2.[24] See 25 for a review. The activation of the MRX complex is essential for the choice of repair system. When inactive, the MRX complex fosters NHEJ and, when active, the resection activity initiated by the clipping and exonuclease activities is essential for a HDR based repair.[7,8,26]

MRX activation (and thereby the DSB repair system choice) is governed by CDK (Cyclin Dependent Kinase) activity.[7,8] In S-phase and G$_2$, the CDK phosphorylates and activates Sae2[24] which, in turn, is needed for the MRX clipping and exonuclease activities. This then initiates the DNA resection carried out by the 5′-3′ exonuclease Exo1, the helicase Sgs1 and maintained and extended, again, by the CDK phosphorylation on Dna2.[27] A long recession of the 5′ end is essential for the rest of the HDR components to come into (for a review see 28).

The Ku complex is, alongside other functions (see below), essential for the correct functioning of NHEJ, minimizing the potential errors intrinsic to this type of repair[13] as suggested by the high frequency of imprecise joins in cells whose Ku function is affected.[10,29–31]

In summary, the Ku heterodimer encircles and binds DNA DSBs throughout the cell cycle. The two heterodimers (one at each end of the DNA) form a bridging complex that recruits the rest of the proteins needed for NHEJ.[14,15] Ku protects DNA ends from 5′ end resection[26,32] and, as a consequence, permits NHEJ and precludes HDR.[7,8,26,33] For reviews on HDR, see 3,34.

By contrast, reports about the cell cycle regulation of NHEJ are more scarce; the main evidence in this regard was obtained in the fission yeast *Schizosaccharomyces pombe* where a key component for NHEJ, namely Xlf1 (Nej1 in budding yeast and *XLF/Cernunnos* in humans,[35] is phosphorylated by CDK during the S/G$_2$ phases. This process is essential for NHEJ inhibition during this period.[36]

Apart from its function in DNA repair, Ku is involved in other cellular processes such telomere metabolism, gene silencing[37,38] and chromatin compaction.[39] Regarding telomeres, Ku is known to bind directly to telomeric DNA ends permitting the following: First, telomere capping which is essential for the inhibition of the telomere 5′-end resection,[40,41] secondly, the telomere position effect (TPE),[37,40,42] thirdly, the intranuclear positioning of telomeres[43] and lastly, Ku prevents telomeres end-fusions.[36] How Ku differentiates between DSBs and telomeres is not fully understood, although some hypotheses have been proposed[44] and some details described.[45]

CDKs are a family of kinases that regulate the cell cycle progression.[46,47] The name comes from the fact that the CDKs' activity is tightly regulated by the cyclic expression of another family of proteins called cyclins.[48–50] The yeast *S. cerevisiae* has two CDKs that control cell cycle: the essential Cdc28, which regulates the major events in cell cycle progression, and the –supposed– superfluous Pho85, which plays essential roles under specific environmental conditions[51] and responsible of the fine-tuning of several events during the normal cell cycle.[52] Several models have been proposed to explain why two CDKs are needed to control the yeast cell cycle.[53–55] The most accepted is based on the different substrate specificities of the CDK.[51,56] Focusing on Pho85, this CDK essentially plays 2 types of roles depending on the family of cyclins that interact with 52. On the one hand, when Pho85 binds to Pho80 family cyclins, it controls phosphate metabolism.[57] On the other hand, when it binds cyclins from the Pcl1,2 family, Pho85 is involved in cell cycle control.[52,58–62] A more complex scenario is present in mammalian cells where more CDKs and cyclins are present.[50,63] Nevertheless, the general traits shown by the yeast genetic model are maintained and conserved in mammalian cells.

In this study, we identified Yku80 as a substrate for the CDK Pho85-Pcl1. We have devoted our efforts to establish the physiological relevance of this new CDK target in NHEJ mechanisms and we found that the non-phosphorylatable *yku80* mutant displays increased NHEJ, reduced HDR and compromised survival upon treatment with the DNA DSB-producer bleomycin. Our results show that Yku80 phosphorylation is involved in inhibiting NHEJ during the S and G$_2$ phases of the cell cycle and, consequently, provokes the DSB repair strategy switch from error-prone NHEJ to the more conservative and safer HDR.

Results

Yku80 is an in vitro and in vivo substrate of Pho85-Pcl1

In a genome-wide search for protein–protein interaction events in *S. cerevisiae*, Yku80 was found as a physical interactor to the CDK Pho85.[64] Furthermore, *pho*85D cells are sensitive to hydroxyurea, agent that by inhibiting dNTPs synthesis produces DNA damage[65] suggesting Pho85 has a role in DNA repair mechanisms. These clues together point to a mechanism linking cell cycle machinery (the CDK Pho85) and DNA repair (Yku80).

The aforementioned evidence drove us to search for the ability of Pho85 to phosphorylate Yku80 *in vitro*. Specifically, Pho85 can produce two different enzymes; on the one hand, Pho85, when activated by any of the Pho80 family of cyclins, is involved in phosphate metabolism.[66] On the other hand, Pho85 acts on cell cycle progression regulation when activated by cyclins from the Pcl1/2 family.[51,52] To determine which, if any, of the enzymatic forms of Pho85 is able to act on Yku80, we performed *in vitro* kinase experiments as described in 67 using bacteria produced Pho85 as kinase, Pcl1 and Pho80 as cyclins, Yku80 different mutant alleles as substrates and Pho4 as positive control. These experiments show that Pho85 phosphorylates Yku80 specifically when it is activated by Pcl1. This indicates that whatever function it could play; it must be in a process related to cell cycle progression (Figure 1(a)). Yku80 has 4 SP/TP consensus sites for CDK phosphorylation, we mutated all of them to Ala and made all the necessary mutant combinations to determine that the change S623A practically eliminates the *in vitro* enzymatic activity of Pho85-Pcl1 on Yku80, indicating that S623 is the Yku80 residue phosphorylated by Pho85-Pcl1 *in vitro* (Figure 1(b)).

To determine whether this phosphorylation process also takes place *in vivo*, we decided to produce genomic TAP-tag versions of *YKU80* and *yku80*^{S623A}. We analysed cell extracts from both strains (YEB77 and YBS1039) in a Phos-tag gel, and found increased gel mobility in Yku80-TAP cell extracts when treated with alkaline phosphatase (AP). This change is not present in the *yku80*^{S623A} extracts, suggesting that Yku80 is *in vivo* phosphorylated at residue Ser623 (Figure 1(c)) left panel). Interestingly the migration shift indicative of the phosphorylation is absent in both *pho*85D and in *pcl*1D cell extracts, suggesting that Pho85-Pcl1 is the CDK-cyclin complex phosphorylating Yku80. To further confirm this result, we analysed the cell extracts from the above-mentioned strains using two-dimensional electrophoresis, two dots can be appreciated in the wild-type extract, one of which disappears in the *yku80*^{S623A} (Figure 1(c)) right panel). We can therefore conclude that Yku80 is phosphorylated at Ser623 by Pho85-Pcl1 (see discussion).

Pho85-Pcl1 phosphorylates Yku80 *in vivo*. Pcl1 expression is cell cycle regulated, it occurs at the end of G_1 and during S-phase.[68] We decided to investigate whether Yku80 phosphorylation varies during cell cycle. We synchronised wild-type and *yku80*^{S623A} cells using a-factor and we did not detect any motility shift in the phos-tag gels between both strains suggesting that in these a-factor conditions Yku80 is not phosphorylated. We decided to explore a different synchronization method, phosphate starvation. For this, we kept the cells 7 h without phosphate source obtaining a reasonably good proportion of cells in early G_1. We released the cells in YPD and analysed the motility shift in phos-tag gels. In Figure 1(d)) it can be appreciated the slow migrating form of Yku80, which is apparent after 60 min, when the cells are about to enter S-phase as showed by the FACS analysis. This result indicates that Yky80 is phosphorylated during the G_1 to S-phase transition.

Yku80 phosphorylation by Pho85 is not involved in silencing or telomere maintenance

Before analysing the physiological relevance of Yku80 phosphorylation, we determined that the S623A mutation does not produce statistically significant changes in the amount of Yku80 protein (Figure 2(a)). We also checked whether the *yku80*^{S623A} mutant protein is still functional; for this, we investigated the ability of cells bearing the mutation S623A to grow at 37 °C, the temperature at which *YKU80* knockout cells are unable to grow.[69,70] The spot analysis showed in Figure 2(b)) demonstrate that the temperature sensitivity of the *yku80*D cells is not shared by the *yku80*^{S623A} cells suggesting that the mutation does not simply inactivate the protein. In summary, we conclude that the S623A mutation produces a partially functional protein (at least regarding the temperature sensitivity and other phenotypes, as presented below).

Next, we devoted our work to determining the physiological relevance of Ser623 phosphorylation by Pho85. Yku80 is involved in telomere protection as many reports demonstrate (see introduction). To check whether the phosphorylation of Yku80 by Pho85 regulates telomere length, we analysed the telomeres length of our *yku80*^{S623A} by southern blot. We confirmed the short telomeres presented by *yku80*D cells[71] while similar telomere length is presented by *yku80*^{S623A} and wild-type cells, suggesting that the phosphorylation of S623 is not involved in telomere maintenance (Figure 2(c)). Note that in our hands *pho*85D cells do not show short telomeres as described in 72 and contrary to presented in 73. Yku80 has also been involved in gene silencing at telomeres.[37,38] To check silencing in *yku80*^{S623A} cells, we used a system developed by 74 in which the *URA3* gene is located in a telomere or at the *HML* locus where it is efficiently silenced, yielding auxotrophic Ura- cells. Our results show that the non-phosphorylatable mutant of Yku80 is still fully able to silence *URA3* gene in both loci indicating independency between *yku80*^{S623A} mutation and gene silencing. (Figure 2(d)).

has a role in DNA repair mechanisms. These clues together point to a mechanism linking cell cycle machinery (the CDK Pho85) and DNA repair (Yku80).

The aforementioned evidence drove us to search for the ability of Pho85 to phosphorylate Yku80 *in vitro*. Specifically, Pho85 can produce two different enzymes; on the one hand, Pho85, when activated by any of the Pho80 family of cyclins, is involved in phosphate metabolism.[66] On the other hand, Pho85 acts on cell cycle progression regulation when activated by cyclins from the Pcl1/2 family.[51,52] To determine which, if any, of the enzymatic forms of Pho85 is able to act on Yku80, we performed *in vitro* kinase experiments as described in 67 using bacteria produced Pho85 as kinase, Pcl1 and Pho80 as cyclins, Yku80 different mutant alleles as substrates and Pho4 as positive control. These experiments show that Pho85 phosphorylates Yku80 specifically when it is activated by Pcl1. This indicates that whatever function it could play; it must be in a process related to cell cycle progression (Figure 1(a)). Yku80 has 4 SP/TP consensus sites for CDK phosphorylation, we mutated all of them to Ala and made all the necessary mutant combinations to determine that the change S623A practically eliminates the *in vitro* enzymatic activity of Pho85-Pcl1 on Yku80, indicating that S623 is the Yku80 residue phosphorylated by Pho85-Pcl1 *in vitro* (Figure 1(b)).

To determine whether this phosphorylation process also takes place *in vivo*, we decided to produce genomic TAP-tag versions of *YKU80* and *yku80*^{S623A}. We analysed cell extracts from both strains (YEB77 and YBS1039) in a Phos-tag gel, and found increased gel mobility in Yku80-TAP cell extracts when treated with alkaline phosphatase (AP). This change is not present in the *yku80*^{S623A} extracts, suggesting that Yku80 is *in vivo* phosphorylated at residue Ser623 (Figure 1(c)) left panel). Interestingly the migration shift indicative of the phosphorylation is absent in both *pho*85D and in *pcl*1D cell extracts, suggesting that Pho85-Pcl1 is the CDK-cyclin complex phosphorylating Yku80. To further confirm this result, we analysed the cell extracts from the above-mentioned strains using two-dimensional electrophoresis, two dots can be appreciated in the wild-type extract, one of which disappears in the *yku80*^{S623A} (Figure 1(c)) right panel). We can therefore conclude that Yku80 is phosphorylated at Ser623 by Pho85-Pcl1 (see discussion).

Pho85-Pcl1 phosphorylates Yku80 *in vivo*. Pcl1 expression is cell cycle regulated, it occurs at the end of G_1 and during S-phase.[68] We decided to investigate whether Yku80 phosphorylation varies during cell cycle. We synchronised wild-type and *yku80*^{S623A} cells using a-factor and we did not detect any motility shift in the phos-tag gels between both strains suggesting that in these a-factor conditions Yku80 is not phosphorylated. We decided to explore a different synchronization method, phosphate starvation. For this, we kept the cells 7 h without phosphate source obtaining a reasonably good proportion of cells in early G_1. We released the cells in YPD and analysed the motility shift in phos-tag gels. In Figure 1(d)) it can be appreciated the slow migrating form of Yku80, which is apparent after 60 min, when the cells are about to enter S-phase as showed by the FACS analysis. This result indicates that Yky80 is phosphorylated during the G_1 to S-phase transition.

Yku80 phosphorylation by Pho85 is not involved in silencing or telomere maintenance

Before analysing the physiological relevance of Yku80 phosphorylation, we determined that the S623A mutation does not produce statistically significant changes in the amount of Yku80 protein (Figure 2(a)). We also checked whether the *yku80*^{S623A} mutant protein is still functional; for this, we investigated the ability of cells bearing the mutation S623A to grow at 37 °C, the temperature at which *YKU80* knockout cells are unable to grow.[69,70] The spot analysis showed in Figure 2(b)) demonstrate that the temperature sensitivity of the *yku80*D cells is not shared by the *yku80*^{S623A} cells suggesting that the mutation does not simply inactivate the protein. In summary, we conclude that the S623A mutation produces a partially functional protein (at least regarding the temperature sensitivity and other phenotypes, as presented below).

Next, we devoted our work to determining the physiological relevance of Ser623 phosphorylation by Pho85. Yku80 is involved in telomere protection as many reports demonstrate (see introduction). To check whether the phosphorylation of Yku80 by Pho85 regulates telomere length, we analysed the telomeres length of our *yku80*^{S623A} by southern blot. We confirmed the short telomeres presented by *yku80*D cells[71] while similar telomere length is presented by *yku80*^{S623A} and wild-type cells, suggesting that the phosphorylation of S623 is not involved in telomere maintenance (Figure 2(c)). Note that in our hands *pho*85D cells do not show short telomeres as described in 72 and contrary to presented in 73. Yku80 has also been involved in gene silencing at telomeres.[37,38] To check silencing in *yku80*^{S623A} cells, we used a system developed by 74 in which the *URA3* gene is located in a telomere or at the *HML* locus where it is efficiently silenced, yielding auxotrophic Ura- cells. Our results show that the non-phosphorylatable mutant of Yku80 is still fully able to silence *URA3* gene in both loci indicating independency between *yku80*^{S623A} mutation and gene silencing. (Figure 2(d)).

Yku80 phosphorylation at Ser623 regulates DSB repair

As well as for telomere maintenance and gene silencing, Ku proteins are essential for DSB NHEJ.[17,75,76] Probably as a part of the NHEJ function, Ku is involved in the inhibition of HDR in G_1[26,77] a cell cycle phase where the genome is not replicated, no homologous copies exist and, as a consequence, it is pointless or even detrimental to activate HDR. Lastly, Ku involvement in DSB DNA repair is conserved in mammalian cells.[78]

To evaluate NHEJ in the *yku80*^{S623A} strains, we used the method described in 76. It consists of transforming a linearized plasmid; only those cells able to re-ligate the plasmid will become pro-

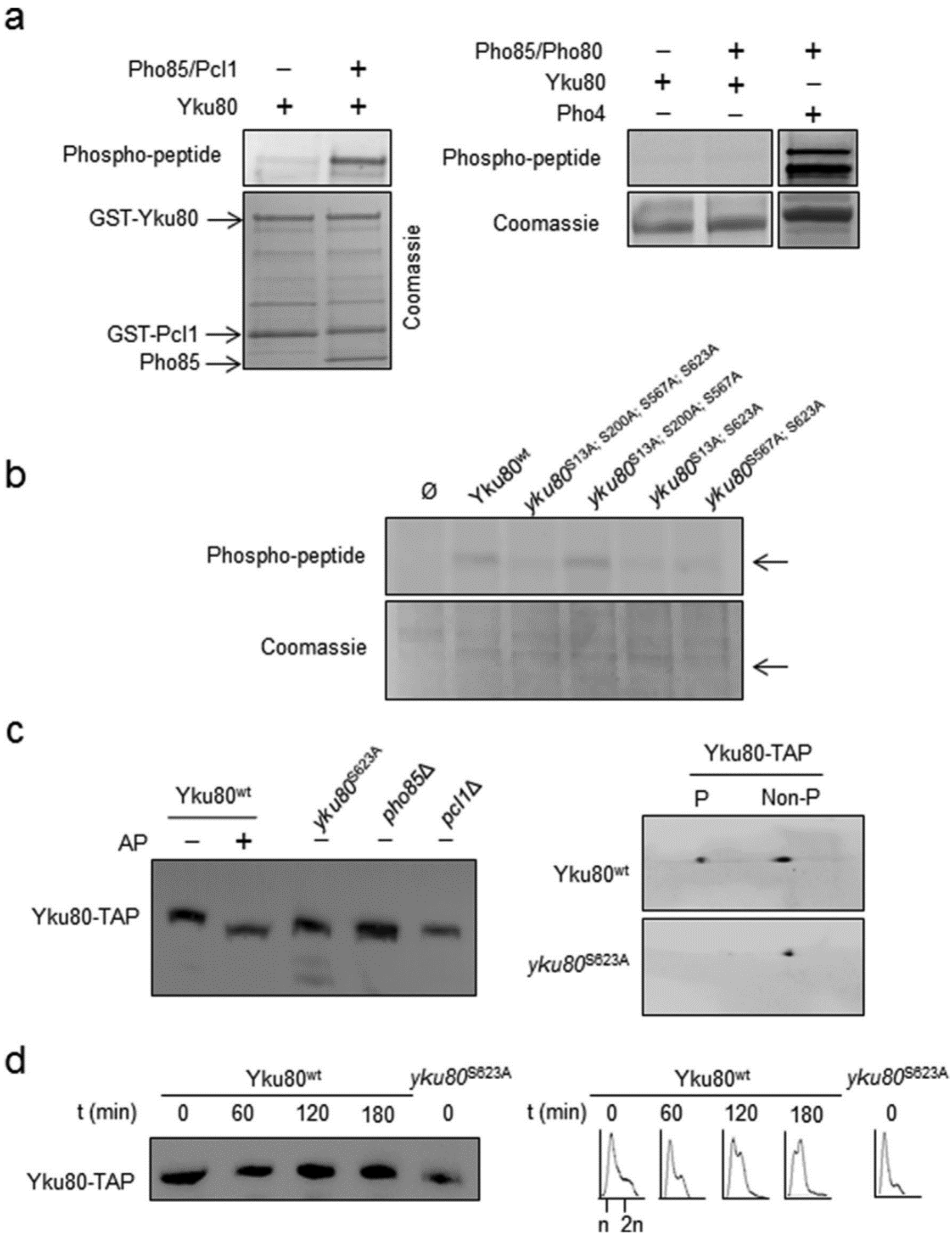

totrophic by using the plasmid auxotrophic marker and grow on an appropriate selective plate. Interestingly, the strain carrying the genomic *yku80*^{S623A} allele presents a statistically significant higher amount on NHEJ than the wild-type strain (Figure 3(a)). To further support this finding, we employed a different method to measure NHEJ; the system is based on the so-called “suicide system”.[79,80] In short, the cells were engineered to bear two HO endonuclease cutting sites flanking the *HO* endonuclease gene governed by the *GAL1* promoter. When galactose is present, the HO endonuclease is produced, the fragment is clipped, and for the cell to survive the DNA ends have to be repaired by NHEJ (the only available repair method in this genetic system because no intact homologous sequence is present). Strikingly, using this method, we found a 50-fold increase in NHEJ in the non-phosphorylatable mutant version of Yku80 (Figure 3(b)). We performed the analysis using two different mutant and wild-type (engineered exactly as the mutants were, except for the inclusion of the S623A mutation) clones and, as can be appreciated in Figure 3(b)), the effect of the S623A mutation is independent of the clone. As expected, *yku*80D cells do not have NHEJ and *pcl*1D cells show more NHEJ than wild-type cells; however, their NHEJ is much less than in *yku80*^{S623A}. It should be noted that *pcl*1D cells grow very poorly on galactose plates affecting the NHEJ measurement system. This problem is even worse in the *pho*85D strain, the cells did not grow and it was impossible to perform the analysis. The quantitative difference between the two strategies for measuring NHEJ (repairing a plasmid or a genomic DSB) may rely on the fact that cells respond differently to a genome DSB than to repairing naked DNA transformed by applying a genotoxic treatment.[4,81] We cannot rule out the possibility that the different microhomology between the DNA plasmid ends and the HO clipping could engage alternative NHEJ mechanisms.[33] To get more evidence, we used a third system to check NHEJ, this one is based on a system described in 11. We induced a genomic DSB at the *MATa* locus by the HO endonuclease expressed under the *GAL* promoter. Cells lack *HML* and *HMR* loci so the DSB can only be repaired by NHEJ. Using this system we, again, found the same result, *yku80*^{S623A} cells display higher NHEJ than wild-type cells (Figure 3(c)). Our conclusion is that *yku80*^{S623A} cells have more HNEJ than wild-type cells. As mentioned in the introduction, NHEJ is an error-prone repair system; we decided to study the influence of S623A mutation on the fidelity of NHEJ. To this end, we used a method that measures the ability to grow in auxotrophic plates when an error-free repair process occurred. Briefly, we used a plasmid bearing *LEU2* and *URA3* genes, the plasmid was digested using an enzyme cutting into *URA3* gene and transformed linearized. Leu+ colonies represent repair and Ura+ colonies represent fidelity in the repair because changes in the sequence will determine inactive *ura3* gene versions. We found no statistically significant differences in fidelity between the wild-type and the S623A mutant strains (Figure 3(d)).

Ku proteins are at the DSB ends to protect them from end-resection and to promote NHEJ. In this scenario, the increased NHEJ activity showed by the S623A mutant should be accompanied by a reduction in HDR. To test this hypothesis, we measured HDR in S623A mutant cells using a system based on the genome integration of previously linearized integrative plasmid in the non-functional *ura3* locus.[36] Cells able to integrate the plasmid by homologous recombination will grow on selective Ura-plates. We detected a statistically significant reduction in HDR when Yku80 cannot be phosphorylated (Figure 3(e)). Addition-

Figure 1. Yku80 is phosphorylated by Pho85-Pcl1 at Ser 623 both *in vitro* and *in vivo*. (a) The complex Pho85/Pcl1, but not the Pho85-Pho80, phosphorylates Yku80 *in vitro*. In vitro kinase assay using bacteria produced recombinant GST-Pho85 (digested with PreScission to eliminate GST) and GST-Pcl1 (left panel) or GST-Pho85 (digested with PreScission to eliminate GST) and GST-Pho80 (right panel). Pho85 together with the correspondent cyclin were assayed with GST-Yku80 (and GST-Pho4 as a positive control). Proteins were separated by SDS-PAGE and phosphopeptides were detected with Pro-Q™ Diamond Phosphoprotein Gel Stain. Coomassie staining of the membranes is presented as load control. (b) Pho85-Pcl1 *in vitro* phosphorylates Yku80 at Ser 623. The indicated mutant versions of Yku80 protein were obtained, assayed for Pho85-Pcl1 phosphorylation, separated by SDS-PAGE and phosphopeptides detected as in A. Arrows indicate Yku80. Coomassie is as load control. (c) Yku80 is *in vivo* phosphorylated at Ser 623 by Pho85-Pcl1. Phos-tag gel experiment (left panel) in which cell extracts of genomic *YKU80*-TAP and *yku80*^{S623A}-TAP were analyzed. Wild-type cell extract was treated with alkaline phosphatase (AP) before being electrophoretically separated in phos-tag gels *pho*85Δ and *pcl*1Δ cell extracts were included. In the right panel, 2D electrophoresis analysis (first dimension was SDS-PAGE and second was electrofocusing) of the wild-type and *yku80*^{S623A} cell extracts. Yku80 was detected by immunoblotting with anti-PAP antibodies detecting TAP-tag. (d) Yku80 phosphorylation is cell cycle dependent. Wild-type and *yku80*^{S623A} cells were synchronized in early G_1 by phosphate starvation. Cells were changed to YPD to resume cell cycle synchronously, aliquots were collected at the noted times after release and cell extracts were analyzed in phos-tag gels (left panel). FACS analysis of the same time points is presented in the right panel.

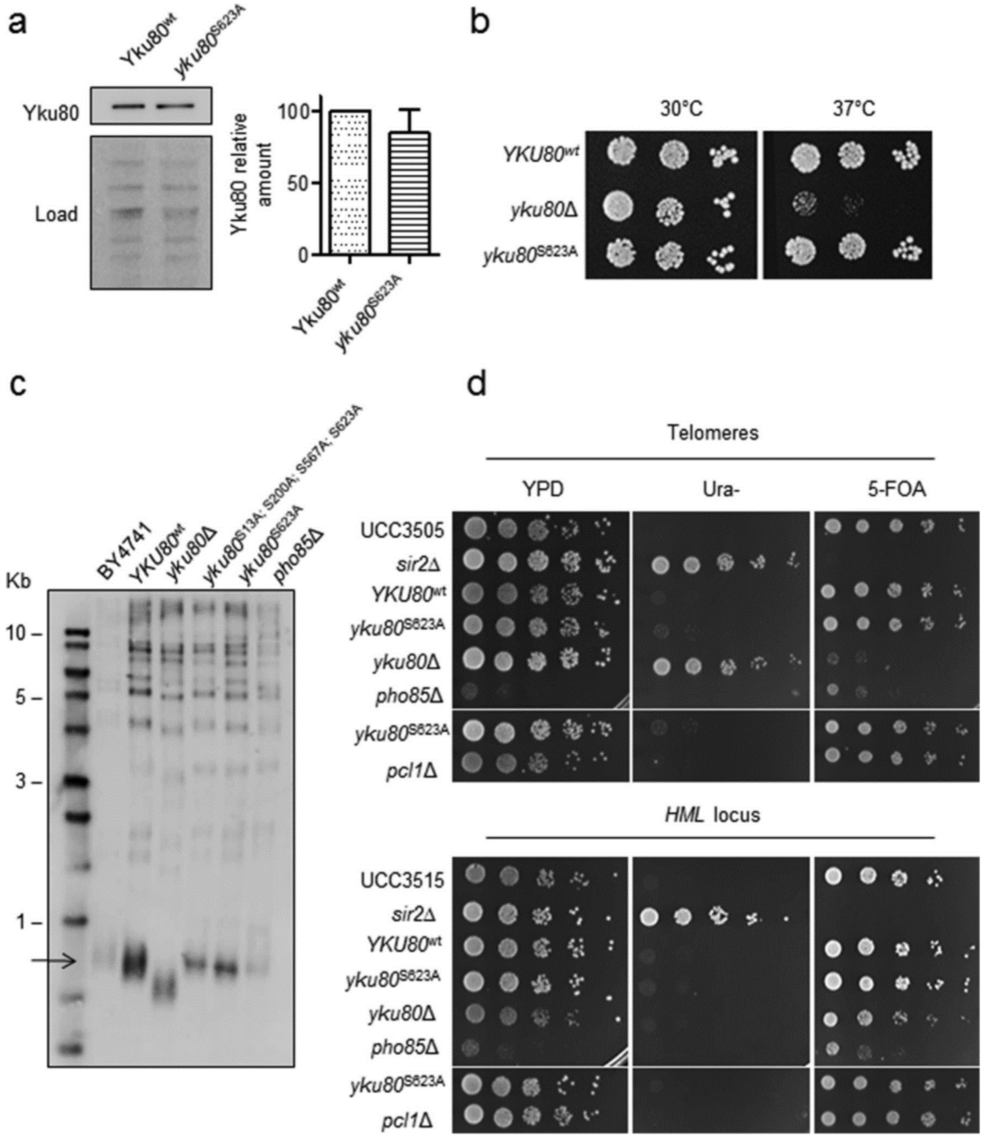
a
Yku80wt
yku80S623A
Yku80
Load
Yku80 relative amount
100
50
0
Yku80wt
yku80S623A
b
30°C
37°C
YKU80wt
yku80Δ
yku80S623A
c
Kb
BY4741
YKU80wt
yku80Δ
yku80S13A; S200A; S567A; S623A
yku80S623A
pho85Δ
10 –
5 –
3 –
1 –
d
Telomeres
YPD
Ura-
5-FOA
UCC3505
sir2Δ
YKU80wt
yku80S623A
yku80Δ
pho85Δ
yku80S623A
pcl1Δ
HML locus
UCC3515
sir2Δ
YKU80wt
yku80S623A
yku80Δ
pho85Δ
yku80S623A
pcl1Δ

Figure 2. *yku80*^{S623A} genomic mutant is functional and does not affect telomere maintenance or gene silencing. (a) Yku80 protein amount is not altered by the *yku80*^{S623A} mutation. Western blot of TAP-tagged wild-type and *yku80*^{S623A} mutant strains growing exponentially. Ponceau staining of the membrane was used as loading control. The graph represents the quantification of 10 different experiments. (b) *yku80*^{S623A} genomic mutant restores the high temperature growing defect of *yku*80Δ cells. Spot assay of *YKU80*^{wt}, *yku80*Δ and *yku80*^{S623A} at 30 °C and 37 °C. 3 μl of three fold sequential dilutions were spotted onto YPD plates starting from $A_{\lambda 660} = 0.05$ and incubated at the noted temperature for 24 h. (c) *yku80*^{S623A} displays normal telomere length. Southern blot of *Xho*I-digested genomic DNA probed with Y′ specific sequences of yeast telomeres from the noted strains. BY4741 is the original unmodified strain and *YKU80*^{wt} represents the strain that suffered the same genetic modification as the genomic mutants except for the pursued mutations. The arrow indicates the specific fragment detected by the probe. (d) *yku80*^{S623A} does not interfere with gene silencing at telomeres nor at the *HML* locus. 10-fold serial dilutions of the exponentially growing noted strains.[110] were spotted on the indicated plates at an initial $A_{\lambda 660} = 0.05$. Cells silencing properly should not grow on Ura- plates and the opposite should be observed on the 5-FOA plates.

ally, we used a method to monitor genomic DSB repair, for this we used a system described in 82. In this system, HO endonuclease is induced by addition of galactose to the medium and generates a DSB in the *MATa* gene (chromosome III). Because the cells lack *HML* and *HMR* genes, the DSB cannot be repaired by intrachromosomal homologous recombination. Instead, the cells contain *MATa-inc* sequences on chromosome V; in consequence, DSB at *MATa* can be repaired by ectopic recombination by using the *MATa-inc* sequence as a homologous donor (*MATa-inc* cannot be re-cut by HO). Using this system we obtained a consistent, although not statistically significant ($p = 0.3$) reduction in HDR in cells bearing the S623A mutation (Figure 3(f)). Our conclusion is that, at least in one of the genetic systems used, S623A mutant shows less HDR.

To continue with the analysis of the phosphorylation of Yku80 we tried to produce the *yku80*^{S623EE} phophomimetic mutant. After different attempts and strategies, we were unable to obtain that genomic mutant. Finally, we transformed wild-type cells with plasmids bearing *YKU80* or *yku80*^{S623EE} versions and while we obtained normal number of colonies using *YKU80*, we did not obtained a single colony when we used *yku80*^{S623EE}, suggesting toxicity.

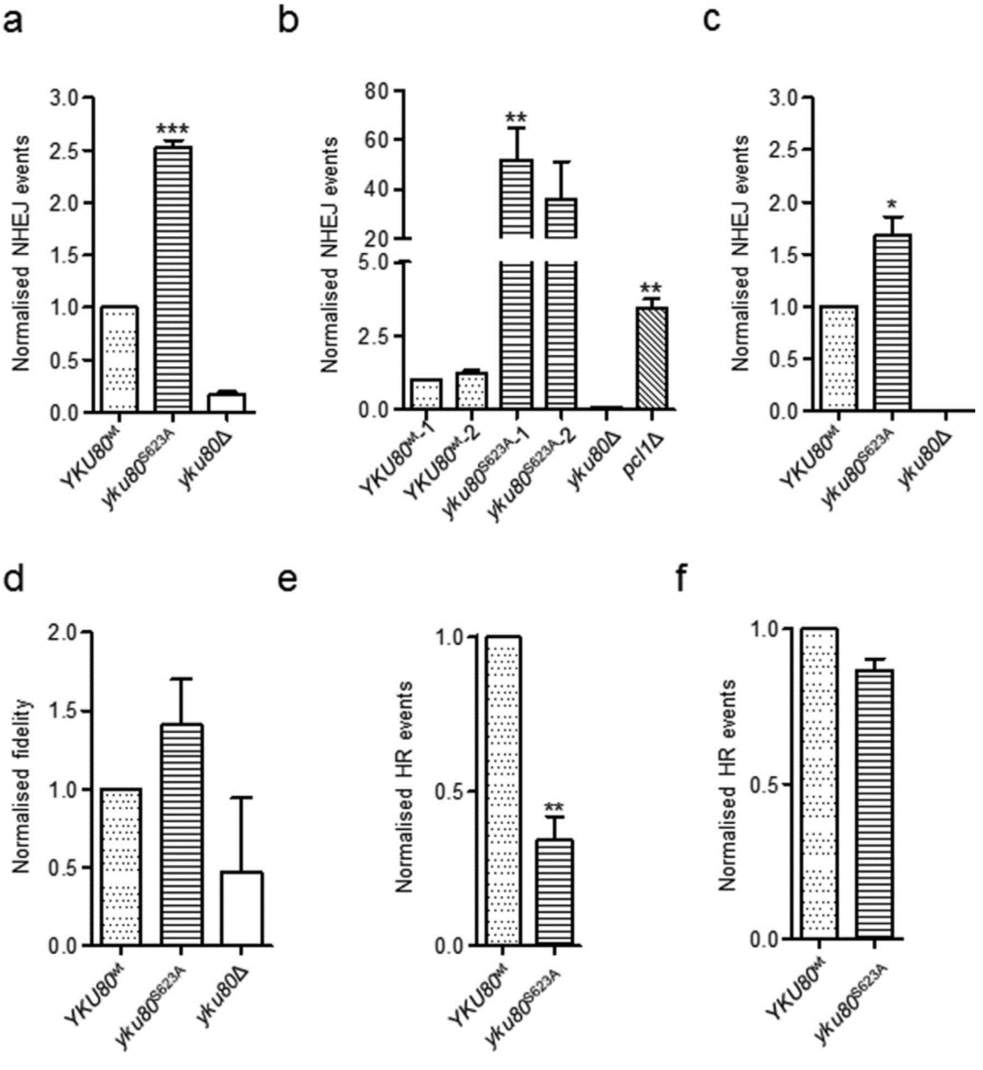

Yku80 phosphorylation hampers NHEJ in the S-G_2 phases of the cell cycle

In the experiments presented so far, the DSBs induced were either somehow artificial (cleaved plasmids) or genomic single cuts determined by the HO endonuclease system. Moving to a more physiological context, we decided to investigate the effect of bleomycin (a molecule able to produce DNA DSBs[83] in the non-phosphorylatable mutant strain of Yku80. In order to achieve this, we incubated the different strains that were growing exponentially with 300 mg/ml of bleomycin for 30 min and plated them on fresh rich plates. We found no differences in viability, quantified by counting colonies, between the S623A mutant and the wild-type (Figure 4(a)).

Damaging the cells in asynchronous cultures where cells are in different cell cycle phases and, therefore, with a differing influence on the different repair mechanisms, could conceal the putative role played by Yku80.[84] Moreover, considering our previous results showing the inhibition of HDR by the S623A mutation, we decided to analyse the effect of the S623A mutation specifically in G_2 phase synchronised cells where HDR takes place. For this, we synchronised cells in G_1 using a-factor, released them and let them to progress synchronously for 70 min until their genome was mostly replicated (as demonstrated by FACS analysis in Figure 4(b)). At this point, we produced DSB damage by adding 300 μg/ml bleomycin. Under these conditions, S623A cells presented reduced viability (Figure 4(b)), most likely due to the reduced HDR that S623A cells have (showed previously in Figure 3(e) and (f)). Additionally, we must consider the possibility that error-prone NHEJ produces viable cells explaining the relatively small reduction of viability shown by *yku80*^{S623A} strain. Our next experiment was to eliminate the possibility of HDR by deleting the *RAD52* gene; in this instance and with the same experimental set-up, we observed the expected reduction in the viability of the *rad*52D *YKU80* wild-type strain compared to the *RAD52 YKU80* since no HDR mechanisms could take place (Figure 4(b)). Additionally, we observed the recovery of viability in the *yku80*^{S623A} *rad*52D cells compared to *YKU80 rad*52D, suggesting that in the absence of HDR, the increase in viability is determined by the increased NHEJ shown in S623A cells.

Yku80 regulation is a conserved mechanism

Ku proteins, despite showing a modest level of identity in terms of the aminoacid sequence, are, at least in eukaryotic cells, functionally and

Figure 3. *yku80*^{S623A} mutant cells display enhanced NHEJ and reduced HDR. (a) *yku80*^{S623A} cells present increased plasmid repair by NHEJ. The strains YRC1061 (*YKU80*^{wt}), YRC1062 (*yku80*^{S623A}) and YRC1057 (*yku*80Δ) were simultaneously transformed with *Bam*HI digested pRS416 (*URA3* as marker) and with non-digested pRS415 (*LEU2* as marker). Leu + colonies were used to assess transformation efficiency of the different strains and repair efficiency was measured as the ratio of Ura$^+$ to Leu$^+$ colonies. (b) *yku80*^{S623A} cells present increased genomic DSB repair by NHEJ. The *HO* suicide deletion system was employed to analyze genomic repair by NHEJ. HO endonuclease is expressed under *GAL* promoter producing a DSB in the genome, only those cells able to repair by NHEJ will produce colonies. Exponentially growing cells from strains YRC1047 and 1048 (*YKU80*^{wt}), YRC1061 and 1063 (*yku80*^{S623A}), YRC1051 (*yku*80Δ) and YRC1147 (*pcl*1Δ) were plated on galactose or glucose containing plates. Relative repair efficiency was measured as the ratio of colonies grown in galactose (where HO is induced) to colonies on glucose plates. (c) *yku80*^{S623A} cells present increased genomic DSB repair by NHEJ. A different genetic system than in B is used. In this case, the *GAL* promoter expressed HO endonuclease produces a DSB at its natural site in the *MAT*α locus in cells lacking *HML* and *HMR* genes and, consequently, only repairing by NHEJ. Exponentially growing cells from strains YRC1131 (*YKU80*^{wt}), YRC1132 (*yku80*^{S623A}) and YRC1133 (*yku*80Δ) were plated on galactose or glucose containing plates. Relative repair efficiency (NHEJ) was measured as the ratio of colonies grown on galactose (where HO is induced) to colonies on glucose plates. (d) Plasmid repair fidelity is independent of Ser 623 phosphorylation. Noted strains were transformed with a *Nco*I digested plasmid bearing *URA3* and *LEU2* gene markers (*Not*I site lays in *URA3* gene). Colonies on Leu- plates reflect plasmid repair, colonies growing on Ura- plates reflect accurate repair. Data are plotted as the ratio of Ura$^+$ to Leu$^+$ colonies. (e) The *yku80*^{S623A} strain shows reduced HDR plasmid repair events. Noted strains were transformed with both *Eco*RV digested YIpLac211 (Bearing *URA3* gene) and non-digested pRS415 (bearing *LEU2* gene). Relative repair efficiency was measured as the ratio of Ura$^+$ to Leu$^+$ colonies. (f) The *yku80*^{S623A} strain shows a slight and consistent, although not statistically significant ($p = 0.3$), reduced HDR in an HO endonuclease-induced genomic DSB system. HO endonuclease is under *GAL* promoter, when expressed produces a DSB in *MAT*α locus that can only be repaired by HDR using a copy of *MATa-inc* placed at chromosome V. Exponentially growing cells from strains YRC1128 (*YKU80*^{wt}) and YRC1177 (*yku80*^{S623A}) were plated on galactose or glucose containing plates. Relative repair efficiency (HDR) was measured as the ratio of galactose to glucose colonies. In all experiments, values were normalised to wild-type = 1. The mean ± SEM of a minimum of three independent experiments with internal duplicates is shown. $p < 0.05$ was considered significant (*); (**) indicates $p < 0.005$ and (***) indicates $p < 0.0001$.

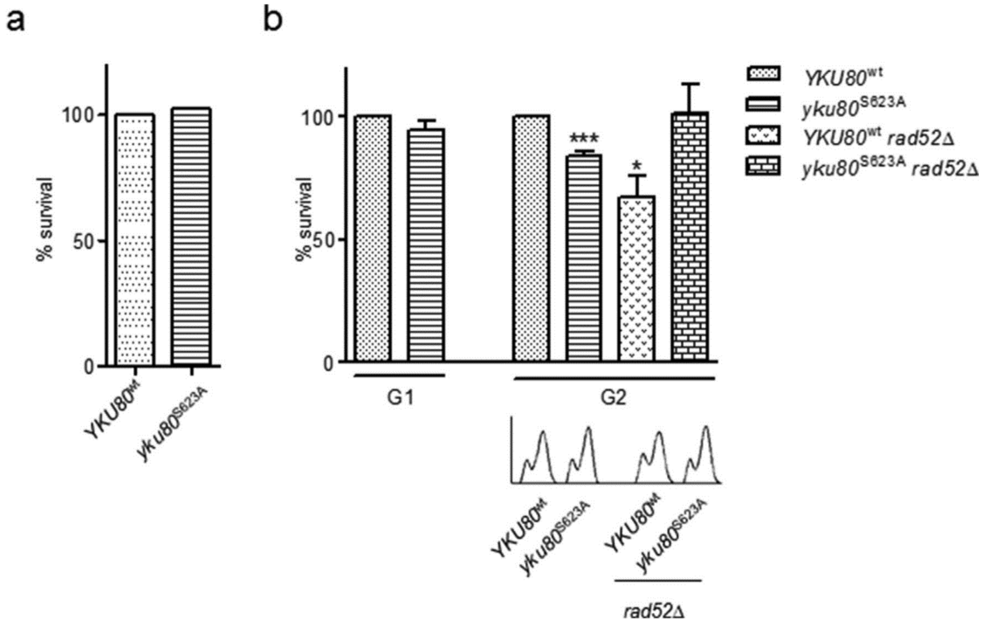

Figure 4. ***yku80*^{S623A} displays reduced viability in G$_2$ after bleomycin treatment.** (a) Cell survival measured as colony formation of asynchronous exponentially growing cultures after 30 min of 300 µg/ml bleomycin treatment. (b) Cells were synchronized in G$_1$ with α-factor, released and damage was produced after 10 min (G$_1$) or 70 min (G$_2$). DSB damage was induced by adding 300 µg/ml bleomycin for 30 min and, afterwards, cells were plated on SD plates. Repair efficiency was measured as the number of colonies after bleomycin treatment relative to the non-treated cells. The cell cycle phase in the moment of bleomycin treatment was assessed by FACS analysis, a representative experiment is presented below the survival graph. Values were normalised to wild-type = 1. The mean ± SEM of a minimum of three independent experiments with internal duplicates is shown. $p < 0.05$ was considered significant (*) and (***) indicates $p < 0.0001$.

structurally well conserved.[70] The phosphorylation site found in this study lies close to a putative nuclear localization signal in a disorganized domain at the C-terminal part or the protein. At the C-terminal domain of the human KU80 there is a consensus site for CDK phosphorylation (T629, see Figure 5(a)) that, even though it is not in exactly the same position as it is in yeast, the modest degree of sequence conservation led us to wonder whether the function of this residue might be conserved. Unfortunately, neither the expression using BL21 *E. coli* expression system, (that gives a modest amount of soluble KU80) nor the production from insect cells (that produces a KU80 co-purifying with a resident kinase) provides us with KU80 for testing the *in vitro* phosphorylation.

To show the potential relevance of T629, we decided to analyse the influence of the mutation *KU80*^{T629A} on the viability of cells after a DSB inducing treatment. For this, we cloned the wild-type and the non-phosphorylatable mutant in the viral vectors pWPI and infected A549 (lung carcinoma), MCF7 (breast adenocarcinoma) and MDA-MB-231 (breast cancer) human cancer cell lines. We treated them with 0.1 µg/ml bleomycin to induce DSBs and analysed the viability by colony forming assay. In two of the cell lines, we found a statistically significant reduction in the colony formation when the cells were overexpressing the non-phosphorylatable mutant (Figure 5(b)) indicating the *in vivo* relevance of T629 that reinforces the phenotype observed in yeast. This later result tempted us to speculate about the possibility of a conserved mechanism between species.

Discussion

Simply put, the cell cycle can be seen as a group of processes ending with the duplication of cells. However, in addition to the processes strictly related to cell division, there are several other processes taking place which are somewhat dependent on and/or closely related to cell cycle progression. One such process is DNA double strand break repair. DNA must be intact for a faithful duplication of cells, and for this reason, the cell cycle and DNA repair must be tightly coordinated. There are several examples where the cell cycle master regulators (CDKs) are also

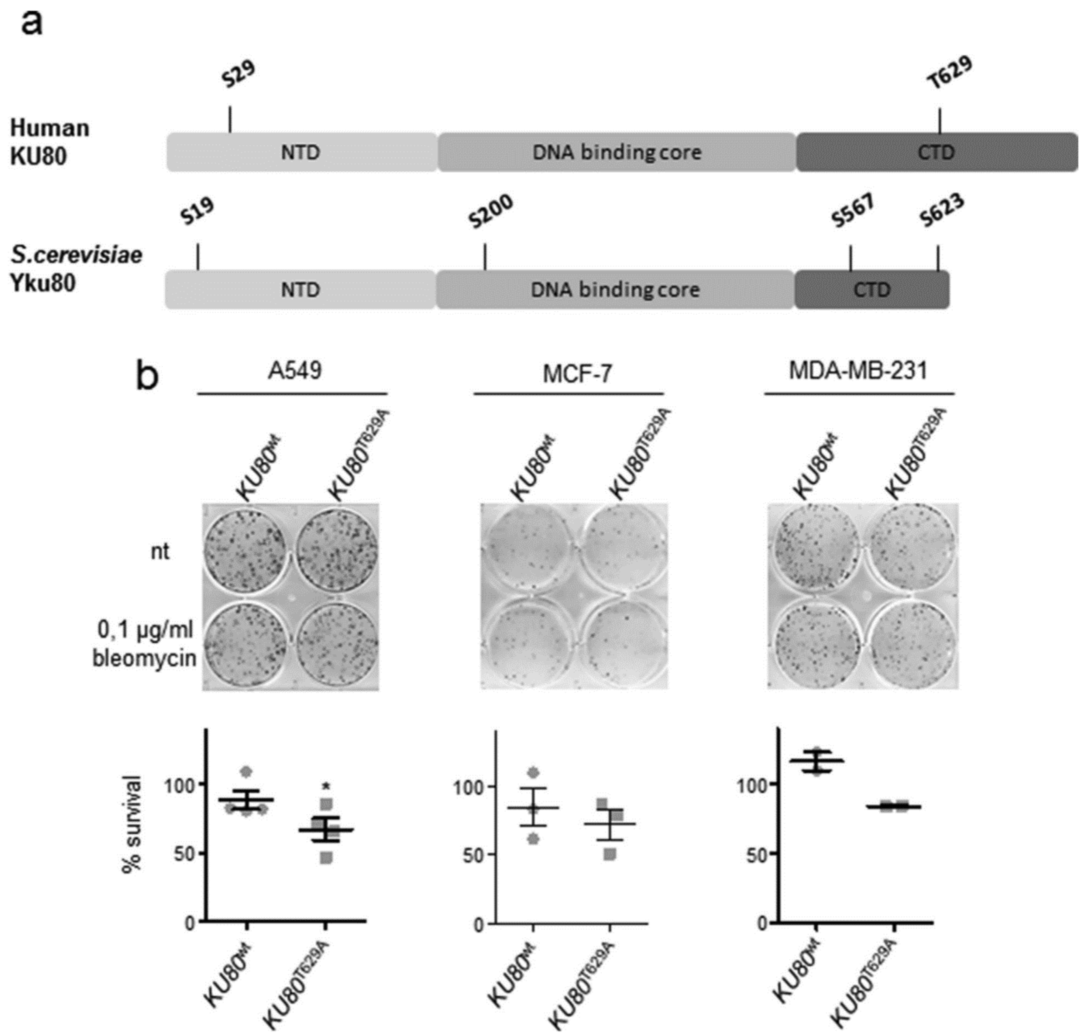

Figure 5. Overexpression of human $KU80^{\mathrm{T629A}}$ increases sensitivity to bleomycin in cancer human cell lines. (a) Schematic representation of human Ku80 where the CDK consensus sites are noted. (b) Noted cell lines were infected with the empty lentiviral pWPI vector, or with pWPI containing either $KU80^{\mathrm{wt}}$ or $KU80^{\mathrm{T629A}}$ genes. Cells were treated with 0.1 µg/ml bleomycin for 2 h. The percentage of survival was calculated as the ratio of treated versus not treated colonies after 14 days at 37 °C. The mean ± SEM of at least three independent experiments is shown. $p < 0.05$ was considered significant (*).

in charge of controlling these parallel processes. Our group has discovered some of them, such as the coordination between nutrient availability and the cell cycle[61,62] or nucleus-cytoplasmic traffic.[85] In both cases, Pho85 plays a crucial role in coordinating those events. In this study, we have explored another link, in this case, between the cell cycle machinery and DNA repair. We present a new mechanism by which cell cycle machinery coordinates the cell cycle and DNA repair to ensure a well-oiled and successful cell division.

Yku80 phosphorylation by cell cycle machinery

Yku80 is a phosphoprotein,[86] although the kinase or the responsible mechanisms remain undescribed.[86,87] We found that the CDK Pho85 is able to phosphorylate Yku80 at Serine 623. Although we have not check the ability of Cdc28, (the other CDK involved in cell cycle progression), the *in vivo* phosphorylation evidence presented in which Yku80 shows a very similar migration pattern in both *pho*85D and in wild-type alkaline phosphatase treated cell extracts, points to Pho85 as the kinase responsible for this reaction.

Synchronizing cells is an inherently artifact-producing process. We have no explanation for the absence of Yku80 phosphorylation in a-factor synchronized cells. Pho85 is essential for cell cycle resume after phosphate starvation,[61] representing an environmental situation in which Pho85 is active and in consequence a set-up in which its activity could be detected. Our results indicate that Yku80 is phosphorylated during the G_1 to S-phase transition which is precisely the moment in which Pcl1 is expressed.[68]

A new mechanism for the cell cycle control of DSB repair

The term NHEJ was introduced by Moore and Haber to describe the repair process that takes place when non-homologous donors are present.[11] Accordingly, NHEJ can be considered a default repair mechanism, an early responder mechanism to DNA ends not presenting an extensive ssDNA tail.[88] As such, NHEJ operates throughout the cell cycle while HDR is largely restricted to the cell cycle phases where a homologous DNA sequence is available (S-phase and G_2).[6] It is worth mentioning that entry into mitosis involves chromatin structural changes that prevent DSB repair and cells undertake mitosis in the presence of DNA damage.[89] The key element for the selection of the repair mechanism is the 5′–3′ end resection process, which is essential for HDR (see below).

CDKs act on DSB repair mechanisms only in S and G_2 cell cycle phases, permitting DNA end resection and, consequently, HDR.[7,8,24,90–95] It is notorious that in all the mechanisms described so far, the cell cycle machinery acts directly on the HDR mechanisms, activating them in the appropriate moment of the cycle.

The term NHEJ includes a group of mechanisms that are thought to be active throughout the cell cycle both in yeast[4] and in mammalian cells.[6] At least in yeast (in more complex genomes such as in mammalian cells NHEJ is thought to be the most relevant mechanism.[88,96] HDR mechanisms are quantitatively greater than NHEJ.[84] NHEJ must be inhibited to some extent or at least hampered[36,86] to permit HDR to take place. As mentioned before, several mechanisms for activating HDR have been described but, so far, none of them directly involves the regulation of NHEJ at least in *S. cerevisiae* or mammals.

Our work unveils a new mechanism by which cell cycle machinery regulates DNA DSB repair, a mechanism that hampers the error-prone NHEJ in the cell cycle phases where homologous sequences are present and consequently the error-free HDR could represent an advantage because it maintains DNA unmodified. In addition, the phosphorylation on Yku80 represents the first described mechanism occurring directly on the NHEJ machinery (Figure 6). The group of Doherty described a mechanism in *S. pombe* involving phosphorylation by CDKs on Xlf1, an essential piece for NHEJ.[36] Similarly to the mechanism found by us, the Xlf1 phosphorylation by CDKs ensures the inhibition of NHEJ in cell cycle phases where HDR could take place, shifting the balance of the repair to the error free system HDR.

Is KU regulation a conserved mechanism?

KU is a functionally well conserved family of proteins even though the sequence identity is surprisingly low.[70] Yku80-Ser623 residue, which is the one found by us to be phosphorylated by the CDK Pho85, is located at the structurally poorly organized C-terminal domain. Looking at the human KU sequence, a consensus sequence for CDK is also present in the homologous poorly organized domain at the C-terminus of the protein (Figure 5(a)). The CDK phosphorylation preference for disorganized domains[97] allows us to speculate about the possibility of conserved mechanisms.

CDK5 is the closest Pho85 homolog in human cells.[47,98] The activity of CDK5 is controlled by several cyclins, among them, the cyclin CCNI,[50] sharing homology with the yeast Pcl1 cyclin. We predict that CDK5/CCNI may be involved in KU phosphorylation and, thus, in DNA related processes. Interestingly, CDK5 has been linked to the DNA damage repair processes several times[99] and our work points to the idea that KU might be one of its targets.

We selected different human tumor cell lines and found a reduced ability to form colonies after DSB in some of them suggesting a reduced ability to deal with this insult. This result is somewhat surprising, considering that NHEJ is the predominant DSB repair system in cyclin mammalian cells.[34,84,88,96] The reduced viability in mammalian cells after DSBs is not consistent with the phenotype of increased NHEJ found in yeast, suggesting a different balance between NHEJ and HDR mechanisms for dealing with DSBs. Based on this evidence, we propose a conserved function of KU80 proteins in the regulation of DSB repair.

Structural and functional considerations

In this article, we present evidence supporting the inhibitory role of Yku80 phosphorylation by the CDK Pho85 on the NHEJ. Serine 623 is the Yku80 residue targeted by the CDK. This residue is at the C-terminal domain of the protein, a domain that has been reported to establish physical contact with Dnl4,[80] the DNA ligase required for the NHEJ.[100] A simple and tempting possibility is that the phosphorylation could produce conformational changes, hampering the inter-

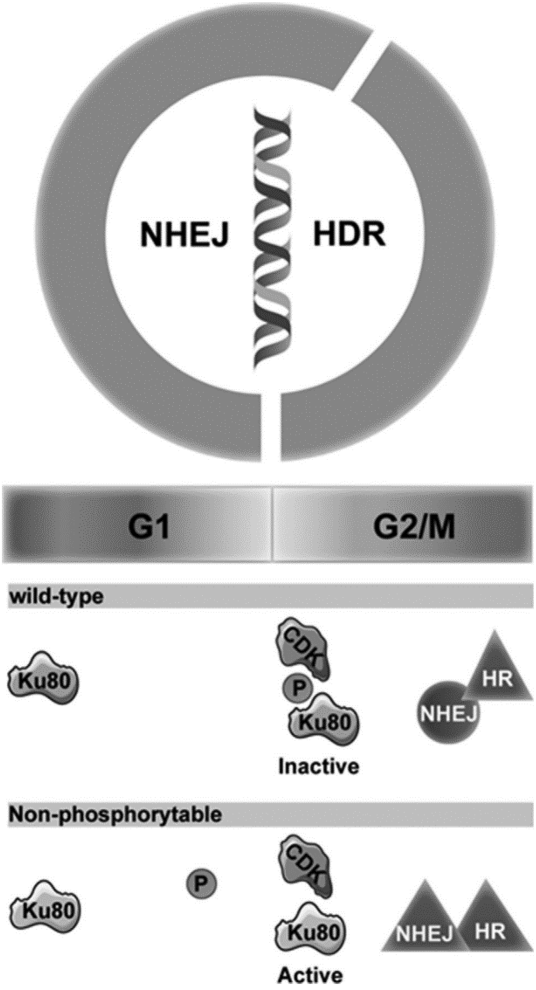

Figure 6. Working model. At the end of G_1 the CDK phosphorylates Yku80 at Ser623 contributing to the inactivation of NHEJ and favoring the activation of the error free HDR in G_2. Consequently, the NHEJ activity in the non-phosphorylatable *yku80*^{S623A} mutant remains active throughout the entire cell cycle hampering the HDR repair system.

action with the DNA ligase and consequently inhibiting NHEJ in particular phases of the cell cycle. It is relevant to mention that the cyclin Pcl1, activator of Pho85 and used for the *in vitro* kinase assay, is only present in late G_1 and during the S-phase[68]; suggesting that Yku80 could be inactivated during the G_1 to S-phase transition to permit HDR mechanisms to take place. This idea is supported by the fact that Yku80 phosphorylation is cell cycle regulated as indicated by the results presented in this work.

In the specific case of human KU80, the C-terminal domain is also essential for NHEJ; it has been shown to be responsible for the DNA-PKcs recruitment to the DNA end complex.[16,17] Although initially, DNA-PKcs activity was thought essential for NHEJ,[101] it has been recently uncovered that these proteins have repair-independent functions that protect irradiated cells from mitotic slippage.[102] We cannot rule out that this mechanism might also be an important step for the recruitment of the DNA-PKcs during gamma irradiation insults. The proteins interacting with the C-terminal domain of the yeast Yku80 and the human Ku80 are different, but in both cases, those elements are essential for NHEJ suggesting that the CDK phosphorylation could be a convergent evolutionary system to regulate NHEJ.

Materials and methods

Yeast strains, growth conditions and tagging

All strains used are shown in Table 1. Yeast were grown in water shakers at 30 °C under vigorous agitation (200 rpm) in either YPD medium (1% yeast extract, 2% peptone, and 2% glucose) or complete synthetic dextrose (SD) medium (0.67% yeast nitrogen base, 0.5% NH_4SO_4, and 2% glucose) supplemented with auxotrophic requirements (15 mg/ml of leucine and uracil, 5 mg/ml of histidine, and 10 mg/ml of tryptophan). For the 5-FOA plates, SD with all the required amino acids was supplemented with 1 mg/ml 5-FOA, (Thermo Scientific™) sterilized by filtering, and added to the medium just before plating. In all experiments, to reduce experiment's variability, the number of cells inoculated for the overnight cultures was always constant and ranging between $A_{\lambda 660}$ = 0.01–0.05 depending on the experiment.

Tagging and detentions were performed using the toolbox system[103] and confirmed by PCR and western blot or fluorescence microscopy.

Plasmids

All plasmids are in Table 2. pRS415-*URA3* was constructed by amplifying the *URA3* gene from pRS416 with the primers: URA3F4: 5′CGCAAGCTTTTCAATTCAATTCATCATTTTTTTTTTATTC3′ (*Hin*dIII restriction site underlined) and URA3R4: 5′CGCGGATCCTTAGTTTTGCTGGCCGCATC3′ (*Bam*HI restriction site underlined). The fragment was introduced into pRS415.

Cell synchrony and flow cytometry analysis

Apha-factor G_1 synchronization. Yeast cells were grown exponentially in YPD or SD to a density of approximately 1×10^7 cells/ml and a-factor (Biomedal) was added to a final concentration of 20 lg/ml. After 100 min, the cells were collected, washed and released into fresh medium.

Phosphate deprivation G_1 synchronization. As described in 104. Briefly, yeast nitrogen base without phosphate was used (MP Biomedicals) to prepare SD medium without phosphate. Phosphate deprivation experiments were performed with cells growing exponentially in SD for 16 h until they reached an optical density at 600 nm ($A_{\lambda 600}$) of 0.3–0.4, the cells were collected by filtration and, after a quick wash, resuspended at the same cellular concentration in pre-warmed SD medium lacking the phosphate source. Cells were kept phosphate deprived for 7 h and released by centrifuging and resuspending in fresh YPD.

For nocodazole synchronization, exponential growing cells were treated twice with nocodazole

Table 1 Yeast strains.

Name	Background	Relevant genotype	Source
W303-1a	W303-1a	*MATa leu2-3,112 trp1-1 can1-100 ura3-1 ade2-1 his3-11,15*	111
BY4741	BY4741	*MATa his3Δ1 leu2-Δ-200 met15-Δ-0 ura3Δ-0*	112
YBS1058	W303-1a	*yku80::hph*	This study
YBS1071	W303-1a	*YKU80-KanMX*	This study
YBS1066	W303-1a	*yku80*^{S623A}*-KanMX*	This study
YBS1061	BY4741	*YKU80-KanMX*	This study
YBS1062	BY4741	*yku80*^{S623A}*-KanMX*	This study
YBS1057	BY4741	*yku80::hph*	This study
UCC3505	YPH499	*MATa ura3-52 lys2-801 ade2-101 trp1Δ63 his3Δ200 leu2Δ1 ppr1::HIS3 adh4::URA-TEL DIA5-1*	108
YBS1015	YPH499	*MATa ura3-52 lys2-801 ade2-101 trp1Δ63 his3Δ200 leu2Δ1 ppr1::HIS3 adh4::URA-TEL DIA5-1 sir2::KanMX*	This study (derived from UCC3505)
YBS1073	YPH499	*MATa ura3-52 lys2-801 ade2-101 trp1Δ63 his3Δ200 leu2Δ1 ppr1::HIS3 adh4::URA-TEL Dia5-1 YKU80-KanMX*	This study (derived from UCC3505)
YBS1074	YPH499	*MATa ura3-52 lys2-801 ade2-101 trp1Δ63 his3Δ200 leu2Δ1 ppr1::HIS3 adh4::URA-TEL Dia5-1 yku80*^{S623A}*-KanMX*	This study (derived from UCC3505)
UCC3515	YPH499	*MATa ura3-52 lys2-801 ade2-101 trp1Δ63 his3Δ200 leu2Δ1 hml::URA3*	108
YRC1150	YPH499	*MATa ura3-52 lys2-801 ade2-101 trp1Δ63 his3Δ200 leu2Δ1 hml::URA3 pho85::TRP1*	This study (derived from UCC3515)
YRC1165	YPH499	*MATa ura3-52 lys2-801 ade2-101 trp1Δ63 his3Δ200 leu2Δ1 hml::URA3 pcl1::KanMX*	This study (derived from UCC3515)
YBS1016	YPH499	*MATa ura3-52 lys2-801 ade2-101 trp1Δ63 his3Δ200 leu2Δ1 hml::URA3 sir2::KanMX*	This study (derived from UCC3515)
YBS1050	YPH499	*MATa ura3-52 lys2-801 ade2-101 trp1Δ63 his3Δ200 leu2Δ1 hml::URA3 YKU80*-6HA-*KanMX*	This study (derived from UCC3515)
YRC1167	YPH499	*MATa ura3-52 lys2-801 ade2-101 trp1Δ63 his3Δ200 leu2Δ1 ppr1::HIS3 adh4::URA-TEL DIA5-1 pho85::KanMX*	This study (derived from UCC3505)
YRC1160	YPH499	*MATa ura3-52 lys2-801 ade2-101 trp1Δ63 his3Δ200 leu2Δ1 ppr1::HIS3 adh4::*	This study (derived

(*continued on next page*)

Table 1 (*continued*)

Name	Background	Relevant genotype	Source
		URA-TEL DIA5-1 pcl1::KanMX	from UCC3505)
YBS1051	YPH499	*MATa ura3-52 lys2-801 ade2-101 trp1Δ63 his3Δ200 leu2Δ1 hml::URA3 yku80-*^{S623A}-6HA-*KanMX*	This study (derived from UCC3515)
YBS1059	YPH499	*ppr1::HIS3 adh4::URA-TEL Dia5-1 yku80::hph*	This study (derived from UCC3505)
YBS1060	YPH499	*MATa ura3-52 lys2-801 ade2-101 trp1Δ63 his3Δ200 leu2Δ1 hml::URA3 yku80::hph*	This study (derived from UCC3515)
YEB126	BY4741	*YKU80*-TAP-*KanMX*	This study
YEB77	BY4741	*yku80*^{S623A}-TAP	This study
YBS1039	BY4741	*yku80*^{S623A}-TAP-*KanMX*	This study
YEB122	BY4741	*YKU80*-TAP-*KanMX pho85::LEU2*	This study
YEB94	BY4741	*YKU80*-TAP-*KanMX pcl1::LEU2*	This study
YRC1029	W303-1a	*YKU80*-eGFP-*HIS3*	This study
YRC1031	W303-1a	*yku80*^{S623A}*-eGFP-HIS3*	This study
YRC1120	BY4741	*YKU80-KanMX rad52::hph*	This study
YRC1124	BY4741	*yku80*^{S623A}*-KanMX rad52::hph*	This study
JKM179		*matα HO hml:ADE1 hmr::ADE1 ade1-100 leu2-3, 112 trp::hisG lys5 ura3-52 ade3::GAL::HO arg5, 6::MATa-inc::HPH1*	82
YRC1131		*matα HO hml:ADE1 hmr::ADE1 ade1-100 leu2-3, 112 trp::hisG lys5 ura3-52 ade3::GAL::HO arg5,6::MATa-inc::HPH1 YKU80-KanMX*	This study (derived from JKM179)
YRC1132		*matα HO hml:ADE1 hmr::ADE1 ade1-100 leu2-3, 112 trp::hisG lys5 ura3-52 ade3::GAL::HO arg5, 6::MATa-inc::HPH1 yku80-*^{S623A}*-KanMX*	This study (derived from JKM179)
YRC1133		*matα HO hml:ADE1 hmr::ADE1 ade1-100 leu2-3, 112 trp::hisG lys5 ura3-52 ade3::GAL::HO arg5,6::MATa-inc::HPH1 yku80::KanMX*	This study (derived from JKM179)
YJK17		*MATα hoΔ hmlΔ::ADE1 hmrΔ::ADE1 ade1-100 leu2-3,112 trp::hisG lys5 ura3-52 ade3::GAL::HO arg5,6::MATa*-inc::*HPH1*	82
YRC1128		*MATα hoΔ hmlΔ::ADE1 hmrΔ::ADE1 ade1-100 leu2-3,112 trp::hisG lys5 ura3-52 ade3::GAL::HO arg5,6::MATa*-inc::*HPH1 YKU80-KanMX*	This study (derived from YJK17)
YRC1177		*MATα hoΔ hmlΔ::ADE1 hmrΔ::ADE1 ade1-100 leu2-3,112 trp::hisG lys5 ura3-52 ade3::GAL::HO arg5,6::MATa*-inc::*HPH1 yku80*^{S623A}*-KanMX*	This study (derived from YJK17)
YRC1178		*MATα hoΔ hmlΔ::ADE1 hmrΔ::ADE1 ade1-100 leu2-3,112 trp::hisG lys5 ura3-52 ade3*::GAL::*HO arg5,6::MATa*-inc::HPH1 *yku80*^{S623A}*-KanMX*	This study (derived from YJK17)
YRC1172		*MATα hoΔ hmlΔ::ADE1 hmrΔ::ADE1 ade1-100 leu2-3,112 trp::hisG lys5 ura3-52 ade3*::GAL::*HO arg5,6::MATa*-inc::HPH1 *yku80::KanMX*	This study (derived from YJK17)
YW1276		MATα-inc ade2::HOSD(+1)::STE3-MET15 his3Δ1 leu2Δ met15Δ ura3Δ	80
YRC1047		MATα-inc ade2::HOSD(+1)::STE3-MET15 his3Δ1 leu2Δ met15Δ ura3Δ *YKU80-KanMX*	This study (derived from YW1276)
YRC1048		MATα-inc ade2::HOSD(+1)::STE3-MET15 his3Δ1 leu2Δ met15Δ ura3Δ *YKU80-KanMX*	This study (derived from YW1276)
YRC1051		MATα-inc ade2::HOSD(+1)::STE3-MET15 his3Δ1 leu2Δ met15Δ ura3Δ *yku80::KanMX*	This study (derived from YW1276)
YRC1061		MATα-inc ade2::HOSD(+1)::STE3-MET15 his3Δ1 leu2Δ met15Δ ura3Δ *yku80*^{S623A}*-KanMX*	This study (derived from YW1276)
YRC1063		MATα-inc ade2::HOSD(+1)::STE3-MET15 his3Δ1 leu2Δ met15Δ ura3Δ *yku80*^{S623A}*-KanMX*	This study (derived from YW1276)
YRC1147		MATα-inc ade2::HOSD(+1)::STE3-MET15 his3Δ1 leu2Δ met15Δ ura3Δ *pcl1::LEU2*	This study (derived from YW1276)

Table 2 Plasmids.

Name	Relevant characteristics	Source
pJC1043	pRS316	103
pJC2287	YIplac211	113
pJC1314	pRS415-empty	103
pJC2170	pRS415-*URA3* (cloned between *Hin*dIII and *Bam*HI)	This study
pJC1491	pRS414	103
pJC2242	pRS414-*YKU80*	This study
pJC2246	pRS414-*yku80*^{S629A}	This study
pJC1759	pWPI	Addgene ref 12254
pWPI KU	pWPI-KU80	This study
pWPI KU	pWPI-KU80^{T629A}	This study

(15 μg/ml final concentration) for 60 min. Nocodazole was washed by centrifugation and cells resuspended in fresh growing medium to resume cell cycle.

The flow cytometry analysis was as in 105. In short, cells were fixed in 70% ethanol, washed with 50 mM Na-citrate, treated with 0.1 mg/ml RNase A at 37 °C for 3 h to overnight, stained with 4 μg/ml propidium iodide, slightly sonicated to disrupt cell aggregates, and analysed in a FACSCalibur flow cytometer (BD Biosciences, San Jose, CA). 10^4 cells were analysed for each time point.

Dot assays

Cells were grown overnight in YPD medium, diluted to $A_{\lambda 660}$ = 0.05 and tenfold sequentially diluted in fresh YPD. 3 ll were spotted on the appropriate plates and incubated for 48 h at the indicated temperature.

Cell extract and immunoblot

For western blot analysis, cells were treated as described in 106. The primary antibody was anti-PAP 1:4.000 (Sigma, P1291). The secondary antibody was donkey anti-goat-HRP 1:25000 (from Jackson Laboratories). Immunoblots were developed using Luminata Forte Western HRP Substrate (Millipore) and images were taken using GeneSnap (Syngene) and quantified using Image Studio Lite (Li-Cor).

For Phos-tag experiments, the stacking gel buffer was 350 mM Bis–Tris (pH 6.8), 0.1% v/v TEMED, and 0.05% w/v ammonium persulfate (APS); acrylamide concentration was 4% (w/v). The resolving gel buffer was 350 mM Bis–Tris (pH 6.8), 100 lM Phos-Tag™, 40 lM Zn $(NO_3)_2$, 0.05% v/v TEMED, 0.01% w/v APS; acrylamide concentration was 6% (w/v). The running buffer consisted of 50 mM Tris-HCl pH = 7.5, 50 mM MOPS, 0.1% (w/v) SDS and 5 mM $NaHSO_3$ pH = 7.2. Gels were run for 1 h at 100 V for optimal separation of protein species. The transfer buffer was 25 mM Tris, 192 mM glycine, pH 8.3, 20% v/v methanol, 5 mM $NaHSO_3$ pH = 7.2 and 2.5 mM NaPPi. Proteins were transferred to PVDF membranes (Immobilon-P; Millipore) at 20 V and 4 °C overnight.

Protein extraction from human cell lines

Cells were washed with ice-cold phosphate-buffered saline (PBS) and placed on lysis buffer (20 mM TRIS, 5 mM EDTA, 1% NP40 (IGEPAL CA-630), 150 mM NaCl, pH 7.4) supplemented with Pierce Phosphatase Inhibitor Mini tablets and Protease Inhibitor tablets from Thermo Fisher Scientific (refs: 88,667 and 88,266 respectively). Cell extracts were prepared by vortex following centrifugation at 14,000 rpm for 20 min at 4 °C. Finally, the supernatants were collected and protein concentration was quantified by Bradford assay (BioRad). A total protein of 30 μg was used for immunodetection by western blot.

Recombinant protein purification

GST fusion proteins were expressed using *Escherichia coli* strain BL21 (DE3) (Stratagene). Protein expression was induced with 1 mM isopropyl b-D-thiogalactopyranoside (IPTG) for 3 h at 25 °C. Cells were collected by centrifugation, resuspended in 600 μl of phosphate-buffered saline (PBS) with 0.1% Triton X-100 (PBS-T) and a protease inhibitor mixture (2 mg/ml of pepstatin, 2 mg/ml of leupeptin, 1 mM pepstatin leupeptin phenylmethylsulfonyl fluoride, or PMSF, and 1 mM benzamidine), and subjected to mechanical rupture by sonication. Cell debris was removed by centrifugation, and the supernatants were purified using glutathione-Sepharose chromatography (GE Healthcare), as described in the manufacturer's protocol. After incubation with rotation for 2 h at 4 °C, the beads were collected by centrifugation (1000 rpm for 1 min at 4 °C) and washed three times with PBS-T. The elution was performed by adding 10 mM glutathione.

In vitro kinase assay

Kinase assays were performed as previously described.[107] Briefly, 0.5 μg of Pho85 and 1 μg of GST-Pcl1 were added to 1 μg of the different GST-substrates (recombinant proteins expressed and purified from *E. coli.* In the case of Pho85, GST was eliminated by digestion with the protease pre-Scission from GenScript) to be checked in the presence of 100 μM ATP in kinase buffer (50 mM Tris–HCl pH 7.5, 10 mM $MgCl_2$, 2 mM DTT). The mix was incubated at 30 °C for 30 min. The reaction was stopped by adding SDS-PAGE sample buffer, boiled for 5 min and resolved in 8% polyacrylamide gels. The gels were stained for detecting phosphoproteins following the protocol provided by the manufacturer (Pro-Q Diamond phosphoprotein gel stain kit from Invitrogen).

Southern blot

Genomic DNA from overnight cultures was isolated using phenol–chloroform. DNA samples where digested with *Xho*I, separated in a 1% agarose gel and transferred to Amersham™ Protran™ NC Nitrocellulose Membranes (10600001). Membranes were incubated with the DIG labelled telomere probe: 5′-TGTGGGTGTGG TGTGTGGGTGTGGTG-3′.[70] The probe was detected with anti-digoxigenin-AP, Fab fragments (Roche Applied Science, 11175033910).

Two-dimensional electrophoresis

Protein extracts were obtained as described above. A maximum of 50 μg of protein was used. Proteins were isoelectrically focused in the first dimension using 11 cm Ready Strips™ IPG (pH 3.0–10.0; Bio Rad) in an Ettan IPGphor II (Amershan Biosciences) system following the indications of the manufacturer. Proteins were resolved in the second dimension by SDS-PAGE using 4–15% gradient acrylamide gels. Proteins were transferred to PVDF membranes (Immobilon-P; Millipore) at 20 V and 4 °C overnight. The western blot was performed as described above.

Silencing assay

All yeasts strains are derived from UCC3505 and UCC3515.[108] Cell suspensions were adjusted to $A_{\lambda 660}$ = 0.05, they were 10-fold serially diluted, spotted onto YPD or 5-FOA (Thermo Scientific™) plates and incubated at 30 °C for 3–4 days.

DSB plasmid repair assay

The non-homologous end joining (NHEJ) repair assay was as in 109. In short, 300–350 ng of *Bam*HI digested pRS316 and 50–100 ng of uncut pRS415 (used to normalise the transformation process) were transformed into the pertinent strains. NHEJ efficiency was calculated as the ratio of uracil prototrophic growing colonies to leucine prototrophic growing colonies. The homologous recombination (HR) repair assay was as in 36. That is to say, 500 ng *Eco*RV digested integrative YIpLac211 and 50–100 ng of uncut pRS415 were transformed into the pertinent strains. HR efficiency was calculated as the ratio of uracil prototrophic growing colonies that have successfully integrated the *URA3* gene (the yeast background to perform these HDR experiments was BY4741 where the *URA3* has been deleted) to leucine prototrophic colonies.

Suicide deletion assay to measure NHEJ

All strains used in the suicide deletion system derived from YW1276 (MATa-inc ade2::*HOSD*(+1)::STE3-MET15 his3D1 leu2D met15D ura3D). The assay was performed as previously described in 80. In short, cells were grown exponentially in SD supplemented with 120 μg/ml adenine, plated in either 2% glucose or 2% galactose plates and incubated at 30 °C for 3–4 days. The frequency of DSB repair by NHEJ was measured as the ratio of colonies formed on the galactose plates compared to the glucose plates.

HR genomic assay

All strains used in these experiments are derived from YJK17 (*MATa ho*D *hml*D::*ADE1 hmr*D::*ADE1 ade1-100 leu2-3,112 trp*::*hisG lys5 ura3-52 ade3*::GAL::*HO arg5,6*::*MAT***a**-inc::HPH1).[82] That is, cells were grown overnight in SD 2% raffinose to $A_{\lambda 660}$ = 0.6–0.8. Cells were plated on either 2% glucose or 2% galactose SD plates. The frequency of DSB repair by HR was measured as the ratio of colonies formed on galactose plates compared to the glucose plates.

NHEJ fidelity assay

Fidelity in the NHEJ process was measured as follows, 200–300 ng of *Nco*I digested pJC2170 plasmid was transformed into the pertinent strains: pJC2170 plasmid is based on pRS415 in which *URA3* has been cloned between *Hin*dIII and *Bam*HI restriction sites. The *Nco*I site is in the *URA3* sequence. Consequently, Leu+ colonies are those able to repair the plasmid, and Ura+ those that repaired and kept the *URA3* intact. Fidelity was measured as the ratio of uracil prototrophic colonies to leucine prototrophic colonies.

Sensitivity to bleomycin

Cells were synchronised in G_1 as described above. To specifically induce the double strand breaks in the G_2 phase, cells were released from the a-factor arrest and, after 70 min, 300 μg/ml of bleomycin (AB142977, Abcam) was added. Cells were kept with the drug for 30 min, plated in 2% glucose plates and incubated at 30 °C for 2–3 days.

Colony formation assay

Cells were incubated for 2 h with 0.1 lg/ml of bleomycin (Abcam). Afterwards, cells were trypsinised, counted and seeded in 6-well plates at a density of: 1200 (A549), 2500 (MCF-7) and 1200 (MDA-MB-231) cells per well. After 2 weeks of incubation when colonies became visible, they were fixed with 1 ml of 100% methanol at −20 °C for 5 min, washed twice with PBS, stained with 0.1% crystal violet for 30 min at room temperature in the dark, washed 3–4 times with PBS, and colonies were automatically counted by using ImageJ program. To get a quantitative measure that includes the difference in growth between the colonies, the cells from the different wells were harvested and the crystal violet staining was measured as absorbance at 570 nm. The percentage of cell survival was calculated as the ratio of cells treated with bleomycin versus the control.

Viral cloning and transduction

The KU80 gene was amplified from A549 cells. Either KU80$^{\text{wt}}$ or Ku80$^{\text{T629A}}$ were cloned into pWPI lentiviral expression vector (Addgene, ref: 12254,) at the *Pme*I restriction site. For lentivirus production, 45 lg pWPI-KU80 (wt and variants)

Two-dimensional electrophoresis

Protein extracts were obtained as described above. A maximum of 50 μg of protein was used. Proteins were isoelectrically focused in the first dimension using 11 cm Ready Strips™ IPG (pH 3.0–10.0; Bio Rad) in an Ettan IPGphor II (Amershan Biosciences) system following the indications of the manufacturer. Proteins were resolved in the second dimension by SDS-PAGE using 4–15% gradient acrylamide gels. Proteins were transferred to PVDF membranes (Immobilon-P; Millipore) at 20 V and 4 °C overnight. The western blot was performed as described above.

Silencing assay

All yeasts strains are derived from UCC3505 and UCC3515.[108] Cell suspensions were adjusted to $A_{\lambda 660}$ = 0.05, they were 10-fold serially diluted, spotted onto YPD or 5-FOA (Thermo Scientific™) plates and incubated at 30 °C for 3–4 days.

DSB plasmid repair assay

The non-homologous end joining (NHEJ) repair assay was as in 109. In short, 300–350 ng of *Bam*HI digested pRS316 and 50–100 ng of uncut pRS415 (used to normalise the transformation process) were transformed into the pertinent strains. NHEJ efficiency was calculated as the ratio of uracil prototrophic growing colonies to leucine prototrophic growing colonies. The homologous recombination (HR) repair assay was as in 36. That is to say, 500 ng *Eco*RV digested integrative YIpLac211 and 50–100 ng of uncut pRS415 were transformed into the pertinent strains. HR efficiency was calculated as the ratio of uracil prototrophic growing colonies that have successfully integrated the *URA3* gene (the yeast background to perform these HDR experiments was BY4741 where the *URA3* has been deleted) to leucine prototrophic colonies.

Suicide deletion assay to measure NHEJ

All strains used in the suicide deletion system derived from YW1276 (MATa-inc ade2::*HOSD*(+1)::STE3-MET15 his3D1 leu2D met15D ura3D). The assay was performed as previously described in 80. In short, cells were grown exponentially in SD supplemented with 120 μg/ml adenine, plated in either 2% glucose or 2% galactose plates and incubated at 30 °C for 3–4 days. The frequency of DSB repair by NHEJ was measured as the ratio of colonies formed on the galactose plates compared to the glucose plates.

HR genomic assay

All strains used in these experiments are derived from YJK17 (*MATa ho*D *hml*D::*ADE1 hmr*D::*ADE1 ade1-100 leu2-3,112 trp*::*hisG lys5 ura3-52 ade3*:: GAL::*HO arg5,6*::*MAT***a**-inc::HPH1).[82] That is, cells were grown overnight in SD 2% raffinose to $A_{\lambda 660}$ = 0.6–0.8. Cells were plated on either 2% glucose or 2% galactose SD plates. The frequency of DSB repair by HR was measured as the ratio of colonies formed on galactose plates compared to the glucose plates.

NHEJ fidelity assay

Fidelity in the NHEJ process was measured as follows, 200–300 ng of *Nco*I digested pJC2170 plasmid was transformed into the pertinent strains: pJC2170 plasmid is based on pRS415 in which *URA3* has been cloned between *Hin*dIII and *Bam*HI restriction sites. The *Nco*I site is in the *URA3* sequence. Consequently, Leu+ colonies are those able to repair the plasmid, and Ura+ those that repaired and kept the *URA3* intact. Fidelity was measured as the ratio of uracil prototrophic colonies to leucine prototrophic colonies.

Sensitivity to bleomycin

Cells were synchronised in G$_1$ as described above. To specifically induce the double strand breaks in the G$_2$ phase, cells were released from the a-factor arrest and, after 70 min, 300 μg/ml of bleomycin (AB142977, Abcam) was added. Cells were kept with the drug for 30 min, plated in 2% glucose plates and incubated at 30 °C for 2–3 days.

Colony formation assay

Cells were incubated for 2 h with 0.1 lg/ml of bleomycin (Abcam). Afterwards, cells were trypsinised, counted and seeded in 6-well plates at a density of: 1200 (A549), 2500 (MCF-7) and 1200 (MDA-MB-231) cells per well. After 2 weeks of incubation when colonies became visible, they were fixed with 1 ml of 100% methanol at −20 °C for 5 min, washed twice with PBS, stained with 0.1% crystal violet for 30 min at room temperature in the dark, washed 3–4 times with PBS, and colonies were automatically counted by using ImageJ program. To get a quantitative measure that includes the difference in growth between the colonies, the cells from the different wells were harvested and the crystal violet staining was measured as absorbance at 570 nm. The percentage of cell survival was calculated as the ratio of cells treated with bleomycin versus the control.

Viral cloning and transduction

The KU80 gene was amplified from A549 cells. Either KU80$^{\mathrm{wt}}$ or Ku80$^{\mathrm{T629A}}$ were cloned into pWPI lentiviral expression vector (Addgene, ref: 12254,) at the *Pme*I restriction site. For lentivirus production, 45 lg pWPI-KU80 (wt and variants) was cotransfected with 12.9 lg of pMD2.G and 29.1 lg of psPAX2 into HEK293-T cells using the calcium phosphate system and plated in 10 cm plates. The virus-containing supernatant was collected at 24 h and 48 h post-transfection, concentrated using the Sartorius VS2042 Vivaspin 20 concentrator and titrated. MDA-MB-231 and MCF-7 cells were infected with 15 MOI of lentivirus and A549 cells with 5 MOI of lentivirus.

Statistical analysis

Data were expressed as mean and the standard error of the mean was included (mean ± SEM). Statistical significance was determined using the Student's test. A *p* value <0.05 was considered significant.

Acknowledgements

We want to express our sincere gratitude to the people who shared their materials with us: P. Belhumeur for the silencing strains, T. Wilson for the suicide system, F. Prado for the plasmids for measuring HR, J. Haber for the strains to check HR and J Masson for human KU80 protein. To J. Haber and A. Doherty for critical reading. To F. Prado and M.G. Blanco for discussion. Marta Pérez, our lab technician, for thousand details. Funding was provided by Ministerio de Ciencia, Innovación y Universidades (MCIU) from the Spanish Government (ref: PGC2018-096597-B-I00) to JC and JJ. RC was the recipient of a grant from the Agència de Gestió d'Ajuts Universitaris i de Recerca AGAUR (ref: 2018FI_B1 00180).

Author contribution

Reyes Carballar and Joan Marc Martínez conducted most of the experiments. Samuel Bru, Bàrbara Samper, Elisabet Bállega and Oriol Mirallas conducted specific experiments. Natalia Ricco helped in designing some of the experiments, Josep Clotet and Javier Jiménez funded, designed, supervised the experiments and wrote the article.

Declaration of Competing Interest

The authors declare that they have no known competing financial interests or personal relationships that could have appeared to influence the work reported in this paper.

Received 7 May 2020;
Accepted 11 November 2020;
Available online 17 November 2020

Keywords:
Ku80;
Pho85;
NHEJ;
HDR;
DNA repair

† Authors contributed equally.

References

1. Hanahan, D., Weinberg, R.A., (2011). Hallmarks of cancer: the next generation. *Cell*, **144**, 646–674.
2. Ciccia, A., Elledge, S.J., (2010). The DNA damage response: making it safe to play with knives. *Mol. Cell*, **40**, 179–204.
3. Jasin, M., Rothstein, R., (2013). Repair of strand breaks by homologous recombination. *Cold Spring Harb Perspect. Biol.*, **5**, a012740.
4. Daley, J.M., Palmbos, P.L., Wu, D., Wilson, T.E., (2005). Non-homologous end joining in yeast. *Annu. Rev. Genet.*, **39**, 431–451.
5. Wilson, T.E., Sunder, S., (2019). Double-strand breaks in motion: implications for chromosomal rearrangement. *Curr. Genet.*, **66**, 1–6.
6. Takata, M., Sasaki, M.S., Sonoda, E., Morrison, C., Hashimoto, M., Utsumi, H., Yamaguchi-Iwai, Y., Shinohara, A., Takeda, S., (1998). Homologous recombination and non-homologous end-joining pathways of DNA double-strand break repair have overlapping roles in the maintenance of chromosomal integrity in vertebrate cells. *Embo J.*, **17**, 5497–5508.
7. Aylon, Y., Liefshitz, B., Kupiec, M., (2004). The CDK regulates repair of double-strand breaks by homologous recombination during the cell cycle. *Embo J.*, **23**, 4868–4875.
8. Ira, G., Pellicioli, A., Balijja, A., Wang, X., Fiorani, S., Carotenuto, W., Liberi, G., Bressan, D., Wan, L., Hollingsworth, N.M., Haber, J.E., Foiani, M., (2004). DNA end resection, homologous recombination and DNA damage checkpoint activation require CDK1. *Nature*, **431**, 1011–1017.
9. Karanam, K., Kafri, R., Loewer, A., Lahav, G., (2012). Quantitative live cell imaging reveals a gradual shift between DNA repair mechanisms and a maximal use of HR in mid S phase. *Mol. Cell*, **47**, 320–329.
10. Chen, S., Inamdar, K.V., Pfeiffer, P., Feldmann, E., Hannah, M.F., Yu, Y., Lee, J.W., Zhou, T., Lees-Miller, S. P., Povirk, L.F., (2001). Accurate in vitro end joining of a DNA double strand break with partially cohesive 3'-overhangs and 3'-phosphoglycolate termini: effect of Ku on repair fidelity. *J. Biol. Chem.*, **276**, 24323–24330.
11. Moore, J.K., Haber, J.E., (1996). Cell cycle and genetic requirements of two pathways of nonhomologous end-joining repair of double-strand breaks in *Saccharomyces cerevisiae. Mol. Cell. Biol.*, **16**, 2164–2173.
12. Jiang, G., Plo, I., Wang, T., Rahman, M., Cho, J.H., Yang, E., Lopez, B.S., Xia, F., (2013). BRCA1-Ku80 protein interaction enhances end-joining fidelity of chromosomal double-strand breaks in the G1 phase of the cell cycle. *J. Biol. Chem.*, **288**, 8966–8976.

13. Emerson, C.H., Lopez, C.R., Ribes-Zamora, A., Polleys, E.J., Williams, C.L., Yeo, L., Zaneveld, J.E., Chen, R., Bertuch, A.A., (2018). Ku DNA end-binding activity promotes repair fidelity and influences end-processing during non-homologous end-joining in *Saccharomyces cerevisiae. Genetics*, **209**, 115–128.
14. Cary, R.B., Peterson, S.R., Wang, J., Bear, D.G., Bradbury, E.M., Chen, D.J., (1997). DNA looping by Ku and the DNA-dependent protein kinase. *Proc. Natl. Acad. Sci. U. S. A.*, **94**, 4267–4272.
15. Ramsden, D.A., Gellert, M., (1998). Ku protein stimulates DNA end joining by mammalian DNA ligases: a direct role for Ku in repair of DNA double-strand breaks. *Embo J.*, **17**, 609–614.
16. Walker, J.R., Corpina, R.A., Goldberg, J., (2001). Structure of the Ku heterodimer bound to DNA and its implications for double-strand break repair. *Nature*, **412**, 607–614.
17. Gottlieb, T.M., Jackson, S.P., (1993). The DNA-dependent protein kinase: requirement for DNA ends and association with Ku antigen. *Cell*, **72**, 131–142.
18. Haber, J.E., (2000). Partners and pathways repairing a double-strand break. *Trends Genet.*, **16**, 259–264.
19. Emerson, C.H., Bertuch, A.A., (2016). Consider the workhorse: Non-homologous end-joining in budding yeast. *Biochem. Cell Biol.*, **94**, 396–406.
20. Rulten, S.L., Grundy, G.J., (2017). Non-homologous end joining: Common interaction sites and exchange of multiple factors in the DNA repair process. *Bioessays*, **39** https://doi.org/10.1002/bies.201600209.
21. Lisby, M., Barlow, J.H., Burgess, R.C., Rothstein, R., (2004). Choreography of the DNA damage response: spatiotemporal relationships among checkpoint and repair proteins. *Cell*, **118**, 699–713.
22. Gobbini, E., Cesena, D., Galbiati, A., Lockhart, A., Longhese, M.P., (2013). Interplays between ATM/Tel1 and ATR/Mec1 in sensing and signaling DNA double-strand breaks. *DNA Repair (Amst)*, **12**, 791–799.
23. Paull, T.T., Gellert, M., (1998). The 3’ to 5’ exonuclease activity of Mre 11 facilitates repair of DNA double-strand breaks. *Mol. Cell*, **1**, 969–979.
24. Huertas, P., Cortes-Ledesma, F., Sartori, A.A., Aguilera, A., Jackson, S.P., (2008). CDK targets Sae2 to control DNA-end resection and homologous recombination. *Nature*, **455**, 689–692.
25. D’Amours, D., Jackson, S.P., (2002). The Mre11 complex: at the crossroads of dna repair and checkpoint signalling. *Nat. Rev. Mol. Cell Biol.*, **3**, 317–327.
26. Clerici, M., Mantiero, D., Guerini, I., Lucchini, G., Longhese, M.P., (2008). The Yku70-Yku80 complex contributes to regulate double-strand break processing and checkpoint activation during the cell cycle. *EMBO Rep.*, **9**, 810–818.
27. Chen, X., Niu, H., Chung, W.H., Zhu, Z., Papusha, A., Shim, E.Y., Lee, S.E., Sung, P., Ira, G., (2011). Cell cycle regulation of DNA double-strand break end resection by Cdk1-dependent Dna2 phosphorylation. *Nat. Struct. Mol. Biol.*, **18**, 1015–1019.
28. Hustedt, N., Durocher, D., (2016). The control of DNA repair by the cell cycle. *Nat. Cell Biol.*, **19**, 1–9.
29. Boulton, S.J., Jackson, S.P., (1996). *Saccharomyces cerevisiae* Ku70 potentiates illegitimate DNA double-strand break repair and serves as a barrier to error-prone DNA repair pathways. *Embo J.*, **15**, 5093–5103.
30. Liang, F., Jasin, M., (1996). Ku80-deficient cells exhibit excess degradation of extrachromosomal DNA. *J. Biol. Chem.*, **271**, 14405–14411.
31. Feldmann, E., Schmiemann, V., Goedecke, W., Reichenberger, S., Pfeiffer, P., (2000). DNA double-strand break repair in cell-free extracts from Ku80-deficient cells: implications for Ku serving as an alignment factor in non-homologous DNA end joining. *Nucleic Acids Res.*, **28**, 2585–2596.
32. Symington, L.S., Rothstein, R., Lisby, M., (2014). Mechanisms and regulation of mitotic recombination in *Saccharomyces cerevisiae. Genetics*, **198**, 795–835.
33. Ceccaldi, R., Rondinelli, B., D’Andrea, A.D., (2016). Repair pathway choices and consequences at the double-strand break. *Trends Cell Biol.*, **26**, 52–64.
34. Scully, R., Panday, A., Elango, R., Willis, N.A., (2019). DNA double-strand break repair-pathway choice in somatic mammalian cells. *Nat. Rev. Mol. Cell Biol.*, **20**, 698–714.
35. Valencia, M., Bentele, M., Vaze, M.B., Herrmann, G., Kraus, E., Lee, S.E., Schar, P., Haber, J.E., (2001). NEJ1 controls non-homologous end joining in *Saccharomyces cerevisiae. Nature*, **414**, 666–669.
36. Hentges, P., Waller, H., Reis, C.C., Ferreira, M.G., Doherty, A.J., (2014). Cdk1 restrains NHEJ through phosphorylation of XRCC4-like factor Xlf1. *Cell. Rep.*, **9**, 2011–2017.
37. Mishra, K., Shore, D., (1999). Yeast Ku protein plays a direct role in telomeric silencing and counteracts inhibition by rif proteins. *Curr. Biol.*, **9**, 1123–1126.
38. Roy, R., Meier, B., McAinsh, A.D., Feldmann, H.M., Jackson, S.P., (2004). Separation-of-function mutants of yeast Ku80 reveal a Yku80p-Sir4p interaction involved in telomeric silencing. *J. Biol. Chem.*, **279**, 86–94.
39. Thrower, D.A., Bloom, K., (2001). Dicentric chromosome stretching during anaphase reveals roles of Sir2/Ku in chromatin compaction in budding yeast. *Mol. Biol. Cell*, **12**, 2800–2812.
40. Gravel, S., Larrivee, M., Labrecque, P., Wellinger, R.J., (1998). Yeast Ku as a regulator of chromosomal DNA end structure. *Science*, **280**, 741–744.
41. Polotnianka, R.M., Li, J., Lustig, A.J., (1998). The yeast Ku heterodimer is essential for protection of the telomere against nucleolytic and recombinational activities. *Curr. Biol.*, **8**, 831–834.
42. Boulton, S.J., Jackson, S.P., (1998). Components of the Ku-dependent non-homologous end-joining pathway are involved in telomeric length maintenance and telomeric silencing. *Embo J.*, **17**, 1819–1828.
43. Laroche, T., Martin, S.G., Gotta, M., Gorham, H.C., Pryde, F.E., Louis, E.J., Gasser, S.M., (1998). Mutation of yeast Ku genes disrupts the subnuclear organization of telomeres. *Curr. Biol.*, **8**, 653–656.
44. Ribes-Zamora, A., Mihalek, I., Lichtarge, O., Bertuch, A. A., (2007). Distinct faces of the Ku heterodimer mediate DNA repair and telomeric functions. *Nat. Struct. Mol. Biol.*, **14**, 301–307.
45. Larcher, M.V., Pasquier, E., MacDonald, R.S., Wellinger, R.J., (2016). Ku Binding on Telomeres Occurs at Sites Distal from the Physical Chromosome Ends. *PLoS Genet.*, **12**, e1006479.
46. Nurse, P., Bissett, Y., (1981). Gene required in G1 for commitment to cell cycle and in G2 for control of mitosis in fission yeast. *Nature*, **292**, 558–560.

47. Malumbres, M., (2014). Cyclin-dependent kinases. *Genome Biol.*, **15**, 122.
48. Evans, T., Rosenthal, E.T., Youngblom, J., Distel, D., Hunt, T., (1983). Cyclin: a protein specified by maternal mRNA in sea urchin eggs that is destroyed at each cleavage division. *Cell*, **33**, 389–396.
49. Hydbring, P., Malumbres, M., Sicinski, P., (2016). Non-canonical functions of cell cycle cyclins and cyclin-dependent kinases. *Nat. Rev. Mol. Cell Biol.*, **17**, 280–292.
50. Quandt, E., Ribeiro, M.P.C., Clotet, J., (2019). Atypical cyclins: the extended family portrait. *Cell Mol. Life Sci.*, **77**, 231–242.
51. Jimenez, J., Ricco, N., Grijota-Martinez, C., Fado, R., Clotet, J., (2013). Redundancy or specificity? The role of the CDK Pho85 in cell cycle control. *Int. J. Biochem. Mol. Biol.*, **4**, 140–149.
52. Huang, D., Friesen, H., Andrews, B., (2007). Pho85, a multifunctional cyclin-dependent protein kinase in budding yeast. *Mol. Microbiol.*, **66**, 303–314.
53. Stern, B., Nurse, P., (1996). A quantitative model for the cdc2 control of S phase and mitosis in fission yeast. *Trends Genet.*, **12**, 345–350.
54. Swaffer, M.P., Jones, A.W., Flynn, H.R., Snijders, A.P., Nurse, P., (2016). CDK substrate phosphorylation and ordering the cell cycle. *Cell*, **167**, 1750–1761.e16.
55. Uhlmann, F., Bouchoux, C., Lopez-Aviles, S., (2011). A quantitative model for cyclin-dependent kinase control of the cell cycle: revisited. *Philos. Trans. R. Soc. Lond. B. Biol. Sci.*, **366**, 3572–3583.
56. Andrews, B., Measday, V., (1998). The cyclin family of budding yeast: abundant use of a good idea. *Trends Genet.*, **14**, 66–72.
57. Lee, Y.S., Huang, K., Quiocho, F.A., O'Shea, E.K., (2008). Molecular basis of cyclin-CDK-CKI regulation by reversible binding of an inositol pyrophosphate. *Nat. Chem. Biol.*, **4**, 25–32.
58. Schneider, K.R., Smith, R.L., O'Shea, E.K., (1994). Phosphate-regulated inactivation of the kinase PHO80-PHO85 by the CDK inhibitor PHO81. *Science*, **266**, 122–126.
59. Espinoza, F.H., Ogas, J., Herskowitz, I., Morgan, D.O., (1994). Cell cycle control by a complex of the cyclin HCS26 (PCL1) and the kinase PHO85. *Science*, **266**, 1388–1391.
60. Truman, A.W., Kristjansdottir, K., Wolfgeher, D., Hasin, N., Polier, S., Zhang, H., Perrett, S., Prodromou, C., Jones, G.W., Kron, S.J., (2012). CDK-dependent Hsp70 phosphorylation controls G1 cyclin abundance and cell-cycle progression. *Cell*, **151**, 1308–1318.
61. Menoyo, S., Ricco, N., Bru, S., Hernandez-Ortega, S., Escote, X., Aldea, M., Clotet, J., (2013). Phosphate-activated CDK stabilizes G1 cyclin to trigger cell cycle entry. *Mol. Cell. Biol.*, **33** (7), 1273–1284.
62. Jimenez, J., Truman, A.W., Menoyo, S., Kron, S.J., Clotet, J., (2013). The yin and yang of cyclin control by nutrients. *Cell. Cycle*, **12**, 865–866.
63. Cao, L., Chen, F., Yang, X., Xu, W., Xie, J., Yu, L., (2014). Phylogenetic analysis of CDK and cyclin proteins in premetazoan lineages. *BMC Evol. Biol.*, **14** 10-2148-14-10.
64. Ho, Y., Gruhler, A., Heilbut, A., Bader, G.D., Moore, L., Adams, S.L., Millar, A., Taylor, P., Bennett, K., Boutilier, K., Yang, L., Wolting, C., Donaldson, I., Schandorff, S., Shewnarane, J., Vo, M., Taggart, J., Goudreault, M., Muskat, B., Alfarano, C., Dewar, D., Lin, Z., Michalickova, K., Willems, A.R., Sassi, H., Nielsen, P.A., Rasmussen, K. J., Andersen, J.R., Johansen, L.E., Hansen, L.H., Jespersen, H., Podtelejnikov, A., Nielsen, E., Crawford, J., Poulsen, V., Sorensen, B.D., Matthiesen, J., Hendrickson, R.C., Gleeson, F., Pawson, T., Moran, M. F., Durocher, D., Mann, M., Hogue, C.W., Figeys, D., Tyers, M., (2002). Systematic identification of protein complexes in *Saccharomyces cerevisiae* by mass spectrometry. *Nature*, **415**, 180–183.
65. Lenburg, M.E., O'Shea, E.K., (2001). Genetic evidence for a morphogenetic function of the *Saccharomyces cerevisiae* Pho85 cyclin-dependent kinase. *Genetics*, **157**, 39–51.
66. Lee, Y.S., Mulugu, S., York, J.D., O'Shea, E.K., (2007). Regulation of a cyclin-CDK-CDK inhibitor complex by inositol pyrophosphates. *Science*, **316**, 109–112.
67. Jeffery, D.A., Springer, M., King, D.S., O'Shea, E.K., (2001). Multi-site phosphorylation of Pho4 by the cyclin-CDK Pho80-Pho85 is semi-processive with site preference. *J. Mol. Biol.*, **306**, 997–1010.
68. Ballega, E., Carballar, R., Samper, B., Ricco, N., Ribeiro, M.P., Bru, S., Jimenez, J., Clotet, J., (2019). Comprehensive and quantitative analysis of G1 cyclins. A tool for studying the cell cycle. *PLoS One*, **14**, e0218531.
69. Gravel, S., Wellinger, R.J., (2002). Maintenance of double-stranded telomeric repeats as the critical determinant for cell viability in yeast cells lacking Ku. *Mol. Cell. Biol.*, **22**, 2182–2193.
70. Boulton, S.J., Jackson, S.P., (1996). Identification of a *Saccharomyces cerevisiae* Ku80 homologue: roles in DNA double strand break rejoining and in telomeric maintenance. *Nucleic Acids Res.*, **24**, 4639–4648.
71. Mozdy, A.D., Podell, E.R., Cech, T.R., (2008). Multiple yeast genes, including Paf1 complex genes, affect telomere length via telomerase RNA abundance. *Mol. Cell. Biol.*, **28**, 4152–4161.
72. Askree, S.H., Yehuda, T., Smolikov, S., Gurevich, R., Hawk, J., Coker, C., Krauskopf, A., Kupiec, M., McEachern, M.J., (2004). A genome-wide screen for *Saccharomyces cerevisiae* deletion mutants that affect telomere length. *Proc. Natl. Acad. Sci. U. S. A.*, **101**, 8658–8663.
73. Gatbonton, T., Imbesi, M., Nelson, M., Akey, J.M., Ruderfer, D.M., Kruglyak, L., Simon, J.A., Bedalov, A., (2006). Telomere length as a quantitative trait: genome-wide survey and genetic mapping of telomere length-control genes in yeast. *PLoS Genet.*, **2**, e35.
74. Clement, M., Deshaies, F., de Repentigny, L., Belhumeur, P., (2006). The nuclear GTPase Gsp1p can affect proper telomeric function through the Sir4 protein in *Saccharomyces cerevisiae. Mol. Microbiol.*, **62**, 453–468.
75. Taccioli, G.E., Gottlieb, T.M., Blunt, T., Priestley, A., Demengeot, J., Mizuta, R., Lehmann, A.R., Alt, F.W., Jackson, S.P., Jeggo, P.A., (1994). Ku80: product of the XRCC5 gene and its role in DNA repair and V(D)J recombination. *Science*, **265**, 1442–1445.
76. Milne, G.T., Jin, S., Shannon, K.B., Weaver, D.T., (1996). Mutations in two Ku homologs define a DNA end-joining repair pathway in *Saccharomyces cerevisiae. Mol. Cell. Biol.*, **16**, 4189–4198.

77. Zhang, Y., Hefferin, M.L., Chen, L., Shim, E.Y., Tseng, H. M., Kwon, Y., Sung, P., Lee, S.E., Tomkinson, A.E., (2007). Role of Dnl4-Lif1 in non-homologous end-joining repair complex assembly and suppression of homologous recombination. *Nat. Struct. Mol. Biol.*, **14**, 639–646.
78. Fattah, F., Lee, E.H., Weisensel, N., Wang, Y., Lichter, N., Hendrickson, E.A., (2010). Ku regulates the non-homologous end joining pathway choice of DNA double-strand break repair in human somatic cells. *PLoS Genet.*, **6**, e1000855.
79. Karathanasis, E., Wilson, T.E., (2002). Enhancement of *Saccharomyces cerevisiae* end-joining efficiency by cell growth stage but not by impairment of recombination. *Genetics*, **161**, 1015–1027.
80. Palmbos, P.L., Daley, J.M., Wilson, T.E., (2005). Mutations of the Yku80 C terminus and Xrs2 FHA domain specifically block yeast non-homologous end joining. *Mol. Cell. Biol.*, **25**, 10782–10790.
81. Haghnazari, E., Heyer, W.D., (2004). The DNA damage checkpoint pathways exert multiple controls on the efficiency and outcome of the repair of a double-stranded DNA gap. *Nucleic Acids Res.*, **32**, 4257–4268.
82. Kim, J.A., Haber, J.E., (2009). Chromatin assembly factors Asf1 and CAF-1 have overlapping roles in deactivating the DNA damage checkpoint when DNA repair is complete. *Proc. Natl. Acad. Sci. U. S. A.*, **106**, 1151–1156.
83. Benitez-Bribiesca, L., Sanchez-Suarez, P., (1999). Oxidative damage, bleomycin, and gamma radiation induce different types of DNA strand breaks in normal lymphocytes and thymocytes. A comet assay study. *Ann. N. Y. Acad. Sci.*, **887**, 133–149.
84. Gao, S., Honey, S., Futcher, B., Grollman, A.P., (2016). The non-homologous end-joining pathway of *S. cerevisiae* works effectively in G1-phase cells, and religates cognate ends correctly and non-randomly. *DNA Repair (Amst)*, **42**, 1–10.
85. Mirallas, O., Ballega, E., Samper-Martin, B., Garcia-Marquez, S., Carballar, R., Ricco, N., Jimenez, J., Clotet, J., (2018). Intertwined control of the cell cycle and nucleocytoplasmic transport by the cyclin-dependent kinase Pho85 and RanGTPase Gsp1 in *Saccharomyces cerevisiae. Microbiol. Res.*, **206**, 168–176.
86. Zhang, Y., Shim, E.Y., Davis, M., Lee, S.E., (2009). Regulation of repair choice: Cdk1 suppresses recruitment of end joining factors at DNA breaks. *DNA Repair (Amst)*, **8**, 1235–1241.
87. Ptacek, J., Devgan, G., Michaud, G., Zhu, H., Zhu, X., Fasolo, J., Guo, H., Jona, G., Breitkreutz, A., Sopko, R., McCartney, R.R., Schmidt, M.C., Rachidi, N., Lee, S.J., Mah, A.S., Meng, L., Stark, M.J., Stern, D.F., De Virgilio, C., Tyers, M., Andrews, B., Gerstein, M., Schweitzer, B., Predki, P.F., Snyder, M., (2005). Global analysis of protein phosphorylation in yeast. *Nature*, **438**, 679–684.
88. Shibata, A., Conrad, S., Birraux, J., Geuting, V., Barton, O., Ismail, A., Kakarougkas, A., Meek, K., Taucher-Scholz, G., Lobrich, M., Jeggo, P.A., (2011). Factors determining DNA double-strand break repair pathway choice in G2 phase. *Embo J.*, **30**, 1079–1092.
89. Rieder, C.L., Cole, R.W., (1998). Entry into mitosis in vertebrate somatic cells is guarded by a chromosome damage checkpoint that reverses the cell cycle when triggered during early but not late prophase. *J. Cell Biol.*, **142**, 1013–1022.
90. Caspari, T., Murray, J.M., Carr, A.M., (2002). Cdc2-cyclin B kinase activity links Crb2 and Rqh1-topoisomerase III. *Genes Dev.*, **16**, 1195–1208.
91. Tomimatsu, N., Mukherjee, B., Catherine, H.M., Ilcheva, M., Vanessa, C.C., Louise, H.J., Porteus, M., Llorente, B., Khanna, K.K., Burma, S., (2014). Phosphorylation of EXO1 by CDKs 1 and 2 regulates DNA end resection and repair pathway choice. *Nat. Commun.*, **5**, 3561.
92. Makharashvili, N., Paull, T.T., (2015). CtIP: A DNA damage response protein at the intersection of DNA metabolism. *DNA Repair (Amst)*, **32**, 75–81.
93. Yu, T.Y., Garcia, V.E., Symington, L.S., (2019). CDK and Mec1/Tel1-catalyzed phosphorylation of Sae2 regulate different responses to DNA damage. *Nucleic Acids Res.*, **47**, 11238–11249.
94. Chen, X., Niu, H., Yu, Y., Wang, J., Zhu, S., Zhou, J., Papusha, A., Cui, D., Pan, X., Kwon, Y., Sung, P., Ira, G., (2016). Enrichment of Cdk1-cyclins at DNA double-strand breaks stimulates Fun30 phosphorylation and DNA end resection. *Nucleic Acids Res.*, **44**, 2742–2753.
95. Luo, K., Deng, M., Li, Y., Wu, C., Xu, Z., Yuan, J., Lou, Z., (2015). CDK-mediated RNF4 phosphorylation regulates homologous recombination in S-phase. *Nucleic Acids Res.*, **43**, 5465–5475.
96. Brandsma, I., Gent, D.C., (2012). Pathway choice in DNA double strand break repair: observations of a balancing act. *Genome Integr.*, **3** 9-9414-3-9.
97. Holt, L.J., Tuch, B.B., Villen, J., Johnson, A.D., Gygi, S.P., Morgan, D.O., (2009). Global analysis of Cdk1 substrate phosphorylation sites provides insights into evolution. *Science*, **325**, 1682–1686.
98. Nishizawa, M., Suzuki, K., Fujino, M., Oguchi, T., Toh-e, A., (1999). The Pho85 kinase, a member of the yeast cyclin-dependent kinase (Cdk) family, has a regulation mechanism different from Cdks functioning throughout the cell cycle. *Genes Cells*, **4**, 627–642.
99. Huang, E., Qu, D., Park, D.S., (2010). Cdk5: Links to DNA damage. *Cell. Cycle*, **9**, 3142–3143.
100. Wilson, T.E., Grawunder, U., Lieber, M.R., (1997). Yeast DNA ligase IV mediates non-homologous DNA end joining. *Nature*, **388**, 495–498.
101. Davis, A.J., Chen, B.P., Chen, D.J., (2014). DNA-PK: a dynamic enzyme in a versatile DSB repair pathway. *DNA Repair (Amst)*, **17**, 21–29.
102. Liu, Y., Efimova, E.V., Ramamurthy, A., Kron, S.J., (2019). Repair-independent functions of DNA-PKcs protect irradiated cells from mitotic slippage and accelerated senescence. *J. Cell. Sci.*, **132** https://doi.org/10.1242/jcs.229385.
103. Janke, C., Magiera, M.M., Rathfelder, N., Taxis, C., Reber, S., Maekawa, H., Moreno-Borchart, A., Doenges, G., Schwob, E., Schiebel, E., Knop, M., (2004). A versatile toolbox for PCR-based tagging of yeast genes: new fluorescent proteins, more markers and promoter substitution cassettes. *Yeast*, **21**, 947–962.
104. Gallego, C., Gari, E., Colomina, N., Herrero, E., Aldea, M., (1997). The Cln3 cyclin is down-regulated by translational repression and degradation during the G1 arrest caused by nitrogen deprivation in budding yeast. *Embo J.*, **16**, 7196–7206.
105. Yaakov, G., Duch, A., Garcia-Rubio, M., Clotet, J., Jimenez, J., Aguilera, A., Posas, F., (2009). The stress-activated protein kinase Hog1 mediates S phase delay in response to osmostress. *Mol. Biol. Cell*, **20**, 3572–3582.

106. Bell, M., Capone, R., Pashtan, I., Levitzki, A., Engelberg, D., (2001). Isolation of hyperactive mutants of the MAPK p38/Hog1 that are independent of MAPK kinase activation. *J. Biol. Chem.*, **276**, 25351–25358.
107. Hernandez-Ortega, S., Bru, S., Ricco, N., Ramirez, S., Casals, N., Jimenez, J., Isasa, M., Crosas, B., Clotet, J., (2012). Defective in Mitotic Arrest 1 (Dma1) ubiquitin ligase controls G1 cyclin degradation. *J. Biol. Chem.*, **288** (7), 4704–4714.
108. Singer, M.S., Gottschling, D.E., (1994). TLC1: template RNA component of *Saccharomyces cerevisiae* telomerase. *Science*, **266**, 404–409.
109. Bertuch, A.A., Lundblad, V., (2003). The Ku heterodimer performs separable activities at double-strand breaks and chromosome termini. *Mol. Cell. Biol.*, **23**, 8202–8215.
110. Abramov, A.Y., Fraley, C., Diao, C.T., Winkfein, R., Colicos, M.A., Duchen, M.R., French, R.J., Pavlov, E., (2007). Targeted polyphosphatase expression alters mitochondrial metabolism and inhibits calcium-dependent cell death. *Proc. Natl. Acad. Sci. U. S. A.*, **104**, 18091–18096.
111. Thomas, B.J., Rothstein, R., (1989). Elevated recombination rates in transcriptionally active DNA. *Cell*, **56**, 619–630.
112. Brachmann, C.B., Davies, A., Cost, G.J., Caputo, E., Li, J., Hieter, P., Boeke, J.D., (1998). Designer deletion strains derived from *Saccharomyces cerevisiae* S288C: a useful set of strains and plasmids for PCR-mediated gene disruption and other applications. *Yeast*, **14**, 115–132.
113. Gietz, R.D., Sugino, A., (1988). New yeast-Escherichia coli shuttle vectors constructed with in vitro mutagenized yeast genes lacking six-base pair restriction sites. *Gene*, **74**, 527–534.

RESEARCH ARTICLE

Comprehensive and quantitative analysis of G_1 cyclins. A tool for studying the cell cycle

Elisabet Bállega☯, Reyes Carballar☯, Bàrbara Samper, Natalia Ricco, Mariana P. Ribeiro, Samuel Bru, Javier Jiménez*, Josep Clotet*

Basic Sciences Department, Faculty of Medicine and Health Sciences, Universitat Internacional de Catalunya, Barcelona, Spain

☯ These authors contributed equally to this work.
* jjimenez@uic.es (JJ); jclotet@uic.cat (JC)

Abstract

In eukaryotes, the cell cycle is driven by the actions of several cyclin dependent kinases (CDKs) and an array of regulatory proteins called cyclins, due to the cyclical expression patterns of the latter. In yeast, the accepted pattern of cyclin waves is based on qualitative studies performed by different laboratories using different strain backgrounds, different growing conditions and media, and different kinds of genetic manipulation. Additionally, only the subset of cyclins regulating Cdc28 was included, while the Pho85 cyclins were excluded. We describe a comprehensive, quantitative and accurate blueprint of G_1 cyclins in the yeast *Saccharomyces cerevisiae* that, in addition to validating previous conclusions, yields new findings and establishes an accurate G_1 cyclin blueprint. For the purposes of this research, we produced a collection of strains with all G_1 cyclins identically tagged using the same and most respectful procedure possible. We report the contribution of each G_1 cyclin for a broad array of growing and stress conditions, describe an unknown role for Pcl2 in heat-stress conditions and demonstrate the importance of maintaining the 3'UTR sequence of cyclins untouched during the tagging process.

OPEN ACCESS

Citation: Bállega E, Carballar R, Samper B, Ricco N, Ribeiro MP, Bru S, et al. (2019) Comprehensive and quantitative analysis of G_1 cyclins. A tool for studying the cell cycle. PLoS ONE 14(6): e0218531. https://doi.org/10.1371/journal.pone.0218531

Editor: Michael Polymenis, Texas A&M University College Station, UNITED STATES

Received: December 21, 2018

Accepted: June 4, 2019

Published: June 25, 2019

Copyright: © 2019 Bállega et al. This is an open access article distributed under the terms of the Creative Commons Attribution License, which permits unrestricted use, distribution, and reproduction in any medium, provided the original author and source are credited.

Data Availability Statement: All data are included in the manuscript.

Funding: RC was awarded with a Generalitat de Catalunya grant. JC received a grant from the Spanish Government (MINECO Grant Ref: BFU 2013-44189-P and PGC2018-096597-B-I00). JJ received a grant from the Spanish Government (PGC2018-096597-B-I00). The funders had no role in study design, data collection and analysis, decision to publish or preparation of the manuscript.

Introduction

The cell cycle–the basis for perpetuating life–can be described as a set of events unfolding in a cell that result in the generation of two new cells that are virtually identical to the original. Cell cycle processes are tightly controlled to produce viable cells as nearly identical as possible to the original. Cell cycle control is mastered by a family of proteins called cyclin dependent kinases (CDKs), responsible for the phosphorylation of many different substrates directly involved in processes that successfully multiply cells [1–5]. Despite their structural similarity, not all CDKs are involved in cell cycle progression [6].

The main focus of this work is not CDKs as such but cyclins, a family of proteins capable of making specific complexes with the CDKs and in charge of controlling their activity [7–11]. Cyclins are so called because of their oscillatory presence in the cell cycle, due to specific sequences and regulators in both their promoters and the three prime untranslated regions

Competing interests: The authors have declared that no competing interests exist.

(3'UTR) (for reviews see [12, 13]) and to post-translational regulation [14]. The diversity and oscillation of cyclins are thought to be crucial for substrate selection by the CDKs and, consequently, in triggering the orderly succession of events that is essential for faithful cell cycle progression and cell multiplication [15]. Nevertheless, increasingly available experimental data indicate a more complex scenario in the orderly regulation of cell cycle events than mere succession in cyclin expression. A quantitative model has been proposed based on increasing CDK activity along the cell cycle and using different thresholds in the affinity of the different cell cycle phase substrates to be phosphorylated [16–18]. Intermediate kinase/phosphatase ratio models have also been described based on balancing CDK phosphorylation activity and counteracting phosphatase activity [19].

Cyclins are grouped into families according to different criteria. Based on temporal expression and action, we can distinguish between G_1 cyclins [20, 21], S-phase cyclins [22, 23], G_2 cyclins and M-phase cyclins [24]. Specific cyclin families modulate the activity of Cdc28, the main CDK in *S. cerevisiae* [21, 25], and other cyclin families are specifically related to the other CDK involved in cell cycle progression in the G_1 phase in budding yeast, namely Pho85 [15, 26]. Cdc28 is modulated by two families of cyclins that are also structurally different, namely, Cln1-Cln3 and Clb1-Clb6, while Pho85 is regulated by Pcl1-Pcl10 and Pho80. Cdc28 cyclins bear two conserved sequences called the 'cyclin box', responsible for cyclin-CDK physical interaction; in contrast, Pho85 cyclins have only one conserved sequence [26, 27]. Temporal expression and correlation between expression and cell cycle phases for Cdc28 and Pho85 has been documented to be as follows: in G_1, Cdc28 is modulated by Cln1, Cln2 and Cln3, whereas Pho85 is activated by Pcl1 and Pcl2; in the S-phase, Cdc28 is modulated by Clb5 and Clb6 and Pho85 is (probably) activated by Pcl7; in G_2, Cdc28 is modulated by Clb3 and Clb4; and finally, in the M-phase, Cdc28 is controlled by Clb2 and Clb1 while Pho85 is (apparently) controlled by Pcl9 [19, 28, 29].

The complex scenario of several CDKs and cyclins governing the cell cycle is even more intricate in the case of mammalian cells [30–32]. A long-standing question is why so many CDK/cyclin complexes are needed at a particular moment of the cell cycle; in other words, are they redundant or are they specific? [28, 29].

Regarding cyclin expression, limited quantitative information is available, although it has been established that Cln3 expression is low compared to that of other Clns; in one study, a set of tagged Clns with the 3'UTR intact was produced in an attempt to understand the difference in Cln3 regulation compared to Cln1and Cln2 regulation [33]. Subsequently described was an analysis of all Cdc28 cyclins in a set of strains where the 3'UTR was deleted [34]. Overall, the general picture of cyclin demeanour comes from a patchwork of data obtained in different laboratories that have used different strain backgrounds, different growing conditions, different detection systems and different kinds of genetic manipulation. As for the Pho85 cyclins, only qualitative data are available regarding the cell cycle phase where these are expressed [26, 28]. To date, therefore, no research has comprehensively quantified and studied all the G_1 cyclins (both Clns and Pcls) together.

In an attempt to inject some coherence into the data on the *S. cerevisiae* G_1 cyclins, we designed and produced a set of strains and identically tagged the different cyclins in order to comparatively analyse their levels of expression. We selected a clean tagging system, respectful of the 3'UTR sequence and designed to avoid some of the artefacts detected in an earlier phase of our research (these artefacts, which are not considered in the current G_1 cyclin expression model, are discussed further below). We used our set of strains to shed some light on the question of the specificity or redundancy of cyclins and CDKs in different environmental conditions and identified a previously unreported role for Pcl2 in cell cycle progression at high temperatures. Below we describe a tool, in the form of a set of identically tagged strains, for studying the G_1 phase and how cell cycle progression may be affected by environmental stress conditions or external treatments such as chemotherapeutic drugs.

Results

G_1 cyclin tagging

In our endeavour to provide the cell cycle community with a unified and comprehensive study of the pattern of expression of all G_1 cyclins in *S. cerevisiae*, we investigated the G_1 cyclins in exactly the same growing conditions, using exactly the same tagging strategy and using a single and widely used *S. cerevisiae* genetic background, namely, BY4741.

Cyclin amounts have frequently been evaluated by tagging the cyclins at their C-terminus and inserting a marker for the selection of transformants; this separates the 3'UTR from the gene and eliminates its putative regulatory function. However, growing evidence points to the importance of the 3'UTR for gene expression and protein amount regulation in both mammalian cells [35, 36] and yeast [37] (for a recent review see [38]). Therefore, before we tagged all the cyclins, we evaluated the influence of the 3'UTR sequence on two different G_1 cyclins. We did so by monitoring the amount and timing of Pcl1 expression in a *PCL1-3HA* tagged strain where the 3'UTR sequence was replaced by a selection marker (*KanMX*) as an inherent feature of the tagging strategy (as done in the classical strategy). We then compared this to a *PCL1-3HA* strain in which the 3'UTR was not altered using a strategy called *delitto perfetto* [39]. *Delitto perfetto* permits a DNA sequence to be tampered with while leaving no trace other than the desired modification (see Materials and Methods). Fig 1A and Fig 1B show that the amount of Pcl1-3HA was notably higher in the classically tagged strain. Similar results were obtained when the same approach was applied to *CLB5*, indicating that integrity of the 3'UTR might be key to cell regulation of the amount of cyclins and may, consequently, be a requirement for correct evaluation of the G_1 cyclin blueprint.

To reduce interference with the amount of the protein as much as possible, we performed an analysis aimed at determining the most appropriate tag to use. TAP (a large tag) and 3HA (a small tag) detected the cyclins reasonably well. Although our results indicated that tag size does have a minor impact on the amount of Clb5, applying Occam's razor principle for simplicity sake, we nevertheless decided to use the smaller 3HA tag. In the course of our research, it has been reported [40] that the 3HA module developed by Longtine et al. [41] uses a linker between the protein to be tagged and the 3HA epitope that greatly affects the stability of the tagged protein. In our research we used the tool-box system [42], which uses a different linker that does not affect protein stability [40].

Altering the level of cyclins is usually detrimental to normal cell cycle progression [43]. To check whether a variation in the amount of cyclins as determined by the presence or absence of the 3'UTR had any physiological impact, we studied the duplication time of cells bearing cyclins with or without the 3'UTR. As can be appreciated in Fig 1C, eliminating the *PCL1* 3'UTR produced a statistically significant increase in duplication time (from 89 to 102 min), which confirms that the extra amount of Pcl1 alters cell physiology. Interestingly, an increase in the amount of Clb5 in the strain *CLB5-3HA*-Δ3'UTR did not produce any significant difference in duplication time (in standard growing conditions at least); this is consistent with the existence of differential compensatory mechanisms depending on which cyclins are affected.

In view of the above results, we tagged each G_1 cyclin in a separate strain (since tagging several cyclins in the same strain could have resulted in the additive effect of small perturbations) in the most respectful way possible, i.e., maintaining their 3'UTR intact and using the 3HA tag from the tool-box module. We also tagged Clb5 and Sic1 using the same strategy and used them as landmark cairns to assess the biochemical border for G_1-S transition.

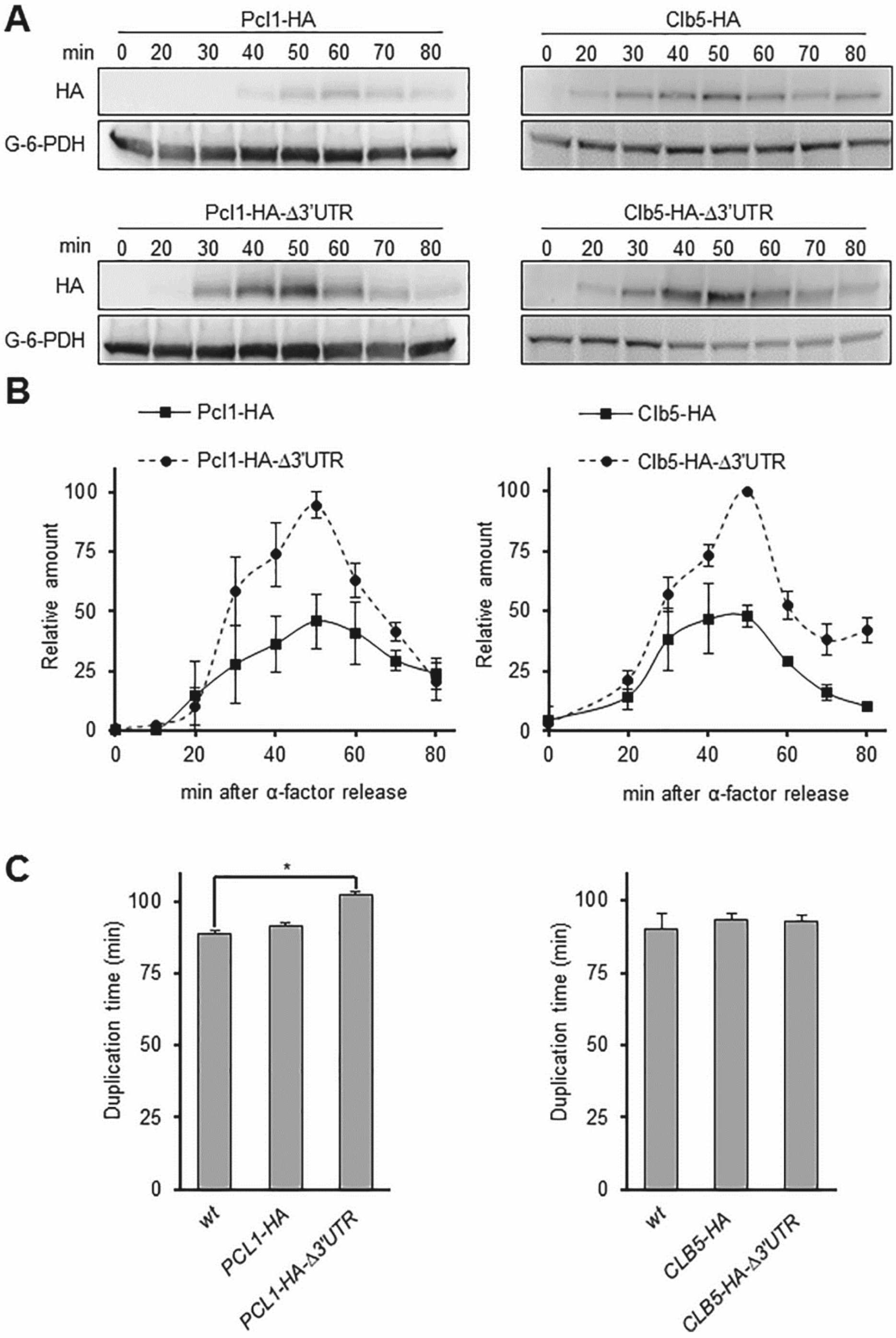
A
Pcl1-HA
min 0 20 30 40 50 60 70 80
HA
G-6-PDH
Clb5-HA
0 20 30 40 50 60 70 80
Pcl1-HA-Δ3'UTR
min 0 20 30 40 50 60 70 80
HA
G-6-PDH
Clb5-HA-Δ3'UTR
0 20 30 40 50 60 70 80
B
Pcl1-HA
Pcl1-HA-Δ3'UTR
Relative amount
100
75
50
25
0
0 20 40 60 80
min after α-factor release
Clb5-HA
Clb5-HA-Δ3'UTR
Relative amount
100
75
50
25
0
0 20 40 60 80
min after α-factor release
C
*
Duplication time (min)
100
75
50
25
0
wt
PCL1-HA
PCL1-HA-Δ3'UTR
Duplication time (min)
100
75
50
25
0
wt
CLB5-HA
CLB5-HA-Δ3'UTR

Fig 1. The 3'UTR sequence of cyclin genes is important for protein levels. A) Protein amounts for Clb5 (right) and Pcl1 (left), Cdc28 and Pho85 cyclins, respectively. The genes of both cyclins were modified to introduce the 3HA tag sequence, either eliminating or retaining the 3'UTR sequence. Cells were grown to the exponential phase in YPD (see Materials and Methods), synchronized in G_1 with α-factor and released in fresh YPD medium. At specific times, samples were taken and protein amounts were determined by western blot analysis using Image Studio Lite software. Representative western blot images are depicted. Although the blots for cyclins with and without 3'UTR are presented as separate images, they were realized, analysed and developed in the same membrane. B) Quantification of the amount of Pcl1-3HA and Clb5-3HA with and without 3'UTR. As in A), the signal from the western blots was quantified using Image Studio Lite software. Values were standardized using loading control and were relativized to the maximum expression amounts. Mean±SEM values for three and four independent experiments for Clb5 and Pcl1, respectively, are shown. C) Duplication time of strains bearing *PCL1-3HA* or *CLB5-3HA* with or without the 3'UTR sequence. Cells were grown overnight in YPD at 30°C, diluted to OD = 0.4 in fresh medium and incubated in a water shaker at 30°C. Samples were taken every 10 min over 420 min. Optical density (wavelength 660 nm) was used as a measure of cell density. Mean±SEM values for three independent experiments are shown. An asterisk indicates a statistically significant difference ($p \leq 0.05$).

https://doi.org/10.1371/journal.pone.0218531.g001

Monitoring seven G_1 cyclins

To reliably and efficiently monitor the seven selected proteins, we pooled the tagged strains in groups (see below). To do this, we first checked whether all the strains grew at the same rate, by growing them simultaneously in a microtiter plate at 30°C under agitation in a spectrophotometer, which permitted us to continuously monitor optical density. No statistically significant differences were detected in their duplication times (S1A Fig). Furthermore, to better validate the pooling strategy, under a microscope, we counted the cells of all the separately growing strains at different moments of the experiment and also counted the proportion of budding at 35 min after α-factor release. In all cases all the separately growing strains behaved very similarly (S1B and S1C Fig). Finally, using western blot we monitored all cyclins from the separately growing strains, finding that the pattern of expression was very similar to the pattern observed when the strains were pooled (see below and see S1D Fig).

Overnight cultures of cells with the different tagged cyclins were pooled in strictly controlled quantities in three mixes, designed according to the size of the cyclins to ensure correct detection of all cyclins in the same blot (see Fig 2A). The mixes were grown exponentially for 3 h, synchronized in G_1 by incubation with α-factor and released synchronously into the cell cycle. To minimize experimental noise, expression of all G_1 cyclins was monitored in a single western blot (see representative images in Fig 2B). The specificity of signals was checked using a non-tagged strain. Note that, for the two western blot images from independent experiments included in Fig 2A, we obtained reproducible data on the relative amounts and the appearance-disappearance dynamics of the different G_1 cyclins. This information can be considered accurate and reliable, as the cells were grown at the same time, in the same incubator, using the same polyacrylamide gel for the electrophoresis, using the same transfer conditions and the same transfer device and using the same antibody solution, developed and exposed in an identical way. Since α-factor synchronization produces intrinsic artefacts, we repeated the analysis using elutriation as a very different synchronization method, with the results depicted in Fig 2C.

In our analysis, we also included the cyclins specific for the Pho85 CDK (Pcl1, Pcl2 and Pcl7). This meant that we could obtain evidence on the relative importance of the Cln and Pcl sets of cyclins, so as to hypothesize regarding the contribution of their respective CDKs (Cdc28 and Pho85) to G_1 progression in both normal growing conditions and, more importantly, in environmentally different growing conditions (explained further below).

A cyclin map for G_1/S-phase transition in *S. cerevisiae*

We quantified at least three independent experiments (in the case of α-factor synchronization)–like those depicted in Fig 2B–to produce cyclin blueprints that included both amplitude

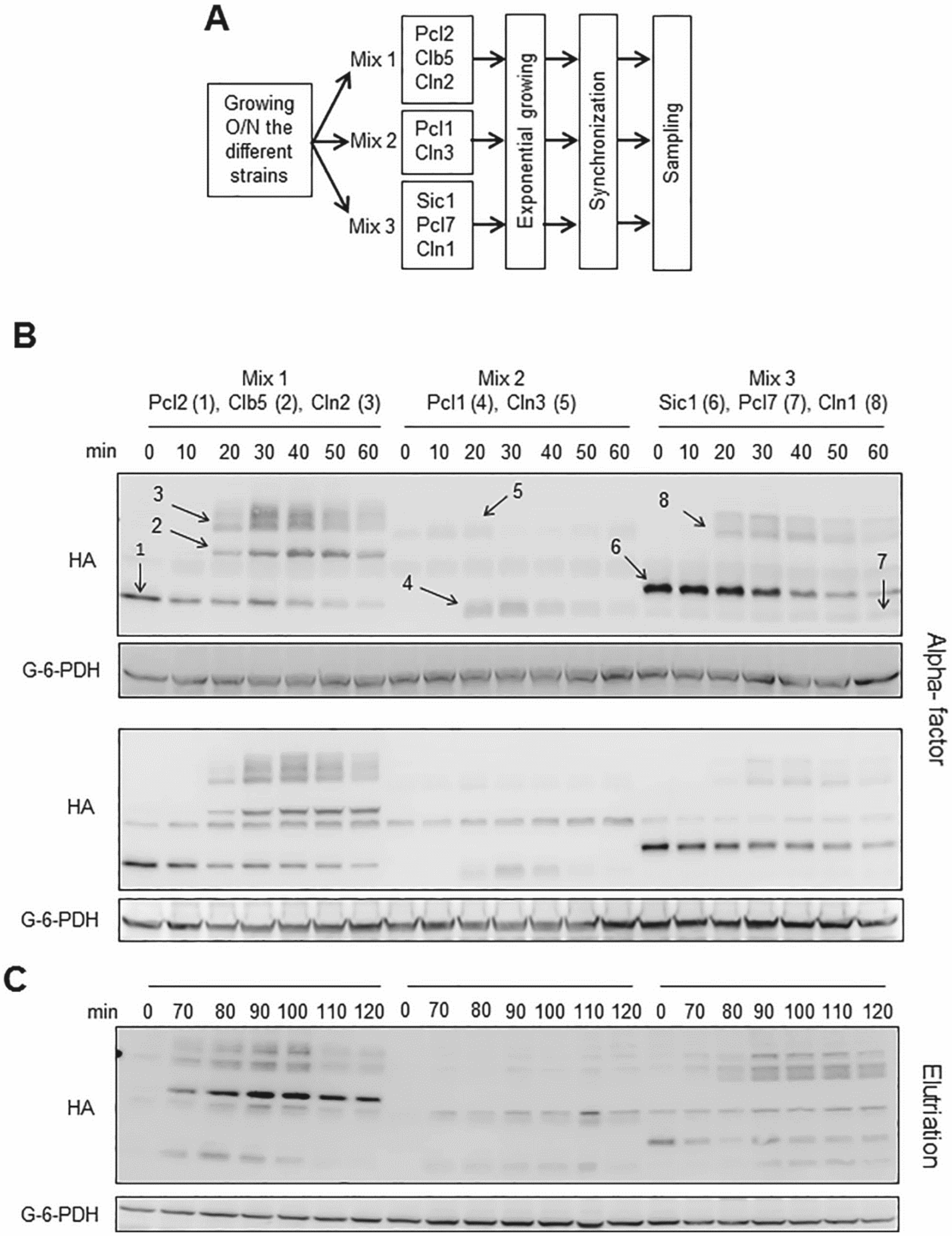
A
Growing O/N the different strains
Mix 1
Mix 2
Mix 3
Pcl2
Clb5
Cln2
Pcl1
Cln3
Sic1
Pcl7
Cln1
Exponential growing
Synchronization
Sampling
B
Mix 1
Pcl2 (1), Clb5 (2), Cln2 (3)
Mix 2
Pcl1 (4), Cln3 (5)
Mix 3
Sic1 (6), Pcl7 (7), Cln1 (8)
min
0 10 20 30 40 50 60
0 10 20 30 40 50 60
0 10 20 30 40 50 60
HA
1
2
3
4
5
6
7
8
G-6-PDH
HA
G-6-PDH
Alpha- factor
C
min
0 70 80 90 100 110 120
0 70 80 90 100 110 120
0 70 80 90 100 110 120
HA
G-6-PDH
Elutriation

Fig 2. Experimental setup for determining G_1 cyclin amounts. A) Workflow and pooling scheme. Strains were grown overnight in YPD at 30˚C in a water shaker, diluted in fresh medium, mixed in three different sets according to the molecular weight of the tagged proteins, grown in the exponential phase, synchronized, released in fresh medium and subjected to the designed stress or treatment (see Materials and Methods). B) Two representative and independent western blot images (to show reproducibility) used to quantify G_1 cyclin amounts. Cells were synchronized using α-factor and samples were obtained as described in A), separated by SDS-PAGE and blotted and developed (see Materials and Methods). The different cyclins are indicated by numbers in the upper image. C) Same procedure as in B), except that cells were synchronized by elutriation, with time 0 corresponding to the moment the cells were retrieved from the elutriation device, after which the cells were incubated under agitation at 30˚C.

https://doi.org/10.1371/journal.pone.0218531.g002

(temporal expression) and height (protein expression) of the G_1 cyclin waves. To simplify visualization, the Cdc28 and Pho85 cyclins (Clns and Pcls, respectively) are shown in different graphs. We also used Clb5 and Sic1 levels together with the budding index (virtually identical for all the strains; (see S1C Fig) to establish the precise moment of START, defined as the moment in which Clb5 and Sic1 amounts are identical (see Materials and Methods and Fig 3). All together, these produced an accurate picture of the G_1 cyclin universe in a yeast cell (Fig 3).

We found some differences between the two synchronization methods, specifically, the presence of Pcl2 with α-factor synchronization, as previously reported [26], a slightly delay in the expression of Cln1 compared to Cln2 and an increased level of Clb5 in elutriation. We also found some similarities: the low level of Cln3 (although higher for elutriation than for α-factor) and the bulk of Cln1 and 2 expression taking place after START. At this point, we decided to perform the rest of our experiments using α-factor synchronization method rather than centrifugal elutriation, which, although it has been used to study cyclin expression on several occasions [44, 45], is a more complex method for the purposes of the research described in this article.

Looking at the cyclin pattern resulting from α-factor synchronization, we can first confirm very low-level and slightly cyclic Cln3 behaviour [33]. Second, Cln1 and Cln2, which are typically plotted as a single curve (for simplification sake), are present in different amounts, as already reported for expression from plasmids [46] and for interference with 3'UTR sequences [47]. Third, our temporal map of Cln expression in relation to START is noticeably different to the current widely used model, with the maximum level reached in the S-phase (Fig 3A). Finally, for the first time, Pcl cyclins are included in the G_1 cyclin picture (Fig 3A).

Cyclin and cyclin family amounts in different conditions and stresses

The amounts of specific cyclins depend on the environmental stress conditions to which cells are exposed. Some examples are Cln2 in response to osmotic shock [48], Cln1 in response to glucose [49] and Cln1, Cln2, Cln3 and Clb5 in response to heat shock [50]. However, those studies feature some of the drawbacks mentioned above, mainly, modification of the 3'UTR and failure to include all the cyclins. To obtain a more accurate description of cyclin behaviour in stress conditions, we used the strains and setup described above, synchronized the cells using α-factor and released them under four different stress conditions: heat shock (37˚C), osmotic stress (0.4M NaCl), reductive stress (100 mM N-acetyl cysteine) and oxidative stress (10 μM menadione). We also tested cyclin levels when cells were growing in different mediums: SD at 30˚C and malt-based medium (as a more physiological growth medium for yeast) at 30˚C and at 37˚C. The corresponding analyses pointed to variations in the expression pattern of the G_1 cyclins with respect to standard lab growing conditions (i.e., YPD at 30˚C). Western blots of all the conditions and stresses analysed, along with quantifications and graphical representations of all the G_1 cyclins in the different conditions, are depicted in S2–S5 Figs.

To produce a more comprehensive view of changes, we depicted the contribution of each G_1 cyclin in single graphs that showed cyclin amounts from α-factor release to START (see Fig 4A for an example). In our experimental setup, Clns and Pcls were expressed at similar levels

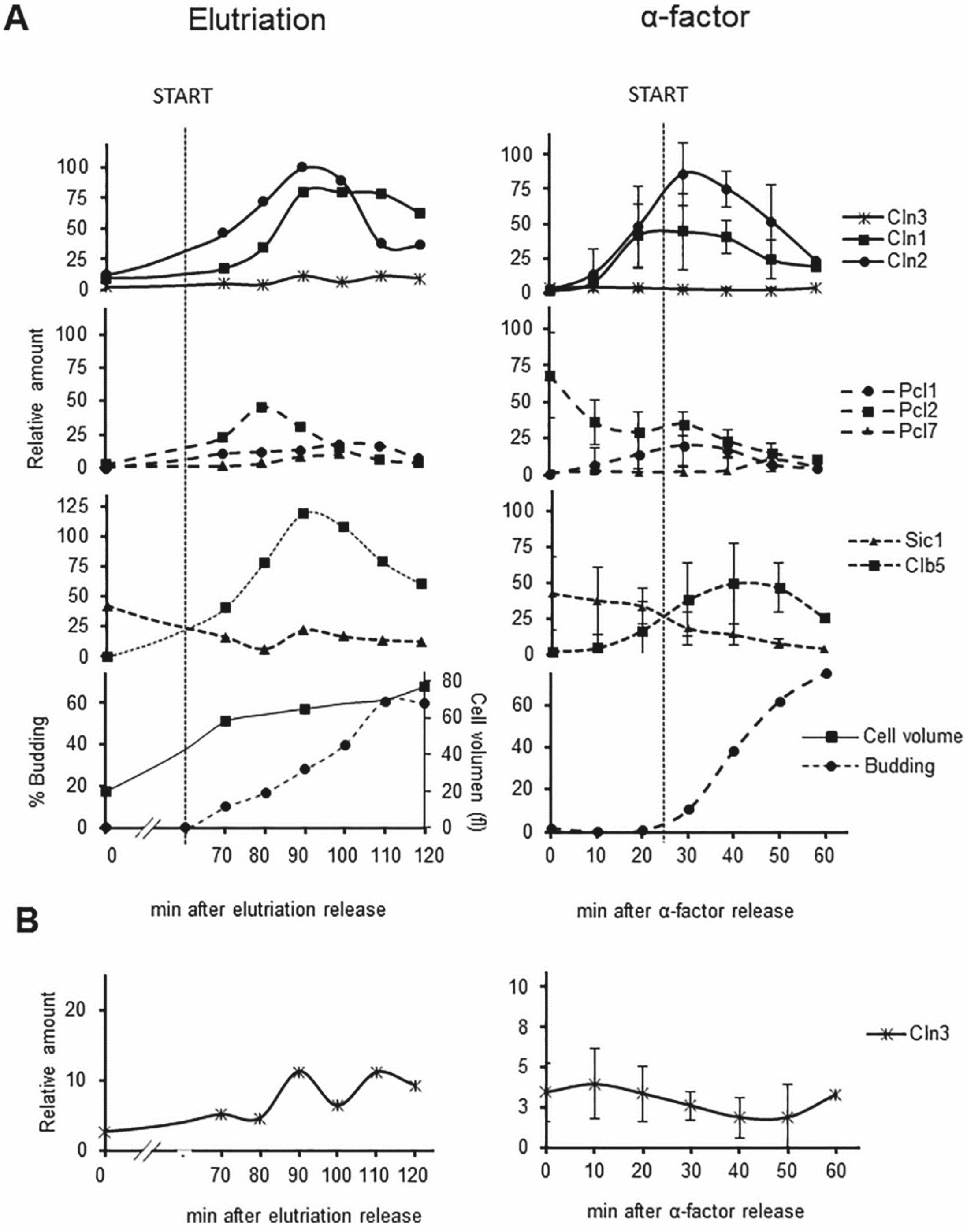
A
Elutriation
α-factor
START
START
Relative amount
Cln3
Cln1
Cln2
Pcl1
Pcl2
Pcl7
Sic1
Clb5
% Budding
Cell volumen (fl)
Cell volume
Budding
0
70 80 90 100 110 120
0 10 20 30 40 50 60
min after elutriation release
min after α-factor release
B
Relative amount
Cln3
min after elutriation release
min after α-factor release

Fig 3. Cyclin waves in *S. cerevisiae* growing in normal lab conditions (YPD at 30˚C). G_1 cyclin waves as determined in this research. From top to bottom, the panels show the Cdc28 G_1 cyclins, the Pho85 G_1 cyclins and the different molecular markers (Clb5 and Sic1) and morphological markers (budding percentage and size for elutriation). START, determined as the moment in which Sic1 and Clb5 amounts were identical, is extrapolated as a dashed line to all the panels. A) Cells were synchronized by centrifugal elutriation (left panels) or α-factor (right panels). Time 0 corresponds to the moment of cell removal from the elutriation device or α-factor removal, after which cells were incubated under agitation at 30˚C. Note that the time elapsed before the cells resumed the cell cycle was greater after elutriation than after α-factor treatment. B) Since the amount of Cln3-3HA is very low, it is plotted both with the other Clns and individually so as to clearly represent levels. In the case of α-factor synchronization, at least three independent western blot experiments as in Fig 2B were quantified, standardized using loading control and relativized to the maximum expression amounts (Cln2). Values are expresed as mean±SEM.

https://doi.org/10.1371/journal.pone.0218531.g003

in most of the tested conditions (Fig 4B), reinforcing the idea that both groups of cyclins are necessary for correct cell cycle passage through the G_1 phase. This scenario was generally maintained, except for heat shock and the malt-based medium: for the cells growing at a high temperature (37˚C) in the malt-based medium, Pho85 cyclin amounts rose to 80% and even 90% (Fig 4B).

Variations in cyclin family components

Another level of complexity is represented in Fig 4C, which shows the contribution of each cyclin to the overall picture (also see Fig 4A). Noticeable is the prominent presence of Pcl2, most significantly for the malt-based medium at a high temperature. On the basis of these results we speculated that *pcl2Δ* cells might face difficulties in surpassing START when released from α-factor arrest at 37˚C. The FACS analysis of cell cycle progression revealed this to be the case: *pcl2Δ* cells showed some cell cycle progression difficulties in heat-shock conditions (Fig 5A), but no difficulties in other conditions such as, for instance, osmotic stress. To evaluate the relevance of the role played by Pcl2 in high temperature conditions, we repeated the analysis using elutriation as the synchronization method (S6 Fig). Since we did not detect any notable increase in the level of Pcl2 in these conditions, we conclude that the role of Pcl2 in thermal stress is restricted to α-factor conditions.

Interestingly, the magnitude of the *pcl2Δ* cell cycle phenotype depended on the genetic background. Despite cell cycle impairment, in a spotting assay using the BY4741 background we were unable to find a growth phenotype that is clearly present in the W303 background (Fig 5C). Our results corroborate *pho85Δ* thermosensitivity, as other studies have also documented *pho85Δ* difficulties in growing at 37˚C [51, 52]. Additionally, the inclusion of the different Pcl mutant strains in the dot assay growing analysis suggests that the thermosensitivity of *pho85Δ* might be determined by the regulation exerted by Pcl2, since Pcl2 deletion is the only deletion leading to thermosensitivity (Fig 5C), at least in the W303 background. Focusing on the *pcl2Δ* thermosensitive phenotype, we detected an interesting trait in the appearance of a significant proportion of *pcl2Δ* cells showing a 'mickey mouse' phenotype consisting of double-budded cells (Fig 5D) appearing after incubation for 5 h at 37˚C. This phenotype was not present when Pcl1, another cyclin from the Pcl family, was deleted. Note that, despite the apparent increase in size of the *pcl2Δ* cells, we found no statistically significant differences when volumes were calculated using the Scepter cell counter (Millipore) or when cell diameter was directly measured under the microscope (Fig 5E).

We present the correlation between the change in Pcl2 amounts and particular physiological consequences as a proof of principle for the potential usefulness of our set of tagged strains, whether to unveil the physiological relevance of cyclins in specific environmental settings or to analyse cell cycle progression in different types of treatments (including chemotherapeutic drugs). However, Pcl2 is not the only cyclin that changes; important differences can also be appreciated in many other cyclins–e.g., Cln2 and Cln1, which clearly increase in response to reductive stress or in the SD medium (Fig 4B). These notable changes in expression will be analysed in detail in future research.

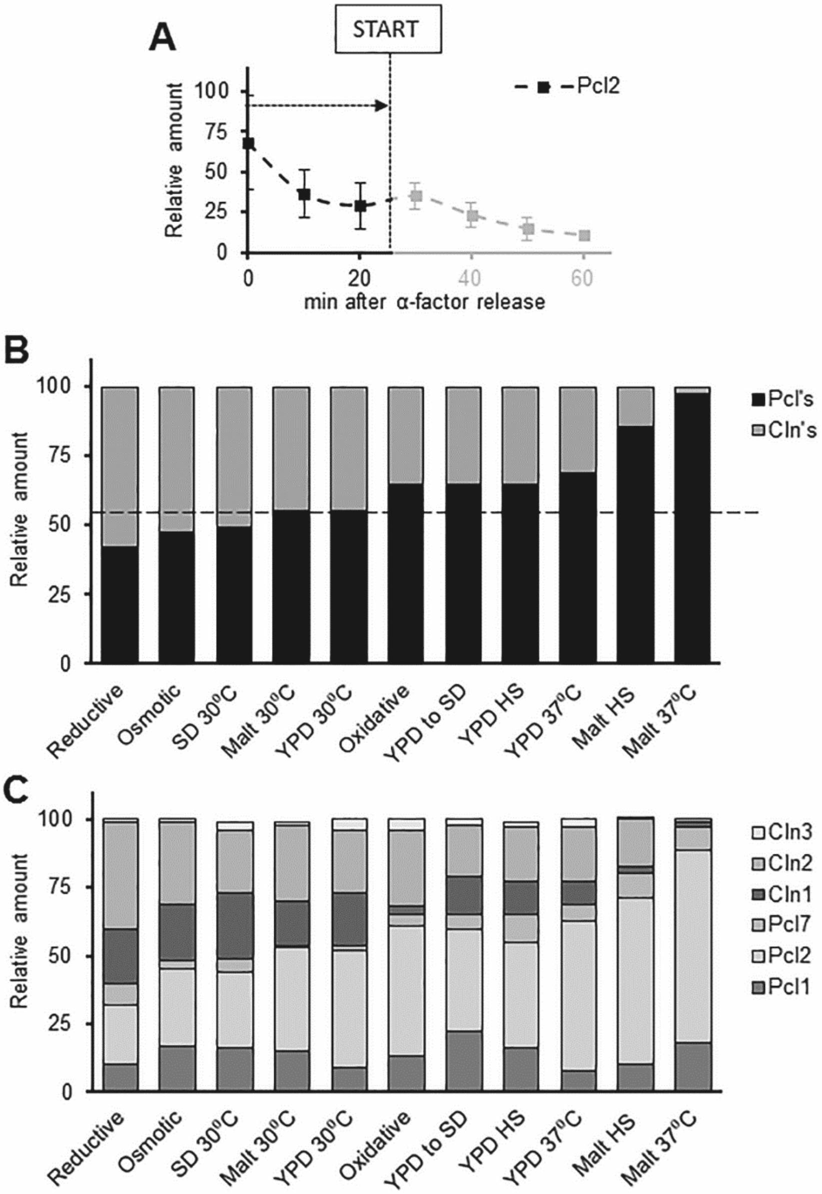

Fig 4. Cyclin amounts in different conditions and stresses. Strains were grown and processed as described in Fig 2B. Western blots were quantified, values were standardized using loading control, relativized to the maximum expression amounts and plotted as in Figs 1B and 3B. A) Cyclin amounts in particular environmental or stress conditions were obtained by calculating the area under the curve from α-factor release to START. B) Pcl and Cln amounts were calculated as for A). Conditions are ordered according to increasing amounts of Pcl. C) Same procedure as in A) but with the different members of the two cyclin families separated. Conditions are ordered according to increasing amounts of Pcl. Values are expressed as means of at least three independent experiments.

https://doi.org/10.1371/journal.pone.0218531.g004

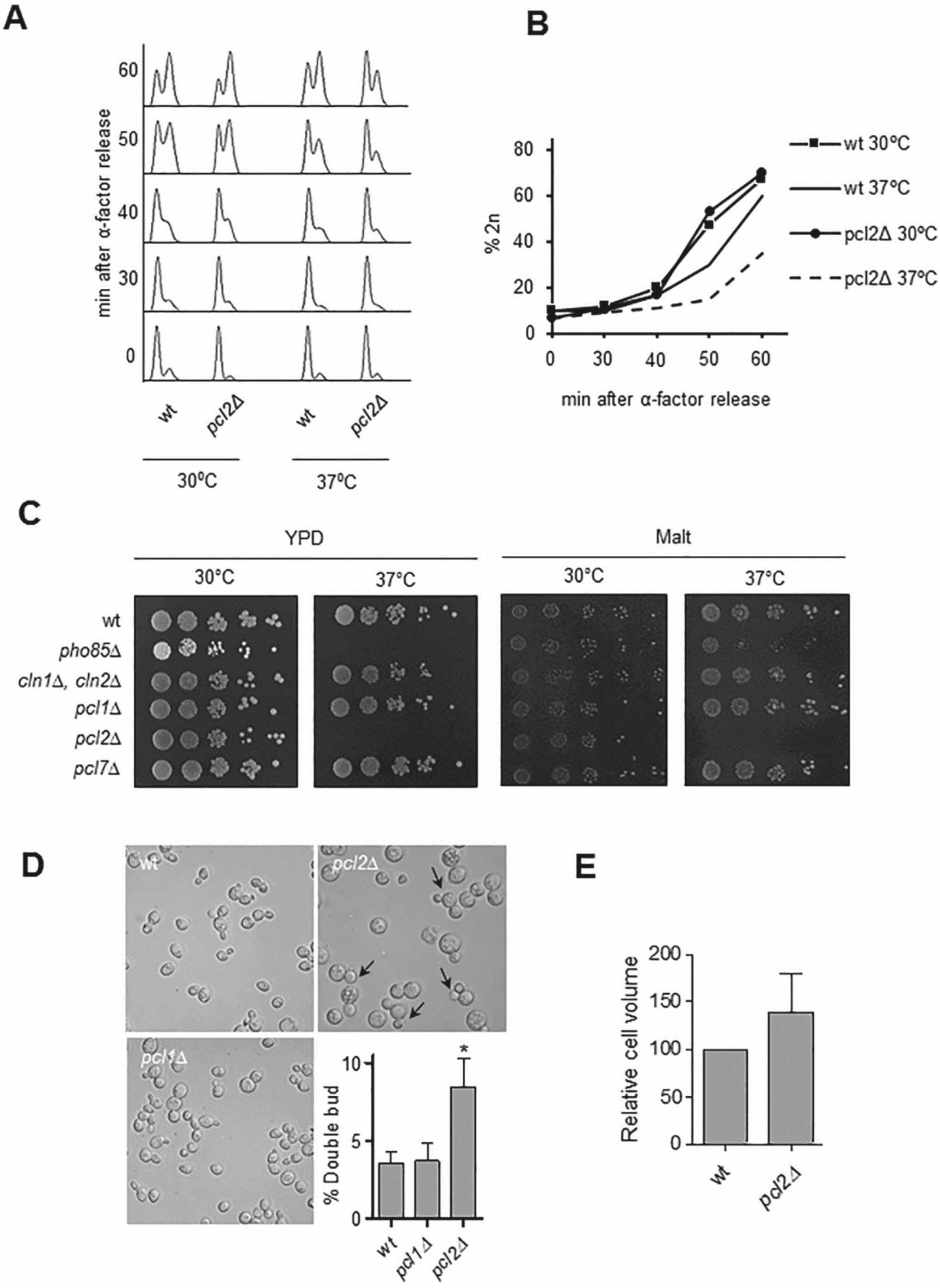
A
60
50
40
30
0
min after α-factor release
wt
pcl2Δ
wt
pcl2Δ
30°C
37°C
B
% 2n
80
60
40
20
0
0
30
40
50
60
min after α-factor release
wt 30°C
wt 37°C
pcl2Δ 30°C
pcl2Δ 37°C
C
YPD
Malt
30°C
37°C
30°C
37°C
wt
pho85Δ
cln1Δ, cln2Δ
pcl1Δ
pcl2Δ
pcl7Δ
D
wt
pcl2Δ
pcl1Δ
% Double bud
10
5
0
*
wt
pcl1Δ
pcl2Δ
E
Relative cell volume
200
150
100
50
0
wt
pcl2Δ

Fig 5. Cell cycle progression and thermosensitivity of *pcl2*Δ cells. A) FACS analysis of wild-type and *pcl2*Δ cells from the BY4741 background. Cells were grown exponentially at 30°C in YPD, synchronized in G_1 with α-factor and released in fresh YPD medium at 30°C or 37°C. B) Quantification of cells with 2n DNA content from A). C) Spot assay. W303 background cells were grown in YPD or a malt-based medium to the exponential phase and diluted to an optical density of 0.05 (wavelength 660 nm). Spotted on plates were 5 μl of tenfold sequential dilution for incubation at the indicated temperature. D) Nomarski images of the strains after 5 h at 37°C. Arrows indicate cells showing a 'mickey mouse' phenotype and the bar represents 10 μm. The 'mickey mouse' cells were quantified (mean±SEM) for three different experiments. E) Relative cell volume (mean±SEM), based on measurement of some 30 cells from each of the three independent experiments.

https://doi.org/10.1371/journal.pone.0218531.g005

Discussion

Several studies have been carried out to produce a view of gene expression and the proteome of yeast cells, for instance, a gene expression assay depending on the cell cycle [53]. However, despite the great value of that study, since it was designed to provide data on variations in the amount of mRNA in all genes (including G_1 cyclins) relative to initial expression, it tells us very little about the level of expression of a particular protein relative to other proteins. For this reason, while it is useful for assessing the temporal framework of cyclin expression, it yields little information regarding relative amounts of the G_1 cyclins.

In addition to transcriptomic analysis, efforts have been invested in analysing the proteome of yeast cells under many different conditions [54–56] and also in proteome variations throughout the cell cycle [57]. Unfortunately, however, the dynamic range of proteome approaches greatly limits the detection of low abundance proteins [58] like cyclins. Another systematic study of Cdc28 cyclins used a collection of strains in which 3'UTR was deleted [34]. However, we have not been able to find data in the literature regarding the relative amounts of the different G_1 cyclins in *S. cerevisiae* throughout the cell cycle. A direct consequence is that, to date, no quantitative picture of the G_1 cyclin waves including Pcls has been available.

3'UTR sequence in cyclins

Apart from the issues mentioned above, the current Cln wave model is seriously affected by technical artefacts; not only was it produced in different labs using different tags, it is also affected by the tags used and the genetic modifications inherent to the tagging procedure. The effect of using different tags (even though they had little influence in our case) has been recently pointed out for high-throughput analyses [54–56]. In the course of our research, an artefact was reported to affect the tagging of proteins [40], specifically, that a dramatic reduction occurred in the stability of tagged proteins due to the presence of a particular linker sequence in the 3HA module used for the Longtine system [41], for which it was reported that the use of a different linker sequence (as in our case) had less impact on the amount of proteins. It should be noted that a seminal study on the level of Clns [33] published by the Futcher laboratory did not use the Longtine tagging system but a genomic tagging approach [59] that also keeps 3'UTR sequences intact.

Importantly, our results demonstrate a role for 3'UTR sequences in cyclin genes in the amount of the proteins coded by them. The regulatory role of this gene sequence in stabilizing the mRNA and, consequently, in regulating protein levels [60, 61]–and also in relation to the proteins involved in the cell cycle [43]–is well known. We have shown that disrupting the 3'UTR of cyclins appears to have no effect either on expression timing or cyclin destruction, which may suggest that 3'UTR disruption affects mRNA stability more than promoter regulation or destruction mechanisms. However, although an interesting topic, it was not our aim to understand the molecular mechanisms behind cyclin level regulation by the 3'UTR. What is relevant to our research is the fact that the 3'UTR role points to an important issue in cyclin analysis. As one example, if the level of Clb5 is altered by affecting the 3'UTR, and this level, relative to the CDK inhibitor Sic1, is essential to defining S-phase entry, then relocating this landmark would appear to be necessary. Changes like this are likely to have a major impact on modelling studies.

The fact that it has been reported for a G_2 cyclin that protein increases when the 3'UTR sequence is eliminated [54] would suggest a more general scenario rather than one confined to yeast. The deletion of the 3'UTR in cyclins D, B and CCND1 in mammalian cells leads to significant upregulation of the proteins [62–64]. The translational repression of the 3'UTR in cyclin B, among many other genes, has also been demonstrated for *Xenopus* oocytes [65], although the opposite has also been reported, namely, a role for the 3'UTR in the stabilization of cyclin E [66].

A quantitative blueprint of G_1 cyclins

To perform a cell cycle analysis like that performed for this research, the cells must first be synchronized. Several methods for doing this exist, each with their intrinsic strengths and weaknesses [67, 68]. Choosing a method therefore results in a limitation inherent to the experimental design. We chose α-factor synchronization–while accepting the limitation of synchronizing cells in the late G_1 phase–for several reasons: first, α-factor arrest is a physiological situation for yeast, especially when they are growing in nature, but is not the case for most of the remaining systems (drugs, temperature sensitive mutants, elutriation, etc); second, since α-factor arrest has been commonly used for cell cycle studies, a great deal of evidence is available regarding its use, so a comparison with the existing model should be performed using the same approach; and finally, α-factor arrest is easy to perform and is highly reproducible. With the aim of generating a more general view that considers synchronization artefacts, we also investigated cyclin waves using elutriation synchronization. Some differences with the α-factor method included the higher amount of Clb5, the delayed expression of Cln1 and the already documented different behaviour of Pcl2 [26] (very elevated at the moment of α-factor release but reflecting a more typical cyclin wave pattern in elutriation). We also found some similarities in the two methods: the previously documented low level of Cln3, the shifted expression peak of Cln1 and Cln2 with respect to START and the very low levels of Pcl1 and Pcl7. In sum, our comparison of data from different synchronization methods suggest that cyclin wave studies need to be interpreted with care and should bear in mind the synchronization method.

Another important assumption on which our research is based is that we used the biochemical definition of START: the moment in which relative amounts of Clb5 and Sic1 are the same [69, 70]. Our evidence indicate that this definition is in good agreement with the budding index, a morphological parameter for assessing START [71, 72]. Note that this definition also reflects a subcellular definition of START as the exit from the nucleus of the main START repressor Whi5, which is strictly necessary for the Cln1 and Cln2 positive feedback loop and S-phase entry [73].

Taking into account the above facts (or limitations), our results nevertheless demonstrate, first, that most Cln1 and Cln2 are actually produced significantly beyond START and well into the S-phase. This is not entirely surprising, given their morphogenetic role in the polarized growth taking place over a significant period of time within the S-phase [74–76]. Second, we detected substantially differing expression for Cln1 and Cln2 than proposed elsewhere for systems where the 3'UTR was respected [33] or not [46, 47]. Bearing in mind the similarity of the SBF boxes in the promoters of both genes and, consequently, their fairly similar levels of mRNA, it is tempting to speculate that the molecular nature of their differential regulation may depend on the protein sequences, as already suggested elsewhere [14]. Finally, it is interesting to note that our analysis corroborates the very low levels of Cln3—in comparison with the rest of the cyclins—reported years ago [33, 77].

Pcls: The overlooked cyclins

The Pho85 CDK is not considered essential in standard lab growing conditions, which may explain why its cyclins have never been represented in cyclin blueprints. Nevertheless, the fact that the presence of several families of CDKs controlling passage through G$_1$ has been conserved through evolution to mammals [78] would point to the importance of these CDKs. One of our goals was to account for the corresponding knowledge gap by producing a full map of the G$_1$ cyclins that included Pcls and, in this way, to throw some light on the problem of the redundancy of the different CDK/cyclin complexes [29]. Analysis of the Pcls led to the findings discussed below.

First, in the release from α-factor arrest, the relative amount of Pcls is surprisingly high, bearing in mind that Pcls are regulators of a 'non-essential' CDK. In practically all tested conditions, Pcls accounted for over 50% of total cyclins (taking into account the definition of START used by us). This could be interpreted in terms of an understated role for Pho85-Pcls in the biology of yeast cells. The role of master cell cycle regulator has deservedly been attributed to Cdc28 (Cdk1 in mammals), with a secondary, redundant or supporting role attributed to Pho85 as the other CDK involved in cell cycle progression. Nevertheless, according to a basic cell economy principle, the high level of expression of the Pho85 cyclins would point to a more active role for Pho85, at least when cells are released from α-factor arrest (a situation which, as mentioned before, is absolutely physiological for yeast in a natural environment). Second, contributions in terms of amounts of Clns and Pcls are clearly dependent on environmental conditions, and interestingly, Pcls seem to be very important in general terms, since they are always noticeably present; even more importantly, Pcls clearly take the lead in high temperature or heat-shock conditions.

Does this mean, therefore, that the two CDKs are more specific than redundant? That the absence of one cannot be fully compensated for by the presence of the other? And, regarding a different layer of regulation, do subtleties in cell cycle control result from the interaction of each CDK with different cyclins?

In addition to providing an accurate blueprint of the G$_1$ cyclins, therefore, we also pondered the fundamental question of why eukaryotic cells have or need more than one CDK to control cell cycle progression and also more than one cyclin to control each CDK. We propose two possible explanations. One is that cell cycle machinery may incorporate a certain degree of redundancy in order to gain robustness. The other is that the different apparently redundant elements may have specific functions–related to the broad array of eventualities that all cells must cope with during their life–that are only apparent when cells are growing in particular conditions (whether in terms of stress or specific nutrients). The results reported here support the second possibility.

Pcl2 and thermal control

Our analysis suggests specific roles for certain cyclins depending on the environmental conditions to which cells are exposed. The most striking finding was the increase in Pcl2 during both heat shock and permanent growing at a high temperature, especially when the cells grew in a more 'natural' condition (in a malt-based medium). As predicted by the increased amount of Pcl2, *pcl2Δ* cells had problems progressing through START and the S-phase in the malt-based medium and at 37°C (that is, the conditions in which this cyclin is highly expressed). While this effect was only slightly evident in the BY4741 background, when the same analysis was done in the W303 background, the phenotype of absent Pcl2 was striking, not only in cell cycle progression but also in thermosensitivity terms, as revealed by the dot assay. In view of this observation, we performed the dot assay for other, less widely used genetic backgrounds, such as YPH499 [79] and 1700, derived from 1783 [80] and, again, we detected partial thermosensitivity.

While we have no clear explanation for the enhanced thermosensitivity, we venture that it may depend on differences in the relative level of expression of the cyclins in the different backgrounds. Leaving aside background differences, microscopic inspection of the *pcl2*Δ cells revealed a 'mickey mouse' phenotype based on double-budded cells. This phenotype has been described in the absence of the GPI-anchored wall protein Gas1 [81]. Expression of Gas1, which is essential for normal cell wall synthesis, is regulated during the G_1 phase [82, 83]. The null mutant shows a thermosensitive phenotype and reduced viability at 37°C [84–86]. Altogether, it is possible to speculate that regulation of Gas1 in G_1 by Pcl2 in thermal stress conditions cannot be supplanted by any other G_1 cyclin. Finally, we detected no increment in Pcl2 when we used elutriation; nevertheless, we were able to find phenotypes in *pcl2*Δ cells for heat shock in conditions where α-factor was not present, indicating a role for Pcl2 in thermal stress independently of the synchronization method used.

We found other remarkable variations in the amount of cyclins in different stress conditions. One was the increase in Cln1 and Cln2 in response to osmotic or reductive stress. Although we attempted to determine whether those increases were reflected in the appearance of a phenotype when the cyclins were deleted, we found no differences in either dot assays or growing kinetics. This result leads us to suggest the following. First, another cyclin could take over the work of Cln1 and Cln2 in dealing with these stresses, given that Cln3 alone is able to drive cell cycle progression showing only a minor G_1 delay [33]. Second, since the variation we detected in the tested conditions was not sufficient to produce a phenotype, a more sensitive analysis is needed to reveal the importance of Cln1 and Cln2 responses to osmotic and reductive stress. Finally, although consistent in the different replications of the experiment, the variations in Cln1 and Cln2 in the tested conditions were not reflected biologically.

A new tool for assessing G_1

G_1 allows cells time to check internal and external environments and to ensure that conditions are appropriate and preparations are complete before major cellular processes are undertaken in the S- and M-phases. G_1 is important for cells to decide their fate: to enter in quiescence, to sporulate, to wait for better nutrient conditions, to check their size, or to acquire confidence about successful transit through cell division and not perform this process blindly. In metazoans, misregulated G_1 can lead to developmental problems and disease [87]. Yeast cells represent a good model for testing drugs or treatments affecting cell cycle progression in G_1. Our set of strains can be used both as a tool for accurately assessing G_1 cell cycle progression and as a testing bench for gaining biochemical insights into the mechanisms by which a compound could affect the expression patterns of cyclins and, consequently, cell cycle progression.

To sum up, we produced a set of strains tagged in the most respectful way possible so as to produce a quantitative and accurate picture of the G_1 cyclins for a broad array of environmental conditions. We propose using this set of strains to monitor G_1 cell cycle progression and to study the molecular mechanisms sustaining cell cycle effects, the use of drugs, treatments, compounds, stresses, etc. All the strains are fully available upon request.

Materials and methods

Yeast strains

Yeast background (except when otherwise mentioned) was always BY4741 [88]. A list of all the strains used in this work is provided in Table 1. For tagging, we followed a system based on *delitto perfetto* [39]. Briefly, for a protein to be tagged, we first deleted the complete open

Table 1. Yeast strains.

Name	Background	Genotype	Source
BY4741	BY4741	*MATa his3Δ1 leuΔ200 met15Δ0 ura3Δ0*	[88]
YJJ1024	W303-1a	*MATa leu2-3,112 trp1-1 can1-100 ura3-1 ade2-1 his3-11,15*	[89]
YPC502	YPH499	*MATa ura3-52 lys2-801 ade2-101 trp1-Δ63 his3-Δ200 leu2-Δ*	[79]
1700	1700	*MATa leu2-3,112 ura3-52 trp1-1 his4 can1*^{r}	This study
YEB27	W303-1a	*PCL1-3HA*	This study
YEB56	W303-1a	*PCL1-3HA-KanMX4*	This study
YEB53	BY4741	*CLB5-3HA-KanMX4*	This study
YEB11	BY4741	*sic1::URA3-kanMX4-3HA*	This study
YEB112	BY4741	*PCL1-3HA*	This study
YEB113	BY4741	*PCL2-3HA*	This study
YEB114	BY4741	*PCL7-3HA*	This study
YEB116	BY4741	*CLN1-3HA*	This study
YEB117	BY4741	*CLN2-3HA*	This study
YEB118	BY4741	*CLN3-3HA*	This study
YEB119	BY4741	*CLB5-3HA*	This study
YEB120	BY4741	*SIC1-3HA*	This study
YEB182	BY4741	*CLB5-TAP*	This study
YEB181	BY4741	*pcl2::URA3*	This study
YEB189	W303-1a	*cln1::URA3-KanMX4 cln2::URA3*	This study
YEB184	W303-1a	*pcl2::URA3*	This study
YEB32	W303-1a	*pcl1::URA3-hyg*	This study
YEB30	W303-1a	*pcl7::URA3-KanMX4*	This study
YNR60	W303-1a	*pho85::KanMX4*	This study

https://doi.org/10.1371/journal.pone.0218531.t001

reading frame (ORF) and replaced it with a *URA3-KanMX4-3HA* double marker and tag. We then transformed the deleted cells using a DNA fragment containing the eliminated ORF and fused the fragment to the previously introduced tag (3HA) sequence using 40 nucleotide flanking tails so as to allow the recombination (integration) process to take place. To eliminate the possibility of different recombination events–due to the presence of the three times repeated sequence of the HA tag potentially leading to proteins tagged with different numbers of HA repetitions–we modified the *3HA* DNA sequence but maintained the amino acid sequence. The *3HA* sequence was as follows (underlined are the bases changed to ensure the desired integration): `5′ TCAGCACTGAGCAGCGTAGTCTGGGACGTCATACGGATAGGATCCTGCGTAATCTGGGACGTCATACGGATAGCCCGCATAGTCAGGAACATCGTATGGGTA3′`. Tagging, furthermore, was always checked by tag sequencing. Knock-ins were grown in plates containing 1mg/ml of the antimetabolite 5-fluoroorotic acid (5-FOA; Sigma) and were confirmed by replica plating in plates containing geneticine 0.4 mg/ml (Gibco). Selected were colonies able to grow in 5-FOA and not in geneticine.

Classical tagging to obtain the strains *PCL1*-3HA-Δ3'UTR and *CLB5*-3HA-Δ3'UTR was performed using the tool-box system [42] (a variation of a method developed previously [90, 91]), in which the original 3'UTR of the gene to be tagged is interrupted (and consequently inactivated) by the tagging (3HA in our case), the 3'UTR from *ADH1* and the selection marker.

Growth conditions

The growing media used were yeast extract-peptone-dextrose (YPD: 1% yeast extract, 2% peptone and 2% dextrose) and complete synthetic (SD) medium (0.67% yeast nitrogen base, 0.5%

NH_4SO_4, 2% glucose, supplemented with amino acids for auxotrophic requirements). For solid media, 2% of agar-agar (w/v) was added and melted during the autoclave process. For the malt-based medium plates, 1 g of malt medium from Bulldog Brews was dissolved in 7.69 ml of distilled water. For the 5-FOA plates, SD with all the required amino acids was supplemented with 5-FOA 1 mg/ml, sterilized by filtering, and added to the medium just before plating. Cells were always grown, except when otherwise specified, at 30°C under vigorous agitation (200 rpm) in water shakers. To reduce experimental variability, the overnight yeast cultures were always inoculated in strictly controlled conditions: the cells to be inoculated were obtained from a fresh colony and the number of cells to be inoculated was always constant ($OD_{660} = 0.01$).

Cell synchrony, flow cytometry analysis and size measure

To synchronize the cells in G_1, yeast cultures were grown exponentially in YPD or SD at a density of 1×10^7 cells/ml, treated with α-factor (Biomedal) to a final concentration of 20 μg/ml; after 100 min, the cells were collected, washed and released into fresh medium to resume the cell cycle in a synchronous manner. Afterwards, aliquots were collected and processed as described elsewhere [92]. DNA was stained with propidium iodide and analysed in a FACS Calibur cytometer (Becton Dickinson) as described elsewhere [93].

Centrifugal elutriation was performed as described elsewhere [94], using a Beckman-Coulter J-26XPI centrifuge equipped with a JE-5.0 elutriator rotor. Briefly, one litre of cells was incubated in YPD under continuous agitation at 30°C during 16 h, to arrival at an optical density of around 6 (660 nm wavelength). The culture was brought into the elutriator using a peristaltic pump and equilibrated at 1900 rpm at 20°C. The G_1 cells were then obtained from the elutriator by increasing the pump flow (total elutriation process time was 2 h). Synchrony was checked in situ by microscopic inspection. The different unbudded fractions were collected and mixed until the needed number of cells was obtained. Cells were diluted in YPD to an optical density of 1. Synchrony was checked by FACS analysis. Cells were immediately incubated in an agitated water bath at 30°C and aliquots were taken for western blot analysis.

The size of the elutriated cells was assessed using a Scepter Cell Counter (Millipore) and strictly following manufacturer indications. Briefly, cells to be measured were diluted in PBS buffer at a final concentration of around 10^5 cells/ml.

Cell extract and immunoblot

One ml of the yeast cell culture (1×10^7 cells) was treated with 10 M trichloroacetic acid (TCA) to a final concentration of 20% (v/v) for 10 min and centrifuged at full speed for 1 min. The resulting pellets were dissolved in 100 μl of 0.5% SDS, 42 mM Tris-HCl at pH 6.8. Then 300 μl of glass beads (Sartorius, BBI-8541701) were added, bead-beaten twice at maximum force for 30 sec and boiled for 5 min. Around 40 μg to 60 μg of protein from each sample was separated at 90 V (10% polyacrylamide/SDS gel) and transferred to PVDF membranes (Immobilon-P; Millipore). The primary antibodies used were anti-HA 1:100 (12CA5), anti-PAP 1:4.000 (Sigma, P1291), anti-PSTAIRE 1:5000 (Abcam, ab10345) and anti-G6PDH 1:500 (Sigma, A9521). The secondary antibodies used were donkey anti-goat-HRP, donkey anti-mouse-HRP and goat anti-rabbit-HRP 1:25000 (all from Jackson Laboratories). Immunoblots were developed using Luminata Forte Western HRP Substrate (Millipore) and images were taken using GeneSnap (Syngene) and quantified using Image Studio Lite (Li-Cor).

Measuring relative amounts of cyclins

To detect all cyclins in the same blot, we mixed different strains in the same test tube. Due to their different levels of expression we included different quantities as follows: in mix 1, 0.1 OD of each strain to a final cell concentration of $OD_{660} = 0.3$ (0.3 ODs); in mix 2, 0.1 OD and 0.2 OD from the strains bearing *PCL1-3HA* and *CLN3-3HA*, respectively; and in mix 3, 0.05 OD from *CLN1-3HA*, 0.1 OD from *PCL7-3HA* and 0.15 OD from *SIC1-3HA*. Note that we inoculated the same number of cells for the overnight culture and before mixing the strains, and we also checked that all cells had grown to the same extent to ensure that culture phase influence was minimized (see Fig 2A). The different quantities of cells included in the mixes were mathematically corrected after western blot quantification to revert any differences introduced in mixing.

The sampling and sample processing for separation by SDS-PAGE was as described above and in Fig 2A and Fig 2B. The bands were quantified using Image Studio Lite (Li-Cor), the amounts were corrected according to mixing (see immediately above), normalized according to load control, and relativized to the maximum signal in the blot. Using this data, we produced plots representing the relative amounts of cyclins in relation to time after release.

To produce the bar graphs representing the total amounts of the cyclins, we used the plots representing relative amounts over time, determined the START point (defined as the moment when Sic1 and Clb5 amounts were identical) and integrated the area under the curve up to START using GraphPad Prism 5 software. The obtained values represent the amounts of each cyclin at START.

Growth curves and duplication time

Strains were grown in YPD medium overnight and were diluted to $OD_{660} = 0.01$. Culture cell density at 660 nm wavelength was measured continuously for 24 h under agitation at 30˚C in a spectrophotometer (Biotek Synergy HT). Once cultures were growing in the exponential phase, data were plotted and duplication time was calculated.

Dot assays

Strains were grown in YPD medium overnight, diluted to $OD_{660nm} = 0.05$ and tenfold sequentially diluted in fresh YPD. Spotted in the appropriate plates were 5 μl of culture for incubation at the desired temperature for 24 h or 48 h.

Statistical analysis

Data were expressed as mean±standard error of the mean (mean±SEM). Statistical significance was determined using the Mann-Whitney U test. A p value of less than 0.05 was considered significant.

Supporting information

S1 Fig. Validation of the pooling strategy. A) The presence of the 3HA tag (obtained by *delitto perfetto*, then keeping the 3'UTR intact) does not significantly alter duplication time in any of the strains used. Cells were grown overnight in YPD at 30˚C, diluted to OD = 0.1 in fresh medium and incubated at 30˚C in a thermostated spectrophotometer under constant agitation. Optical density (wavelength 660nm) constantly measured for 420 min was used as a measure of cell density. Mean±SEM values for three independent experiments are shown. B) Number of cells, counted in a Newbauer chamber for four independent experiments, at indicated moments of the experiment (immediately after the O/N culture dilution, before α-factor addition for synchronization and at the moment of α-factor release). Values are expressed as mean±SEM for four independent experiments. C) Proportion of cells budding 35 min after α-factor release, reported as mean±SEM values for four independent experiments. D)

Comparison of western blot signals obtained from pooled and individually growing strains. Exponentially growing cultures were synchronized and release and aliquots were taken at the indicated times. E) Quantification of D). Note that, other than the fact that the amount of protein could be affected by using different blots, there was no difference in expression time of the cyclins depending on the pooling strategy.
(PDF)

S2 Fig. Cyclin amounts in different growing media. Representative western blot for the different mixes of cells growing in different culture media (YPD, SD and malt). Experiments were performed as described in Fig 2A and Fig 2B. Mean±SEM values quantify at least three independent experiments.
(PDF)

S3 Fig. Cyclin amounts in different growing media in heat-shock or high temperature conditions. Same procedure as for S2 Fig. In heat-shock conditions, cells were grown at 30˚C and then moved to 37˚C on α-factor release. In heat-stress conditions, cells were exponentially grown at 37˚C and temperature was kept constant after α-factor release. A representative western blot is depicted. The graphs show mean±SEM values for at least three independent experiments.
(PDF)

S4 Fig. Cyclin amounts in different stress conditions. Same procedure as for S2 Fig. Cells were subjected to different stresses on α-factor release: osmotic stress (0.4 M NaCl), reductive stress (100 mM N-acetyl cysteine), and oxidative stress (10 μM menadione). A representative western blot is depicted. The graphs show mean±SEM values for at least three independent experiments.
(PDF)

S5 Fig. Cyclin amounts after change to growing medium. Same procedure as for S2 Fig. Cells were grown in YPD and released from α-factor arrest into an SD medium. A representative western blot is depicted. The graphs show mean±SEM values quantifying at least three independent experiments.
(PDF)

S6 Fig. Cyclin amount after elutriation in normal lab conditions and upon heat shock. The noted strains were grown as described in methods section. Cells were synchronized by centrifugal elutriation. Time 0 corresponds to the moment of obtaining the cells form the elutriation device. After this moment, cells were incubated under agitation at 30˚C (upper panel) or 37˚C (lower panel). We took aliquots at the indicated times and processed them for western blot analysis as in the rest of the α-factor experiments.
(PDF)

Acknowledgments

We thank F. Storici for the *delitto perfetto* plasmids, F. Posas, H. Martín and J. Ayté for antibodies, M. Aldea for helpful discussion and F. Posas (and his team) for sharing the elutriator. We thank all the members of our group (S. Hernández-Ortega, O. Mirallas, L. Gasa, A. Sánchez, E. Quandt, and N. Massip) for day-by-day discussions, and Marta Pérez for technical assistance. This work was supported by funding from the Spanish Government (MINECO Grant Ref: BFU 2013-44189-P) to J Clotet. The funders had no role in study design, data collection or interpretation, or in the decision to submit the work for publication. The authors declare no conflict of interest. Ailish Maher edited the English in a version of the manuscript.

Author Contributions

Conceptualization: Javier Jiménez, Josep Clotet.

Funding acquisition: Josep Clotet.

Investigation: Elisabet Bállega, Reyes Carballar, Bàrbara Samper, Samuel Bru.

Project administration: Natalia Ricco.

Supervision: Mariana P. Ribeiro, Samuel Bru, Javier Jiménez, Josep Clotet.

Validation: Josep Clotet.

Writing – original draft: Javier Jiménez.

References

1. Nurse P, Bissett Y. Gene required in G1 for commitment to cell cycle and in G2 for control of mitosis in fission yeast. Nature. 1981. 292(5823): 558–560. https://doi.org/10.1038/292558a0 PMID: 7254352
2. Reed SI, Hadwiger JA, Lorincz AT. Protein kinase activity associated with the product of the yeast cell division cycle gene CDC28. Proc Natl Acad Sci U S A. 1985. 82(12): 4055–4059. https://doi.org/10.1073/pnas.82.12.4055 PMID: 3889921
3. Reed SI, Wittenberg C. Mitotic role for the Cdc28 protein kinase of *Saccharomyces cerevisiae*. Proc Natl Acad Sci U S A. 1990. 87(15): 5697–5701. https://doi.org/10.1073/pnas.87.15.5697 PMID: 2165600
4. Nurse P. Universal control mechanism regulating onset of M-phase. Nature. 1990. 344(6266): 503–508. https://doi.org/10.1038/344503a0 PMID: 2138713
5. Morgan DO. Principles of CDK regulation. Nature. 1995. 374(6518): 131–134. https://doi.org/10.1038/374131a0 PMID: 7877684
6. Liu J, Kipreos ET. Evolution of cyclin-dependent kinases (CDKs) and CDK-activating kinases (CAKs): Differential conservation of CAKs in yeast and metazoa. Mol Biol Evol. 2000. 17(7): 1061–1074. https://doi.org/10.1093/oxfordjournals.molbev.a026387 PMID: 10889219
7. Evans T, Rosenthal ET, Youngblom J, Distel D, Hunt T. Cyclin: A protein specified by maternal mRNA in sea urchin eggs that is destroyed at each cleavage division. Cell. 1983. 33(2): 389–396. 0092-8674(83)90420-8. PMID: 6134587
8. Pines J, Hunt T. Molecular cloning and characterization of the mRNA for cyclin from sea urchin eggs. Embo J. 1987. 6(10): 2987–2995. PMID: 2826125
9. Standart N, Minshull J, Pines J, Hunt T. Cyclin synthesis, modification and destruction during meiotic maturation of the starfish oocyte. Dev Biol. 1987. 124(1): 248–258. 0012-1606(87)90476-3. PMID: 15669148
10. Swenson KI, Farrell KM, Ruderman JV. The clam embryo protein cyclin A induces entry into M phase and the resumption of meiosis in *Xenopus* oocytes. Cell. 1986. 47(6): 861–870. 0092-8674(86)90801-9. PMID: 2946420
11. Mendenhall MD, Hodge AE. Regulation of Cdc28 cyclin-dependent protein kinase activity during the cell cycle of the yeast *Saccharomyces cerevisiae*. Microbiol Mol Biol Rev. 1998. 62(4): 1191–1243. PMID: 9841670
12. de Bruin RA, Kalashnikova TI, Wittenberg C. Stb1 collaborates with other regulators to modulate the G1-specific transcriptional circuit. Mol Cell Biol. 2008. 28(22): 6919–6928. https://doi.org/10.1128/MCB.00211-08 PMID: 18794370
13. Bertoli C, Skotheim JM, de Bruin RA. Control of cell cycle transcription during G1 and S phases. Nat Rev Mol Cell Biol. 2013. 14(8): 518–528. https://doi.org/10.1038/nrm3629 PMID: 23877564
14. Quilis I, Igual JC. Molecular basis of the functional distinction between Cln1 and Cln2 cyclins. Cell Cycle. 2012. 11(16): 3117–3131. https://doi.org/10.4161/cc.21505 PMID: 22889732
15. Andrews B, Measday V. The cyclin family of budding yeast: Abundant use of a good idea. Trends Genet. 1998. 14(2): 66–72. PMID: 9520600
16. Stern B, Nurse P. A quantitative model for the cdc2 control of S phase and mitosis in fission yeast. Trends Genet. 1996. 12(9): 345–350. S0168-9525(96)80016-3. PMID: 8855663

17. Swaffer MP, Jones AW, Flynn HR, Snijders AP, Nurse P. CDK substrate phosphorylation and ordering the cell cycle. Cell. 2016. 167(7): 1750–1761.e16. S0092-8674(16)31606-3. https://doi.org/10.1016/j.cell.2016.11.034 PMID: 27984725
18. Coudreuse D, Nurse P. Driving the cell cycle with a minimal CDK control network. Nature. 2010. 468 (7327): 1074–1079. https://doi.org/10.1038/nature09543 PMID: 21179163
19. Uhlmann F, Bouchoux C, Lopez-Aviles S. A quantitative model for cyclin-dependent kinase control of the cell cycle: Revisited. Philos Trans R Soc Lond B Biol Sci. 2011. 366(1584): 3572–3583. https://doi.org/10.1098/rstb.2011.0082 PMID: 22084384
20. Hadwiger JA, Wittenberg C, Richardson HE, de Barros Lopes M, Reed SI. A family of cyclin homologs that control the G1 phase in yeast. Proc Natl Acad Sci U S A. 1989. 86(16): 6255–6259. https://doi.org/10.1073/pnas.86.16.6255 PMID: 2569741
21. Wittenberg C, Sugimoto K, Reed SI. G1-specific cyclins of *S. cerevisiae*: Cell cycle periodicity, regulation by mating pheromone, and association with the p34CDC28 protein kinase. Cell. 1990. 62(2): 225–237. 0092-8674(90)90361-H. PMID: 2142620
22. Schwob E, Nasmyth K. CLB5 and CLB6, a new pair of B cyclins involved in DNA replication in *Saccharomyces cerevisiae*. Genes Dev. 1993. 7(7A): 1160–1175. https://doi.org/10.1101/gad.7.7a.1160 PMID: 8319908
23. Epstein CB, Cross FR. CLB5: A novel B cyclin from budding yeast with a role in S phase. Genes Dev. 1992. 6(9): 1695–1706. https://doi.org/10.1101/gad.6.9.1695 PMID: 1387626
24. Surana U, Robitsch H, Price C, Schuster T, Fitch I, Futcher AB, et al. The role of CDC28 and cyclins during mitosis in the budding yeast *S. cerevisiae*. Cell. 1991. 65(1): 145–161. 0092-8674(91)90416-V. PMID: 1849457
25. Pines J, Hunter T. Isolation of a human cyclin cDNA: Evidence for cyclin mRNA and protein regulation in the cell cycle and for interaction with p34cdc2. Cell. 1989. 58(5): 833–846. 0092-8674(89)90936-7. PMID: 2570636
26. Measday V, Moore L, Retnakaran R, Lee J, Donoviel M, Neiman AM, et al. A family of cyclin-like proteins that interact with the Pho85 cyclin-dependent kinase. Mol Cell Biol. 1997. 17(3): 1212–1223. https://doi.org/10.1128/mcb.17.3.1212 PMID: 9032248
27. Malumbres M, Barbacid M. Mammalian cyclin-dependent kinases. Trends Biochem Sci. 2005. 30(11): 630–641. S0968-0004(05)00276-8. https://doi.org/10.1016/j.tibs.2005.09.005 PMID: 16236519
28. Huang D, Friesen H, Andrews B. Pho85, a multifunctional cyclin-dependent protein kinase in budding yeast. Mol Microbiol. 2007. 66(2): 303–314. https://doi.org/10.1111/j.1365-2958.2007.05914.x PMID: 17850263
29. Jimenez J, Ricco N, Grijota-Martinez C, Fado R, Clotet J. Redundancy or specificity? the role of the CDK Pho85 in cell cycle control. Int J Biochem Mol Biol. 2013. 4(3): 140–149. PMID: 24049669
30. Malumbres M. Physiological relevance of cell cycle kinases. Physiol Rev. 2011. 91(3): 973–1007. https://doi.org/10.1152/physrev.00025.2010 PMID: 21742793
31. Malumbres M BM. Cell cycle, CDKs and cancer: A changing paradigm. Nat Rev Cancer. 2009. 9(3): 153–66. https://doi.org/10.1038/nrc2602 PMID: 19238148
32. Doonan JH, Kitsios G. Functional evolution of cyclin-dependent kinases. Mol Biotechnol. 2009. 42(1): 14–29. https://doi.org/10.1007/s12033-008-9126-8 PMID: 19145493
33. Tyers M, Tokiwa G, Futcher B. Comparison of the *Saccharomyces cerevisiae* G1 cyclins: Cln3 may be an upstream activator of Cln1, Cln2 and other cyclins. Embo J. 1993. 12(5): 1955–1968. PMID: 8387915
34. Cross FR, Archambault V, Miller M, Klovstad M. Testing a mathematical model of the yeast cell cycle. Mol Biol Cell. 2002. 13(1): 52–70. https://doi.org/10.1091/mbc.01-05-0265 PMID: 11809822
35. Jackson RJ. Cytoplasmic regulation of mRNA function: The importance of the 3' untranslated region. Cell. 1993. 74(1): 9–14. 0092-8674(93)90290-7. PMID: 7687524
36. Matoulkova E, Michalova E, Vojtesek B, Hrstka R. The role of the 3' untranslated region in post-transcriptional regulation of protein expression in mammalian cells. RNA Biol. 2012. 9(5): 563–576. https://doi.org/10.4161/rna.20231 PMID: 22614827
37. Tuller T, Ruppin E, Kupiec M. Properties of untranslated regions of the *S. cerevisiae* genome. BMC Genomics. 2009. 10: 391-2164-10-391. https://doi.org/10.1186/1471-2164-10-391 PMID: 19698117
38. Geissler R, Grimson A. A position-specific 3'UTR sequence that accelerates mRNA decay. RNA Biol. 2016. 13(11): 1075–1077. https://doi.org/10.1080/15476286.2016.1225645 PMID: 27565004
39. Storici F, Lewis LK, Resnick MA. In vivo site-directed mutagenesis using oligonucleotides. Nat Biotechnol. 2001. 19(8): 773–776. https://doi.org/10.1038/90837 PMID: 11479573

40. Saiz-Baggetto S, Mendez E, Quilis I, Igual JC, Bano MC. Chimeric proteins tagged with specific 3xHA cassettes may present instability and functional problems. PLoS One. 2017. 12(8): e0183067. https://doi.org/10.1371/journal.pone.0183067 PMID: 28800621

41. Longtine MS, McKenzie A,3rd, Demarini DJ, Shah NG, Wach A, Brachat A, et al. Additional modules for versatile and economical PCR-based gene deletion and modification in *Saccharomyces cerevisiae*. Yeast. 1998. 14(10): 953–961. https://doi.org/10.1002/(SICI)1097-0061(199807)14:10<953::AID-YEA293>3.0.CO;2-U PMID: 9717241

42. Janke C, Magiera MM, Rathfelder N, Taxis C, Reber S, Maekawa H, et al. A versatile toolbox for PCR-based tagging of yeast genes: New fluorescent proteins, more markers and promoter substitution cassettes. Yeast. 2004. 21(11): 947–962. https://doi.org/10.1002/yea.1142 PMID: 15334558

43. Tarn WY, Lai MC. Translational control of cyclins. Cell Div. 2011. 6(1): 5-1028-6-5. https://doi.org/10.1186/1747-1028-6-5 PMID: 21314915

44. Thorburn RR, Gonzalez C, Brar GA, Christen S, Carlile TM, Ingolia NT, et al. Aneuploid yeast strains exhibit defects in cell growth and passage through START. Mol Biol Cell. 2013. 24(9): 1274–1289. https://doi.org/10.1091/mbc.E12-07-0520 PMID: 23468524

45. Zapata J, Dephoure N, Macdonough T, Yu Y, Parnell EJ, Mooring M, et al. PP2ARts1 is a master regulator of pathways that control cell size. J Cell Biol. 2014. 204(3): 359–376. https://doi.org/10.1083/jcb.201309119 PMID: 24493588

46. Quilis I, Igual JC. A comparative study of the degradation of yeast cyclins Cln1 and Cln2. FEBS Open Bio. 2016. 7(1): 74–87. https://doi.org/10.1002/2211-5463.12157 PMID: 28097090

47. Ball DA, Marchand J, Poulet M, Baumann WT, Chen KC, Tyson JJ, et al. Oscillatory dynamics of cell cycle proteins in single yeast cells analyzed by imaging cytometry. PLoS One. 2011. 6(10): e26272. https://doi.org/10.1371/journal.pone.0026272 PMID: 22046265

48. Gonzalez-Novo A, Jimenez J, Clotet J, Nadal-Ribelles M, Cavero S, de Nadal E, et al. Hog1 targets Whi5 and Msa1 transcription factors to downregulate cyclin expression upon stress. Mol Cell Biol. 2015. 35(9): 1606–1618. https://doi.org/10.1128/MCB.01279-14 PMID: 25733686

49. Flick K, Chapman-Shimshoni D, Stuart D, Guaderrama M, Wittenberg C. Regulation of cell size by glucose is exerted via repression of the CLN1 promoter. Mol Cell Biol. 1998. 18(5): 2492–2501. https://doi.org/10.1128/mcb.18.5.2492 PMID: 9566870

50. Li X, Cai M. Recovery of the yeast cell cycle from heat shock-induced G(1) arrest involves a positive regulation of G(1) cyclin expression by the S phase cyclin Clb5. J Biol Chem. 1999. 274(34): 24220–24231. https://doi.org/10.1074/jbc.274.34.24220 PMID: 10446197

51. Sambuk EV, Popova I, Fizikova AI, Padkina MV. Genetic analysis of pleiotropic effects of pho85 mutations in yeast *Saccharomyces cerevisiae*. Genetika. 2003. 39(8): 1039–1045. PMID: 14515459

52. Sambuk EV, Fizikova AY, Savinov VA, Padkina MV. Acid phosphatases of budding yeast as a model of choice for transcription regulation research. Enzyme Res. 2011. 2011: 356093. https://doi.org/10.4061/2011/356093 PMID: 21785706

53. Spellman PT, Sherlock G, Zhang MQ, Iyer VR, Anders K, Eisen MB, et al. Comprehensive identification of cell cycle-regulated genes of the yeast *Saccharomyces cerevisiae* by microarray hybridization. Mol Biol Cell. 1998. 9(12): 3273–3297. https://doi.org/10.1091/mbc.9.12.3273 PMID: 9843569

54. Ghaemmaghami S, Huh WK, Bower K, Howson RW, Belle A, Dephoure N, et al. Global analysis of protein expression in yeast. Nature. 2003. 425(6959): 737–741. https://doi.org/10.1038/nature02046 PMID: 14562106

55. Horak CE, Snyder M. Global analysis of gene expression in yeast. Funct Integr Genomics. 2002. 2(4–5): 171–180. https://doi.org/10.1007/s10142-002-0065-3 PMID: 12192590

56. Ho B, Baryshnikova A, Brown GW. Unification of protein abundance datasets yields a quantitative *Saccharomyces cerevisiae* proteome. Cell Syst. 2018. S2405-4712(17)30546-X.

57. Flory MR, Lee H, Bonneau R, Mallick P, Serikawa K, Morris DR, et al. Quantitative proteomic analysis of the budding yeast cell cycle using acid-cleavable isotope-coded affinity tag reagents. Proteomics. 2006. 6(23): 6146–6157. https://doi.org/10.1002/pmic.200600159 PMID: 17133367

58. Zubarev RA. The challenge of the proteome dynamic range and its implications for in-depth proteomics. Proteomics. 2013. 13(5): 723–726. https://doi.org/10.1002/pmic.201200451 PMID: 23307342

59. Field J, Nikawa J, Broek D, MacDonald B, Rodgers L, Wilson IA, et al. Purification of a RAS-responsive adenylyl cyclase complex from *Saccharomyces cerevisiae* by use of an epitope addition method. Mol Cell Biol. 1988. 8(5): 2159–2165. https://doi.org/10.1128/mcb.8.5.2159 PMID: 2455217

60. Kuersten S, Goodwin EB. The power of the 3' UTR: Translational control and development. Nat Rev Genet. 2003. 4(8): 626–637. https://doi.org/10.1038/nrg1125 PMID: 12897774

61. Andreassi C, Riccio A. To localize or not to localize: mRNA fate is in 3'UTR ends. Trends Cell Biol. 2009. 19(9): 465–474. https://doi.org/10.1016/j.tcb.2009.06.001 PMID: 19716303

62. Deshpande A, Pastore A, Deshpande AJ, Zimmermann Y, Hutter G, Weinkauf M, et al. 3'UTR mediated regulation of the cyclin D1 proto-oncogene. Cell Cycle. 2009. 8(21): 3592–3600. https://doi.org/10.4161/cc.8.21.9993 PMID: 19823025

63. Schnerch D, Follo M, Felthaus J, Engelhardt M, Wasch R. The 3' untranslated region of the cyclin B mRNA is not sufficient to enhance the synthesis of cyclin B during a mitotic block in human cells. PLoS One. 2013. 8(9): e74379. https://doi.org/10.1371/journal.pone.0074379 PMID: 24058555

64. Slotta-Huspenina J, Koch I, Richter M, Bink K, Kremer M, Specht K, et al. Cyclin D1 positive multiple myeloma: Predominance of the short, 3'UTR-deficient transcript is associated with high cyclin D1 mRNA levels in cases with t(11;14) translocation, but does not correlate with proliferation rate or genomic deletions. Leuk Res. 2008. 32(1): 79–88. S0145-2126(07)00240-8. https://doi.org/10.1016/j.leukres.2007.05.021 PMID: 17629555

65. Radford HE, Meijer HA, de Moor CH. Translational control by cytoplasmic polyadenylation in *Xenopus* oocytes. Biochim Biophys Acta. 2008. 1779(4): 217–229. https://doi.org/10.1016/j.bbagrm.2008.02.002 PMID: 18316045

66. Slevin MK, Gourronc F, Hartley RS. ElrA binding to the 3'UTR of cyclin E1 mRNA requires polyadenylation elements. Nucleic Acids Res. 2007. 35(7): 2167–2176. gkm084. https://doi.org/10.1093/nar/gkm084 PMID: 17355986

67. Juanes MA. Methods of synchronization of yeast cells for the analysis of cell cycle progression. Methods Mol Biol. 2017. 1505: 19–34. https://doi.org/10.1007/978-1-4939-6502-1_2 PMID: 27826853

68. Rosebrock AP. Methods for synchronization and analysis of the budding yeast cell cycle. Cold Spring Harb Protoc. 2017. 2017(1): pdb.top080630. https://doi.org/10.1101/pdb.top080630 PMID: 28049810

69. Barberis M, Klipp E, Vanoni M, Alberghina L. Cell size at S phase initiation: An emergent property of the G1/S network. PLoS Comput Biol. 2007. 3(4): e64. 06-PLCB-RA-0291R4. https://doi.org/10.1371/journal.pcbi.0030064 PMID: 17432928

70. Adrover MA, Zi Z, Duch A, Schaber J, Gonzalez-Novo A, Jimenez J, et al. Time-dependent quantitative multicomponent control of the G(1)-S network by the stress-activated protein kinase Hog1 upon osmostress. Sci Signal. 2011. 4(192): ra63. https://doi.org/10.1126/scisignal.2002204 PMID: 21954289

71. Charvin G, Oikonomou C, Siggia ED, Cross FR. Origin of irreversibility of cell cycle start in budding yeast. PLoS Biol. 2010. 8(1): e1000284. https://doi.org/10.1371/journal.pbio.1000284 PMID: 20087409

72. Doncic A, Falleur-Fettig M, Skotheim JM. Distinct interactions select and maintain a specific cell fate. Mol Cell. 2011. 43(4): 528–539. https://doi.org/10.1016/j.molcel.2011.06.025 PMID: 21855793

73. Cross FR, Tinkelenberg AH. A potential positive feedback loop controlling CLN1 and CLN2 gene expression at the start of the yeast cell cycle. Cell. 1991. 65(5): 875–883. 0092-8674(91)90394-E. PMID: 2040016

74. Lew DJ, Reed SI. Morphogenesis in the yeast cell cycle: Regulation by Cdc28 and cyclins. J Cell Biol. 1993. 120(6): 1305–1320. https://doi.org/10.1083/jcb.120.6.1305 PMID: 8449978

75. Benton BK, Tinkelenberg AH, Jean D, Plump SD, Cross FR. Genetic analysis of cln/Cdc28 regulation of cell morphogenesis in budding yeast. Embo J. 1993. 12(13): 5267–5275. PMID: 8262069

76. Cross FR. Starting the cell cycle: What's the point? Curr Opin Cell Biol. 1995. 7(6): 790–797. 0955-0674(95)80062-X. PMID: 8608009

77. Levine K, Huang K, Cross FR. *Saccharomyces cerevisiae* G1 cyclins differ in their intrinsic functional specificities. Mol Cell Biol. 1996. 16(12): 6794–6803. https://doi.org/10.1128/mcb.16.12.6794 PMID: 8943334

78. Hydbring P, Malumbres M, Sicinski P. Non-canonical functions of cell cycle cyclins and cyclin-dependent kinases. Nat Rev Mol Cell Biol. 2016. 17(5): 280–292. https://doi.org/10.1038/nrm.2016.27 PMID: 27033256

79. Sikorski RS, Hieter P. A system of shuttle vectors and yeast host strains designed for efficient manipulation of DNA in *Saccharomyces cerevisiae*. Genetics. 1989. 122(1): 19–27. PMID: 2659436

80. Lee KS, Irie K, Gotoh Y, Watanabe Y, Araki H, Nishida E, et al. A yeast mitogen-activated protein kinase homolog (Mpk1p) mediates signalling by protein kinase C. Mol Cell Biol. 1993. 13(5): 3067–3075. https://doi.org/10.1128/mcb.13.5.3067 PMID: 8386319

81. Popolo L, Vai M, Gatti E, Porello S, Bonfante P, Balestrini R, et al. Physiological analysis of mutants indicates involvement of the *Saccharomyces cerevisiae* GPI-anchored protein gp115 in morphogenesis and cell separation. J Bacteriol. 1993. 175(7): 1879–1885. https://doi.org/10.1128/jb.175.7.1879-1885.1993 PMID: 8458831

82. Popolo L, Alberghina L. Identification of a labile protein involved in the G1-to-S transition in *Saccharomyces cerevisiae*. Proc Natl Acad Sci U S A. 1984. 81(1): 120–124. https://doi.org/10.1073/pnas.81.1.120 PMID: 6364132

83. Popolo L, Cavadini P, Vai M, Alberghina L. Transcript accumulation of the GGP1 gene, encoding a yeast GPI-anchored glycoprotein, is inhibited during arrest in the G1 phase and during sporulation. Curr Genet. 1993. 24(5): 382–387. PMID: 8299152

84. Sinha H, David L, Pascon RC, Clauder-Munster S, Krishnakumar S, Nguyen M, et al. Sequential elimination of major-effect contributors identifies additional quantitative trait loci conditioning high-temperature growth in yeast. Genetics. 2008. 180(3): 1661–1670. https://doi.org/10.1534/genetics.108.092932 PMID: 18780730

85. Auesukaree C, Damnernsawad A, Kruatrachue M, Pokethitiyook P, Boonchird C, Kaneko Y, et al. Genome-wide identification of genes involved in tolerance to various environmental stresses in *Saccharomyces cerevisiae*. J Appl Genet. 2009. 50(3): 301–310. https://doi.org/10.1007/BF03195688 PMID: 19638689

86. Ruiz-Roig C, Vieitez C, Posas F, de Nadal E. The Rpd3L HDAC complex is essential for the heat stress response in yeast. Mol Microbiol. 2010. 76(4): 1049–1062. https://doi.org/10.1111/j.1365-2958.2010.07167.x PMID: 20398213

87. Johnson A, Skotheim JM. Start and the restriction point. Curr Opin Cell Biol. 2013. 25(6): 717–723. https://doi.org/10.1016/j.ceb.2013.07.010 PMID: 23916770

88. Brachmann CB, Davies A, Cost GJ, Caputo E, Li J, Hieter P, et al. Designer deletion strains derived from *Saccharomyces cerevisiae* S288C: A useful set of strains and plasmids for PCR-mediated gene disruption and other applications. Yeast. 1998. 14(2): 115–132. https://doi.org/10.1002/(SICI)1097-0061(19980130)14:2<115::AID-YEA204>3.0.CO;2-2 PMID: 9483801

89. Thomas BJ, Rothstein R. Elevated recombination rates in transcriptionally active DNA. Cell. 1989. 56 (4): 619–630. 0092-8674(89)90584-9. PMID: 2645056

90. Wach A, Brachat A, Pohlmann R, Philippsen P. New heterologous modules for classical or PCR-based gene disruptions in *Saccharomyces cerevisiae*. Yeast. 1994. 10(13): 1793–1808. PMID: 7747518

91. Wach A, Brachat A, Alberti-Segui C, Rebischung C, Philippsen P. Heterologous HIS3 marker and GFP reporter modules for PCR-targeting in *Saccharomyces cerevisiae*. Yeast. 1997. 13(11): 1065–1075. https://doi.org/10.1002/(SICI)1097-0061(19970915)13:11<1065::AID-YEA159>3.0.CO;2-K PMID: 9290211

92. Haase SB, Reed SI. Improved flow cytometric analysis of the budding yeast cell cycle. Cell Cycle. 2002. 1(2): 132–136. PMID: 12429922

93. Yaakov G, Duch A, Garcia-Rubio M, Clotet J, Jimenez J, Aguilera A, et al. The stress-activated protein kinase Hog1 mediates S phase delay in response to osmostress. Mol Biol Cell. 2009. 20(15): 3572–3582. https://doi.org/10.1091/mbc.E09-02-0129 PMID: 19477922

94. Gordon CN, Elliott SC. Fractionation of *Saccharomyces cerevisiae* cell populations by centrifugal elutriation. J Bacteriol. 1977. 129(1): 97–100. PMID: 318655

Microbiological Research 206 (2018) 168–176

Contents lists available at ScienceDirect

Microbiological Research

journal homepage: www.elsevier.com/locate/micres

Intertwined control of the cell cycle and nucleocytoplasmic transport by the cyclin-dependent kinase Pho85 and RanGTPase Gsp1 in *Saccharomyces cerevisiae*

Oriol Mirallas, Elisabet Ballega, Bàrbara Samper-Martín, Sergio García-Márquez, Reyes Carballar, Natalia Ricco, Javier Jiménez*, Josep Clotet*

Department of Basic Sciences, Faculty of Medicine and Health Sciences, Universitat Internacional de Catalunya, Barcelona, Spain

ARTICLE INFO

Keywords:
Cell cycle
Pho85
Gsp1
RAN-GTP
Saccharomyces cerevisiae

ABSTRACT

Deciphering the molecular mechanisms that connect cell cycle progression and nucleocytoplasmic transport is of particular interest: this intertwined relationship, once understood, may provide useful insight on the diseases resulting from the malfunction of these processes. In the present study we report on findings that indicate a biochemical connection between the cell cycle regulator CDK Pho85 and Ran-GTPase Gsp1, an essential nucleocytoplasmic transport component. When Gsp1 cannot be phosphorylated by Pho85, the cell cycle progression is impaired. Accordingly, a nonphosphorylatable version of Gsp1 abnormally localizes to the nucleus, which impairs the nuclear transport of molecules, including key components of cell cycle progression. Furthermore, our results suggest that the physical interaction of Gsp1 and the Kap95 karyopherin, essential to the release of nuclear cargoes, is altered. Altogether, the present findings point to the involvement of a biochemical mechanism in the interlocked regulation of the cell cycle and nuclear transport.

1. Introduction

In all eukaryotic cells, the nucleocytoplasmic transport of proteins greater than ~40 kDa is an energy-dependent process requiring the participation of a very complex group of proteins governed by Ran-GTPase (Nachury and Weis, 1999), which cycles between GTP-bound and GDP-bound states (Pemberton and Paschal, 2005). Besides Ran-GTPase, the nucleocytoplasmic traffic is supported by a family of proteins generally known as karyopherins (Radu et al., 1995) that includes importins (α and β) (Gorlich et al., 1994) and exportins (Stade et al., 1997), as well as many adaptors and helping proteins (Chook and Blobel, 2001; Chook and Suel, 2011; Conti and Izaurralde, 2001; Conti et al., 2006; Gorlich and Kutay, 1999; Madrid and Weis, 2006; Mosammaparast and Pemberton, 2004; Pemberton and Paschal, 2005; Stewart, 2007) as briefly described below.

In the import process, the importin-β-family of proteins—Kap95 being the most relevant, although others are found in *Saccharomyces cerevisiae*—specifically recognizes and binds itself to nuclear localization signals (NLSs) present in the cargoes to be imported (Kalderon et al., 1984; Lange et al., 2007). Helped by importin-α (Srp1 in *S. cerevisiae*), importin-β proteins carry NLS-containing proteins through the nuclear pore complex into the nucleus. Once in the nucleus, they bind with Ran-GTPase (Gsp1 in *S. cerevisiae*) in GTP form and destabilize the importin-cargo complex, releasing the cargo into the nucleus (Pemberton and Paschal, 2005; Stewart, 2007). In the export process, the exportin (Xpo1 in *S. cerevisiae*) forming a complex with the Ran-GTPase in its GTP form, binds to the nuclear export signal (NES) present in the cargoes to be exported (Chook and Suel, 2011), and this process is aided by adaptor proteins (Yrb2 in *S. cerevisiae*). The complex goes through the nuclear pore complex into the cytoplasm, where Ran-GTPase changes into its GDP form to allow for cargo release (Weis, 2003), a process that is also helped by other proteins such as Yrb1 (Oki and Nishimoto, 2000) and Mog1 (Oki and Nishimoto, 1998).

As mentioned above, the keystone in nucleocytoplasmic transport relays on the GTP/GDP cycle of the Ran-GTPase, a cycle that is catalysed by the nuclear GEF (GTP Exchanging Factor) Prp20 (also known as Srm1) in *S. cerevisiae* (Akhtar et al., 2001; Vijayraghavan et al., 1989) and the cytoplasmic GAP (GTPase Activating Protein) Rna1 in *S. cerevisiae* (Becker et al., 1995). In *S. cerevisiae*, Ran-GTPase Gsp1 is an essential protein with a paralog, Gsp2 which is very little expressed (Belhumeur et al., 1993). The overexpression of Gsp1 has a pleiotropic phenotype: abnormal cell cycle progression in G_1 (Stevenson et al., 2001), altered chromosome stability (Ouspenski et al., 1999), decreased telomeric silencing (Clement et al., 2006), and decreased vegetative

---

* Corresponding author at: Universitat Internacional de Catalunya, Avda. Dr. Trueta S/N, 08195, Sant Cugat del Vallès, Barcelona, Spain.
E-mail addresses: jjimenez@uic.es (J. Jiménez), jclotet@uic.cat (J. Clotet).

http://dx.doi.org/10.1016/j.micres.2017.10.008
Received 19 July 2017; Received in revised form 9 October 2017; Accepted 17 October 2017
Available online 26 October 2017
0944-5013/ © 2017 Elsevier GmbH. All rights reserved.

Table 1
Yeast strains used in this study.

Strain	Background	Genotype	Source
W303-1a	W303-1a	MATa leu2-3,112 trp1-1 can1-100 ura3-1 ade2-1 his3-11,15	(Thomas and Rothstein, 1989)
YJJ1091	W303-1a	GSP1-wt-KanMX, gsp2Δ:LEU2	This Study
YJJ1092	W303-1a	gsp1-S181A-KanMX, gsp2Δ:LEU2	This Study
YEB145	W303-1a	GSP1-wt-KanMX, WHI51-eGFP-HIS3	This Study
YEB146	W303-1a	gsp1-S181A-KanMX, WHI5-eGFP-HIS3	This Study
YEB147	W303-1a	GSP1-wt-KanMX, MBP1-eGFP-HIS3	This Study
YEB148	W303-1a	gsp1-S181A-KanMX, MBP1-eGFP-HIS3	This Study
YJJ1081	W303-1a	GSP1-wt-KanMX, MIG1-eGFP-HIS3	This Study
YJJ1082	W303-1a	gsp1-S181A-KanMX, MIG1-eGFP-HIS3	This Study
YJJ1117	W303-1a	NAT pADH-yeGFP GSP1-wt-KanMX	This Study
YJJ1118	W303-1a	NAT pADH-yeGFP gsp1-S181A KanMX	This Study
YEB159	W303-1a	GSP1-wt-KanMX, gsp2Δ:LEU2, PHO85-eGFP	This Study
YEB160	W303-1a	gsp1-S181A- KanMX, gsp2Δ:LEU2, PHO85-eGFP	This Study

growth (Sopko et al., 2006).

From a structural point of view, several components of the transport machinery have been well characterized, including crystal structures of the Ran-GTPase, karyopherins, and other components of the complex, information that is essential to understanding the steric changes that allow the assembling and disassembling of different import and export complexes (Forwood et al., 2010; Lee et al., 2005; Stewart, 2007).

The transport of molecules to and from the nucleus has been shown to correlate with cell cycle progression machinery. Cell cycle repressors, such as Whi5, are excluded from the nucleus at the appropriate time point (Costanzo et al., 2004; Taberner et al., 2009), checkpoint protein localization is regulated (Kobayashi and Matsuura, 2013), and cell cycle activators are introduced so that the cycle may proceed (e.g. Mbp1, Swi4, and Sw6) (Koch et al., 1993). Phosphorylation of consensus sites around NLS signals have been shown to modulate the activity of the NLS in question. CDK-dependent phosphorylation of NLS confers cell cycle-dependent nucleocytoplasmic shuttling of proteins such as Swi5, Swi6, and Mcm3 (Kosugi et al., 2009). Taken together, these findings provide evidence that cell cycle machinery has a certain level of control over the nucleocytoplasmic traffic of molecules.

Cell cycle machinery is mastered by a family of cyclin-dependent kinases (CDKs) (Nurse and Bissett, 1981; Nurse, 1990; Reed et al., 1985; Reed and Wittenberg, 1990) (for a more recent review see (Malumbres, 2014)), enzymes that contain a serine/threonine-specific catalytic core and carry out activity that is modulated by their interaction with oscillatory regulatory subunits known as cyclins (Evans et al., 1983; Pines and Hunt, 1987; Standart et al., 1987; Swenson et al., 1986). Several models have been proposed to explain how CDKs control the cell cycle (Coudreuse and Nurse, 2010; Stern and Nurse, 1996; Swaffer et al., 2016), but the most accepted is based on the different substrate specificities of the CDK, which are determined by the cyclin the CDK interacts with (Andrews and Measday, 1998; Jimenez et al., 2013a). It is also important to note that these proteins fine-tune a multitude of biological pathways through phosphorylation (Hydbring et al., 2016).

The yeast *S. cerevisiae* has 2 CDKs that control cell cycle events: the essential CDK Cdc28, which is believed to be responsible for the major processes in cell cycle progression, and the relatively superfluous CDK Pho85, which has been described as playing essential roles under specific environmental conditions (Jimenez et al., 2013a) and fine-tuning many different processes during the normal cell cycle (Huang et al., 2007). To understand the nuances of cell cycle regulation, our group has focused on the role of Pho85 in cellular processes that, in one way or another, must correlate with cell cycle progression.

Pho85 essentially plays 2 types of roles depending on the family of cyclins that are attached to it (Huang et al., 2007). When attached to Pho80 family cyclins, Pho85 controls phosphate metabolism (Lee et al., 2008) and as a consequence cell cycle (Truman et al., 2012; Menoyo et al., 2013; Jimenez et al., 2013b). When it binds cyclins from the Pcl1,2 family, meanwhile, it is involved in cell cycle control (Espinoza et al., 1994; Huang et al., 2007; Schneider et al., 1994).

In the present work, we report on findings related to the relationship between cell cycle control and nucleocytoplasmic transport. We will show that Pho85-Pcl1, but not Pho85-Pho80, is able to phosphorylate, at least in vitro, Ran-GTPase Gsp1 at Ser181. The nonphosphorylatable *gsp1* mutant shows a reduced nuclear intensity, as do some of the nuclear cargoes, and the interaction with the karyopherin Kap95 appears to be clearly impaired. Phenotypically, cells bearing the nonphosphorylatable version of *gsp1* show impaired cell cycle progression, which compromises its behaviour in culture.

2. Materials and methods

2.1. Yeast strains and growth conditions

Yeast cells were grown in either rich yeast peptone dextrose (YPD) medium (1% yeast extract, 2% peptone, and 2% glucose) or complete synthetic dextrose (SD) medium (0.67% yeast nitrogen base and 2% glucose) containing the auxotrophic amino acid requirements (76 mg/l except for leucine and adenine, which are present at 380 mg/l and 150 mg/l, respectively).

The yeast strains and plasmids used in the present study are listed in Tables 1 and 2, respectively. All gene modifications in yeast were achieved by homologous recombination at the chromosomal loci using the toolbox system (Janke et al., 2004), with the exception of *gsp2:LEU2*, in which the YDp plasmid system was used (Berben et al., 1991). All constructed strains were verified by PCR, and the tagged strains were additionally confirmed by Western blot analysis.

2.2. Genomic site-directed mutation of GSP1

We designed a PCR-based system for genomic site-directed mutation

Table 2
Plasmids used in this study.

Name	Relevant characteristics	Source
pJC1159	pGEX6P1-empty	This Study
pJC1168	pGEX6P1-*PHO85* (Cloned in *Bam*HI)	This Study
pJC1177	pGEX6P1-*PCL1* (Cloned in *Bam*HI)	This Study
pJC1406	pGEX6P1-*GSP1* (Cloned between *Bam*HI and *Eco*RI)	This Study
pJC1407	pGEX6P1-*gsp1*-S181A (Cloned between *Bam*HI and *Eco*RI)	This Study
pJC1974	pRSETA-*KAP95* (Cloned between *Bam*HI and *Eco*RI)	This Study
pJC2007	pRSETA-*YRB1* (Cloned between *Bam*HI and *Eco*RI)	This Study
pFT043	pRS416-NLS-4GFP	(Fernandez-Cid et al., 2012b)

Table 3
Oligonucleotides used for the genomic site-directed mutation of *GSP1* underlined are the mutation. In upper case, sequence corresponding to the *GSP1* locus. In lower case, KanMX gene from pYM14 toolbox plasmid.

Name	Sequence 5′-3′
F1wt	CAGAAAATTGGCTGGTAACCCACAATTAGAATTTGTTGCTTCTCCAGCTT
F1A	CAGAAAATTGGCTGGTAACCCACAATTAGAATTTGTTGCTGCTCCAGCTT
R1	cccggcggggacgaggcaagctTTAGACAAGCCAAATACGTT
F2	AACGTATTTGGCTTGTCTAAagcttgcctcgtccccgccggg
R2	GCTTGCTTTGGTATGCCTTTAACGCAAGTTGAAGGAGACGaaactggatggcggcgttag

of serine 181 to alanine (S181A), system that maintains intact 250 bases downstream from the ORF of the gene. For a first PCR reaction, two pairs of oligonucleotides were designed (Table 3); two forward primers (named F1 wt and F1A) containing the wild-type or the S181A mutation of the *GSP1* gene, and a reversal oligonucleotide (R1) designed 250 bp downstream the genomic sequence of *GSP1* gene (in order to respect the gene termination signals) and including an additional tail of 15 nucleotides hybridizing to the 5′ end of the KanMX gene in the pYM14 plasmid from the toolbox (Janke et al., 2004). PCR reactions, using as template genomic DNA from W303 strain and combining the different forward primers (producing wild-type or mutant version) and the reverse oligonucleotide, were performed to obtain DNA fragments corresponding to the 3′ end part of *GSP1* gene containing or not the desired mutation.

To add the KanMX selection marker to the cassette, we first amplify the KanMX gene bearing the appropriate hanging tails as follows: we performed a PCR using a F2 forward primer (hybridizing 250 base-pair downstream the 3′ end of *GSP1* gene) and including a 3′tail hybridizing to the 5′end of the KanMK sequence included in pYM14 from toolbox (Janke et al., 2004) and a R2 reversal primer including a sequence hybridizing 300 bp downstream the *GSP1* gene and a sequence for the 3′ end part of the KanMK sequence included in pYM14.

Finally, to produce the recombination cassette we performed a PCR reaction using F1 (wt or A) and R2 primers. As template, we used an equimolecular mix of the *GSP1* PCR fragment generated as described above (wild-type and mutant) and the KanMX PCR fragment.

The wild-type and S181A mutation cassettes were transformed in wild-type W303 strain. The *GSP1* locus was totally sequenced in all the strains to assure that not mutations further than the desired one was included during the PCR reactions.

2.3. Recombinant protein purification

For expression of glutathione S-transferase (GST) or 6xHIS fusion proteins, the *Escherichia coli* strain BL21 (DE3) (Stratagene) was transformed with the corresponding plasmids. Protein expression was induced with 1 mM isopropyl β-D-thiogalactopyranoside (IPTG) for 5 h at 25 °C. Cells were collected by centrifugation, resuspended in 10 ml of cold extraction buffer A (50 mM Tris, pH: 8, 15 mM EDTA, 15 mM EGTA, and 0.1% Triton X-100) containing protease inhibitors (2 mg/ml of pepstatin, 2 mg/ml of leupeptin, 1 mM pepstatin leupeptin phenylmethylsulfonyl fluoride, or PMSF, and 1 mM benzamidine), phosphatase inhibitors (10 mM sodium orthovanadate, 25 mM β-glycerophosphate, 1 mM sodium pyrophosphate, and 10 mM sodium fluoride), and 2 mM DTT. Cells were ruptured by sonication on ice, lysates were removed by centrifugation (1000 rpm for 1 min at 4 °C), and the supernatants were purified using glutathione-sepharose column chromatography for GST-fused proteins and nickel-chelating resin (Ni-NTA) for 6xHIS-fused proteins as described in each manufacturer's instructions. After incubation for 1 h at 4 °C with rotation, the beads were collected by centrifugation (1000 rpm for 1 min at 4 °C) and washed with buffer A 3 times. The elution was performed by adding 10 mM glutathione or 250 mM imidazole.

2.4. In vitro kinase assays

Kinase assays were performed mainly as previously described (Hernandez-Ortega et al., 2012). GST-Pho85, GST-Pcl1, GST-Pho80, GST-Gsp1, and GST-*gsp1*-S181A were purified from bacteria. Phosphorylated proteins were detected using the Pro-Q Diamond phosphoprotein gel stain kit (Invitrogen).

2.5. Cell extracts and immunoblot analysis

Proteins were isolated from yeast strains by treating cell culture samples with trichloroacetic acid at a final concentration of 20% for 1 h. Next, pellets were dissolved in PAGE-SDS sample buffer (100 µl of 50% SDS, 42 mM Tris-HCl at pH 6.8), lysed using glass beads, and boiled for 5 min. Anti-glucose-6-phosphate dehydrogenase antibody (anti-G6PDH; Sigma) was used at 1:500, anti-Clb5 polyclonal antibody (Santa Cruz, sc-6704) was used at 1:100, and anti-Gsp1 polyclonal antibody (Abnova Ref: PAB12340) was used at 1:1000. The secondary antibodies used were donkey anti-goat-HRP 1:2000 and goat anti-rabbit-HRP 1:25000 (both from Jackson laboratories). Immunoblots were developed using Luminata Forte Western HRP Substrate (Millipore) and images were taken with a GeneSnap (Syngene) and quantified with Image Studio Lite (Li-Cor).

2.6. Co-immunoprecipitation assays

Exponential-phase yeast cells were harvested (500 ml at 0.8 OD_{600nm}) and resuspended in 5 ml of cold extraction buffer A (50 mM Tris, pH8, 15 mM EDTA, 15 mM EGTA, 0.1% Triton X-100) containing protease inhibitors (2 µg/ml of pepstatin, leupeptin, phenylmethylsulfonyl fluoride (PMSF), and benzamidine) and phosphatase inhibitors (10 mM sodium orthovanadate and 250 mM β-glycerophosphate). Cells were ruptured by vortexing with glass beads, and the resulting extract was centrifuged at 4 °C for 15 min at 13,000 rpm. Three-mg samples of crude extract were incubated overnight at 4 °C with 25 µl of GFP-Trap (ChromoTek). After washing with extraction buffer, the proteins bound to the beads were resuspended in 30 µl of SDS-PAGE sample buffer, heated at 95 °C for 5 min, and loaded onto SDS-PAGE gels.

2.7. Cell synchronization and cytometry analysis

To synchronize the cells, yeast cultures were grown exponentially in YPD at a density of 1×10^7 cells/ml. For G_1 arrest, cells were treated with α-factor (Biomedal) to a final concentration 20 µg/ml; after 2 h, cells were collected, washed twice with fresh YPD, and released to resume the cell cycle. Next, samples were collected and processed as previously described (Haase and Reed, 2002). DNA was stained with propidium iodide and analysed in a FACS Calibur cytometer (Becton Dickinson) as detailed in (Yaakov et al., 2009).

2.8. Fluorescence microscopy

Strains tagged with eGFP or yeGFP were grown overnight with SD complete medium plus adenine to a final concentration of 120 µg/ml to avoid autofluorescence. Cells were diluted in the same medium to OD_{660nm} = 0.4 and allowed to grow to a mid-log phase for approximately 2 h at 30 °C; next, cells were centrifuged at 1500 rpm for 1 min and resuspended in the appropriate volume of medium to produce the optimal cell concentration for the observation. Five μl of cells were placed onto a slide and mounted with a coverslip. The intensity of the GFP signal was measured using NIS-Elements software as follows: a circular area in the nucleus was selected and the intensity was measured, and the same area was measured in different nuclei. The same was carried out to measure cytoplasmic fluorescence; in this case, areas with low intensity were ruled out to avoid areas or organelles where the proteins were excluded.

2.9. Protein binding assay

All full-length proteins used were purified from bacteria as stated above, except for Gsp1 or *gsp1*-S181A, which were left attached to the Sepharose beads. After 4 washes with buffer A, Gsp1 and *gsp1*-S181A were washed with 1 ml of buffer 1 (PBS containing 10 mM EDTA, 1 mM PMSF, and 1 mM DTT) twice and left rotating at 4 °C for 1 h. Next, beads were washed twice with 1 ml of buffer 2 (PBS containing 10 mM Mg^{+2}, 1 mM PMSF, 1 mM DTT, and 1 mM GTP). Fifty μg of RanGTP were added with 70 μg of importin-β or Xpo1 and Yrb1, based on the binding assay, with buffer 2 in the same eppendorf tube at a final volume of 50 μl. The mixture was incubated for 1 h at 30 °C and the beads were centrifuged at 1500 rpm and washed 3 times with buffer 2. The beads were resuspended with 5 μl of PAGE-SDS sample buffer concentrated 5 times and heated at 95 °C for 5 min, loaded onto SDS-PAGE gels, and stained with Bio-Safe Coomassie stain.

2.10. Statistical analysis

Data were expressed as mean value ± standard error of the mean (SEM). Statistical significance was determined using the Mann-Whitney *U* test. A *p* value of less than 0.05 was considered statistically significant.

3. Results

3.1. The biochemical relationship between Gsp1 and Pho85

To investigate the molecular mechanisms that account for the necessary coordination between the cell cycle and nucleocytoplasmic transport, we reviewed the literature in search for clues about such a relationship and found that in a genome-wide search for phosphorylation events in *S. cerevisiae,* Gsp1 had been proposed as a substrate for the CDK Pho85 (Ptacek et al., 2005). This led us to the question of whether nucleocytoplasmic transport might be regulated by the availability of phosphate and/or the cell cycle, processes that involve Pho85. This prompted us to ask what activity is responsible for Gsp1 phosphorylation, either Pho85-Pho80 suggesting that the availability of phosphate could regulate nucleocytoplasmic transport, or, alternatively, Pho85-Pcl1, which would suggest a regulation by cell cycle. Our first approach involved producing all the proteins in a bacterial system and performing in vitro kinase assays using both kinase complexes to address whether nutrients (through Pho80) or cell cycle (through Pcl1) were responsible for the phosphorylation process that had been previously described (Ptacek et al., 2005). Our result shows that Pho85-Pcl1, and not Pho85-Pho80, is responsible for in vitro phosphorylation of Gsp1, suggesting that the cell cycle regulates nucleocytoplasmic transport through the CDK Pho85 (Fig. 1A and B). Gsp1 bears a single S/PT (Ser181) that is site-specific for CDK phosphorylation; we directly mutated it to Ala and, according to the result shown in Fig. 1A, in vitro phosphorylation disappears, thus demonstrating that Ser181 is the residue targeted by Pho85-Pcl1 in Gsp1.

To obtain in vivo evidence about Pho85-Pcl1/Gsp1 regulation, we performed co-immuno-precipitation assays in which Pho85-eGFP was pulled down and Gsp1 presence was determined by an anti-Gsp1-specific antibody. The transient nature of the kinase-substrate physical interaction is well known, and this could be the reason for very low coprecipitation of Gsp1 and Pho85 (Fig. 1C). However, since kinases interact more strongly when their substrates cannot be phosphorylated (Belozerov et al., 2014), we decided to pull down Pho85 in a strain carrying the nonphosphorylatable version of Gsp1. In this experiment, we obtained a clear increase in the pulled-down amount of *gsp1*-S181A (Fig. C), indicating that Gsp1 and Pho85 *in vivo* interact in *S. cerevisiae.*

3.2. The involvement of Gsp1 in the cell cycle

The next question we asked was directed toward understanding the role of Gsp1 in the cell cycle, which was prompted by our biochemical experiments. Since Pho85-Pcl1 is known to play several roles in G_1 progression and G_1/S transition (Huang et al., 2007; Jimenez et al., 2013a), we decided to synchronize cells bearing a genomic *gsp1*-S181A mutation (see Materials and Methods) at late G_1 by incubating them with alpha-factor. We performed this analysis, and those that followed, in a yeast strain deleted for the orthologue *GSP2* to avoid unexpected interference by the presence of this very similar although non-expressing orthologue. The release of these cells into the cell cycle showed a faster entrance into the S-phase in the mutant strain, which began 40–45 min after release in the nonphosphorylatable *gsp1* cells, while in the wild-type cells the replication began 45–50 min after release, as shown by FACS analysis (Fig. 2A). This impairment in the progression of the cell cycle, while relatively small, was consistent and statistically significant. Fig. 2B shows the quantification of 4 independent experiments.

To confirm that the nonphosphorylatable *gsp1* mutant affects cell cycle progression, we analysed the appearance of the cyclin Clb5, which has been described as a biochemical marker for the G_1/S-phase transition (Skowyra et al., 1997), by Western blot using specific antibodies. In Fig. 2C we present a representative time course of Clb5 after alpha-factor synchronization and release and the quantification of 4 different Western blot experiments (Fig. 2D), which provides biochemical evidence to support the faster cell cycle progression we found by measuring DNA content by FACS analysis.

To further confirm our cell cycle impairment findings, and to avoid artefacts from the alpha-factor treatment of the cells, we decided to analyse the growth of nonphosphorylatable *gsp1* cells in long-term experiments. We placed exponentially growing cells on a microtiter plate and incubated them with constant shaking and controlled temperature in a spectrophotometer to continuously measure the optical density of the culture and thus measure growth. The resulting data, seen in Fig. 2E, is coherent with the faster progression during the G_1/S-phase transition we observed, showing that *gsp1*-A181S grows slightly faster and therefore arrives faster to the stationary phase than wild-type strains when both are grown in a liquid culture with constant monitoring of the culture cell density. Interestingly, when monitored for longer periods under these conditions (24 h), the wild-type culture reached a final concentration of 3.7×10^7 cells/ml, while the mutant concentration was consistently lower at 3.3×10^7 cells/ml.

3.3. The subcellular localization of nonphosphorylatable gsp1

Gsp1 travels from the cytoplasm to the nucleus and vice versa to assist in the transit of different cargo molecules. To confirm the effect of the S181A mutation in nucleocytoplasmic transport, we investigated the subcellular localization of Gsp1and *gsp1*-S181A. The importance of the C terminal part of Gsp1 in the functionality of the protein had previously been described (Lee et al., 2005; Nilsson et al., 2001). This was confirmed when we were unable to obtain a viable cell with a C-terminus GFP-tagged Gsp1 (not shown). However, the N terminus tagging of Gsp1 permitted us to follow the in vivo localization and

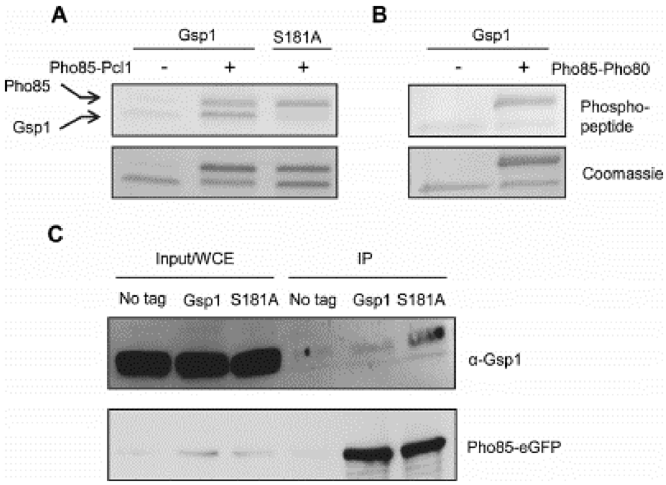

Fig. 1. Gsp1 biochemically interacts with Pho85/Pcl1.
A) and B), in vitro kinase assays. Recombinant Pho85 and GST-Pcl1 or GST-Pho80 purified from bacteria was incubated with GST-Gsp1, either with the wild-type or the indicated mutation versions (see Materials and Methods). The arrows indicate the specific proteins. Coomassie staining of the membrane is presented as a load control. B) Coimmunoprecipitation assay. YJJ1117 (pADH-yeGFP-*GSP1*), YJJ1118 (pADH-yeGFP-*gsp1*-S181A), and a non-tagged strain, all in the exponential growing phase, underwent protein extraction. The extracts were pull-down using GFP-Trap beads. Whole cell extracts (WCE) show the quantity of Gsp1 and Pho85 used in the assay and IP shows the immuno-precipitated samples. The proteins trapped in the GFP-beads after extensive washing were resuspended in SDS-PAGE sample buffer, boiled, and electrophoretically separated. Gsp1 was detected by using anti-Gsp1-specific polyclonal antibodies.

dynamics of Gsp1. We took exponentially growing cells and analysed the subcellular localization of yeGFP-Gsp1 by fluorescence microscopy in both wild-type and S181A mutant cells. In both cases, we obtained a signal that was coherent with nuclear localization. By means of in vivo video-microscopy assays in alpha-factor-synchronised cells, we did not find any apparent differences in the dynamics of Gsp1 and *gsp1*-S181A (data not shown). But a careful quantification of the GFP intensity signal revealed a lower nuclear amount of *gsp1*-S181A than in the wild-type strain (Fig. 3A) and a higher intensity of the mutant in the cytoplasm (Fig. 3B). It is important to note that according to Western blot analysis, the amount of both proteins, (wild-type and S181A) is roughly the same (Fig. 3C).

3.4. Localization of cargo proteins in the nonphosphorylatable gsp1 mutant

To determine whether *gsp1*-S181A functionality is affected, we analysed the intensity of the nuclear localization of some well-described cargoes in which nuclear localization depends on Gsp1. To this end, we tagged *WHI5*, *MBP1*, *MIG1* at their genomic loci with eGFP and used a plasmid bearing an NLS (Nuclear Localization Signal) tagged with 4 GFP copies (Fernandez-Cid et al., 2012a). In all cases, we could detect a different intensity in the GFP-tagged proteins when comparing the nonphosphorylatable mutant of Gsp1 and the wild-type strain (Fig. 3D), thus revealing impaired nuclear localization of the cargo and suggesting either difficulties in the cargo entrance or a more efficient cargo export.

3.5. The physical interaction of Gsp1 with the karyopherin Kap95

The experiments described above suggested that the interaction capabilities of Gsp1 wild-type and the nonphosphorylatable mutant may be different and responsible for the altered cargo localization shown in Fig. 4. For this reason, we decided to analyse the in vitro binding ability of the *gsp1*-S181A mutant to the karyopherin Kap95, which is needed for the nuclear import of cargoes, as well as its binding ability to Yrb1, one of the proteins involved in the export traffic of cargoes to the cytoplasm. To perform these experiments, all the proteins were produced in *E. coli* bearing the tags needed for attachment to agarose beads, (see Materials and Methods and Fig. 4 legend). Our binding experiments showed a drastic reduction in the ability of nonphosphorylatable *gsp1* to bind with Kap95, while we detected a very similar level of interaction with Yrb1. These results are shown in Fig. 4A and B.

4. Discussion

The development of separate compartments for gene expression and protein synthesis in eukaryotic cells, while an evolutionary advantage, has the disadvantage of requiring a tightly controlled system to move molecules in and out of these compartments. However, this aspect gives also room to new possibilities for the regulation of the main cell processes, including signal transduction, gene expression, and cell cycle progression, among many others. The present work adds another piece to the puzzle of the cell cycle and nucleocytoplasmic transport and their intertwined regulation by identifying a biochemical relationship, very probably involving phosphorylation, between a CDK in charge of cell cycle control (Pho85-Pcl1) and the master regulator of in-and-out nuclear transport, Ran-GTPase Gsp1.

4.1. Cell cycle control on transport and vice versa

Our biochemical results suggest that cell cycle machinery controls the nucleocytoplasmic apparatus, and when this control is disturbed it produces an alteration in the amount of at least some of the cargoes. Impairment of the amount of cargoes in the nucleus may be explained by a reduced nuclear amount of Ran-GTPase or impaired interaction with the karyopherin-β (importin-β) Kap95. Our binding assays support the latter; *gsp1*-S181A was shown to barely bind to Kap95. Although we do not know the extent of this effect in a physiological context, phenotypic analysis of the nonphosphorylatable *gsp1* mutant showed a defect in cell cycle progression, suggesting that nucleocytoplasmic transport has some control over the cell cycle. The 2 possibilities are not mutually exclusive and may suggest a close interaction between the 2 processes. It is important to note that cell cycle machinery affects traffic, including traffic of cell cycle regulators such as the transcription factors Swi4 and Swe6, and the repressor Whi5.

4.2. The cell cycle is faster in nonphosphorylatable gsp1

All phenotypic analysis carried out in our study clearly demonstrates that *gsp1*-S181A mutant cells proceed faster through G_1/S-phase. Two possibilities could explain this: on one hand, impaired transport may tamper with a checkpoint mechanism in charge of the quality control of G_1/S-phase processes, including START, while on the other hand, the altered localization of cell cycle repressors such as Whi5 allows for an unscheduled entry into S-phase. In both cases, one might expect that this faster cycling would produce viability problems in the

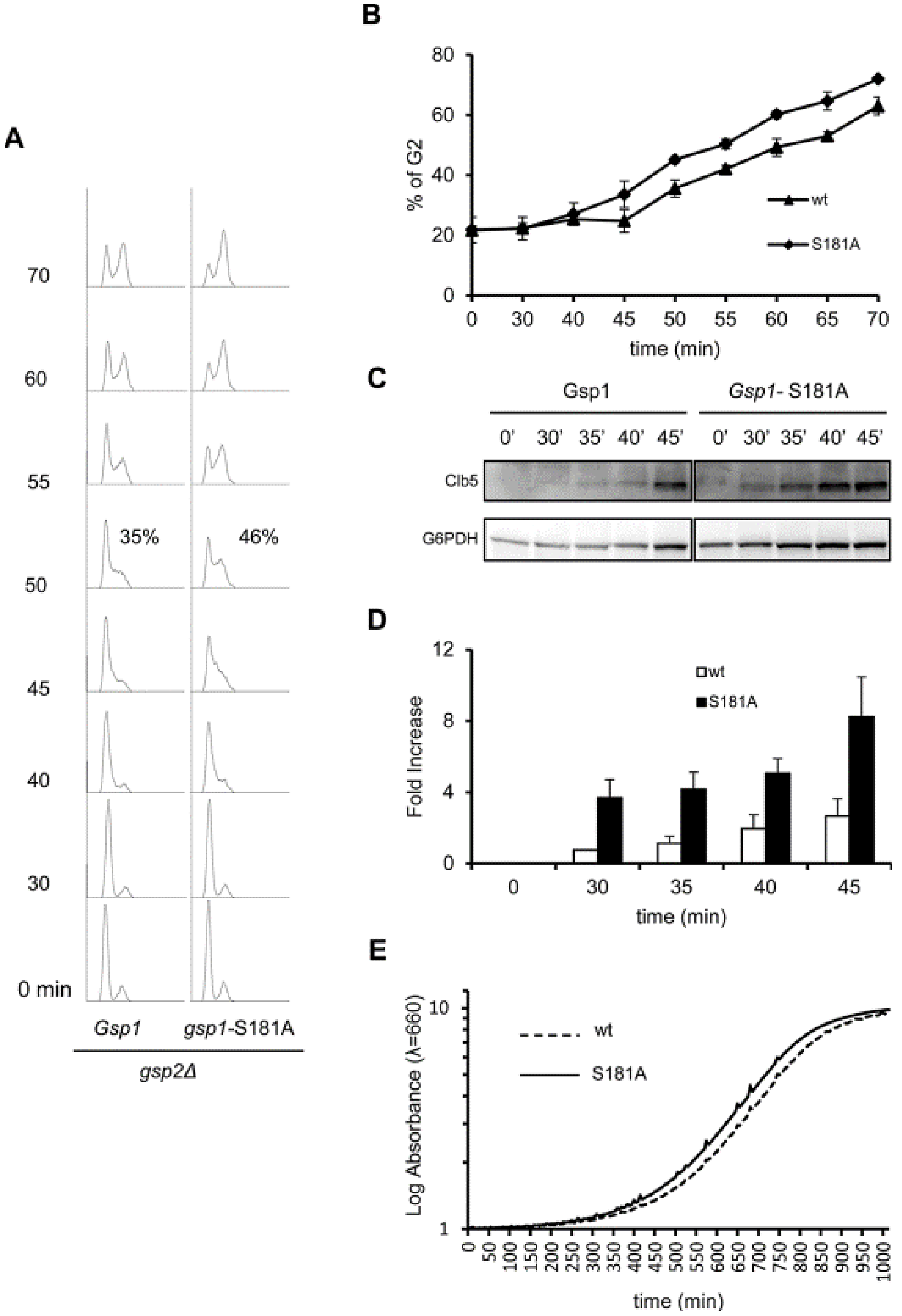

(caption on next page)

Fig. 2. Cell cycle progression and the culture behaviour of *gsp1*-S181A mutant cells.
A) Cell cycle progression of YJJ1091 (wild-type) and YJJ1092 (*gsp1*-S181A), both in a *gsp2Δ* background. Wild-type and *gsp1* mutant cells were synchronized in G_1 using alpha-factor and released in YPD medium at 30 °C. Samples were taken at the indicated times and processed to measure DNA content by FACS analysis. The proportion of 2n cells is indicated in the relevant time point. B) Quantification of 2n DNA content cells. The amount of 2n cells for each time point was calculated using WinMDI free software. The quantification of 4 independent experiments is shown (mean ± SEM). C) Clb5 protein amount in YJJ1091 (wild-type) and YJJ1092 (gsp1-S181A). Cells were treated as in A). Aliquots were taken at the indicated times and proteins were extracted for PAGE-SDS and immunoblotting using specific anti-Clb5 antibodies. D) The quantification of 4 independent experiments, like that of C), is shown (mean ± SEM). Protein amount was normalized using G6PDH and standardized to the amount of protein in the wild-type strain at time 0. E) YJJ1091 (wild-type) and YJJ1092 (*gsp1*-S181A) strains were grown in YPD medium overnight, diluted to OD_{660nm} = 0.01, and followed for 24 h at 30 °C and when agitated in a spectrophotometer to continuously measure culture cell density. The mean result of 3 independent experiments is shown. Note that the large number of time points makes error bar representation impossible.

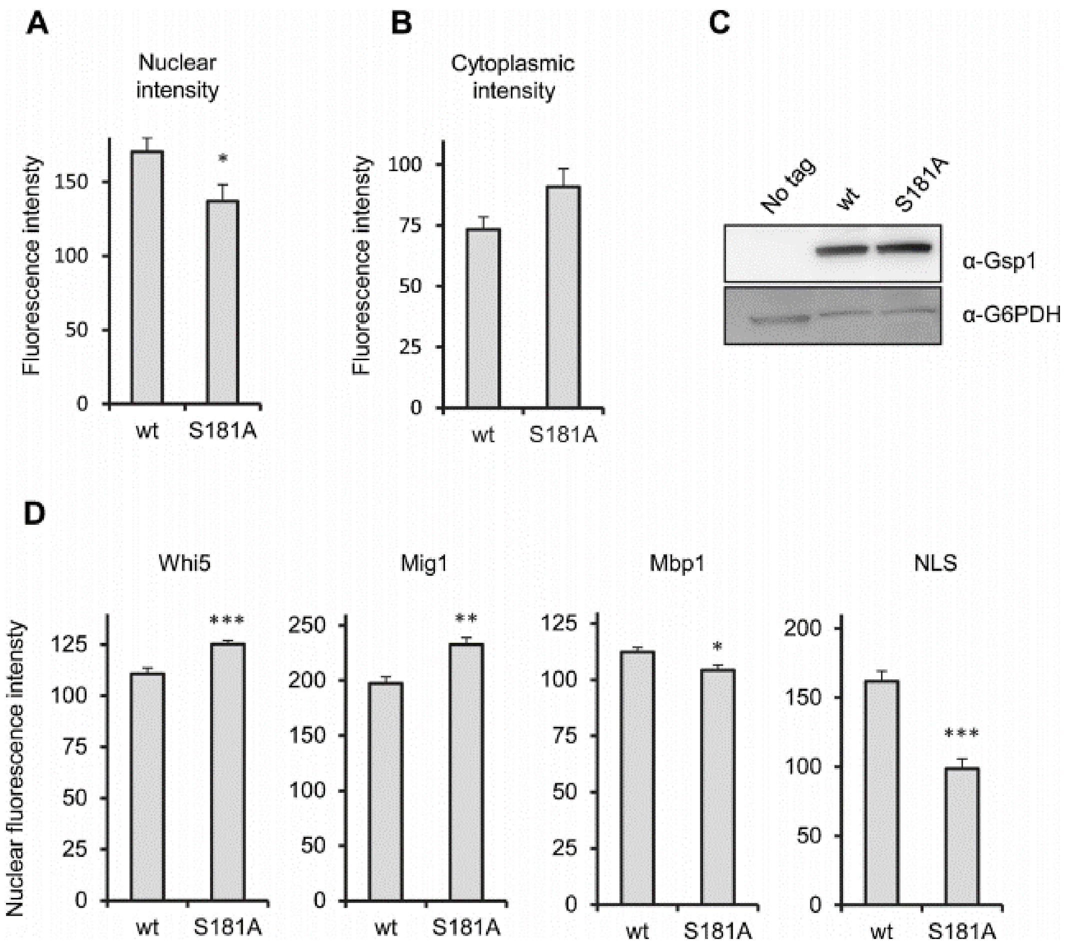

Fig. 3. Subcellular localization of *gsp1*-S181A and different cargoes.
A and B) YJJ1117 (p*ADH*-yeGFP-*GSP1*) and YJJ1118 (p*ADH*-yeGFP-*gsp1*-S181A) strains were grown in SD at 30 °C. After 3 h of growth in the exponential phase, the nuclear and cytoplasmic GFP signal intensity was measured using the NIS-Elements software. The quantification of more than 100 cells obtained from 3 independent experiments is shown (mean ± SEM). The asterisk indicates a statistically significant difference ($p < 0.05$). C) Cell extracts from YJJ1117 (p*ADH*-yeGFP-*GSP1*), YJJ1118 (p*ADH*-yeGFP-*gsp1*-S181A), and a no-tag strain were grown as described in A), with the exception that YPD was used. After 3 h of exponential growth, the protein concentration was assessed by immunoblotting. D) Nuclear intensity of the indicated proteins in YJJ1091 (*GSP1* wild-type) and YJJ1092 (*gsp1*-S181A) strains. Cells were treated and analysed as in A). At least 100 cells from 3 independent experiments were quantified (mean ± SEM). In all cases the GFP tagging was in the genomic (see Table 1) locus except for the NLS in which YJJ1091 (*GSP1* wild-type) and YJJ1092 (*gsp1*-S181A) were transformed with the pFT043 plasmid bearing a NLS-4GFP sequence. The asterisks indicate a statistically significant difference ($p < 0.05$, 0.01, and 0.001).

long term. Indeed, we detected a repetitive and consistent reduction in cellular density during the stationary phase in the nonphosphorylatable mutant that may have been a reflection of cell cycle impairment. Other explanations are possible, like for example metabolic difficulties during the stationary phase. It is worth mentioning that nucleocytoplasmic transport is essential for the proper movement of energy metabolism regulators such as Mig1 and Mig2, which are involved in the repression of galactose metabolism genes in the presence of glucose (Fernandez-Cid et al., 2012a; Fernandez-Cid et al., 2012b).

4.3. Ser181: an important residue for Gsp1/Kap95 interaction

Our binding results point to the residue Ser181 as a participant in the modulation of the interaction between Gsp1 and the importin β

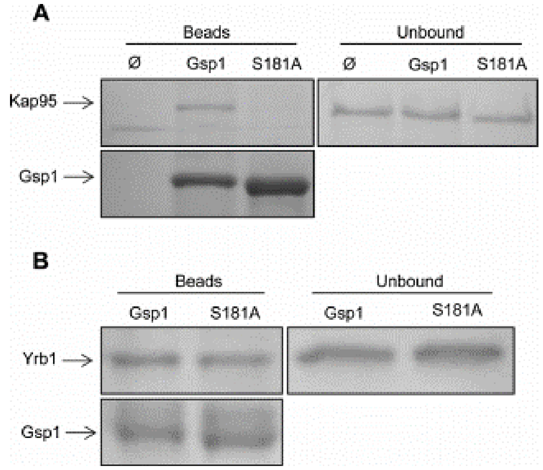

Fig. 4. In vitro binding assays of Gsp1 and *gsp1*-S181A with Kap95 and Yrb1.
A) GST-Gsp1, GST-*gsp1*-S181A proteins, and 6xHIS-Kap95 purified from bacteria. The GST tag proteins were kept attached to glutathione agarose beads and incubated for 1 h at 30 °C with Kap95 before washing 3 times. The attached proteins were eluted by adding PAGE-SDS sample buffer and boiling for 5 min. The proteins were electrophoretically separated and stained using Coomassie. Gsp1 (lower panel) is shown as a loading control. The input amount of Kap95 is shown in B) (left panel), which used the same approach as in A) but involved 6xHIS-Yrb1 and 6xHIS-Xpo1 (Xpo1 was included in the assay because it is important in the Gsp1-Yrb1 complex formation). Gsp1 (lower panel) is presented as a loading control.

Kap95. Mimicking mammalian Ran/Kap95 interaction, the yeast Gsp1 could produce the key salt bridge interactions between Arg29 and Asn154, or the hydrogen bonding interaction between Lys37 and 152, with the C-terminal domain of Kap95. The presence of a serine residue in position 181 of Gsp1 could produce another hydrogen bond, not yet described, that may be playing an important interactive role together with Kap95. In this context, the Stewart group (Lee et al., 2005; Stewart, 2007) has described mutations Lys37Asp/Lys152Asp or Gln69Lys, finding them not sufficient to displace Kap95 from Gsp1. Therefore, Gsp1 Ser181 may be responsible for the previously predicted additional hydrogen bond interaction which, when phosphorylated, increases the disassociation rate of the complex. Such a role would represent a putative cornerstone in the regulation of Gsp1-Kap95 interaction, and thus in nuclear in-and-out cargo traffic. The evidence obtained from our in vitro binding experiments is limited, however, and could lead to overestimating physiological conditions. Further research must be carried out to confirm this hypothesis. In future, binding experiments should be performed in conjunction with the already known mutations of Gsp1 involved in Kap95 interaction in order to determine what residues are essential to this synergy.

Ser181 is not conserved in the human Ran-GTPase, although the homology between Gsp1 and Ran is very high (83% at amino acid level); we might argue that this is due to the complexity of the CDK family in mammalian cells, which is vast when compared to yeast (Malumbres, 2014). This suggests different regulation mechanisms in different types of organisms. Interestingly, however, the same Ser181 residue is conserved in another mammalian small GTPase, ()Rab30, which is involved in the intracellular membrane trafficking (Kelly et al., 2012). This opens up the question of whether this function may also be controlled by cell cycle machinery in metazoans.

The present study is not the first report describing the role of the karyopherin Kap95 in cell cycle progression; Kap95 has been shown to be involved in the nuclear localization of the cell-cycle-related transcription factors Swi4 and Swi6 (Taberner and Igual, 2010).

4.4. A model for Pho85-Gsp1 interaction

Our collected data suggest that the CDK Pho85-Pcl1 involved in the cell cycle biochemically regulates the Ran GTPase Gsp1. According to our results, this phosphorylation may serve as the fine-tuning mechanism necessary for the correct nuclear localization of Gsp1 as well as several other cargoes involved in cell cycle progression, an effect that is mediated by interaction with the importin-β Kap95. We propose that alterations in the nucleocytoplasmic transport of cell cycle regulators may be responsible for the cell cycle impairment we observed in cells that do not have this regulation system. In other words, to phosphorylate Gsp1 during G1/S-phase transition, it is important for the cells to have sufficient time to obtain appropriate levels of cell cycle regulators in the appropriate subcellular location. While it is true that the effect of this mutation in laboratory conditions is subtle, research carried out in physiological situations will lead to a clearer picture of its role.

Acknowledgements

We thank all the members of the lab for their continuous support and scientific contributions, especially M. Pérez for technical assistance, Dr P. Belhumeur for strains, and F. Moreno for the plasmid GFP-NLS. This work was made possible by a UIC grant to O.M. and a grant from the Ministerio de Economia y Competitividad (MINECO) project in Spain (ref: BFU 2013-44189-P) awarded to J.C.

References

Akhtar, N., Hagan, H., Lopilato, J.E., Corbett, A.H., 2001. Functional analysis of the yeast Ran exchange factor Prp20p: in vivo evidence for the RanGTP gradient model. Mol. Genet. Genomics 265, 851–864.

Andrews, B., Measday, V., 1998. The cyclin family of budding yeast: abundant use of a good idea. Trends Genet. 14, 66–72.

Becker, J., Melchior, F., Gerke, V., Bischoff, F.R., Ponstingl, H., Wittinghofer, A., 1995. RNA1 encodes a GTPase-activating protein specific for Gsp1p, the Ran/TC4 homologue of *Saccharomyces cerevisiae*. J. Biol. Chem. 270, 11860–11865.

Belhumeur, P., Lee, A., Tam, R., DiPaolo, T., Fortin, N., Clark, M.W., 1993. GSP1 and GSP2, genetic suppressors of the *prp* 20-1 mutant in *Saccharomyces cerevisiae*: GTP-binding proteins involved in the maintenance of nuclear organization. Mol. Cell. Biol. 13, 2152–2161.

Belozerov, V.E., Ratkovic, S., McNeill, H., Hilliker, A.J., McDermott, J.C., 2014. In vivo interaction proteomics reveal a novel p38 mitogen-activated protein kinase/Rack1 pathway regulating proteostasis in Drosophila muscle. Mol. Cell. Biol. 34, 474–484.

Berben, G., Dumont, J., Gilliquet, V., Bolle, P.A., Hilger, F., 1991. The YDp plasmids: a uniform set of vectors bearing versatile gene disruption cassettes for *Saccharomyces cerevisiae*. Yeast 7, 475–477.

Chook, Y.M., Blobel, G., 2001. Karyopherins and nuclear import. Curr. Opin. Struct. Biol. 11, 703–715.

Chook, Y.M., Suel, K.E., 2011. Nuclear import by karyopherin-betas: recognition and inhibition. Biochim. Biophys. Acta 1813, 1593–1606.

Clement, M., Deshaies, F., de Repentigny, L., Belhumeur, P., 2006. The nuclear GTPase Gsp1p can affect proper telomeric function through the Sir4 protein in *Saccharomyces cerevisiae*. Mol. Microbiol. 62, 453–468.

Conti, E., Izaurralde, E., 2001. Nucleocytoplasmic transport enters the atomic age. Curr. Opin. Cell Biol. 13, 310–319.

Conti, E., Muller, C.W., Stewart, M., 2006. Karyopherin flexibility in nucleocytoplasmic transport. Curr. Opin. Struct. Biol. 16, 237–244.

Costanzo, M., Nishikawa, J.L., Tang, X., Millman, J.S., Schub, O., Breitkreuz, K., Dewar, D., Rupes, I., Andrews, B., Tyers, M., 2004. CDK activity antagonizes Whi5, an inhibitor of G1/S transcription in yeast. Cell 117, 899–913.

Coudreuse, D., Nurse, P., 2010. Driving the cell cycle with a minimal CDK control network. Nature 468, 1074–1079.

Espinoza, F.H., Ogas, J., Herskowitz, I., Morgan, D.O., 1994. Cell cycle control by a complex of the cyclin HCS26 (PCL1) and the kinase PHO85. Science 266, 1388–1391.

Evans, T., Rosenthal, E.T., Youngblom, J., Distel, D., Hunt, T., 1983. Cyclin: a protein specified by maternal mRNA in sea urchin eggs that is destroyed at each cleavage division. Cell 33, 389–396.

Fernandez-Cid, A., Riera, A., Herrero, P., Moreno, F., 2012a. Glucose levels regulate the nucleo-mitochondrial distribution of Mig2. Mitochondrion 12, 370–380.

Fernandez-Cid, A., Vega, M., Herrero, P., Moreno, F., 2012b. Yeast importin-beta is required for nuclear import of the Mig2 repressor. BMC Cell Biol. 13 (31–2121-13-31).

Forwood, J.K., Lange, A., Zachariae, U., Marfori, M., Preast, C., Grubmuller, H., Stewart, M., Corbett, A.H., Kobe, B., 2010. Quantitative structural analysis of importin-beta flexibility: paradigm for solenoid protein structures. Structure 18, 1171–1183.

Gorlich, D., Kutay, U., 1999. Transport between the cell nucleus and the cytoplasm. Annu. Rev. Cell Dev. Biol. 15, 607–660.

Gorlich, D., Prehn, S., Laskey, R.A., Hartmann, E., 1994. Isolation of a protein that is essential for the first step of nuclear protein import. Cell 79, 767–778.

Haase, S.B., Reed, S.I., 2002. Improved flow cytometric analysis of the budding yeast cell cycle. Cell Cycle 1, 132–136.

Hernandez-Ortega, S., Bru, S., Ricco, N., Ramirez, S., Casals, N., Jimenez, J., Isasa, M., Crosas, B., Clotet, J., 2012. Defective in mitotic arrest 1 (Dma1) ubiquitin ligase controls G1 cyclin degradation. J. Biol. Chem. 288 (7), 4704–4714.

Huang, D., Friesen, H., Andrews, B., 2007. Pho85, a multifunctional cyclin-dependent protein kinase in budding yeast. Mol. Microbiol. 66, 303–314.

Hydbring, P., Malumbres, M., Sicinski, P., 2016. Non-canonical functions of cell cycle cyclins and cyclin-dependent kinases. Nat. Rev. Mol. Cell Biol. 17, 280–292.

Janke, C., Magiera, M.M., Rathfelder, N., Taxis, C., Reber, S., Maekawa, H., Moreno-Borchart, A., Doenges, G., Schwob, E., Schiebel, E., Knop, M., 2004. A versatile toolbox for PCR-based tagging of yeast genes: new fluorescent proteins, more markers and promoter substitution cassettes. Yeast 21, 947–962.

Jimenez, J., Ricco, N., Grijota-Martinez, C., Fado, R., Clotet, J., 2013a. Redundancy or specificity? The role of the CDK Pho85 in cell cycle control. Int. J. Biochem. Mol. Biol. 4, 140–149.

Jimenez, J., Truman, A.W., Menoyo, S., Kron, S.J., Clotet, J., 2013b. The yin and yang of cyclin control by nutrients. Cell Cycle 12, 865–866.

Kalderon, D., Roberts, B.L., Richardson, W.D., Smith, A.E., 1984. A short amino acid sequence able to specify nuclear location. Cell 39, 499–509.

Kelly, E.E., Giordano, F., Horgan, C.P., Jollivet, F., Raposo, G., McCaffrey, M.W., 2012. Rab30 is required for the morphological integrity of the Golgi apparatus. Biol. Cell. 104, 84–101.

Kobayashi, J., Matsuura, Y., 2013. Structural basis for cell-cycle-dependent nuclear import mediated by the karyopherin Kap121p. J. Mol. Biol. 425, 1852–1868.

Koch, C., Moll, T., Neuberg, M., Ahorn, H., Nasmyth, K., 1993. A role for the transcription factors Mbp1 and Swi4 in progression from G1 to S phase. Science 261, 1551–1557.

Kosugi, S., Hasebe, M., Tomita, M., Yanagawa, H., 2009. Systematic identification of cell cycle-dependent yeast nucleocytoplasmic shuttling proteins by prediction of composite motifs. Proc. Natl. Acad. Sci. U. S. A. 106, 10171–10176.

Lange, A., Mills, R.E., Lange, C.J., Stewart, M., Devine, S.E., Corbett, A.H., 2007. Classical nuclear localization signals: definition, function, and interaction with importin alpha. J. Biol. Chem. 282, 5101–5105.

Lee, S.J., Matsuura, Y., Liu, S.M., Stewart, M., 2005. Structural basis for nuclear import complex dissociation by RanGTP. Nature 435, 693–696.

Lee, Y.S., Huang, K., Quiocho, F.A., O'Shea, E.K., 2008. Molecular basis of cyclin-CDK-CKI regulation by reversible binding of an inositol pyrophosphate. Nat. Chem. Biol. 4, 25–32.

Madrid, A.S., Weis, K., 2006. Nuclear transport is becoming crystal clear. Chromosoma 115, 98–109.

Malumbres, M., 2014. Cyclin-dependent kinases. Genome Biol. 15, 122.

Menoyo, S., Ricco, N., Bru, S., Hernandez-Ortega, S., Escote, X., Aldea, M., Clotet, J., 2013. Phosphate-activated CDK stabilizes G1 cyclin to trigger cell cycle entry. Mol. Cell. Biol. 33 (7), 1273–1284.

Mosammaparast, N., Pemberton, L.F., 2004. Karyopherins: from nuclear-transport mediators to nuclear-function regulators. Trends Cell Biol. 14, 547–556.

Nachury, M.V., Weis, K., 1999. The direction of transport through the nuclear pore can be inverted. Proc. Natl. Acad. Sci. U. S. A. 96, 9622–9627.

Nilsson, J., Askjaer, P., Kjems, J., 2001. A role for the basic patch and the C terminus of RanGTP in regulating the dynamic interactions with importin beta, CRM1 and RanBP1. J. Mol. Biol. 305, 231–243.

Nurse, P., Bissett, Y., 1981. Gene required in G1 for commitment to cell cycle and in G2 for control of mitosis in fission yeast. Nature 292, 558–560.

Nurse, P., 1990. Universal control mechanism regulating onset of M-phase. Nature 344, 503–508.

Oki, M., Nishimoto, T., 1998. A protein required for nuclear-protein import, Mog1p, directly interacts with GTP-Gsp1p, the Saccharomyces cerevisiae ran homologue. Proc. Natl. Acad. Sci. U. S. A. 95, 15388–15393.

Oki, M., Nishimoto, T., 2000. Yrb1p interaction with the gsp1p C terminus blocks Mog1p stimulation of GTP release from Gsp1p. J. Biol. Chem. 275, 32894–32900.

Ouspenski, I.I., Elledge, S.J., Brinkley, B.R., 1999. New yeast genes important for chromosome integrity and segregation identified by dosage effects on genome stability. Nucleic Acids Res. 27, 3001–3008.

Pemberton, L.F., Paschal, B.M., 2005. Mechanisms of receptor-mediated nuclear import and nuclear export. Traffic 6, 187–198.

Pines, J., Hunt, T., 1987. Molecular cloning and characterization of the mRNA for cyclin from sea urchin eggs. EMBO J. 6, 2987–2995.

Ptacek, J., Devgan, G., Michaud, G., Zhu, H., Zhu, X., Fasolo, J., Guo, H., Jona, G., Breitkreutz, A., Sopko, R., McCartney, R.R., Schmidt, M.C., Rachidi, N., Lee, S.J., Mah, A.S., Meng, L., Stark, M.J., Stern, D.F., De Virgilio, C., Tyers, M., Andrews, B., Gerstein, M., Schweitzer, B., Predki, P.F., Snyder, M., 2005. Global analysis of protein phosphorylation in yeast. Nature 438, 679–684.

Radu, A., Blobel, G., Moore, M.S., 1995. Identification of a protein complex that is required for nuclear protein import and mediates docking of import substrate to distinct nucleoporins. Proc. Natl. Acad. Sci. U. S. A. 92, 1769–1773.

Reed, S.I., Wittenberg, C., 1990. Mitotic role for the Cdc28 protein kinase of Saccharomyces cerevisiae. Proc. Natl. Acad. Sci. U. S. A. 87, 5697–5701.

Reed, S.I., Hadwiger, J.A., Lorincz, A.T., 1985. Protein kinase activity associated with the product of the yeast cell division cycle gene CDC28. Proc. Natl. Acad. Sci. U. S. A. 82, 4055–4059.

Schneider, K.R., Smith, R.L., O'Shea, E.K., 1994. Phosphate-regulated inactivation of the kinase PHO80-PHO85 by the CDK inhibitor PHO81. Science 266, 122–126.

Skowyra, D., Craig, K.L., Tyers, M., Elledge, S.J., Harper, J.W., 1997. F-box proteins are receptors that recruit phosphorylated substrates to the SCF ubiquitin-ligase complex. Cell 91, 209–219.

Sopko, R., Huang, D., Preston, N., Chua, G., Papp, B., Kafadar, K., Snyder, M., Oliver, S.G., Cyert, M., Hughes, T.R., Boone, C., Andrews, B., 2006. Mapping pathways and phenotypes by systematic gene overexpression. Mol. Cell 21, 319–330.

Stade, K., Ford, C.S., Guthrie, C., Weis, K., 1997. Exportin 1 (Crm1p) is an essential nuclear export factor. Cell 90, 1041–1050.

Standart, N., Minshull, J., Pines, J., Hunt, T., 1987. Cyclin synthesis, modification and destruction during meiotic maturation of the starfish oocyte. Dev. Biol. 124, 248–258.

Stern, B., Nurse, P., 1996. A quantitative model for the cdc2 control of S phase and mitosis in fission yeast. Trends Genet. 12, 345–350.

Stevenson, L.F., Kennedy, B.K., Harlow, E., 2001. A large-scale overexpression screen in *Saccharomyces cerevisiae* identifies previously uncharacterized cell cycle genes. Proc. Natl. Acad. Sci. U. S. A. 98, 3946–3951.

Stewart, M., 2007. Molecular mechanism of the nuclear protein import cycle. Nat. Rev. Mol. Cell Biol. 8, 195–208.

Swaffer, M.P., Jones, A.W., Flynn, H.R., Snijders, A.P., Nurse, P., 2016. CDK substrate phosphorylation and ordering the cell cycle. Cell 167, 1750–1761 (e16).

Swenson, K.I., Farrell, K.M., Ruderman, J.V., 1986. The clam embryo protein cyclin A induces entry into M phase and the resumption of meiosis in *Xenopus* oocytes. Cell 47, 861–870.

Taberner, F.J., Igual, J.C., 2010. Yeast karyopherin Kap95 is required for cell cycle progression at Start. BMC Cell Biol. 11 (47–2121-11-47).

Taberner, F.J., Quilis, I., Igual, J.C., 2009. Spatial regulation of the start repressor Whi5. Cell. Cycle 8, 3010–3018.

Thomas, B.J., Rothstein, R., 1989. Elevated recombination rates in transcriptionally active DNA. Cell 56 (4), 619–630.

Truman, A.W., Kristjansdottir, K., Wolfgeher, D., Hasin, N., Polier, S., Zhang, H., Perrett, S., Prodromou, C., Jones, G.W., Kron, S.J., 2012. CDK-dependent Hsp70 phosphorylation controls G1 cyclin abundance and cell-cycle progression. Cell 151, 1308–1318.

Vijayraghavan, U., Company, M., Abelson, J., 1989. Isolation and characterization of pre-mRNA splicing mutants of *Saccharomyces cerevisiae*. Genes Dev. 3, 1206–1216.

Weis, K., 2003. Regulating access to the genome: nucleocytoplasmic transport throughout the cell cycle. Cell 112, 441–451.

Yaakov, G., Duch, A., Garcia-Rubio, M., Clotet, J., Jimenez, J., Aguilera, A., Posas, F., 2009. The stress-activated protein kinase Hog1 mediates S phase delay in response to osmostress. Mol. Biol. Cell 20, 3572–3582.